Volume 1, Number 1

May-June, 1960

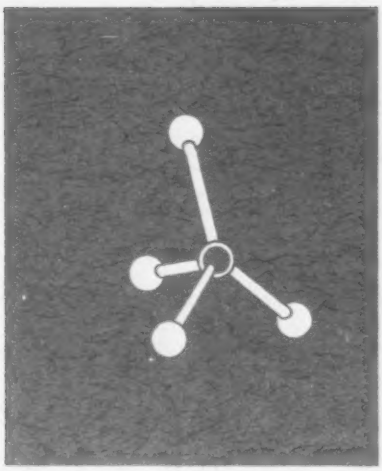

JOURNAL OF

STRUCTURAL CHEMISTRY

ЖУРНАЛ СТРУКТУРНОЙ ХИМИИ / ZHURNAL STRUKTURNOI KHIMII

TRANSLATED FROM RUSSIAN (c/b) CONSULTANTS BUREAU

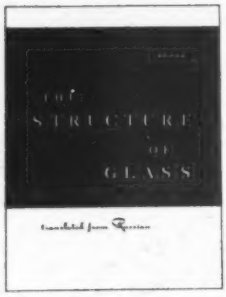

THE STRUCTURE OF GLASS

Volume 2

Proceedings of the Third All-Union Conference on the Glassy State, held in Leningrad, November 16-20, 1959.

This notable volume contains papers presented at the conference convened by the Institute of Silicate Chemistry of the Academy of Sciences, USSR, the D. I. Mendeleev All-Union Chemical Society, and the S. I. Vavilov (Order of Lenin) State Optical Institute for discussion of recent experimental studies of various properties of glass, the principal methods for investigating glass structure, and the problem of glass formation.

A complete account is given of research work on the glassy state since the previous conference. The most modern optical, spectroscopic, and electrical techniques were used in studying the structure of glass in all its aspects, and the results are interpreted in the light of contemporary physical theories of the solid state.

Volume 2: $25.00

CONTENTS include

Investigation of Glass Structures by the Methods of Optical Spectroscopy. *A. A. Lebedev*
Diffraction Methods for the Study of Glassy Substances. *E. A. Porai-Koshits*
The Cellular Structure of Glass. *W. Vogel*
Characteristic Vibrations of the Glass Network and Glass Structure. *A. G. Vlasov*
General Problems of the Structure and Properties of Glasses. *K. S. Evstrop'ev*
Additivity of the Properties of Silicate Glasses in Relation to their Structure. *L. I. Demkina*
Glassy Systems and the Problem of Glass Structure. *M. A. Bezborodov*
Chemical Characteristics of Polymeric Glass-Forming Substances and the Nature of Glass Formation. *R. L. Myuller*
Characteristics of Glass Formation in Chalcogenide Glasses *N. A. Goryunova and B. T. Kolomiets*
Glass as a Polymer. *V. V. Tarasov*
Formation of a Crystalline Phase from a Silicate Melt. *A. I. Avgustinik*
The Vitrification Process and Structure of Glass. *O. K. Botvinkin*
Formation of Glass Structure during the Melting Process. *L. G. Mel'nichenko*
The Structure of Glass in the Light of the Crystal Chemistry of Silicates. *N. V. Belov*

492 pages **illustrated**

Volume 1

Proceedings of the Second All-Union Conference on the Glassy State.

". . . The Glass Division of the American Ceramic Society and the National Science Foundation are to be congratulated for making this inspiring collection available . . ." — *Journal of Chemical Education*

"The book should be of great interest to scientific and technical personnel interested in glass technology, ceramics, the states of matter, and any work involving the vitreous state. They should all have the experience of reading this book." — *Chemistry in Canada*

". . . a stimulating experience . . ." — *Trans. British Ceramic Society*

". . . lively discussions which show the diversity of opinions on every experimental report." — *The Glass Industry*

". . . the volume is excellent . . . the translation was well worth while . . ." — *R. W. Douglas, Nature*

Volume 1: $20.00

Volumes 1 and 2: $40.00 per set

CONTENTS include

The Crystallite Theory of Glass Structure. *K. S. Evstropyev*
Structure and Properties of Organic Glasses. *P. P. Kobeko*
The Structure of Glass. *O. K. Botvinkin*
The Possibilities and Results of X-Ray Methods for Investigation of Glassy Substances. *E. A. Porai-Koshits*
Structural Peculiarities of Vitreous and Liquid Silicates. *O. A. Esin and P. V. Geld*
Raman Spectra and Structure of Glassy Substances. *E. F. Gross and V. A. Kolesova*
The Quantum Theory of Heat Capacity and the Structure of Silicate Glasses. *V. V. Tarasov*
The Infrared Spectra of Simple Glasses and Their Relationship to Glass Structure. *V. A. Florinskaya and R. S. Pechenkina*
The Coordination Principle of Ion Distribution in Silicate Glasses. *A. A. Appen*
Concepts of the Internal Structure of Silicate Glasses Which Follow from the Results of Studies of the Properties of Glasses in Certain Simple Systems. *L. I. Demkina*
Measurement of the Expansion of Glass as a Method for Investigating its Structure. *A. I. Stozharov*
The Theoretical Views of D. I. Mendeleev on the Structure of Silicates and Glasses, and Their Significance for Modern Science. *L. G. Melnichenko*
The Views of D. I. Mendeleev on the Chemical Nature of Silicates. *V. P. Barzakovsky*

296 pages **illustrated**

Complete contents available upon request

c/b
CONSULTANTS BUREAU
227 W. 17 ST., NEW YORK 11, N. Y.

ZHURNAL STRUKTURNOI KHIMII
EDITORIAL BOARD:

S. S. Batsanov *(Secretary)*
G. B. Bokii *(Editor)*
A. V. Nikolaev *(Acting Editor)*
B. V. Ptitsyn
O. Ya. Samoilov
Yu. T. Struchkov
Ya. K. Syrkin
V. V. Voevodskii
M. V. Vol'kenshtein

JOURNAL OF

STRUCTURAL CHEMISTRY

A translation of ZHURNAL STRUKTURNOI KHIMII,

a publication of the Academy of Sciences of the USSR

© 1961 CONSULTANTS BUREAU ENTERPRISES, INC.
227 West 17th Street, New York 11, N. Y.

Volume 1, Number 1 May-June, 1960

CONTENTS

	PAGE ENG.	PAGE RUSS.
Preface	i	
Foreword	1	3
An Electronographic Investigation of the Structure of Molecules of Nitric Acid and Nitric Anhydride in the Vapor. N. A. Akishin, L. V. Vilkov and V. Ya. Rosolovskii	3	5
The Influence of Ions on the Structure of Water. I. G. Mikhailov and Yu. P. Syrnikov	10	12
Proton Relaxation in Aqueous Solutions of Diamagnetic Salts. I. Solutions of Nitrates of Elements in the Second Group of the Periodic System. V. M. Vdovenko and V. A. Shcherbakov	25	28
Vibration Frequencies of the Water Molecules in the First Coordination Layer Around an Ion in an Aqueous Solution. O. Ya. Samoilov	32	36
A Second Chapter in the Chemical Crystallography of the Silicates. N. V. Belov	35	39
The Structure of Epididymite $NaBeSi_3O_7(OH)$. A New Type of $[Si_6O_{15}]$ Chain. E. A. Pobedimskaya and N. V. Belov	44	51
On Phases Formed in the System Chromium – Boron, in the Boron-Rich Region. V. A. Épel'baum N. G. Sevast'yanov, M. A. Gurevich and G. S. Zhdanov	55	64
Crystal Structure of Ternary Phases in the Systems Mo(W) – Fe(Co, Ni) – Si. E. I. Gladyshevskii and Yu. B. Kuz'ma	57	66
Complex Compounds with Multiple Bonds in the Inner Sphere. G. B. Bokii	63	72
Quantitative Evaluations of Maxima in the Three-Dimensional Patterson Function. V. V. Ilyukhin and S. V. Borisov	70	80
Application of Infrared Spectroscopy to the Determination of Silicate Structures. I. Reflection Spectra of Sodium Silicate Crystals in the 7.5-15μ Region. V. A. Florinskaya and R. S. Pechenkina	76	86
The Application of Electron Paramagnetic Resonance to the Study of Molecular Structure of Carbons. N. N. Tikhomirova, I. V. Nikolaeva and V. V. Voevodskii	89	99
New Magnetic Properties of Macromolecular Compounds Containing Conjugated Double Bonds. L. A. Blyumenfel'd, A. A. Berlin, A. A. Slinkin and A. É. Kalmanson	93	103
The Molecular Orbital Self-Consistent-Field Determination of the Ground State of Ferrocene. E. M. Shustorovich and M. E. Dyatkina	98	109
BRIEF COMMUNICATIONS		
Proton Relaxation in Aqueous Solutions of Diamagnetic Salts. II. Alkali Metal Cations and Halide Atoms. V. M. Vdovenko and V. A. Shcherbakov	111	122
The Nuclear Quadrupole Resonance Spectrum of 1,2,3-Trichlorobenzene. É. I. Fedin	114	124
The Coordination of Nickel in $Ni(CH)_2NH_3 \cdot nH_2O$ Crystals. M. A. Porai-Koshits	116	125
CHRONICLE		
Problems of Structural Inorganic Chemistry at the Third All-State Conference on Inorganic Chemistry in Bratislava. T. S. Khodashova	118	127

Annual Subscription: $80 **Single Issue: $20** **Single Article: $12.50**

Note: The sale of photostatic copies of any portion of this copyright translation is expressly prohibited by the copyright owners.

FROM THE PUBLISHER

THE JOURNAL OF STRUCTURAL CHEMISTRY. This important new Soviet journal will make the novel approach of Soviet scientists to many problems of structural chemistry readily accessible to all those working with the problems of the molecular structure of matter.

As a result of the two-year contract signed with Mezhdunarodnaya Kniga, the official Soviet book agency, in 1960, Consultants Bureau is receiving advance page proofs and original art work and photographs for this journal, thus ensuring regular publication of a very high quality. The translation will be published not more than six months after the original Russian by the end of 1961. The translation will bear volume and issue numbers identical with the Russian original. All tabular and illustrative material is reproduced integral with the English text, which is translated by bilingual scientists who are experts in these particular fields. Transliteration is by the British-American system.

The addition of THE JOURNAL OF STRUCTURAL CHEMISTRY to the Consultants Bureau program brings its total of cover-to-cover translations of Soviet scientific and technical journals to 34. More than half of these journals are produced for American learned societies. The company's twelve years of experience in the translation and publication of journals such as this one will be constantly applied toward maintaining and improving the quality of this new translation.

FOREWORD

Translated from Zhurnal Strukturnoi Khimii, Vol. 1, No. 1, pp. 3-4,
May-June, 1960

The Twenty-first Congress of the Communist Party of the Soviet Union stated in its decisions that the most important task for Soviet chemical science comprises all possible extensions of theoretical investigations which aid the development of new and improved technological processes and production of synthetic materials with properties satisfying the demands of modern technology. In 1958 the May Plenary Session of the Central Committee of the Communist Party of the Soviet Union laid down a broad program for accelerated development of the entire chemical industry of the USSR. The Plenary Session of June 1959 adopted a resolution to raise the role of science in technical progress and to accelerate the adoption of scientific advances in industry. Great importance is attached to rational geographical distribution of scientific centers; this is reflected, in particular, in the Government decree for the creation of a scientific center in Siberia in the form of the Siberian Division of the Academy of Sciences of the USSR, where six new chemical institutes are being organized. One of the measures needed for the fulfillment of the great tasks confronting chemical science and industry was the creation of new scientific journals of the Academy of Sciences of the USSR, including the Journal of Structural Chemistry.

The progress of modern theoretical and applied chemistry is closely associated with advances in determination of the atomic structure of matter and elucidation of the nature of the chemical bond. The main task of the new journal is systematic publication and discussion of research results in the structural chemistry of organic and inorganic compounds. The journal will report work on the structure of gases, liquids, and crystals and other solids, performed by modern physical and physicochemical methods. Theoretical and experimental studies of the nature of the chemical bond in substances in various states of aggregation will be considered in the journal. In addition to rigorous methods for solving problems of chemical bonding, the journal will publish researches of a semiquantitative character, reporting on methods whereby particular problems in the theory of interatomic action can be solved rapidly and fairly reliably.

One of the most important tasks of the journal will be detailed presentation of methods for studing the structure of matter, with detailed discussions of new theoretical aspects of structural chemistry which arise in connection with such methods. For example, it is intended to publish work on the development of x-ray, electron, and neutron diffraction methods for studing the atomic structure of matter. Of course, other methods will also be covered, including numerous optical methods, magnetochemistry, colorimetry, and others intended for determination of the structure of matter. The applicability limits of various methods will be discussed, and comparison of the results obtained by these methods, and their practical applications, will be considered.

In view of the extensive use of radiospectroscopic methods (electronic and nuclear magnetic resonance, etc.) in chemistry during the last few years research workers are now able to penetrate into the hitherto inaccessible field of weak interaction between particles of matter, studies of which have already led to the discovery of new properties of matter and explanation of a number of effects, previously not understood, in chemistry, physics, and biology.

Another factor which will greatly influence future successful development of structural chemistry is the speed with which the existing gap will be closed between numerous and diverse experimental investigations and the development of strict theoretical concepts which not only explain known facts but also stimulate further researches in the most important and urgent directions. The first prerequisite for this is that experimental and theoretical workers in this field should exchange information on completed and proposed work as rapidly as possible, and should be well informed on the most recent advances in allied fields. Accordingly, the journal intends to publish not only original papers of a theoretical and experimental character, but also review articles on individual topics in structural chemistry.

The journal will also include brief reports on new methods and results which are of importance in principle. The Journal of Structural Chemistry will publish articles on prospects in the development of structural chemistry and on teaching of its individual aspects, and also book reviews and reports of current events.

The Editorial Board hopes that publication of the journal will lead to closer contacts between chemists, physicists, geochemists, and biologists in a field of vital importance to all these branches of science, namely structural chemistry, and that this cooperation will in its turn assist even more rapid development of our science.

Editorial Board

AN ELECTRONOGRAPHIC INVESTIGATION OF THE STRUCTURE OF MOLECULES OF NITRIC ACID AND NITRIC ANHYDRIDE IN THE VAPOR

P. A. Akishin, L.V. Vilkov and V.Ya. Rosolovskii

M.V. Lomonosov Moscow State University, and the N.S. Kurnakov Institute of General and Inorganic Chemistry of the Academy of Sciences of the USSR

Translated from Zhurnal Strukturnoi Khimii, Vol. 1, No. 1, pp. 5-11, May-June, 1960
Original article submitted November 23, 1959

An electronographic method, involving a visual estimation of the intensity, has been used in an investigation of the structure of the molecules of nitric acid and nitric anhydride. The flowing values have been obtained for the basic parameters of the nitric acid molecule, $HO'-NO_2$: $r(N=O) = 1.22 \pm 0.01$ A; $r(N-O) = 1.40 \pm 0.01$ A; $\angle ONO = 135 \pm 2.5°$; and for the nitric anhydride molecule, $O_2N-O'-NO_2$: $r(N=O) = 1.21 \pm 0.01$ A; $r(N-O) = 1.46 \pm 0.02$ A; $\angle ONO = 134 \pm 5°$; and the angle between the planes of the NO_2 groups, $\alpha = 95 \pm 3°$. A difference has been observed between the length of the single N–O bonds in the molecules of nitric acid and nitric anhydride. Certain problems concerning the geometrical configuration of the molecules of the higher oxides of elements in the Ist, IIIrd, Vth and VIIth groups of the Periodic System are discussed.

The study of the geometrical structure of molecules of inorganic compounds (such as salts, acids, acid anhydrides, and others) in the gas or vapor phase is a problem of current importance in structural chemistry, the solution of which is necessary for the development of the general theory of the structure of molecules. However, data concerning the structure of the "gaseous" molecules of these compounds are very few in number, as well as being frequently lacking in completeness and reliability. See, for example, [1].

The determination of the geometry of the nitric acid molecule, HNO_3, in the vapor phase has been studied by means of electronographic [2] and microwave [3] methods, as a result of which the planar character of the nitric acid molecule has been established, and the basic interatomic distances have been determined. It must be noted, however, that these investigations [2, 3] are not free from certain methodological inadequacies. Thus, no use was made in [2] of the method of radial distribution, and the theoretical curves were not selected in a satisfactory way; while in [3] only the two parameters $r(N-O) = 1.44$ A and $\angle ONO = 137°50'$ were determined, on the assumption that $r(N=O) = 1.203$ A, $r(O-H) = 0.96$ A, and $\angle NOH = 90°$. It is clear, therefore, that the necessity arises for a new investigation to accurately determine the geometrical parameters of nitric acid in the vapor phase. There are no experimental data concerning the structure of nitric anhydride (N_2O_5) in the vapor, and experiments with a view to determining these, undertaken in the old work [4], were without success.

EXPERIMENTAL

Anhydrous nitric acid was obtained by distilling a mixture of 60% nitric acid and oleum under vacuum at a temperature of 80° in a Zinov'ev apparatus [5]. The preparation of nitric anhydride (containing 99.5% N_2O_5) was performed according to the method described in G. Brayer's Handbook [6].

The investigation was carried out using the electronograph described earlier [7]. The interpretation of the

TABLE 1

Results of the Interpretation of the Electronograms of Nitric Acid and Nitric Anhydride in the Vapor Phase.

Maximum	Minimum	HNO_3				N_2O_5			
		I (s)	s_{exp} *	$\frac{\Delta s_{exp}}{s_{exp}}$	$\frac{s_{theor}}{s_{exp}}$, model 5	I (s)	s_{exp} *	$\frac{\Delta s_{exp}}{s_{exp}}$	$\frac{s_{theor}}{s_{exp}}$, model 3
1		+ 5	3,59	0,025	0,989	+ 4	3,43	0,024	(0,863)
	1	—10	4,84	0,013	(0,949)	—10	4,79	0,003	(0,887)
2		+20	6,14	0,011	1,038	+17	6,04	0,004	1,002
	2	—15	7,94	0,005	1,026	—14	8,02	0,008	1,010
3		+10	9,15	0,007	(1,059)	+ 8	9,29	0,005	1,003
	3	— 8	10,55	0,008	1,010	— 3	10,63	0,009	0,983
4		+12	11,93	0,004	1,022	+10	11,86	0,006	1,000
	4	—12	13,54	0,005	0,019	— 9	13,54	0,005	0,980
5		+ 6	15,00	0,007	1,024	+ 6	14,95	0,006	(0,970)
	5	— 4	16,38	0,005	1,013	— 1	16,32	0,004	0,954
6		+ 7	17,72	0,003	1,014	+ 8	17,67	0,000	0,990
	6	— 6	19,34	0,005	1,014	— 6	19,29	0,003	0,993
7		+ 4	20,72	0,007	1,025	+ 5	20,78	0,004	1,002
	7	0	22,06	0,009	0,013	+ 2	21,98	0,004	0,987
8		+ 5	23,34	0,006	1,009	+ 5	23,11	0,005	0,989
	8	— 3	24,89	0,006	1,017	— 4	24,70	0,006	0,991
9		+ 2	26,36	0,007	1,030	+ 4	26,26	0,005	0,999
	9	—	—	—	—	—	—	—	—
10		—	—	—	—	+ 3	28,66	—	—
	10	—	—	—	—	— 2	30,37	—	—
11		—	—	—	—	+ 2	32,02	—	—
Mean value				0,008	1,017			0,006	0,995
Mean deviation					±0,007				±0,007

* The values were obtained by averaging the measurements for seven series of electronograms.

electronogram was performed on the basis of a visual estimate of the intensity by two methods [8]. The first was the method of radial distribution, according to the equation:

$$rD(r) = \Sigma sI(s) \cdot \exp(-as^2) \cdot \sin sr\,\Delta s, \tag{1}$$

where

$$s = \frac{4\pi}{\lambda} \sin \vartheta/2,\ \exp(-as^2_{max}) = 0{,}1,\ \Delta s = 0{,}2\ A^{-1}.$$

The second was the method of the selection of theoretical curves (by a process of trial and error), according to the equation,

$$I(s) = \sum_{i \neq j} nZ_iZ_j \exp(-b_{ij}s^2) \frac{\sin sr_{ij}}{sr_{ij}}, \tag{2}$$

where n is the number of interatomic distances, r_{ij}, of a single type; $Z_{i(j)}$ are the charges on the nuclei of the atoms i(j); $b_{ij} = \frac{\langle l_{ij}^2 \rangle^{1/2}}{2}$; l_{ij} is the effective mean square amplitude of the thermal oscillations.

Nitric acid. Seven series of electronograms were obtained for the vapor of nitric acid (four recordings in each series), for $\lambda = 0.0543 - 0.0552$ A, and a jet-plate distance of 118 mm. From the values found for s and I(s) for the maxima and minima of the diffraction diagram (Table 1), the experimental intensity curve was

TABLE 2

Parameters of Theoretical Curves for Molecules of Nitric Acid and Nitric Anhydride*

No. of curve	HNO_3** r(N—O)	N_2O_5*** ∠ONO	N_2O_5*** ∠NO'N	No. of curve	N_2O_5*** ∠ONO	N_2O_5*** ∠NO'N
1	1,46	124°	90°	7	154°	101°
2	1,44	129°	95°	8	154°	106°
3	1,42	134°	95°	9	134°	98°
4	1,40	139°	95°	10	134°	92°
5	1,38	144°	98°	11	130°	95°
6	1,36	144°	103°			

* Curve 12 for bipyramid.

** The value of r(N=O) = 1.20 A and ∠ONO = 135° did not vary.

*** The values of r(N=O) = 1.22 A and r(N–O) = 1.47 A did not vary, with the exception of curve 11, for which r(N–O) = 1.41 A.

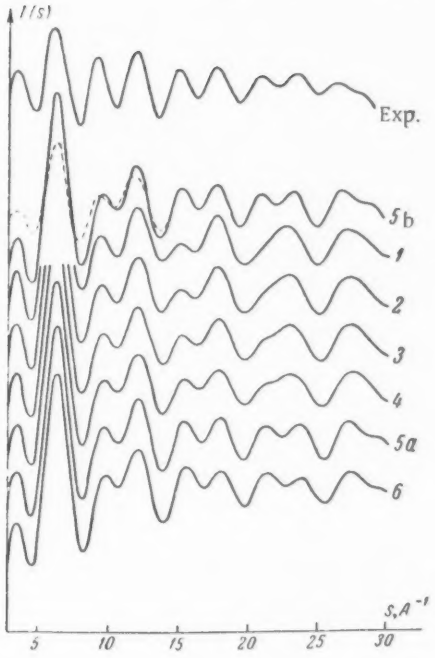

Fig. 1. Experimental and theoretical intensity curves for the nitric acid molecule.

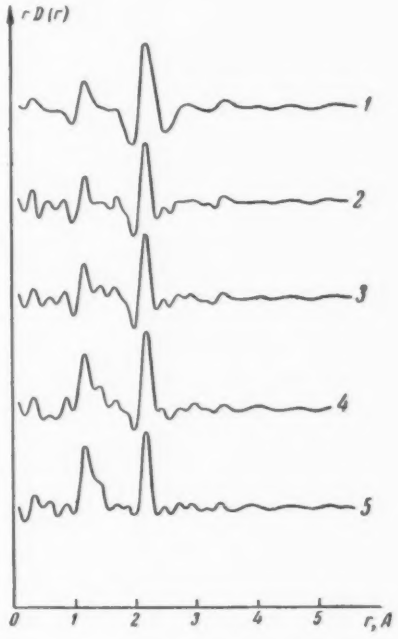

Fig. 2. Radial distribution curves for the nitric acid molecule.

constructed (Fig. 1), and five rD(r) curves were computed (Fig. 2). In the calculation of curves 1 and 2 (Fig. 2), with and without the temperature factor respectively, no extrapolation of the experimental curves for I(s) to the point s = 0 was carried out. The two peaks in curve 1 for the molecule $H-O'-N\lessgtr^{O}_{O}$ may be attributed to the following distances: r(N = O) = 1.21 A, and r(O. . .O, O. . .O') = 2.22 A. In curve 2, in addition to the peaks at 1.20 A and 2.21 A, a weak maximum is found at 1.46 A, close to the expected value of r(N—O), the interpretation of which cannot be given unequivocally on account of the presence of considerable overlapping. Thus, we have obtained from curves 1 and 2 the following values: r(N = O) = 1.20 A, and r(O. . .O, O. . .O') = 2.21 A. The values of the parameters r(N—O) and ∠ONO were made more precise by the selection of theoretical

curves: in doing this the parameter r(N–O) was varied by units of 0.02 A within the range 1.36 A - 1.46 A, and the parameter ∠ ONO by units of 5° within the range 120° to 140° (Table 2 and Fig. 1, on the latter of which only a portion of the curves is depicted). Curve 5a shows the best agreement with the experimental one, though somewhat displaced towards the s axis. Curve 5b was calculated for the same parameters as curve 5a, multiplied by a factor of 1.017 (Table 1). In all the theoretical curves for I(s) (Fig. 1), some lack of correspondence is observed between the inner section and the theoretical curve. The inner part of theoretical curve 5b (shown in broken line) calculated taking into account the form factor [9] is in considerably better correspondence with the experimental curve; in this case the difference in the heights of the third and fourth maxima may be attributed to errors in the visual estimation of intensity. In order to elucidate the part played by errors in the estimation of intensity in this region of the I(s) curve, the rD(r) curves 3, 4 and 5 (Fig. 2) have been calculated, with the extrapolation of the experimental I(s) curve to zero according to the theoretical curve 5b (Fig. 1), taking values of s equal to 5, 7.5 and 10 A^{-1} respectively. Curves 3 to 5 of Fig. 2 then show that inaccuracies in the estimation of intensity of dispersion in the region where s is not greater than 7 A^{-1} make it impossible to obtain sufficient resolution of the peak corresponding to the distance r(N–O).

As a result of interpretations of the curves carried out by the two methods, the following values have been obtained for the geometrical parameters of the planar molecule H–O'–N$\begin{matrix}O\\O\end{matrix}$:

$$r(N=O) = 1{,}22 \pm 0{,}01\,A \qquad r(N-O) = 1{,}40 \pm 0{,}01\,A$$
$$\angle ONO = 135 \pm 2{,}5^\circ \qquad r(O\ldots O) = 2{,}25 \pm 0{,}02\,A.$$
$$r(O\ldots O') = 2{,}19 \pm 0{,}02\,A$$

The position of the hydrogen atom has not been determined. We may note that any deviation of the NO_3 group from planarity would not be detected if it were less than 5°. The parameters for the nitric acid molecule which we have obtained are close to those published in [2].

Nitric anhydride. Seven series of electronograms have been obtained for nitric anhydride in the vapor phase, possessing a similar distribution of intensity to those given by nitric acid vapor (though there was a considerable difference in the shape of the experimental I(s) curves in relation to the fifth and sixth maxima). From the values of s and I(s) for the maxima and minima (with the exclusion of the somewhat unreliable values in the region where s is greater than 27 A^{-1}), the experimental intensity curve has been constructed (Table 1, Fig. 3), and three rD(r) curves have been calculated (Fig. 4). In curve 1 of Fig. 4, obtained from the extrapolation of the experimental I(s) curve from s = 0 to s = 3 by means of the theoretical curve 5b of Fig. 1, five peaks are observed. These are: (a) 1.22 A; (b) nonresolved 1.45-1.46 A; (c) 2.22 A; (d) 2.77 A; and (e) 3.57 A. In curve 2 of Fig. 4, which was calculated without taking the temperature factor into account and without extrapolating the experimental I(s) curve to s = 0, the first (1.22 A) and second (1.46 A) peaks are well resolved; the position of the remaining peaks is unchanged. Curve 3 has been calculated for the difference in intensity between the experimental I(s) curve and the theoretical curve for the nitric anhydride molecule, using only the parameters r(N=O) = 1.22 A and r(O...O, O...O') = 2.22 A. The arrangement of the observed peaks in curve 3 according to the values of r (A) is thus: 1.42, 2.22, 2.77 and 3.60, but it has not been possible to isolate the peak corresponding to r(N–O). Thus, from the rD(r) curves five fundamental distances have been obtained, and have been given the following interpretation in connection with the molecule $\begin{matrix}O\\O\end{matrix}\!\!>\!N-O'-N\!<\!\!\begin{matrix}O\\O\end{matrix}$:

1) $r(N=O) = 1{,}22\,A$
2) $r(N-O) = 1{,}46\,A$
3) $r(O\ldots O,\ O\ldots O',\ N\ldots N) = 2{,}22\,A$
4) $r(N\ldots O,\ O\ldots O) = 2{,}77\,A$
5) $r(O\ldots O) = 3{,}57 - 3{,}60\,A.$

We may note that a possible model for the nitric anhydride molecule may be the bipyramidal model with symmetry D_{3h}. The bipyramidal model may be rejected, however, since: (1) if it were correct, the number of N–O and N=O bonds would not correspond to the height of the maxima on the rD(r) curves; (2) if it is assumed that r(N=O) = 1.22 A and r(N–O) = 1.47 A when r(O...O) = 2.22 A, it is in general impossible to construct a bipyramid; (3) the theoretical I(s) curve 12 (Fig. 3) for a bipyramid is not in agreement with the experimental curve. The "petal shaped" model for nitric anhydride (Fig. 5), which corresponds to the classical structural formula presented

above, can be described by means of five parameters: r (N=O), r (N−O), ∠NO'N, ∠ONO, and the angle of inclination of the two NO_2 groups around the O'−N bond. The curves for rD(r) (Fig. 4) make it possible to determine three of these parameters unequivocally as r(N=O) = 1.22 A; r(N−O) = 1.46 A, and the angle of inclination between the two NO_2 groups, corresponding to a nonplanar configuration with symmetry C_{2v} (Fig. 5); for the parameters indicated, r(N=O) and r(N–O), the magnitude of r(O...O, O...O', N...N) = 2.22 A limits the possible values for the angle ∠ONO as lying between 120° and 150°. The parameters ∠NO'N and ∠ONO have been determined by the selection of theoretical curves (Table 2, Fig. 3); in performing calculations on the basis of equation (2), it was taken that b_{ij} = = 0 for r(N=O), r (N–O), r(O...O') and r(O...O); b_{ij} = 0.001 for r(N...N); b_{ij} = 0.002 for r(N...O) and r($O_{(1)}$ ...$O_{(4)}$); and b_{ij} = = 0.003 for r($O_{(1)}$ ...$O_{(3)}$). The best agreement with the experimental curve was obtained for curve 3 (Table 1, Fig. 3). The variability of ∠ONO and ∠NO'N was determined by their mean value and the mean deviation as: ∠ONO = 134° ± 5°, and ∠NO'N = 95° ± 3°. Since the rD(r) curves reveal an increase in the value of r(N–O) in nitric anhydride compared with that in nitric acid, we have achieved an additional check on the accuracy of this parameter. Computation of the I(s) curves for r(N–O) for values of 1.41 A and 1.43 A, for ∠ONO for values of 130°, 135° and 140°, and for ∠NO'N for values of 92°, 95° and 98° has produced only a deterioration in the correlation between the relevant curves and the experimental curve in comparison with the agreement already obtained in curve 3. (The curves are not shown on Fig. 3 but the best of them approximates to curve 11 on that figure). As a result of these investigations, the following values have been obtained for the values of the parameters of the nitric anhydride molecule (Fig. 5):

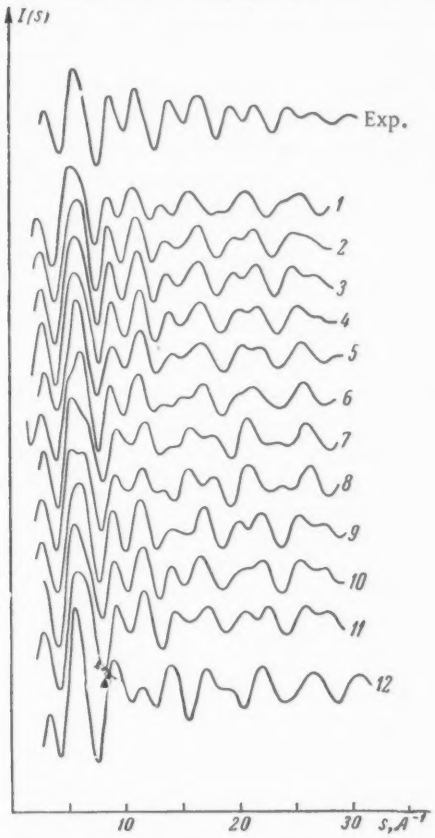

Fig. 3. Experimental and theoretical intensity curves for the nitric anhydride molecule.

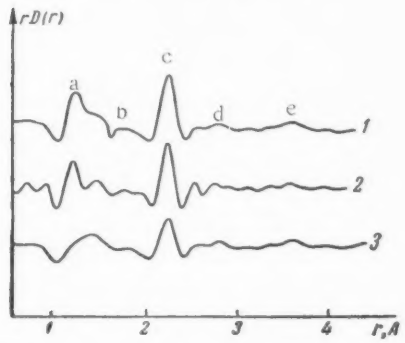

Fig. 4. Radial distribution curves for the nitric anhydride molecule.

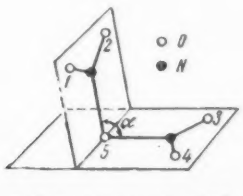

Fig. 5. Model of the nitric anhydride molecule.

$r(N=O) = 1{,}21 \pm 0{,}01$ A $\quad r(N-O) = 1{,}46 \pm 1{,}02$ A
$\angle ONO = 134 \pm 5°$,

angle between planes of NO_2 groups, α = 95° ± 3°;

$r(O...O) = 2{,}24$A $\quad r(N...O) = 2{,}76$ A
$r(O...O') = 2{,}23$ A $\quad r(O_{(1)}...O_{(4)}) = 2{,}85$ A
$r(N...N) = 2{,}15$ A $\quad r(O_{(1)}...O_{(3)}) = 3{,}62$ A.

DISCUSSION OF RESULTS

As a result of our investigations, we have obtained precise values for the geometrical parameters of the nitric acid molecule, and new data for the configuration and geometrical parameters of the nitric anhydride molecule, both in the vapor phase.

In distinction from the plane, triangular ions NO_3^-, with equal interatomic distances, which exist in the crystalline structure, "gaseous" molecules of nitric acid and nitric anhydride have markedly different values for the nitrogen-oxygen distances, whose disposition (if we give them the provisional designations N–O and N=O) correspond to the classical structure formula.

The parameters for the nitric acid and nitric anhydride molecule obtained in the course of the current work are in agreement with the data in the literature for similar molecules. Thus, the length of the N=O bond has been found to have the values: 1.22 A in nitromethane and tetranitromethane [1]; 1.202 A in nitrosyl chloride [10]; 1.180 A in dinitrogen tetroxide [11], as compared with the values of 1.22 A ± 0.01 A and 1.21 A ± 0.01 A in the molecules of nitric acid and nitric anhydride respectively found in this work. The size of the angle ∠ONO in the NO_2 groups of the nitric acid molecule (135°) and the nitric anhydride molecule (134°) is practically the same as those found for nitromethane (135°), nitrosyl chloride (134°), dinitrogen tetroxide (134°) and others. The angle NO'N in the nitric anhydride molecule (95° ± 3°) is rather less than the valence angle of the oxygen in the water molecule (104.45°) [1]. In the nitric anhydride molecule of the configuration discovered (Fig. 5), there can be no appreciable steric hindrance, since the distances between the oxygen atoms not united by valence bond, $O_{(1)}...O_{(4)}$ and $O_{(2)}...O_{(3)}$ are equal to 2.85 A, which is rather larger than twice the intermolecular oxygen radius (≈ 2.80 A).

It should be noted that, although the molecules of nitric acid and nitric anhydride have practically identical values of the parameters r(N=O) and ∠ONO, there is a considerable difference between the lengths of the N–O bonds in these molecules (1.40 and 1.46 A respectively).

In earlier work on the structure of the molecules of perchloric acid and its anhydride [12] a considerable difference was observed between the lengths of the single bonded Cl–O in the molecule of the acid $HClO_4$ (1.64 A) and in that of Cl_2O_7 (1.73A). The increased length of the N–O and Cl–O bonds in the anhydride molecules may be explained by the relatively large (compared with the molecules of the acids HNO_3 and $HClO_4$) reduction of the electronic density in the single bonds under the influence of the strongly electronegative pair of NO_2 or ClO_3 groups respectively.

In the light of this comparison, it may be a matter of great interest to compare the lengths of the N–O and Cl–O bonds in "gaseous" molecules for the acids and their salts; it is to be regretted, however, that no data are to be found in the literature on the geometrical parameters of nitrate or perchlorate salts in the gas phase.

A comparison of the results of electronographic investigations of the geometry of "gaseous" molecules of the higher oxides of the elements of the first, third, fifth and seventh groups of the periodic system - Li_2O [13], B_2O_3 [14], N_2O_5 and Cl_2O_7 [12] - permits of the drawing of general conclusions concerning the regularities of their structures. The molecules of these oxides are constructed according to a single type - that is, from atoms (or groups of atoms) combined to a central oxygen atom, the valence angle of which determines the angular configuration of their molecules. A very high degree of symmetry (such as would be found, for example, in the bipyramidal type and others) is not found in the "gaseous" molecules of these oxides, apparently because of steric hindrance, which makes the bi-tetrahedral structure unstable. It may be mentioned in this connection that in such dimeric oxide molecules as P_4O_6 and P_4O_{10} and others, four- and six-membered bicyclic systems are also not formed.

According to an approximate quantum-mechanical picture, structures containing quinquevalent nitrogen are somewhat improbable, on account of the large energy of the transfer $2s^22p^3 \rightarrow 2s2p^23s$, and the more probable structures possess quadrivalent orientation of the nitrogen; this treatment assumes the equalization of the double and donor-acceptor bonds, with the formation of two equivalent N⋯O bonds, while one single N – O bond is preserved:

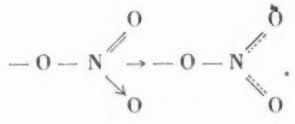

On this basis, it should be noted that any attempt (such, for example, as that made in [15]) to present the length of the N⋯O bonds in the nitrogroups as a mean of the values of r(N=O) and r(N→O) is quite arbitrary, since there is no standard length for the N=O bond, which may vary from 1.14 A in molecules of the type O=N–X (where X is a halogen atom) [1], to 1.22 A in CH_3–O–N=O [1], and similarly there is no standard length for the donor-acceptor bond N→O, which may vary from 1.188 A in the molecule N≡N→O [1] to 1.36 A in the molecule $(CH_3)_3N \rightarrow O$ [1].

SUMMARY

1. An electronographic investigation has been carried out on the structures of molecules of nitric acid and its anhydride in the vapor state. The planar configuration of nitric acid has been confirmed, and its geometrical parameters have been determined more precisely. Here for the first time values have been given for the geometrical parameters and configuration of molecules of nitric anhydride.

2. Certain peculiarities in the structures of the molecules investigated have been discussed.

LITERATURE CITED

1. Sutton, Tables of Interatomic Distances and Configurations in Molecules and Ions (The Chemical Society, London, 1958).
2. L.R. Maxwell and V.M. Mosley, J. Chem. Phys. 8, 738 (1940).
3. D.I. Millen and J.K. Morton, Chem. and Ind. 36, 954 (1956).
4. L.R. Maxwell, V.M. Mosley, and L.S. Deming, J. Chem. Phys. 2, 331 (1944).
5. A.A. Zinov'ev, Zhur. Neorg. Khim. 3, 1205 (1958).
6. G. Brauer, Handbook of Preparative Inorganic Chemistry [in Russian](IL, Moscow, 1956).
7. A.V. Frost, P.A. Akishin, L.V. Gurvich, G.A. Kurkchi, and A.A. Konstantinov, Vestn. Mosk. Universiteta 12, 85 (1953).
8. J. Karle and I. Karle, J. Chem. Phys. 17, 1052 (1949).
9. H. Virvoll and O. Ogrim, Acta crystallogr. 2, 277 (1949).
10. D.I. Millen and K.M. Sinnott, J. Chem. Soc., 350 (1958).
11. D.W. Smith and K. Hedberg, J. Chem. Phys. 25, 282 (1956).
12. P.A. Akishin, L.V. Vilkov, and V.Ya. Rosolovskii, Kristallographiya 4, 353 (1959).
13. P.A. Akishin and N.G. Rambidi, Doklady Akad. Nauk SSSR 118, 973 (1958).*
14. P.A. Akishin and V.P. Spiridonov, Doklady Akad. Nauk SSSR 131, 557 (1960).*
15. T.N. Temnikova, The Theoretical Basis of Organic Chemistry [in Russian] (Goskhimizdat, Moscow, 1959).

* Original Russian pagination. See C.B. translation.

THE INFLUENCE OF IONS ON THE STRUCTURE OF WATER

I.G. Mikhailov and Yu.P. Syrnikov

A.A. Zhdanov Leningrad State University and S.M. Kirov
Leningrad Wood Technology Institute
Translated from Zhurnal Strukturnoi Khimii, Vol. 1, No. 1, pp. 12-27,
May-June, 1960

A model has been suggested for describing the influence of ions on the structure of the "free" water in a solution. According to this model, the electrostatic field of the ions displaces the thermodynamic equilibrium between the structures coexisting in the water towards a more close-packed structure. The proposed model has been used to calculate the relationship between the temperature of the maximum density of a solution and its concentration.

INTRODUCTION

The question of the influence of a dissolved substance on a solvent is one of the most important problems in the theory of solutions. The interaction between a solvent and the dissolved substance is usually taken into account by introducing the concept of solvation, or, in the case of aqueous electrolyte solutions, of ion hydration. It should be noted that there is no accepted single definition of the term solvation. Some authors understand by this term the total sum of the changes produced by the introduction of the ions of an electrolyte into a solution [1] (with the exception of the interaction between the ions themselves). Other authors regard solvation merely as the interaction between an ion and the solvent molecules nearest to it.

According to Bockris [2], the concept of hydration includes the total sum of the changes produced by the introduction of the ions into the solution, but can be divided into two parts—primary and secondary hydration.

Samoilov [3] suggests that these two parts be referred to as "short-range hydration" and "long-range hydration". We shall subsequently use the term "hydration" to mean only short-range hydration. In the study of the hydration of ions in solution, this phenomenon is normally understood to mean that a definite number of water molecules are firmly held by the ions. There are a number of methods for determining hydration numbers, and the hydration numbers of ions, determined by different methods, may differ considerably [4].

Analysis of modern data on hydration [3] shows that these differences are due primarily to the fact that the true interaction between the ions and the water molecules, and the influence of this interaction on the properties of the water in the solution, are replaced by the idea that a given effective number of water molecules are firmly held by the ion. It is quite natural that in order to explain different properties, it is necessary to ascribe different hydration numbers to the same ion. Samoilov [3] has shown that, in the light of modern data, particularly data on spontaneous diffusion in ionic solutions [5], the idea that molecules are firmly held by ions is unsatisfactory and should be reexamined. He suggested that short-range hydration should be regarded as the action of ions on the thermal, and particularly on the translational, movement of the nearest water molecules in the solution. The actual numbers of water molecules closest to the ion—the coordination numbers of the ions in solution—are taken as the so-called hydration numbers. The values for these numbers for a series of monatomic ions, estimated from data on the heats of dissolution of salts in solutions of the acids, are found to be close to 4, i.e., close to the coordination numbers for water molecules themselves in the solution. Thus, the ions, as it were, replace the water molecules. The ions distort the structure of the water, and this is to a considerable extent due

to the difference between the interaction of ions and water molecules on the one hand and the interaction of the water molecules themselves on the other. This difference is most marked for the cation. The water molecules turn their electronegative oxygen atoms towards the cation and the bond which is produced is essentially different in character from the hydrogen bond, which joins the water molecules to one another.

The water molecule turns its proton towards the anion and the nature of the interaction between the anion and the water molecules is similar to that of the hydrogen bond [6, 7], i.e., the bond between the anion and the water molecules is similar in character to that between the water molecules themselves.

The total effect of the distortion of the water structure in the closest coordination sphere can be divided into three components. According to Samoilov [3], the distortion of water by ions when a solution is formed is related firstly to the appearance, in the water, of particles whose radius differs from that of the water molecules; secondly, to a possible difference between the coordination numbers of the ion and the water molecule; and thirdly, to reorientation of the water molecules closest to the ion. "Short-range hydration", in fact, is merely the more or less powerful interaction between the ion and the nearest water molecules; in dilute solutions the number of such molecules is determined by the structure of the water. This interaction affects primarily the translational movement of the water molecules nearest to the ion.

As far as the influence of ions on the structure of the water in the first coordination sphere of the ion is concerned, there is a very great amount of evidence which indicates that the structural changes in the water go far beyond simple polarization under the action of the electrostatic field of the ions. Thus, Bernal and Fowler, in their classical work [8] devoted to the structure of water in ionic solutions, analyzed the experimental data and concluded that a number of ions bring about a change in the structure of water in the direction: structures I→II→III, i.e., a repacking of the water molecules in the direction: ice-like (I)→quartz-like (II)→close-packed (III) structures. Bernal and Fowler introduced the concept of "structural temperature", defined as the temperature at which pure water has the same internal structure and the same viscosity as the water in the solution under study. They considered that some ions increase the structural temperature, while other ions decrease it. Bernal and Fowler did not, however, ascribe any exact physical significance to the concept of "change in structural temperature" and indicated that the problem of the influence of ions on the structure of water required detailed theoretical development.

In their work on the study of the temperature coefficient of the heats of dissolution of electrolytes, Kaganovich and Mishchenko [9] concluded that the change in the heat of dissolution with change in temperature depends to a great extent on the fraction of the energetic effect associated with the change in the structure of the solvent under the influence of the ions. In their work it was noted that a dissolved electrolyte changes the structure of the water in the direction of the changes I→II→III (in the sense of the Bernal–Fowler model).

Frank and Evans [10], who studied the entropy of aqueous electrolyte solutions, and Stewart [11, 12], also concluded that the change in the structure of water extends far beyond the limits of the first coordination sphere. The study of the action of ions on the properties of colloids [13] also shows that the effect of the ions changes the quasi-crystalline structure of the water.

Analogous conclusions were reached in the study of the optical properties of solutions [14, 15]. X-ray data [16] confirm the change in the structure of water in the direction I→II→III (in the sense of the Bernal–Fowler model), and this change in the structure cannot be explained merely by the repacking of the water molecules in direct proximity to the ion. The process is much more extensive and in fact extends throughout the whole volume of the solvent.

In addition, there are effects such as, for example, the change in the temperature of the maximum density of a solution with change in its concentration, which can be explained only if account is taken of the influence of ions on the structure of all the water in the solution.

In the present work, particular attention is paid to the question of the influence of ions on the structure of the water beyond the first coordination sphere, i.e., the problems of "long-range hydration" are considered. The examination is based on the two-structure model of water.

1. The Two-Structure Model of Water and Its Physical Basis

The anomalous properties of water are often attributed to association of the water molecules to form complexes, and the concept of the degree of association is introduced. This concept is also applicable to a number of other liquids, however, although these liquids do not show the anomalies characteristic of water. It is evident that association alone cannot explain the properties of water, and here we shall deal with the deeper structural differences between water and other liquids.

The structure of ice and the structure of water are produced by the formation of hydrogen bonds between the molecules [17, 18]. X-ray diffraction data show that the oxygen nuclei are arranged in the structure of ice in the same way as the atoms of silicon in the tridymite structure [19]. Each H_2O molecule is surrounded by four nearest molecules. There are a number of theories regarding the structure of water, and these have been reviewed in [3]. All the modern theories on the structure of water can be divided into two groups. One group of theories [20] regards water as a mixtures of polymers of the type $(H_2O)_n$. The other group consists of theories which regard water as a mixture of certain three-dimensional structures. The theories of the latter group provide a much better explanation of the properties of water and are to be preferred. The classical theory of this group is that of Bernal and Fowler [8], which is based on x-ray diffraction data and the spectroscopic model of the water molecule. All subsequent theories of this kind are based on the theory of Bernal and Fowler, and merely introduce certain corrections. They regard water as a structure with four-fold coordination and suggest that there exist three forms of arrangement of the water molecules at different temperatures, namely: 1) the ice–tridymite type (with four-fold coordination), which predominates at low temperatures; 2) the quartz type (with four-fold coordination) which predominates between approximately 4° and 200°; and 3) the ammonia type–a close-packed structure which predominates between 200° and 300°.

These forms are not rigorously separated and are converted continuously into one another.

Bernal and Fowler based their theory on x-ray diffraction data, which give merely the relative arrangement of the oxygen atoms. These authors therefore assumed that there are two protons next to each oxygen atom, i.e., that it is possible to speak of separate H_2O molecules in liquid water. Recent studies on neutron diffraction of heavy ice [21] show, however, that one cannot speak of a separate molecule in ice, since the proton does not belong to any definite oxygen atom, but spends equal amounts of time next to the two nearest oxygen atoms. Since the energies of the intermolecular interactions in ice and in liquid water are similar, it may be assumed that the arrangement of the protons is the same in liquid water. Thus, water must be regarded as a particular type of "associated" liquid [22], in which the association penetrates through the whole volume of the liquid, forming a three-dimensional network, and that several configurations of this network can co-exist simultaneously. Each of the co-existing configurations corresponds to a characteristic free energy, dielectric properties, molecular volume, etc. Change in temperature leads to a change in the relative number of molecules associated in each configuration, and this explains the anomalous properties of water. There are a number of works which show that this picture provides a reasonable explanation for the anomalous properties of water. There is no single theory regarding the type and number of coexisting configurations. A number of authors, following Bernal and Fowler, consider that water shows three types of configuration–ice-like, quartz-like, and ammonia-like; others consider that at moderate temperatures it is sufficient to take account of only two configurations. Two- structure models of this type were developed by Hall [23] and by Grjotheim and Krogh-Moe [24]. These authors suggest that rupture of the hydrogen bond must take place when the molecule changes from one structure to another.

Pople [18] proposed another model, according to which the hydrogen bonds become "flexible" when ice melts. The rearrangement of the structure of water with change in temperature takes place as a result of "bending" of the hydrogen bonds*. Pople regards the bending of hydrogen bonds as the production of a finite angle between the line joining the centers of neighboring molecules and the O–H direction of one of these molecules. Pople denies the existence of broken hydrogen bonds in water, and this, generally speaking, is in agreement with

* It is of interest to note that Descartes attributed the anomalies of water to the flexibility of its "particles", and assumed that when water is frozen its "particles" lose their flexibility, so that ice has a "looser packing", and occupies a greater volume, than the water from which it is produced [see Rene Descartes, Discourse on Method and Its Applications, Dioptrics, Meteors, and Geometry [Russian translation] (Izd. AN SSSR, 1953) p. 195].

spectroscopic data, which do not indicate the presence, in water, of any O—H groups which are not present in hydrogen bonds. Certain other data, however, particularly data on spontaneous diffusion [3], require for their explanation the presence in water of at least a small number of broken hydrogen bonds.

The first and most precisely formulated two-structure model of water is that of Hall. Hall used his model to calculate the absorption coefficient of ultrasonic waves in water. According to Hall, two structures exist together in water—one of these is ice-like, with tetrahedral coordination, and the other is close packed. The first state is characterized by a large molar volume V_1 and small thermodynamic potential Φ_1; the second state is characterized by a small molar volume V_2 and high thermodynamic potential Φ_2. Conversion from one structure to another involves the surmounting of a certain potential barrier, and is accompanied by the rupture of hydrogen bonds. The number of molecules in the first and second structure is determined by the Boltzmann distribution law

$$\frac{n_2}{n_1} = e^{-\Delta\Phi/RT}, \qquad (1)$$

where $\Delta\Phi = \Phi_2 - \Phi_1$, Φ_1 is the thermodynamic potential of the first structure (calculated for 1 mole), and Φ_2 is the same for the second structure.

Hall found numerical values for $\Delta\Phi$ and the difference between the molar volumes of the two structures $\Delta V = V_1 - V_2$.

The value of ΔV is calculated as follows: V_1 is taken as approximately equal to the molar volume of ice, and V_2 is taken as the molar volume calculated on the assumption that the H_2O molecules are close-packed in the second state. The calculations give for ΔV the value ~ 8 cm^3; in order to obtain values for the sound absorption coefficient agreeing with the experimental data, it is necessary to assume for $\Delta\Phi$ the value 500 cal/ /mole.

The model proposed by Hall differs considerably from the model of Bernal and Fowler. According to these authors, the quartz-like structure predominates at moderate temperatures, and the close-packed structure is characteristic only of high temperatures. The theory of the quartz-like structure was introduced by Bernal and Fowler to explain the decrease in volume on melting. They point out that a natural assumption following from analysis of the x-ray data is that the structure of water is an irregular version of the structure of ice. This suggestion was rejected by Bernal and Fowler, however, since they considered that there must necessarily be an increase in volume on going from an ordered structure to a less ordered structure. Such an increase does not always take place, however, and when the density of the arrangement of atoms in a solid is sufficiently low, i.e., when the structure is sufficiently open, the density may increase when the disorder increases [3]. On the other hand, the existence of a quartz-like structure in water is not confirmed by examination of modern x-ray diffraction data [3, 18].

The most complete analysis of the data relating to the structure of water has been given by Samoilov [3], who reached the conclusion that the structure of water is a slightly distorted version of the structure of ice, retaining, in general, four-fold coordination, with a certain number of water molecules situated between the lattice sites of this structure. Let us examine this idea of Samoilov's [3] in more detail. The structure of ice is extremely open: it has many open spaces, whose dimensions are even greater than the dimensions of the molecules. Every open space of this type is bounded by six water molecules at a distance of 2.94 A from its center. Around each water molecule in the ice structure there are six open space centers at a distance of 3.47 A. The water molecules which have moved from their equilibrium positions (as a result of the translational movement which becomes possible on fusion) cannot help entering the neighboring open spaces in the structure. Certain relative potential energy minima correspond to these open spaces. At a given moment, a definite quantity of molecules are situated in the open spaces of the structure.

Thus, the idea, introduced by Samoilov, that the open spaces of the structure are filled by molecules undergoing translational movement in fact forms the physical foundation for the second close-packed structure postulated by Hall.

The ideas which have been developed enable us to understand the reason for the difference between water and all other liquids. When ordinary liquids undergo fusion, the order which previously existed is broken down

and a certain quantity of holes appear in the structure; this explains, for example the increase in the volume on fusion, the fluidity of the liquid, etc. When water undergoes fusion, the long-range order also breaks down, chiefly as a result of the flexibility produced in the hydrogen bonds [18], but the formation of holes (in the sense in which this term is used in the theory of liquids) evidently plays almost no part in the process. In fact, the rupture of several hydrogen bonds is necessary in order to form a hole. The energy of one hydrogen bond in water is approximately 5 kcal/mole, so that the energy of hole-formation is excessively high. Estimation of the relative number of such holes, even if it is assumed that only two hydrogen bonds are broken during the formation of a hole, gives a value of approximately 10^{-6}—10^{-7}. The hole which is produced as a result of the removal of a water molecule is immediately "healed" and the molecule which has moved enters the space between the lattice sites, where it may spend some time, so that, as pointed out earlier [3], the presence of an "extra" molecule in the center of an open space in the structure corresponds to a comparatively small breakdown of the neighboring regions of the structure. It may be stated that in water there exists something similar to a "Frenkel' defect" in the crystal [25], but without a vacant site. The change in volume when ice melts, and also the spontaneous diffusion, can be attributed to these "extra" molecules in the open spaces in the structure. When a water molecule enters the space between the lattice sites, a certain number (which is evidently small) of hydrogen bonds must be "broken". If we accept Pople's suggestion [18] that the bonds merely bend, and that there are no "broken" hydrogen bonds in water, we find that a number of the properties of water, related primarily to translational movement (spontaneous diffusion, for example), become understandable. According to Samoilov [3], the water molecules which enter the open spaces are energetically not equivalent to the molecules in the lattice sites, and are to a certain extent free from bonds with neighboring molecules (the bond orientation for molecules in the spaces between the lattice sites is evidently shown to a much smaller extent). At the same time the clearly-defined directional character of the bonds formed by the water molecules occupying the lattice sites hinders the thermal, and particularly the rotational, movement of these molecules. As Samoilov has pointed out [3], the sharp increase in the heat capacity when ice melts is possibly related to the transfer of molecules to the spaces between the lattice sites, where they acquire a greater rotational freedom that in the lattice sites. Thus in water there exist regions with four-fold coordination and regions with coordination greater than 4, i.e., regions of closer packing, in accordance with Hall's model.

Hall considered that the state with the closer packing exhibits a higher thermodynamic potential than the ice-like structure. In [26] it was suggested that the ice-like structure possibly had the greater thermodynamic potential. The authors of [26] reached this conclusion from a study of the relationship between the absorption of ultrasonic waves in water and the pressure and from a comparison of the relationship given by the Hall theory with that obtained experimentally. They assumed that the change in absorption was due only to the change in $\Delta\Phi$ with change in pressure.

As shown in [27], however, the change in the bulk viscosity with change in pressure is due primarily to the change in the energy of activation of the transfer of a molecule from one structure to another with change in pressure, and this possibility was not considered in [26]. Thus the assumption that the ice-like structure has the higher free energy, made by the authors of [26], cannot be regarded as justified. The authors of this work themselves point out that the assumption contradicts all modern theories regarding the structure of water.

In all subsequent calculations, the thermodynamic potential of the second, more close-packed structure will be assumed to be greater than the thermodynamic potential of the ice-like structure.

2. The Influence of Ions on the Structure of the "Free" Water

It was pointed out in Section 1 that the influence of ions on the structure of water is not limited to short-range hydration, but extends throughout the whole bulk of the water. In this section we shall examine a model describing the influence of ions on the structure of the water which is not present in the hydration sheath of the ions, or, in other words, the influence of ions on the structure of the "free" water.

In a solution, the total bulk of the water lies in the strong electrostatic field of the ions. The thermodynamic potential of the water is altered, and the changes are different in the different structures, since it is to be expected that the dielectric characteristics of the different structures are not the same. This leads to a displacement of the equilibrium between the two structures existing together in the water.

The first attempt to examine quantitatively the influence of the displacement of the equilibrium between the two structures on the dielectric constant of the solution was made by Samoilovich and Goryunov [28]. This

work was based, however, on theories, now discarded, which regarded the structure of water as a mixture of monohydrol, dihydrol and trihydrol. At the same time their calculations were applicable only to solutions at infinite dilution.

A rigorous solution of the problem of the influence of ions on the structure of water, applicable over a wide concentration range, is hardly possible at the present time. Even approximate calculations of this kind are extremely difficult. We have,therefore,to construct a model which is sufficiently simple to permit some sort of quantitative calculation, but which nevertheless reflects the most characteristic features of the phenomenon.

We shall assume, like Hall, that the Boltzmann distribution law is applicable to the "mixture" of the two structures, i.e., that the ratio between the numbers of molecules associated in the first and second structures is given by formula (1).

Let us find the numbers of molecules n_1 and n_2 in each of the structures in 1 mole of water, assuming that the total number of molecules $n_1 + n_2 = N$ is equal to Avogadro's number:

$$n_2 = n_1 e^{-\Delta\Phi/RT}; \quad n_1 = (N - n_2).$$

From this we have

$$n_2 = \frac{Ne^{-\Delta\Phi/RT}}{1+e^{-\Delta\Phi/RT}}; \quad n_1 = \frac{N}{1+e^{-\Delta\Phi/RT}}. \tag{2}$$

A number of changes take place when ions dissolve in water. Firstly, a certain quantity of water molecules take part in a direct interaction with the ions (short-range hydration). Secondly, structural changes take place in the remaining fraction of the water under the influence of the ionic field, and this involves primarily a displacement of the equilibrium between the ice-like and close-packed structures. This displacement should take place as a result of the fact that the thermodynamic potentials will change to different extents in the different structures. There should, in fact, be differences between the polarizability of the ice-like structure, where each molecule is bound to the others by directed hydrogen bonds, and the polarizability of the close-packed structure, in which, as pointed out above, the directional properties of the bonds are much less marked. This difference in the polarizability evidently affects primarily the orientational fraction of the polarizability.

For the complete calculation of this effect, it is necessary to know the magnitude of the change in the thermodynamic potential for each of the structures, as a function of the intensity of the field created by the ions, and the magnitude of this intensity as a function of concentration. Detailed calculation of this kind is extremely difficult, but it can be simplified considerably by making a number of assumptions. It must first of all be noted that it is necessary for us to know only the change in the free energy difference between the two structures. In addition, the approximation should be that which best corresponds to the case of strong fields (i.e., "closer" to strong fields than to weak), since the intensities of the fields created by the ions in the solutions are extremely high—of the order of 10^5–10^6 v/cm.

Semenchenko [29] has shown that for systems with no phase changes, the relationship

$$F = F_{id} + \bar{U}, \tag{3}$$

where F is the free energy of the real system, F_{id} is the free energy of the ideal system, and $\bar{U}$ is the average potential energy of the molecules, holds fairly satisfactorily.

Since, however,

$$\Phi = F + pV,$$

a similar relationship can also be written for the thermodynamic potential.

Thus, if the system is situated in an external field, we may write

$$\Phi_{\text{excit}} \simeq \Phi_0 + \bar{U}, \tag{4}$$

where Φ_0 is the thermodynamic potential of the unexcited system, and $\bar{U}$ is the average potential energy resulting from the presence of the external field.

Let $\bar{U}_1$ be the supplementary average potential energy, produced by the presence of the external field, of the water molecules entering the first structure, and let $\bar{U}_2$ be the same for the second structure. The thermodynamic potential of the first structure in the electric field is then

$$\Phi_1 = \Phi_1^0 + \bar{U}_1 \tag{5}$$

and for the second structure:

$$\Phi_2 = \Phi_2^0 + \bar{U}_2, \tag{6}$$

where Φ_1^0 and Φ_2^0 are the thermodynamic potentials of the first and second structures respectively, in the absence of an external field.

The difference in the thermodynamic potentials of the two structures when an ionic field is present is

$$\Delta\Phi = \Delta\Phi_0 + \Delta\bar{U}, \tag{7}$$

where

$$\Delta\bar{U} = (\bar{U}_2 - \bar{U}_1) \text{ and } \Delta\Phi_0 = (\Phi_2^0 - \Phi_1^0). \tag{8}$$

Thus, it is necessary to know ΔU as a function of the concentration of the ions, and the appropriate calculation is an extremely complicated statistical problem. The form of the relationship between $\Delta\bar{U}$ and the concentration can, however, be found without undertaking a tedious statistical calculation.

It has already been pointed out that the orientational components of the polarizabilities of the first and second structures are different, and that the retardation of the rotation in the structure is evidently more marked than that in the first structure, since in the second structure the directional properties of the bonds are much less marked, and the molecules present in the spaces between the lattice sites have a greater individuality than the molecules in the lattice sites. This polarizability difference may be taken into account, as a first approximation, by introducing the concept of the effective dipole moment of a water molecule present in this structure. The term "effective dipole moment" is used in this case to mean the average component of the dipole moment in the direction of the field. According to what has been said above, the effective dipole moment of a water molecule in the second structure will be greater than that of a water molecule in the first structure:

$$\mu_2^{\text{eff}} > \mu_1^{\text{eff}}$$

(subsequently the superscripts "eff" will be omitted). It is known that the potential energy of a dipole in an electric field is

$$U = -\mu E$$

if the directions of the field and dipole coincide. In our case it may be assumed that the direction of the field at a given point in the solvent and the direction of the "effective dipole moment" coincide.

We then have, for the average energies of the structures in an electric field:

$$\left.\begin{aligned} \bar{U}_1 &= -N\mu_1 |\bar{E}| \\ \bar{U}_2 &= -N\mu_2 |\bar{E}| \end{aligned}\right\} \tag{9}$$

and

$$\Delta\bar{U} = -N(\mu_2 - \mu_1)|\bar{E}| \tag{10}$$

where $|\bar{E}|$ is the average value of the absolute intensity of the ionic field at a given point in the solvent. Since $\mu_2 > \mu_1$ it follows that $\Delta\bar{U} < 0$.

Thus, it is necessary, first of all, to know the relationship between $|\bar{E}|$ and the ion concentration. For this purpose it is necessary to find the distribution function for $|\bar{E}|$. If we neglect the correlation between the thermal movement of the ions and the translational thermal movement of the water molecules in the "free" water, then as a first approximation the problem becomes a Holtsmark problem [30-32]. If, however, we take the exact Holtsmark distribution, we obtain integrals which cannot be dealt with by elementary integration. Chandrasekhar [33] has shown, however, that the Holtsmark distribution is given approximately by the nearest neighbor distribution. Appreciable discrepancies between the two are observed only when $|\bar{E}| \to 0$ and even then do not have a significant influence on the results. Thus, when the magnitude of the field is determined, firstly, from the maximum probability based on the Holtsmark distribution and, secondly, from the nearest neighbor distribution, the results differ by less than 5%.

The nearest neighbor distribution law is given by the expression [34]:

$$w(r)\,dr = \exp(-4\pi r^3 n/3)\,4\pi r^2 dr, \tag{11}$$

where w(r) dr is the probability that the nearest neighbor will be found at a distance between r and r + dr from the point under consideration, and n is the number of particles in unit volume.

Since

$$|E| = \frac{q}{\varepsilon r^2}, \tag{12}$$

(where q = ze is the charge on the charge on the ion, z is the valence of the ion, and ε is the dielectric constant), then the probability that the intensity of the ion at that point will lie between $|E|$ and $|E| + d|E|$ will be given by the expression:

$$W(E)\,dE = \exp[-4\pi q^{3/2} n/3\varepsilon^{3/2}E^{3/2}]\,(2\pi q^{3/2} n/\varepsilon^{3/2}E^{5/2})\,dE. \tag{13}$$

From this, regarding the ions as point charges, we obtain for $|\bar{E}|$

$$|\bar{E}| = \frac{\int_0^\infty E\,W(E)\,dE}{\int_0^\infty W(E)\,dE}. \tag{14}$$

For salts for which the charge on the cation is equal to the charge on the anion, i.e., $z_c = z_a = z$, so that $W_c(E) = W_a(E)$, Eq. (14) becomes

$$|\bar{E}| = \frac{\int_0^\infty e^{-a/E^{3/2}} E^{-5/2}\,dE}{\int_0^\infty e^{-a/E^{3/2}} E^{-5/2}\,dE}, \tag{15}$$

where

$$a = 4\pi\,\frac{z^{3/2}e^{3/2}n}{3\varepsilon^{3/2}}. \tag{16}$$

The integral in the numerator can be reduced to

$$-\frac{2}{3}\int_0^\infty e^{-ax}\,\frac{dx}{x^{2/3}} = -{}^2/_3\,\frac{\Gamma\,(1/3)}{a^{1/3}}$$

by substituting

$$E^{3/2} = \frac{1}{x}\,.$$

By the same substitution, the integral in the denominator is reduced to

$$-\frac{2}{3}\int_0^\infty e^{-ax}\,dx = -\frac{2}{3a}\,.$$

From this we obtain for $|\vec{E}|$:

$$|\vec{E}| = \Gamma\left(\frac{1}{3}\right)a^{3/2}. \tag{17}$$

Using the expression (16) for $\underline{a}$, and the fact that $\Gamma\ (^1/_3) = 2.68$, we obtain

$$|\vec{E}| = 2{,}68\left(\frac{4\pi}{3}\right)^{3/2}\frac{ze}{\varepsilon}\,n_{\text{vol}}^{3/2}, \tag{18}$$

where n_{vol} is the number of molecules of the salt in unit volume. In a large number of cases it is more convenient to use the mole fraction of the dissolved salt, i.e., to take as the concentration the number of moles of the salt in 1 mole of water. We then have

$$n_{\text{vol}} = \frac{N}{V}\,n,$$

where N is Avogadro's number, V is the volume of one mole of water, and $\underline{n}$ is the mole fraction of the salt (the volume of the dissolved salt is neglected). Finally, we obtain for $|\vec{E}|$ the following

$$|\vec{E}| = Cn^{3/2}, \tag{19}$$

where

$$C = 2{,}68\left(\frac{4\pi}{3}\right)^{2/3}\frac{ze}{\varepsilon}\,\frac{N^{3/2}}{V^{3/2}}\,.$$

For the difference between the potential energies of the two structures in the field of the ions, we have, from expressions (10) and (19),

$$\Delta\bar{U} = -\gamma n^{3/2}, \tag{20}$$

where

$$\gamma = 2{,}68\left(\frac{4\pi}{3}\right)^{2/3}\frac{ze}{\varepsilon}\,\frac{N^{3/2}}{V^{3/2}}\,(\mu_2 - \mu_1). \tag{20a}$$

A similar expression is also obtained for a salt for which $z_c \neq z_a$, but in this case the relationship between γ and the valencies of the anion and cation is slightly different.

The difference between the thermodynamic potentials of the two structures of the water in the solution will be

$$\Delta\Phi = \Delta\Phi_0 - \gamma n^{2/3}. \tag{21}$$

Taking Eq. (1) into account, we see that, with increase in concentration, the equilibrium is shifted towards an increase in the number of molecules in the second structure. This also takes place, however, with increase in pressure and temperature. This provides justification for the well-known empirical rules: "ions act in the same way as temperature" and "ions act in the same way as pressure."

In a solution, as already pointed out, we also have short-range hydration, and the number of molecules involved in the equilibrium between the "water" structures decreases as a result of the formation of structures of a new type.

If we consider 1 mole of water in a solution, then the number of "free" molecules will be equal to N(1—Zn), where Z is the number of water molecules, per molecule of salt, which are "bound" by short-range hydration, and n is the mole fraction of the salt. The numbers of molecules present in the first and second structures will be, respectively,

$$n_1 = \frac{N(1-Zn)}{1+\exp\left(-\dfrac{\Delta\Phi_0 - \gamma n^{2/3}}{RT}\right)},$$

$$n_2 = N\frac{(1-Zn)\exp\left(-\dfrac{\Delta\Phi_0 - \gamma n^{2/3}}{RT}\right)}{1+\exp\left(-\dfrac{\Delta\Phi_0 - \gamma n^{2/3}}{RT}\right)}. \tag{22}$$

The relationships obtained can be used to calculate a number of effects, for example the change in the temperature of the maximum density of a solution with change in concentration.

3. Calculation of the Relationship Between the Temperature of the Maximum Density of Solutions and their Concentration

One of the most familar anomalies of water is the change in the density with change in temperature, which shows a maximum density at t = 4°. The existence of this maximum results from two processes which take place as the temperature is increased: 1) the ordinary process involving increase in the average intermolecular distances and leading to a decrease in the density, and 2) the process involving rearrangement of the structure towards a more close-packed arrangement, leading to an increase in the density.

It is also known that the temperature of the maximum density is displaced towards lower temperature with increase in the pressure. The temperature of the maximum density of aqueous electrolyte solutions is also displaced towards lower temperatures with increase in the concentration. It is found that this effect can be explained on the basis of the above model, which can also be used to obtain the relationship between the temperature of the minimum molar volume of the water and the pressure and concentration of ions in the solution. In the process it is assumed that at low concentrations, the presence of the ionic lattice in the solution has little influence on the temperature of the maximum density, that the main change in the temperature of the maximum density takes place as a result of the change in the structure of water under the influence of the ionic field, and that the temperature of the minimum molar volume of the water in the solution can be taken as very close to the temperature of the maximum density of the solution itself.

Subsequently, the quantities V_0, $\Delta\Phi_0$, n_1^0 and n_2^0 will be taken as relating to pure water, while the quantities V_1, $\Delta\Phi$, n_1 and n_2 will be taken as relating to the water in the solution. V_1 is the molar volume of the first structure, and V_2 the molar volume of the second structure; $\Delta V = (V_1 - V_2) > 0$, since $V_1 > V_2$. The last three quantities will be assumed to be independent of the ionic field.

The volume occupied by one mole of pure water can be expressed in terms of the volumes occupied by the water molecules in the first and second structures, as follows

$$V_0 = n_1^0 \frac{V_1}{N} + n_2^0 \frac{V_2}{N} . \tag{23}$$

Since, however,

$$n_2^0 = N - n_1^0,$$

we have

$$V_0 = V_2 + n_1^0 \frac{\Delta V}{N} ,$$

or, using formula (2), we have

$$V_0 = V_2 + \frac{\Delta V}{1 + e^{-\Delta\Phi_0/RT}} .$$

Assuming that ΔV is independent of temperature, we obtain for dV_0 / dT:

$$\frac{dV_0}{dT} = \frac{dV_2}{dT} - \frac{\Delta V \frac{\Delta\Phi_0}{RT^2} e^{-\Delta\Phi_0/RT}}{(1 + e^{-\Delta\Phi_0/RT})^2} ,$$

or, using the relationship

$$\frac{e^{-x}}{(1 + e^{-x})^2} = \frac{1}{2(1 + \operatorname{ch} x)} ;$$

we obtain

$$\frac{dV_0}{dT} = \frac{dV_2}{dT} - \frac{\Delta V \Delta\Phi_0}{2RT^2 \left(1 + \operatorname{ch} \frac{\Delta\Phi_0}{RT}\right)} . \tag{24}$$

At low temperatures (below 4°), the major part is played by the second term in the right-hand side of the equation, and the volume decreases. At temperatures above 4°, the major part is played by the term dV_2 / dT, and the volume increases with temperature. The condition for the minimum molar volume ($dV_0/dT = 0$) will be:

$$\frac{dV_2}{dT} = \frac{\Delta\Phi_0 \Delta V}{2R (T_M^0)^2 \left(1 + \operatorname{ch} \frac{\Delta\Phi_0}{RT_M^0}\right)} . \tag{25}$$

Let us derive an analogous expression for the water in a solution. The volume of one mole of water in solution will be equal to

$$V = n_1 \frac{V_1}{N} + n_2 \frac{V_2}{N} + v_{\text{hydr}}, \tag{26}$$

where v_{hydr} is the volume occupied by the water molecules which have left the equilibrium between the structures and are present in the first coordination sphere of the ions.

Using the expression (22), we obtain

$$V = \frac{(1 - Zn) V_1}{1 - e^{-\Delta\Phi/RT}} = \frac{(1 - Zn) V_2 e^{-\Delta\Phi/RT}}{1 + e^{-\Delta\Phi/RT}} + v_{hydr} = \\ = (1 - Zn)\left(V_2 + \frac{\Delta V}{1 + e^{-\Delta\Phi/RT}}\right) + v_{hydr}. \tag{27}$$

If it is assumed that Z, and hence v_{hydr}, are independent of the temperature, then in analogous fashion we obtain, for the minimum value of V, the condition:

$$\frac{dV_2}{dT} = \frac{\Delta\Phi\Delta V}{2RT_M^2\left(1 + \text{ch}\frac{\Delta\Phi}{RT_M}\right)}. \tag{28}$$

Since it can be assumed that dV_2/dT is the same for pure water and for the water in solution, we obtain the following expression for T_M – the temperature of the minimum molar volume of the water in solution – as a function of T_M^0 – the temperature of the minimum molar volume of pure water:

$$\frac{\Delta\Phi_0}{(T_M^0)^2\left(1 + \text{ch}\frac{\Delta\Phi_0}{RT_M^0}\right)} = \frac{\Delta\Phi}{T_M^2\left(1 + \text{ch}\frac{\Delta\Phi}{RT_M}\right)}. \tag{29}$$

Here $\Delta\Phi_0$ is the difference between the thermodynamic potentials of the first and second structures in pure water, and $\Delta\Phi$ is the same for the water which is penetrated by the electrostatic field of the ions, i.e., in solution.

It is quite obvious that a similar equation is also obtained for the temperature of the minimum molar volume of water under an external pressure.

Equation (29) is transcendental and cannot be solved directly. It can, however, be reduced with a good degree of approximation, to a quadratic equation in T_M. Expanding $\text{ch}(\Delta\Phi/RT)$ into a series, we obtain:

$$\text{ch}\frac{\Delta\Phi_0}{RT_M^0} = 1 + \Delta\Phi_0^2/2R^2(T_M^0)^2; \quad \text{ch}\frac{\Delta\Phi}{RT_M^0} = 1 + \Delta\Phi/2R^2T_M^2.$$

From this

$$\frac{\Delta\Phi_0}{(T_M^0)^2[2 + \Delta\Phi_0^2/2R^2(T_M^0)^2]} = \frac{\Delta\Phi}{T_M^2(2 + \Delta\Phi^2/2R^2T_M^2)}.$$

After transformation we obtain:

$$T_M^2 = (T_M^0)^2\frac{\Delta\Phi}{\Delta\Phi_0} + \frac{\Delta\Phi(\Delta\Phi_0 - \Delta\Phi)}{4R^2} \tag{30}$$

and thus

$$T_M = \sqrt{(T_M^0)^2\frac{\Delta\Phi}{\Delta\Phi_0} + \frac{\Delta\Phi(\Delta\Phi_0 - \Delta\Phi)}{4R^2}}.$$

Using the expression (21) obtained above for $\Delta\Phi$, we obtain:

$$T_M = \sqrt{(T_M^0)^2 \frac{\Delta\Phi_0 - \gamma n^{2/3}}{\Delta\Phi_0} + \frac{\gamma n^{2/3}(\Delta\Phi_0 - \gamma n^{2/3})}{4R^2}}. \quad (31)$$

It can be seen from this expression that with increase in the concentration of the solution, the minimum is displaced towards lower temperatures, and this agrees with experimental data. In order to carry out a quantitative comparison with experimental data, it is necessary to know the numerical values of $\Delta\Phi_0$ and γ. As far as $\Delta\Phi_0$ is concerned, its value can, according to Hall, be taken as equal to 500 cal/mole. The value of γ can, in principle, be calculated from formula (20a). For this purpose, however, it is necessary to estimate in some way the difference between the effective dipole moments (μ_2 - μ_1) in the first and second structures respectively. It is extremely difficult to do this by an independent method, however. The only method left for calculating γ is by comparing the formula with the experimental data for a definite concentration, and using the value of γ obtained in this way [according to Eq. (20a), this value will be independent of the concentration] for all other concentrations.

From Eq. (30) we can obtain an equation for $\Delta\Phi$:

$$\Delta\Phi^2 - \left(\frac{4R^2(T_M^0)^2}{\Delta\Phi_0} + \Delta\Phi_0\right)\Delta\Phi + 4R^2T_M^2 = 0.$$

From this

$$\Delta\Phi = \left(\frac{2R^2(T_M^0)^2}{\Delta\Phi_0} + \frac{\Delta\Phi_0}{2}\right) - \sqrt{\left[\frac{2R^2(T_M^0)^2}{\Delta\Phi_0} + \frac{\Delta\Phi_0}{2} - 4R^2T_M^2\right]}.$$

Only one root has physical significance.

We can now find the value of $\Delta\Phi$ at which T_M for the solution becomes equal to 0°. This value is found to be 482 cal/mole. Since $\Delta\Phi = \Delta\Phi_0 - \gamma n^{2/3}$, we obtain the following formula for γ:

$$\gamma = 18/n_0^{2/3} \text{ kcal/mole}, \quad (32)$$

where n_0 is the concentration, in mole fractions, at which the temperature of the maximum density of the solution becomes equal to 0°.

This formula was used to obtain the values of γ for a number of salts. It was found that, in accordance with the relationship (20a), γ is determined primarily by the valencies of the ions of the salt. For the salts NaCl, $NaNO_3$, NaI, KCl, KBr, and KI, the value of γ is of the order of 550 cal/mole. For LiCl, LiBr, and LiI, the value found for γ was 350 cal/mole, and for $ZnSO_4$, $CdSO_4$, and $MgSO_4$ the value found was 800 cal/mole. Thus in accordance with formula (20a), the value of γ for 2,2-valent salts is approximately double the value for 1,1-valent salts.

Formula (20a) does not give the relationship between γ and the radii of the cations and anions, since in the derivation it was assumed that the ions were points. It is obvious, however, that the average intensity of the field created in the solution by the ions should decrease with increase in their radii. From this point of view, the low values of γ for lithium salts appear rather surprising. It is necessary, however, to take account of the fact that the magnitude of the average field produced by the cation is determined not only by its radius but also by the screening effect produced by the first coordination layer of the ion. If the layer is sufficiently "compact", then the "effective radius" of the hydrated cation will be more greater than the crystallo-chemical radius. For the Li^+ cation, which has a very small radius, the first coordination sphere is evidently much more compact than than that of Na^+ or K^+, since the coordination numbers of the Li^+, Na^+ and K^+ ions are close to one another [3].

From formula (20a) and the values obtained for γ, it is possible to estimate the value of the difference (μ_2 - μ_1) in the effective dipole moments of the water molecules associated in the first and second structures respectively. This quantity is found to be approximately equal to 0.8×10^{-18} CGSE. This value is reasonable, when we take account of the fact that the dipole moment of the water molecule in the gaseous state is equal to 1.86×10^{-18} CGSE.

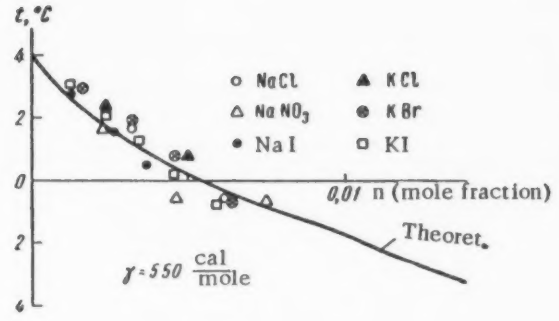

Fig. 1

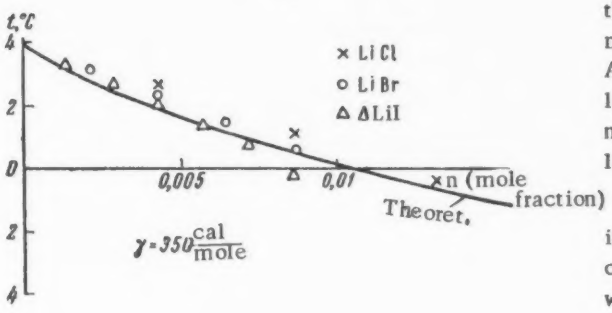

Fig. 2

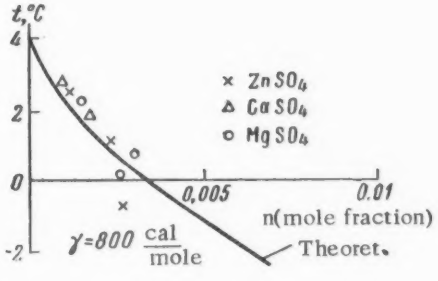

Fig. 3

Figures 1-3 show the relationship between the temperature of the maximum density and the concentration for a number of salts. The solid lines give the theoretical curves calculated from formula (31); the values of γ given above for the three groups of salts were used.

Figure 1 gives data for the group of potassium and sodium salts, Fig. 2 gives data for the lithium halides, and Fig. 3 gives data for some sulfates with divalent cations. The experimental values of T_M were taken from Tables [35].

The curves show that formula (31) gives accurately the relationship between the temperature of the maximum density and the concentration at low concentration. At high concentrations, the use of formula (31), strictly speaking, is unjustified, since in its derivation we neglected the presence of the ionic lattice in the solution.

The model developed in section 2 to describe the influence of ions on the "free" water can be used to calculate a whole series of effects. In [36] this model was used to calculate the change in the volume of the water in the solution.

This treatment, by which account is taken of the influence of ions on the structure of the "free" water, has proved extremely important in the determination of the change in the temperature of the minimum adiabatic compressibility of aqueous solutions with change in concentration. In [37], it was shown that the influence of ions on the structure of the "free" water tends to displace the minimum adiabatic compressibility towards lower temperatures. At low concentrations, the significant part is played by the first effect, and, at high concentrations, the significant part is played by the second effect. It has been shown [38] that by studying the behavior of the minimum adiabatic compressibility, it is possible to estimate the influence of ions on the structure of the "free water".

The model which has been developed can also be used to calculate a number of other effects, for which the influence of ions on the structure of the "free" water is important, for example: the change in viscosity of a solution with change in concentration, the absorption of ultrasonic waves by electrolyte solutions, the heat capacities of solutions, etc.

SUMMARY

The main features of the changes produced by ions in water may be summarized as follows.

1. The ions interact with the nearest water molecules, and this interaction affects primarily the translational movement of the water molecules.

2. The rest of the water beyond the first coordination sphere lies in the strong electrostatic field of the ions. The presence of this field leads to a displacement of the thermodynamic equilibrium between the tetrahedrally-coordinated and close-packed structures towards the latter. In other words, the presence of the ionic

field leads to an increase in the number of molecules which are present in the open spaces in the structure and which undergo translational movement through these open spaces.

The influence of ions on the structure of the "free" water makes it possible to explain a whole series of effects, for example, the decrease in the temperature of the maximum density of a solution with increase in the concentration of the salt.

LITERATURE CITED

1. K.P. Mishchenko, Zhur. Fiz. Khim. 36, 12, 1736 (1952).
2. J.O'M. Bockris, Quart. Rev. 3, 2, 173 (1949).
3. O.Ya. Samoilov, The Structure of Aqueous Electrolyte Solutions and the Hydration of Ions [in Russian] (Izd. AN SSSR, Moscow. 1957).
4. E. Darmois, La Solvation des Ions (Memorial des Sciences Physiques, Paris, 1946).
5. J.H. Wang, J. Phys. Chem. 58, 9, 682 (1954).
6. Yu.P. Syrnikov, Doklady Akad. Nauk SSSR 118, 4, 760 (1958).*
7. R.D. Waldron, J. Chem. Phys. 26, 4, 809 (1957).
8. J. Bernal and R. Fowler, Uspekhi Fiz. Nauk 14, 5, 586 (1934).
9. Yu.Ya. Kaganovich and K.P. Mishchenko, Zhur. Obshch. Khim. 21, 1, 28 (1951).*
10. H.S. Frank and M.W. Evans, J. Chem. Phys. 13, 11, 507 (1945).
11. G.W. Stewart, J. Chem. Phys. 11, 2, 72 (1943).
12. G.W. Stewart, J. Chem. Phys. 12, 2, 321 (1944).
13. A.P. Rudakov, Kolloid. Zhur. 15, 4, 284 (1953).*
14. D.D. Randall and A.M. Taylor, J. Chem. Phys. 22, 5-6, 1149 (1954).
15. R. Lochet, A. Rousset and J. Tourte, Compt. rend. Acad. Sci., Paris 242, 24, 2820 (1956).
16. V.I. Danilov, The Structure and Crystallization of Liquids [in Russian] (Izd. AN SSSR, Kiev, 1956).
17. L. Pauling, The Nature of the Chemical Bond [Russian translation] (Goskhimizdat, Moscow–Leningrad, 1947).
18. J.A. Pople, Proc. Roy. Soc. A205.2, 163 (1951).
19. R.E. Rundle, J. Phys. Chem. 59, 8, 680 (1955).
20. A. Eucken, Electrochem. 52, 4, 255 (1948).
21. E.O. Wallen, W.L. Davison, and C.G. Shull, Phys. Rev. 75, 9, 1348 (1949).
22. V.V. Tarasov and E.G. Ponedel'nikova, Doklady Akad. Nauk SSSR 96, 4, 789 (1954).
23. L. Hall, Phys. Rev. 73, 7, 775 (1948).
24. K. Grjotheim and Krogh - Moe, Acta chem. Scand. 8, 7, 1193 (1954).
25. Ya.I. Frenkel', The Kinetic Theory of Liquids [in Russian] (Izd. AN SSSR, Moscow–Leningrad, 1954).
26. T.D. Litovitz and E.H. Carnevale, J. Appl. Phys. 26, 7, 816 (1955).
27. L.M. Libermann, J. Acoust. Soc. Am. 28, 6, 1253 (1956).
28. A.G. Samoilovich and A.A. Goryunov, Zhur. Éksp. i Teor. Fiz. 4, 9, 892 (1934).
29. V.K. Semenchenko, Vestnik Moskovsk. Univ., 3 (1948).
30. J. Holtsmark, Ann. Phys. 58, 7, 577 (1919).
31. J. Holtsmark, Phys. Z. 20, 7, 162 (1919).
32. J. Holtsmark, Phys. Z. 25, 4, 73 (1924).
33. S. Chandrasekhar, Stochastic Problems in Physics and Astronomy [Russian translation] (IL, Moscow, 1947).
34. C.V. Raman, Phil. Mag. 47, 671 (1924).
35. Supplement to the Technical Encyclopedia, Reference Book of Physical, Chemical, and Technological Quantities [in Russian] (Moscow, 1930) Vol. V.
36. Yu.P. Syrnikov, "The structure of ionic solutions," Technical Information on the Results of Scientific Research Work [in Russian] (Izd. Leningr. Lesotekh. Akad. 1956) Vol. 38, p. 65.
37. I.G. Mikhailov and Yu.P. Syrnikov, Vestnik Leningradsk. Univ. 10, 5 (1958).
38. Yu.P. Syrnikov, Candidate's Dissertation [in Russian] (Leningr. Gos. Un-to, 1958).

* Original Russian pagination. See C.B. translation.

PROTON RELAXATION IN AQUEOUS SOLUTIONS OF DIAMAGNETIC SALTS

I. SOLUTIONS OF NITRATES OF ELEMENTS IN THE SECOND GROUP OF THE PERIODIC SYSTEM

V.M. Vdovenko and V.A. Shcherbakov

V.G. Khlopin Radium Institute, Academy of Sciences of the USSR, Leningrad
Translated from Zhurnal Strukturnoi Khimii, Vol. 1, No. 1, pp. 28-35, May-June, 1960
Original article submitted January 7, 1960

Using the Rivkind method, the authors studied the time of proton relaxation T_1 in aqueous solutions of diamagnetic nitrates of elements in Group II of the Periodic System. It was found that these solutions have a shorter proton relaxation time than water. This is due to the change in the correlation time of proton dipole interaction, which occurs as a result of ion hydration. A hypothesis was advanced with regard to the interrelation between the ratio of times T_1 for solution and pure water and the most important characteristic of inner hydration of the ions – the ratio τ_i/τ. The quantity Δ_M, corresponding to the decrease of T_1 in a molar solution of the given salt, is proposed as a characteristic of the effect of ions on T_1 for protons in aqueous solution. The quantity Δ_M is called the molar relaxation shift in analogy with the molar chemical shift (δ_M) of high-resolution spectra (NMR). A correlation between Δ_M and δ_M for protons under the same conditions was found. Comparison of Δ_M with ionic radii shows sharply different functionalities for A- and B-subgroup ions. On this basis, the hypothesis is advanced that the ion-water bond is covalent in the case of B-subgroup ions, which makes it possible to explain the greater effect of these ions on T_1 in comparison with A-subgroup ions.

At present, the action of paramagetic ions on the relaxation time of protons in water is so well understood that it can be used for purposes, for instance, of physical chemistry [1, 2]. The question of the effect of diamagnetic ions on proton relaxation is in an entirely different state: theoretically and experimentally, it is little-studied, and, correspondingly, the number of works on it is very limited. At the same time, as a review of existing investigations of this question [3, 4, 5, 6] shows, it is of great practical importance inasmuch as the effect of diamagnetic ions on the relaxation of protons in aqueous solutions and the NMR spectra of such protons is very closely connected with their hydration, and is one of the important problems of the modern physical chemistry of solutions.

An interesting theoretical and experimental investigation in this direction was conducted by Broersma [3]. Using the method of magnetic relaxation spectroscopy, he measured the "relaxation number"* and found changes in the latter in aqueous solutions of various diamagnetic ions (Li^+, Na^+, K^+, Mg^{2+}, Ba^{2+}, Al^{3+}). On the basis of the theory under development, the author explains these changes by the fact that the relaxation time of diamagnetic solutions is determined not only by the correlation time of dipole interaction τ_c for pure water, but also the time during which protons remain in the inner sphere of the ion; the rate of departure of the latter from this region disturbs the averaging of "relaxation rates" in the system. The picture of the change in time τ_c

* Authors' term [3].

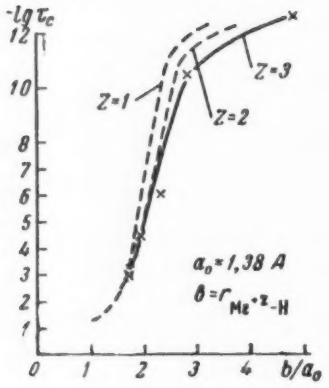

Fig. 1. Relation between the correlation time and the ion–water molecule (ion–proton distance). Curves for Z = 1 and 2 are hypothetical; those for Z = 3 are drawn from the data of Broersma [3].

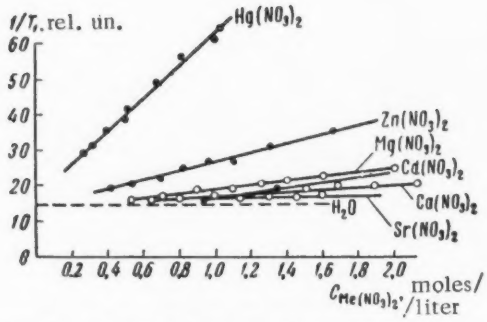

Fig. 2. Change of proton relaxation time in solutions of ions of elements in the second group. The signal of a Mn^{2+} solution of concentration 4.02×10^{-4} M was taken to be 100.0.

with respect to distance from the ion, shown in Fig. 1, is a conclusive argument in favor of Broersma's explanation. The latter also found a very weak negative effect of certain ions, lying almost within the limits of experimental error, an increase of relaxation time. In the author's opinion, this is caused by the appearance of disorder in the structure of water; i.e., in the presence of these ions, the rate of disintegration of liquid crystals, or zones of local order, is greater than the rate of their formation (the existence of such zones was proved by the author's investigation of the temperature dependence of the relaxation of protons in water [3]). Possibly we would not mention this fact, which is allotted only a secondary place even in work [3], if it did not attest to the finding of the phenomenon, which Samoilov called negative hydration [7], by the NMR method.

As Meiboom and co-workers [4] showed in an investigation of proton relaxation in aqueous solutions with various pH values by the spin echo method, the correlation time of proton exchange also may strongly affect τ_c. Connick and Poulson [5], on studying the NMR of O^{17} in aqueous solutions of paramagnetic ions of elements in the first inserted decade, determined the time of departure of water molecules from the first coordination sphere of these ions.

On the basis of the results of work [3] it may be assumed that the length of time during which the proton lies near one ion or another will cause a change in the high-resolution NMR spectrum of protons (or, probably, nuclei of a hydrated ion); i.e., hydration may lead to the appearance of a chemical shift in the NMR spectrum of protons. Recently, Axstmann [6] actually found this phenomenon in nitrate solutions containing bi-, ter-, and quadrivalent cations [7]. The molar chemical shifts δ_M, which he measured for a number of ions, display remarkable correlation with the indices of the acidity constant pK_a for these ions. Since this correlation is observed only when the ion–water bond of the hydration shell is electrostatic and not when the bond is covalent, the author proposes its use as an indicator of the character of the ion–water bond.

We began a systematic study of aqueous solutions of various diamagnetic salts. The results, obtained with solutions of nitrates of elements in the second group of the Periodic System and reported in the present article, are the first step in this direction. We chose second-group elements as the first subject for the investigations, for the following reasons: as Broersma notes [3], alkali-metal ions give a very small effect, the study of third-group ions might be complicated by hydrolysis and the unavailability of certain compounds, which would cause the final picture to be ambiguous and incomplete. The investigation was conducted by the method of measuring relative changes in the relaxation time of protons in water [1]. The solutions were prepared from carefully-recrystallized salts (of purity "CP" and "PAR"). Distilled nitric acid and redistilled water were used; their

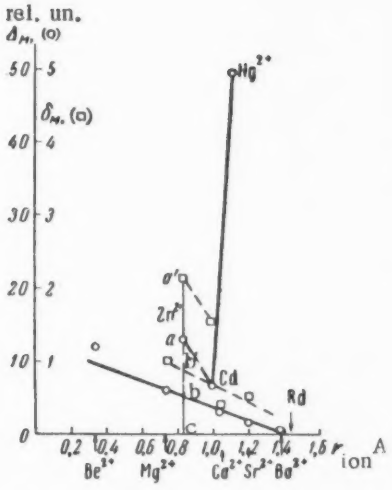

Fig. 3. Relation of ΔM and δ_M [6] to the ionic radius.

freedom from paramagnetic admixtures was checked directly in the apparatus, which was operating under high-sensitivity conditions; the pH of all solutions was about zero (1.5 N HNO_3). Standard solutions of Mn^{2+} were prepared by solution of a manganese sulfate preparation especially intended for calibration. The effect of atmospheric oxygen, which is negligible in concentrated electrolyte solutions, was either taken into account or eliminated by its removal from the solutions. To avoid the complicating effect of macroviscosity, we investigated solutions having nitrate concentrations such that their macroviscosity was practically the same as the viscosity of water. For this, their viscosity was measured with an Ostwald viscometer graduated by means of glycerol ("dynamite" grade) according to tables in [9].

From the experimental results, which are given in Fig. 2, it follows that the studied ions may lead to a considerable decrease in the proton relaxation time in a number of cases, as Broersma also noted [3]. It is also evident that the effectiveness of action of the ions depends on their position in the Periodic System—whether they belong to the A or B subgroup; i.e., it depends on the type of electron shell in the ion.

It is generally known that the relaxation time of pure, liquid water is described, according to Solomon [10], by the following equation:

$$\frac{1}{T_1} = \frac{1}{T_2} = \frac{3}{2} \cdot \frac{\hbar^2 \gamma^4 \tau_c}{b^6} \qquad (1)$$

(T_1 and T_2 are the times of longitudinal and transverse relaxation, $\hbar = h/2\pi$, γ is the gyromagnetic ratio for the proton, $\underline{b}$ is the proton–proton distance, and τ_c is the correlation time of dipole interaction). As follows from [3-5], in the first approximation Eq. (1) may be considered valid for the description of proton relaxation in a diamagnetic solution (i.e., a solution containing diamagnetic ions) if it is assumed that contributions from the interaction of diamagnetic ions with a nuclear magnetic moment are small. This is quite obvious both by virtue of the rarity of individual isotopes in nature and because certain nuclei have no magnetic moment. In the same approximation it may be assumed that in a diamagnetic solution, the distance $\underline{b}$ does not vary enough to affect the relaxation time; i.e., we assume that the contribution from the change in τ_c is much greater than that from the change in $\underline{b}$. This is qualitatively confirmed by Fig. 1.

Let us consider the quantity τ_c. A water molecule in solution has translational and rotational (orientational)degrees of freedom. Thus, the time of energy exchange between the protons of two adjacent water molecules depends on the time during which one molecule remains in an equilibrium position near the other, and the time during which the orientation of these two molecules is favorable for effective energy exchange. These time intervals also determine the value of τ_c. Hence, by determining the ratio of the proton relaxation time for a diamagnetic solution to that for pure water, we obtain the ratio of the correlation time of dipole interaction for the solution (τ_c^i) to that for pure water (τ_c^0). As follows from the definition of τ_c, this ratio is proportional to τ_i/τ, the ratio of the time during which the water molecules remain in the equilibrium position nearest to the ion in the solution structure (τ_i) to the time during which they are surrounded by other water molecules (τ), which is the very important characteristic of inner hydration, first introduced by Samoilov [7]; i.e.,

$$\frac{\tau_c^i}{\tau_c^0} \propto \frac{\tau_i}{\tau}. \qquad (2)$$

This proportionality will be the more strictly fulfilled, the more constant is the relative contribution of rotational motion to τ_c. Thus, by studying proton relaxation in aqueous solutions, one probably can determine the value of τ_i/τ, which until now has only been indirectly evaluated from data on ionic mobilities and coefficients of the self-diffusion of water [8].

Compound	τ_c^i/τ_c^0	Δ_M (±0,3), rel. un.	Compound	τ_c^i/τ_c^0	Δ_M (±0,3), rel. un.
$Be(NO_3)_2$	7,7	12,0	$Cd(NO_3)_2$	5,1	6,5
$Mg(NO_3)_2$	6,4 *,**	6,0	$Ba(NO_3)_2$	1,3	0,25 *
$Ca(NO_3)_2$	3,7 ***	3,0	$Hg(NO_3)_2$	35,0	49,4
$Zn(NO_3)_2$	9,2	13,0	$Ra(NO_3)_2$	0,6	—0,4 *
$Sr(NO_3)_2$	2,2	1,5			

* Values obtained by extrapolation (Fig. 3).

** According to [8], 86.31.

*** According to [8], 2.16.

The relaxation time of the diamagnetic solution may be represented as follows:

$$\left(\frac{1}{T_1}\right)_s = \left(\frac{1}{T_1}\right)_0 + \left(\frac{1}{T_1}\right)_i . \tag{3}$$

Here $(1/T_1)_0$ is the contribution from free water, and $(1/T_1)_i$ is the contribution from water in the hydration shell of the ion. Hence, for the ratio of values of signals from the solution being investigated and pure water we have:

$$\left(\frac{1}{T_1}\right)_s \Big/ \left(\frac{1}{T_1}\right)_0 = \frac{\tau_c^0 N_0 - \tau_c^0 N_i n_i + \tau_c^i N_i n_i}{\tau_c^0 N_0} ,$$

or

$$\left(\frac{1}{T_1}\right)_s \Big/ \left(\frac{1}{T_1}\right)_0 = 1 + KN_i \tag{4}$$

(N_0 and N_i are the concentrations of water and ions in moles/liter in the aqueous solution, and n_i is the hydration number of the given ion), where

$$K = \left(\frac{\tau_c^i}{\tau_c^0} - 1\right)\frac{n_i}{N_0} . \tag{5}$$

Our values of τ_c^i/τ_c^0, calculated for Samoilov's hydration numbers [8], are given in Table 1.

For the ion group chosen by us, unfortunately, there are few data on τ_i/τ; in the future, therefore, it will be necessary to work with ions which have been studied more in this respect. At the same time comparison with existing data shows, for instance, good agreement for Ca^{2+} (table). The inordinately great discrepancy in the case of Mg^{2+} is apparently explained by the fact that the proportion of activated jumps in conjunction with the water molecules nearest to this ion is very great [5, 6, 8]; obviously, their contribution to the effect measured by us is not perceptible, and, hence, the comparison made here is only a forced one. Moreover, there were generally no grounds to expect any better agreement of τ_c^i/τ_c^0 with values of τ_i/τ than that given in the literature for Ca^{2+}, in view of the fact that the quantities τ_c^i/τ_c^0 contain the neglected contribution of the nitrate ion.

It is a very important fact that values obtained for elements of the A-subgroup fall regularly from Be^{2+} to Ba^{2+}, which agrees with modern views on the hydration of these ions [8]. This course of the quantities τ_c^i/τ_c^0 makes it possible to judge the correctness of our hypothesis on the role of the quantity b in relaxation in diamagnetic solutions. According to the views of Frank and Wen [11], the role of Layer B (the layer having the greatest disorder of structure of water near the ion) increases with the ionic radius, i.e., from Be^{2+} to Ba^{2+} in our case. But in just this layer, the distance b may change very substantially owing to the fact that the number of orientations of water molecules with protons is apparently greater than is possible in Layer C (a layer with

unchanged water structure), and still greater than in Layer A (the inner sphere of the ion). If the contribution from changes in $\underline{b}$ were equal to that from changes in τ_c, or exceeded it, either the quantities τ_c^i/τ_c^0 in general would not decrease in the series being considered (equality of both contributions), or a picture opposite to that given in the table would be observed. The decrease in the ratio unambiguously indicates, firstly, that the hypothesis advanced above on the role of the H–H distance in proton relaxation processes in diamagnetic solutions is valid and, secondly, that the decrease in the relaxation time in these solutions is connected with Layer A; i.e., the ratio τ_c^i/τ_c^0 obtained by us characterizes the inner hydration of the ions.

For individualization of the effect of ions on the relaxation time we used a quantity, directly obtainable from experiment, which is defined as the decrease in the relaxation time of protons in water on addition of 1 mole of the given compound (Δ_M). These values for the ions investigated (in arbitrary units), corrected for the change in the number of protons, ocurring on dilution of the water by the salt, are given in the table. In Fig. 3 they are compared with the corresponding ionic radii.

Since the data for ions of alkaline-earth elements are easily plotted on one straight line, a more precise value of Δ_M can be obtained for barium nitrate, the direct experimental determination of which led to a large error, and the quantity Δ_M can be evaluated for radium nitrate, with which no experiments have been performed. More important, of course, is the fact that, by analyzing the picture obtained, one can draw conclusions on the nature of the ion–water bond for second-group ions. This possibility is based on the sharp difference in the relation between Δ_M and the ionic radius for A- and B-subgroup ions. Similar graphical analysis (Fig. 3) of values of δ_M [6] shows that our data fully agree with Axstmann's results. Comparison of these functionalities shows that both the correlation of the chemical shift δ_M of NMR proton spectra with pK_a values and the relation between δ_M and the ionic radius, and the relation found between Δ_M and the ionic radius indicate the character of the ion–water bond. Such agreement of data obtained by different methods is not fortuitous: in both cases we are dealing with a single phenomenon (NMR), and in both cases the measured effect is due to a change in the correlation time of dipole interaction τ_c. The fact that values of Δ_M for zinc, cadmium, and mercuric nitrates do not lie on the same straight line as those for ions of alkaline-earth elements on the graph $\Delta_M = f(r_{ion})$ indicates some covalence in the bond between these ions and the water hydrating them, the degree of which decreases from Zn to Cd and increases from Cd to Hg. This conclusion is consistent with data of the chemistry of complex compounds of these elements and does not contradict Axstmann's results. The correlation found by the latter, for all its undoubted value, apparently only reflects the character of that bond between the ion and water, which predominates with the given ion. This is possibly due in part to the quantity δ_M and mainly to the quantity pK_a, whose comparison with the chemical shift is less useful for determining the character of the ion–water bond, since the index of the acidity constant reflects the character of interactions in the solution only indirectly. The ionic radii directly determine the distribution of particles and their interaction in solution, and hence comparison with them is more worth while.*

Our conclusion is confirmed by the following, interesting experimental fact, discovered by Vdovenko and Kovaleva [11]. The salting-out effect of zinc and cadmium nitrates does not correspond to their ionic radii; i.e., as salting-out agents, they act as if their ionic radii were greater than they actually are. This becomes understandable when the covalent character of the bond between these ions and water molecules is taken into account.

In connection with the above, the position obtained for B-subgroup ions is of special interest. The mechanism of the effect on the proton relaxation time in this case differs from the mechanism obtaining in the case of ions of alkaline-earth elements, where it apparently must be determined only by the change in τ_c. In the case of zinc-subgroup ions this effect is accompanied by another which is due to the covalent character of Me^{2+}–H_2O interaction. Thus, the relaxation time of protons in the solution consists in this case not only of contributions corresponding to water molecules with different τ_c values, but also a third contribution, due to the covalent bond, i.e., the contribution from the paramagnetism of $Me(H_2O)_x^{2+}$ complexes. The formation of these more or less stable particle groups is due to the fact that the activation energy of exchange of their constituents with particles not entering into the group, is large [13]. Values of τ_c^i/τ_c^0 found for this case correspond to just this situation.

---

* Values of Δ_M correlate with pK_a, the same as values of δ_M. In this case a similar smoothing-out of the difference between the A-and B-subgroups occurs in the graph of $\Delta_M = f(pK_a)$.

As Rivkind [14] showed in the case of complexes of metals in the first inserted decade, when a covalent bond is formed with the participation of nd-orbitals of the central ion as a result of partial transfer of electrons with uncompensated spins to the ligands, $1/T_1$ increases, since the ligands become paramagnetic and the "screening" of the central ion is disturbed. Morgan, et al., apparently observed a similar phenomenon in the case of the complex $Cr(H_2O)_6^{3+}$ [15]. Since zinc ions do not have electrons with uncompensated spins, the following explanation seems reasonable: the appearance of a paramagnetic constituent in our case apparently is due to excitation of the ground state of the Me^{2+} ion, or the contribution of the resulting excited states to the decrease of T_1 for protons in the solution. Such excitation of the ground state in ions having an inert-gas electron shell is unlikely from energetic considerations. For B-subgroup ions having an nd^{10} shell in the given case, it is far more probable.* Excitation occurs as a result of overlapping of the wave functions of nd-electrons in the metal ion with unshared electron pairs of oxygen in the water molecule. In this case, as might be supposed on the basis of the general discussion itself, the relative weight of the excited states increases owing to partial compensation of electron spins therein.

Using somewhat more concrete terminology, one may say that in the given case the proton relaxation time gives information on the redistribution of electron density between the metal ion and the water molecules of the hydration shell, which occurs when a covalent bond is formed. The fact that such redistribution actually occurs in the systems being considered is unambiguously indicated by values of δ_M found for zinc and cadmium by Axstmann [6], since the chemical shift of NMR spectra, by its nature, is directly related to the electron-density distribution [16]. The correspondence between values of the molar chemical shift δ_M and the molar decrease of relaxation time Δ_M must again be emphasized in this connection. As shown by the entire discussion, it may be assumed that Δ_M is an additive composite of two contributions: that due to electrostatic (ion-dipole) interaction and that which takes into account covalent bond formation (the additivity of the probabilities of relaxation transitions makes it possible to speak of the additivity of Δ_M). As is evident from Fig. 3, these components are proportional to segments cb and ba, respectively. It is of interest to note the following. If it is assumed that such contributions exist for δ_M, it is found that their ratio for Δ_M in the case of zinc is almost exactly equal to the ratio of the same quantities for δ_M (Fig. 3, segments cb' and b'a', respectively): 1.6_0 and 1.5_6. For Δ_M and δ_M, in the case of cadmium, the equality is very approximate: 0.8_6 and 1.5_6. Possibly this quantitative comparison also indicates the specific character of each of the NMR methods. In the given case it will probably be manifested in the fact that the relaxation time is more sensitive to the paramagnetism of the ion and its state, whereas the value of the chemical shift is more closely connected with the electron density distribution near a resonating nucleus. On the basis of this situation we are justified in calling Δ_M the molar relaxation shift in analogy with δ_M.

Using data of the table and Fig. 3, one may calculate that effective moment which must be ascribed to the ion in the complex $Me(H_2O)_x^{2+}$ as a result of the appearance of a covalent bond. Its values (μ_N) for zinc, cadmium, and mercury are as follows:

Ion Me^{2+}	μ_N $(\pm 0{,}5)\cdot 10^{-2}$, Bohr magnetons
Zn^{2+}	3,2
Cd^{2+}	1,9
Hg^{2+}	6,5

The calculation is performed by the usual method, according to Kozyrev and Rivkind [1]. The magnetic moment of the Mn^{2+} ion is taken to be 5.90 Bohr magnetons. Obviously, values of μ_N, together with those of Δ_M, can be used as a quantitative characteristic of the ion–water molecule bond. They may, possibly, give even more general information on the given ion.

* It would naturally be assumed that a $1s^2$-type shell is more subject to excitation on interaction with electrons of the oxygen in the water, than an $n(s^2p^6)$-type. The fact that the value of Δ_M for $Be(NO_3)_2$ in Fig. 3 occupies a rather special position is understandable from this point of view; i.e., this, evidently, also indicates the covalent character of the interaction of Be^{2+} with water.

The fact that $1/T_1$ for solution protons is affected by the covalent bonds of $Me(H_2O)_x^{2+}$ complexes evidently may be important for understanding the structure of these compounds. Since the proton relaxation time in solutions of paramagnetic ions is very sensitive to the length of the ion–water bond, it may be assumed even on the basis of existing results, that the packing of water molecules (more precisely, oxygen atoms) around the Me^{2+} ion is very far from dense, since the latter case would evidently exclude observation of all effects, altogether. Actually the results of dense packing would be a considerable increase in the effective ionic radii, and "screening" of the paramagnetism induced by the covalent bond.

The authors sincerely thank O.Ya. Samoilov and Yu.V. Gurikov for an interesting discussion and valuable advice.

SUMMARY

1. The proton relaxation time in aqueous solutions of nitrates of elements in the second group of the Periodic System was measured, and it was found that such solutions have a shorter relaxation time T_1 than water.

2. The observed phenomenon is probably due to inner hydration of the ions, as a result of which the correlation time of dipole interaction of protons in the solution changes. Therefore a hypothesis is advanced on the relation between the ratios of correlation times of protons situated near an ion in the solution and those in water itself and the ratios τ_i/τ, which characterize the inner hydration of the ions.

3. On the basis of the difference found in the functionalities of values of the molar relaxation shift Δ_M of the A- and B-subgroup ions investigated, with respect to their radii, it is suggested that in the case of B-subgroup ions the ion–water bond is covalent; this promotes an increase in the effect of these ions on T_1.

LITERATURE CITED

1. B.M. Kozyrev and A.I. Rivkind, Zhur. Éksp. i Teoret. Fiz. 27, 69 (1954); A.I. Rivkind, Zhur. Neorg. Khim. 2, 1263 (1957).
2. P.W. Selwood, Magnetochemistry [Russian translation] (IL, Moscow, 1958).
3. S. Broersma, J. Chem. Phys. 24, 153, 659 (1956); 27, 481 (1957).
4. S. Meiboom, Z. Zuz and D. Gile, J. Chem. Phys. 27, 1410 (1957).
5. R.E. Connick and R.E. Poulson, J. Chem. Phys. 30, 759 (1959).
6. R.K. Axstmann, J. Chem. Phys. 30, 340 (1959).
7. J.N. Shoolery and B.J. Alder, J. Chem. Phys. 23, 805 (1955).
8. O.Ya. Samoilov, Structure of Aqueous Electrolyte Solutions and Hydration of Ions [in Russian] (Izd. AN SSSR, Moscow, 1957).
9. Handbook of Chemistry and Physics (Cleveland, Ohio, 1955).
10. I. Solomon, Phys. Rev. 99, 559 (1955).
11. H.S. Frank and Wen-Jang Wen, Disc. Faraday Soc. 24, 133 (1957).
12. V.M. Vdovenko and T.V. Kovaleva, Zhur. Neorg. Khim. 2, 1682 (1957).
13. O.Ya. Samoilov, Zhur. Fiz. Khim. 33, 1147 (1959).
14. A.I. Rivkind, Zhur. Neorg. Khim. 4, 1291 (1959).
15. L.O. Morgan, A.W. Nolle, R.L. Hull, and J. Murphy, J. Chem. Phys. 25, 206 (1956).
16. E. Andrew, Nuclear Mangetic Resonance [Russian translation] (IL, Moscow, 1958).

VIBRATION FREQUENCIES OF THE WATER MOLECULES IN THE FIRST COORDINATION LAYER AROUND AN ION IN AN AQUEOUS SOLUTION

O. Ya. Samoilov

Kurnakov Institute of General and Inorganic Chemistry,
Academy of Sciences of the USSR
Translated from Zhurnal Strukturnoi Khimii, Vol. 1, No. 1, pp. 36-38,
May-June 1960
Original article submitted July 29, 1959

A study is made of the relation of ΔE_i to the vibration frequencies of the water molecules in the equilibrium positions closest to ions in aqueous solutions of electrolytes. The frequencies and, hence, the j_{0i} increase with ΔE_i.

Quantities ΔE_i are used [1, 2] to specify the effects of ions in aqueous solutions on the translational motion of nearby water molecules, these quantities being the changes induced by the ions in the potential barrier relative to the height E of that barrier, which separates adjacent equilibrium positions for the water molecules. The ΔE_i are important parameters describing the immediate environment of the ions. They are a measure of the strength of the bonds to the nearest water molecules; those strengths are the main factors controlling the frequency of the exchange with other water molecules.

The mean number of activated jumps per sec in water is

$$j = j_0 e^{-E/RT},$$

so the mean number of those jumps from the immediate neighborhood of an ion is

$$j_i = j_{0i} e^{-(E+\Delta E_i)/RT}.$$

The j_{0i} are of interest, in particular, as regards their relation to ΔE_i. This topic has not been dealt with before.

We know [1, 3] that the preexponential factor for the above process in a liquid is

$$j_0 = 2K\nu,$$

in which ν is the mean frequency of oscillation about the equilibrium position and K is some factor that takes account of (for example) the fact that the particle does not traverse the barrier every time it approaches the barrier with an energy greater than E (that factor K also incorporates a steric factor dependent on the shape of the particle). We may assume that K is constant for a given kind of particle (e.g., H_2O^{16}); then j_0 is proportional to ν.

There are many papers on the effects of ions on the intramolecular vibrations of the H_2O molecule [4]. Here we consider the vibrations of the molecule as a whole, the vibrations of the main interest being of course those that can result in exchange between molecules.

Values of ΔE_i and j_0/j_{0i} for Some Simple Ions at 25°C

Ion	Li^+	Na^+	K^+	Cs^+	Cl^-	Br^-	I^-	Mg^{++}	Ca^{++}
ΔE_i, kcal/mole	0,73	0,25	—0,25	—0,33	—0,27	—0,29	—0,32	2,61	0,45
j_0/j_{0i}	0,42	0,79	1,47	1,20	1,26	1,27	1,29	0,017	0,57

There are many papers on the effects of ions on the intramolecular vibrations of the H_2O molecule [4]. Here we consider the vibrations of the molecule as a whole, the vibrations of the main interest being of course those that can result in exchange between molecules.

The frequency of the oscillation about an equilibrium position is related to the slope of the curve representing the interaction energy as a function of distance between particles. The larger the slope, the larger ν. A displacement x (measured from the equilibrium position) results in a restoring force $f = -kx$ (if the oscillations are harmonic). But $f = -dU/dx$, in which U is the potential energy. Then k increases with dU/dx. But $\nu = (1/2\pi)\sqrt{k/m}$, in which m is the mass of a particle. The frequency increases with k and so with the slope of the energy curve.

There are many papers on the relation between ΔE_i and the slope of the energy curve [1, 2, 5]; ΔE_i increases with that slope. If the slope for the interaction between the ion and a water molecule is larger than the slope for the interaction between two water molecules, we have $\Delta E_i > 0$. In the convex case we have $\Delta E_i < 0$ (negative hydration). Finally, $\Delta E_i = 0$, if the two slopes are equal.

These relations can give us the oscillation frequency, and hence j_{0i}, as a function of ΔE_i (clearly, $j_{0i} = j_0$ if $\Delta E_i = 0$:

$$j_{0i} > j_0, \quad \text{if} \quad \Delta E_i > 0,$$

and (1)

$$j_{0i} < j_0, \quad \text{if} \quad \Delta E_i < 0.$$

This result is to be compared with experimental results. An equation that has been given [6] is

$$\rho_i' = \rho' \frac{j_0}{j_{0i}} e^{\Delta E_i/RT}, \tag{2}$$

in which ρ'_i and ρ' are the surface densities of the arrays formed by water molecules respectively in the first coordination layer and in water itself.

$$\rho_i' = \frac{n_i}{4\pi R_i^2} \text{ and } \rho' = \frac{n}{4\pi R_0^2},$$

in which n_i and R_i are the coordination number and radius of the first coordination sphere of an ion, n and R_0 being the corresponding quantities for a water molecule in water. We have $\rho' = 0.044\ A^{-2}$ at 25°C [1]. Then (2) gives us

$$\frac{j_0}{j_{0i}} = \frac{\rho_i'}{\rho'} e^{-\Delta E_i/RT}.$$

We calculated j_0/j_{0i} by means of the ρ_i' and ΔE_i previously given in [1]. The table gives these results.

We see that for $\Delta E_i > 0$ (Mg^{2+}, Ca^{2+}, Li^+, Na^+), we have that $j_0/j_{0i} < 1$ and for $\Delta E_i < 0$ (K^+, Cs^+, Cl^-, Br^-, I^-), that $j_0/j_{0i} > 1$, i.e., that (1) is correct.

Let τ_i be the mean time a molecule spends in an equilibrium position closest to the ion, and let τ be that time for an equilibrium position in water. Then

$$\frac{\tau_i}{\tau} = \frac{\tau_{0i}}{\tau_0} e^{\Delta E_i/RT},$$

in which τ_{0i} is equal (roughly) to half the period of oscillation in an equilibrium position closest to the ion, and τ_0 is the corresponding quantity for water. If we assume that $\tau_{0i} = \tau_0$, we have

$$\frac{\tau_i}{\tau} = e^{\Delta E_i/RT}.$$

This equation is applicable near the transition between positive and negative hydration. Now

$$\frac{\tau_{0i}}{\tau_0} = \frac{j_0}{j_{0i}},$$

so the above argument gives us

$$\frac{\tau_i}{\tau} < e^{\Delta E_i/RT}, \quad \text{if} \quad \Delta E_i > 0,$$

and

$$\frac{\tau_i}{\tau} > e^{\Delta E_i/RT}, \quad \text{if} \quad \Delta E_i < 0.$$

LITERATURE CITED

1. O.Ya. Samoilov, Structure of Aqueous Solutions of Electrolytes and Hydration of Ions [in Russian] (Izd. AN SSSR, Moscow, 1957).
2. O.Ya. Samoilov, Disc. Faraday Soc. 24, 141 (1957).
3. K. Wirtz, Z. Naturforsch. 3a, 12, 672 (1948).
4. G. Sartori and C. Furlani, Z. phys. Chem., Neue Folge (Frankfurter Ausgabe) 15, 336 (1958).
5. O.Ya. Samoilov, Zhur. Fiz. Khim. 33, 5, 1147 (1959).
6. O.Ya. Samoilov, Doklady Akad. Nauk SSSR 126, 2, 330 (1959).

A SECOND CHAPTER IN THE CHEMICAL CRYSTALLOGRAPHY OF THE SILICATES

N.V. Belov

Institute of Crystallography, Academy of Sciences of the USSR
Translated from Zhurnal Strukturnoi Khimii, Vol. 1, No. 1, pp. 39-50,
May-June, 1960
Original article submitted December 12, 1959

The classical studies of the 1930's formed the first chapter in the chemical crystallography of the silicates, which deals mainly with silicates containing small cations (Mg, Fe, Al). The second chapter is derived from studies made on silicates containing large cations. The cations play the decisive part, not the silicon-oxygen radicals; the latter form strong but flexible elements of the structure, whereas the former determine the sizes taken by the octahedra; the flexible elements adapt themselves to the rigid structure formed by the octahedra. The edges of the octahedra formed by large cations (Ca, Na) are comparable in length with the Si_2O_7 groups characteristic of this second class of silicates.

Here we consider from a single point of view, the structures of glass and of silicates containing Zr, Ti, Ta, Nb, Mn, and TR.

The chemical crystallography of silicates is a subject that developed rather late in the USSR. It is true that we can point to Wulff's very early predictions about the structure of mica, which were made in the early 1920's, but this is an isolated feature. These predictions were very penetrating, being based on the epitaxis of KI on mica, but they were to some extent accidental, for they had no solid basis in experiment, as indeed they could not have had at that time.

The start of Soviet chemical crystallography may be dated to 1934-5, when Ferman proposed that we should produce a Russian translation of Hassel's Chemical Crystallography (which had a large section on silicates), and directly afterwards there appeared the third volume 'The Basic Principles of Geochemistry', which contained sections such as Bragg's and Schiebold's 'Structure of the Silicates'. Again, in 1935, Bernal presented (in Leningrad and Moscow) a series of lectures on chemical crystallography, in which he devoted much attention to silicates. A still more important event was Bernal's personal participation in the first complete structure study of a silicate (catapleiite) in the USSR (1935-6), which was performed in the x-ray section of the Laboratory of Crystallography, Academy of Sciences of the USSR, by the creator and first head of that laboratory, Brunovskii [1].

Further progress here and abroad was slow, the reasons being many. Firstly, it was believed (quite without foundation) that the chemistry of the silicates is governed by a minimum number of principles (although those minerals make up 95% of the Earth's crust), and that the very small number of silicon-oxygen radicals had been established once and for always in Bragg's laboratory at Manchester in 1926-1931; those radicals had been standardized in his book of 1930-1. Further, it was considered that the only supplements needed were Pauling's structures for silicates such as mica, the chlorites, etc. The remaining tasks appeared to be only to assign new silicates to the Bragg-Pauling classes. Catapleiite, $Na_2ZrSi_3O_9 \cdot 2H_2O$ appeared to be an example of this; it was the second silicate having $[Si_3O_9]$ rings, which appeared also in Bragg's system in bentonite $BaTiSi_3O_9$. Today it may cause surprise to learn that Bragg and Pauling's structures are still retained as standards and are reproduced after 25 years without changes of any kind in courses on chemical crystallography and mineralogy [see, for

example, Winkler's "Chemical Crystallography" (2nd edition, 1957) and Strunz's "Mineralogical Tables"(also 1957)]. None the less, some few silicates that have been studied since that time can be fitted adequately to those structures; for example, the structure of dioptase $Cu_6[Si_6O_{18}]\cdot 6H_2O$ which has been elucidated in the x-ray laboratory of the Institute of Crystallography, is an example of a silicate with a sixfold silicon-oxygen ring [2]; and ramsayite $Na_2Ti_2Si_2O_9$ (same laboratory), which is another example of pyroxene-type $[SiO_3]_\infty$ rings [3], but with the essential difference that the formula is that of an orthosilicate ($O:Si = 4.5:1$). not that of a metasilicate. A more surprising discovery was that of a new form of silicon-oxygen ring in milarite (same laboratory [4]); the ring again is sixfold, but this time has two layers, the formula being $[Si_{12}O_{30}]$. This was then the sole example of a doubled form of the ring found in beryl, and was all the more surprising, because milarite is a beryllium mineral with a related formula:

Beryl (He) $Be_3Al_2[Si_6O_{18}]$.
Milarite $KBe_2AlCa_2[Si_{12}O_{20}]$*.

Further progress was slow, on account of technical difficulties; the simpler objects had been exhausted, and there remained only complex structures with 20 or 30 parameters or more; such structures could not be solved by means then available. A major breakthrough occurred in 1952, when new direct methods were developed abroad and subsequently (in the main) here. These gave solutions even when the number of unknowns was large, the sole condition (hardly a serious restriction) being that the number of atoms in the unit cell must be less than 80-100. These new methods differ from the classical ones in that they work best when the symmetry is low, and best of all for the monoclinic system, to which most minerals (in particular silicates) belong. Methods of calculation had become very complicated, but these were found to be adaptable to machines. A very important feature was that the Institute of Crystallography was able to organize a training scheme at Gor'kii University, which provided a staff for the laboratories. The result was that a stream of papers began to appear from 1953 onwards from the Moscow laboratories and from the closely associated Gor'kii and Baku workers; these dealt with many silicate structures (ilvaite $CaFe^{\cdot\cdot\cdot}Fe^{\cdot\cdot}{}_2Si_2O_8OH$ [5], epidote [6], β-zoisite [7], $Ca_2Al_2FeSi_3O_{12}OH$ cuspidine $Ca_4[Si_2O_7]F_2$ [8], xonotlite $Ca_6[Si_6O_{17}](OH)_2$ [9], wollastonite $CaSiO_3$ [10], gadolinite $Fe^{\cdot\cdot}Y_2Be_2O_2Si_2O_8$ [11], seidozerite $Na_2(Mn_{0.5}Ti_{0.75}Zr_{0.75})Si_2O_7F_2$ [12], lovenite $(Na, Ca, Mn)_3(Zr, Ti)Si_2O_8F_2$ [13], lovozerite $Na_2ZrSi_6O_{15}\cdot 3H_2O$ [14], epididymite $NaBeSi_3O_7(OH)$ [15], rhodonite $MnSiO_3$ [16], and hillebrandite $2CaO\cdot SiO_2\cdot H_2O$ [17]) and provided material for a reconsideration of the chemical crystallography of the silicates.

Six of the above structures correspond to the orthosilicate formula but have $[Si_2O_7]$ as their silicon-oxygen radical, which was almost entirely neglected in the classical treatment of 1930-53. The binuclear Si_2O_7 group is prominent in chains, strips, grids, and rings in all of the others; these chains etc. differ very greatly from the classical (Bragg) ones. The milarite ring may be interpreted as made up of six Si_2O_7: $6Si_2O_7 - 6\cdot 2O = Si_{12}O_{30}$.

Almost all of these minerals are either pure Ca silicates or are silicates containing (apart from Ca and Na, which are always present) Zr, Ti, Nb, Ta, Mn, TR, and other "heat-resisting" elements. The conclusion was that the large cations have caused the building unit to become Si_2O_7 instead of the SiO_4 of the Bragg silicates, in which the main cations are Mg, Fe, and Al (all small). These purely structural features gave rise to the at-first-sight paradoxical conclusion that the cations (not silica or silicon-oxygen radicals) form the basis of the silicates (usually the cations are simply inserted in rods made up of oxygen octahedra), the silicon-oxygen radicals being fitted around those basic units. Silica, which is chemically very inactive, appears just as inert in crystal structures. The silicon-oxygen chains, strips, grids, and even rings are strong but are not rigid. They are readily deformed and are adaptable to the conditions produced by the cations. It was mentioned previously that dioptase contains sixfold silicon-oxygen rings, which are a basic feature of beryl. This is not exactly so; for the $[Si_6O_{18}]$ ring in beryl has the maximum symmetry (a sixfold axis and a mirror plane), whereas three of the six tetrahedra in dioptase are displaced upwards and the other three downwards. The reason is that the nucleus of the structure of $Cu_6[Si_6O_{18}]\cdot 6H_2O$ is a ring (as it were, taken from ice) consisting of six H_2O having the characteristic rhombohedral symmetry (see [18]). This feature is sufficiently marked to dominate the sixfold silicon-oxygen rings of dioptase.

* Later [25] it became apparent that the milarite rings are basic structures, which have become famous as molecular sieves.

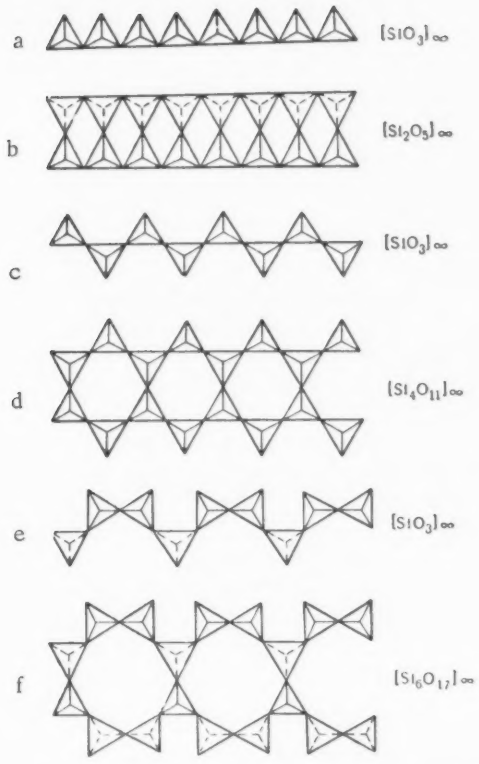

Fig. 1. The basic types of silicon-oxygen chain and strip (doubled chain) in the first and second chapters of the chemical crystallography of the silicates: a) and b) period one Si tetrahedron ($CuGeO_3$ chain and sillimanite strip); c) and d) period two Si tetrahedra (pyroxene chain and amphibole strip); e) and f) period three (2+1) Si tetrahedra (wollastonite chain and xonotlite strip).

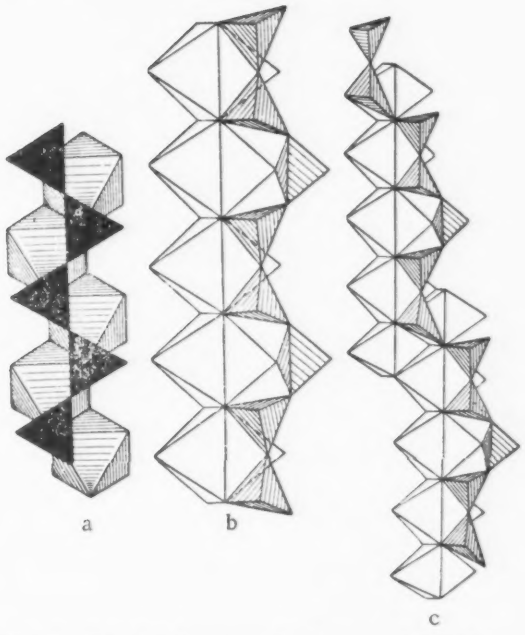

Fig. 2. Relation between the shapes of $[SiO_3]_\infty$ metasilicate chains and the structures of the corresponding columns of cation octahedra: a) in pyroxenes; b) in pyroxenoids (wollastonite); c) in rhodonite.

The best illustration of this feature of silica (and of the radicals based on it) is fused silica (quartz glass), which has a minute thermal-expansion coefficicent; whereas almost all of the thermal expansion of any glass is made up of the contributions from the large cations to the complete exclusion of the Si.

After 25 years, the classical (Bragg) treatment appears only as the first chapter in the subject, and that the one dealing with the relative small cations Mg, Fe, and Al, which produce around themselves octahedra whose edges are comparable (Goldschmidt's term) with the edges of SiO_4 tetrahedra. Large cations (primarily Ca and Na) make the edges of the octahedra no longer comparable with those of SiO_4 tetrahedra (3.8 A as against 2.6 A); the basic unit becomes Si_2O_7 (the edge of the trigonal prism in which that group is inscribed is 4-4.2 A long), and we pass to the second chapter [19].

The single SiO_4 tetrahedra and the comparable Mg octahedra may be arranged quite readily in a close-packed array (see [18]).

The complex radicals (chains, strips, and grids of six-membered rings) made up from SiO_4 tetrahedra do not lose this power to pack in with Mg octahedra, so we find minerals of high density (> 3), which are commonly dark (melanocratic) as a result of extensive isomorphous replacement of Mg and Al by small cations that produce color (Ti, V, Cr, Mn, Co, Ni), especially Fe in both states of oxidation. Light rock-forming minerals of lower density (< 3) are produced when the cations are large, for the basic group is Si_2O_7, which gives rise to relatively open radicals (eight-membered rings form a characteristic feature of these); these minerals are colorless (leucocratic), because the large cations are few (K, Na, Ca) and give no color on account of their completed outer octets.

The beryl-milarite pair is an interesting illustration of this. The first has Al cations in its octahedra, the second Ca (Al partly replaces Be in the tetrahedra in this case). The SiO_4 groups are coupled to aluminium nuclei; the Si_2O_7, to calcium. Both are included in six-member rings, one-layer in beryl and two-layer in milarite. Beryl is a dark-colored mineral (emerald), whereas milarite is leucocratic.

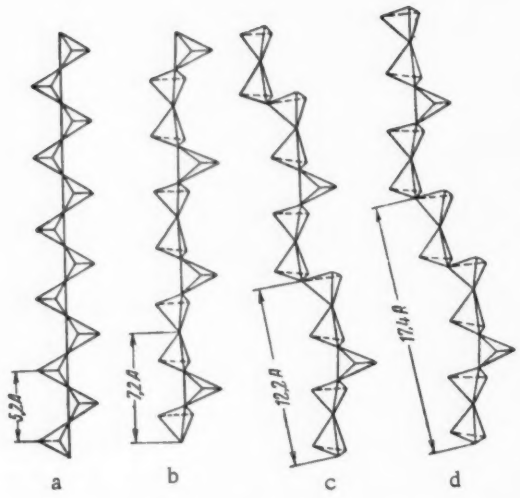

Fig. 3. Various known forms of metasilicate chain of general formula $[SiO_3]_\infty$: a) pyroxene, unit $[Si_2O_6]$; b) pyroxenoid, $[Si_3O_9]$; c) rhodonite, $[Si_5O_{15}]$; d) pyroxomangite, $[Si_7O_{21}]$.

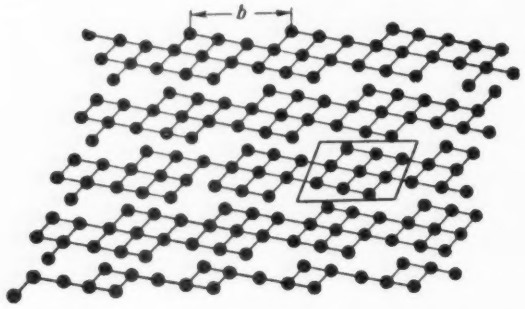

Fig. 4. Arrangement of the $Mn^{"}$ ions in rhodonite. The central three in each set of nine $Mn^{"}$ ions is gripped between the three in front and the three behind. (Unit cell, b× c).

octahedra to another, results in a five-membered unit

Figure 1c and d, shows the silicon-oxygen chain and strip (double chain) that appear in Bragg's system. Nowadays, we recognise far more than these six, and the ones shown at e and f are the most typical of the second chapter, in which the Na and Ca silicates predominate.

We should not be too strict in setting the new silicon-oxygen radicals in opposition to the old ones, for Fig. 1e shows that the $[SiO_3]_\infty = [Si_3O_9]_\infty$ wollastonite chain contains clearly visible Si_2O_7 groups joined together by single SiO_4 tetrahedra. The reason may be found in the lengths quoted above; the height of an Si_2O_7 group (the edge of the prism circumscribing the group) is 4.0-4.2 A, which is longer than the edge of a Ca octahedron (3.7-3.8 A); in this respect the prism has to shorten one edge and lengthen another when it links up with the Ca octahedron, which makes it possible to couple Si_2O_7 groups via a single SiO_4 tetrahedron, as shown in Fig. 2b (another cause of the distortion is that the Si-O-Si angle has to deviate from 180° and approach 109° - see below). While the Mg metasilicates (pyroxenites) require two Si tetrahedra to two octahedra, the Ca metasilicates require three Si tetrahedra to match the height of two Ca octahedra.

Still more complex single metasilicate chains can be based on $[SiO_3]_\infty$ e.g., as in Fig. 3a-d. Let us consider the chain whose link contains five Si tetrahedra in some detail. Each Si_2O_7 section has on one side another Si_2O_7 section and on the other an SiO_4 tetrahedron. This chain occurs in $MnSiO_3$ (rhodonite) and is produced by the cation pattern, which consists of octahedra and which is somewhat unusual, presumably on account of some feature of the $Mn^{"}$ ion. All the columns of Mn octahedra are only nine units in length, the infinite pattern being produced by the means indicated in Fig. 4 and detailed in Fig. 5 (after Mamedov). The silicon-oxygen radical adapts itself to that pattern and, by transferring from one set of nine $[Si_5O_{15}]$, as shown in Fig. 2c *

Figure 6 shows the silicon-oxygen grids of the second chapter; the most characteristic element is the eight-cornered ring (each consisting of four Si_2O_7 groups), which differs from the six-cornered rings typical of kaolin, mica, the chlorites, and other such silicates. Hexagons can fill an unbounded plane completely, whereas octagons cannot; the latter alternate with quadrilaterals and pentagons, a feature that is characteristic of the second chapter [20].

In Fig. 7 a tobermorite grid of the Si tetrahedron is represented, which is particularly characteristic for the second chapter of crystal-chemistry of silicates; it is "pleated" with a disposition of the Si tetrahedrons on two levels, that results in a relation of the number of its eight-cornered rings to the six-cornered and four-cornered ones of 3:1:1 [21].

* All single chains, no matter what the number of tetrahedra in a link, have the formula $[Si_n O_{3n}]_\infty = [SiO_3]_\infty$ but various formulas are obtained when the chains are combined; if the rings have four members (and the links are single) we have $2SiO_3 - O = Si_2O_5$; if six (two units in a link), $4SiO_3 - O = Si_4O_{11}$; if eight (three units in a link), $6SiO_3 - O = Si_6O_{17}$.

A point here (which became apparent some while ago) is that apophyllite (tetragonal mica) and the feldspars contain eight-membered rings alternating with four-membered ones. The latter minerals make up 60% of the Earth's crust, and it is of some value to consider how these are formed in the light of the two chapters. We have stated [22] that nothing is known about the sequence in which natural minerals are produced from a magma** except that we know the melting points of the simplest oxides, so we must proceed as follows. The first to be deposited must be MgO and CaO as having the highest melting points (2800 and 2580°C respectively). These crystallize independently, because their oxygen octahedra (in periclase and lime) are not comparable in size. As the temperature falls, silica combines in steadily increasing amounts with the primary MgO and CaO, but the forms taken are different, because the dimensions must be compatible; the Mg minerals contain single SiO_4 tetrahedra (olivines) and the Ca ones Si_2O_7 (Ca feldspar - anorthite). The original SiO_4 and Si_2O_7 groups condense respectively into the radicals of the first and second chapters as the proportion of SiO_2 in the solid increases. This principle applies to the entire course of crystallization of the main rock-forming minerals; the process is described by Bowen's scheme, in which the left (Mg, Fe) branch contains the minerals of the first chapter and the right (Ca-Na) contains those of the second chapter*:

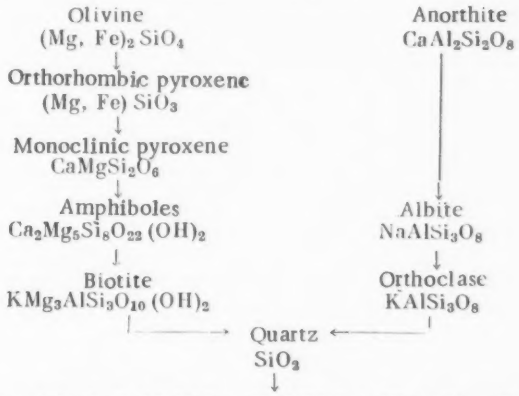

The feldspar sequence on the right is $CaAl_2Si_2O_8 \rightarrow NaAlSi_3O_8$. The silica (25%!) is so inert that it needs the help of alumina (9%) to enter the lattice in the first stage (anorthite contains $SiAlO_7$ groups instead of Si_2O_7); albite contains more Si, but SiO_2 appears as an independent mineral (quartz) only in the low-temperature stage.

Two further features of the silicon-oxygen radicals may be mentioned in order to illustrate the extreme inertness of silica and the tendency for it to adapt itself to the setting governed by the cations. It is very common in the chemistry of glass, cement, and ceramics to speak of platelet structures, of silicon-oxygen grids, and of angular fragments. X-ray and electron-microscope studies have shown that the platey minerals in which a layer of cations in their octahedra is armor-plated by a flat network of silicon and oxygen atoms on one side only (as in Al halloysite and Mg chrysotile) are normally coiled into spiral tubes each nine or ten layers thick. The grid structures are still thinner in silicate masses, and so are even more capable of being deformed into tubes, etc.

---

* We have a useful low-temperature model of this process in the Ca hydrosilicates. If the material is very basic, we get layered portlandite (brucite type) $Ca(OH)_2$ deposited, in which a layer of fully populated Ca octahedra is followed by a layer of empty ones and so on. Between these layers there appear xonotlite chains as the basicity decreases; at first the number of empty layers between the $Ca(OH)_2$ ones greatly exceeds the number of xonotlite chains, but eventually the 1:1 ratio of hillebrandite is reached [17], whose structure may be represented in the form:

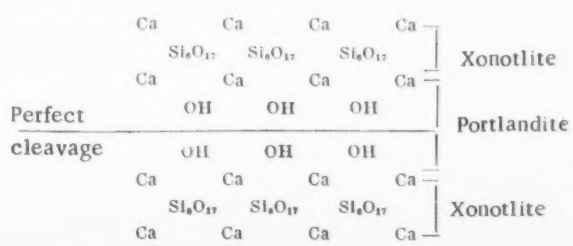

** The composition usually assumed is 50% O, 25% Si, 9% Al, and 3% Mg, Fe, Ca, Na, K, etc.

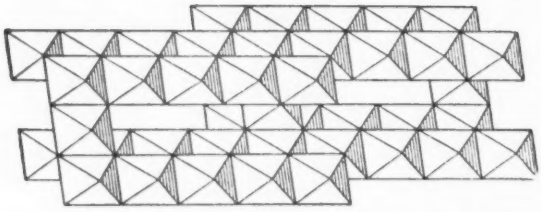

Fig. 5. Combination of sets of nine $Mn^{"}$ octahedra one with another and with similar sets in the next lower level of rhodonite.

The Si ions adapt themselves to the tendency of the O ions to produce by themselves tetrahedral angles of 109°. In quartz we find a compromise Si-O-Si angle of about 150° (i.e., between 109 and 180°). The diorthosilicates contain Si_2O_7, which is to be inscribed in a trigonal prism instead of into a centrosymmetric octahedron, which might appear more suitable to pack in with the cation octahedra; the central O atom of Si_2O_7 is in the equatorial plane of symmetry in the prism; it may be displaced to produce a compromise Si-O-Si angle without the prism losing its symmetry plane.

Thus, the main form in which silica is found in the ordinary Ca-Na glasses is as Si_2O_7 groups, which condense further into broken chains of random length, and into the other structures characteristic of the second chapter. This is why the crystalline phase (surface layer) extracted from glass is commonly composed of crystobalite and tridymite, whose structures most clearly demonstrate the presence of Si_2O_7.

Sometimes the silicon-oxygen radicals adapt themselves to the two main kinds of cation simultaneously. In epidote $Ca_2Al_2FeSi_3O_{12}(OH)$ we have columns of Al octahedra along c and columns (not so straight) of seven-cornered Ca figures (semioctahedron with a half-prism) along a; the expanded formula of the mineral is $CaAl_2FeO[SiO_4][Si_2O_7](OH)$, which contains ortho groups and diortho groups. The first are connected only to the columns of Al octahedra and the second to the Ca polyhedra, but only along the axes of the $O_3Si\text{-}O\text{-}SiO_3$ groups. The short edges (the edges of the bases of the Si tetrahedra in the Si_2O_7) are coupled also to the Al octahedra without injury to the essential compatibility in size. Ilvaite (the first diorthosilicate with the standard formula we succeeded in elucidating) has $Ca_2Fe^{"'}Fe_2^{"}Si_2O_8OH = CaFe^{"'}Fe_2^{"}O[Si_2O_7]OH$, in which both functions are performed (there are columns of Fe octahedra and of Ca polyhedra); a single Si_2O_7 group performs both functions with different O-O edges (short and long).

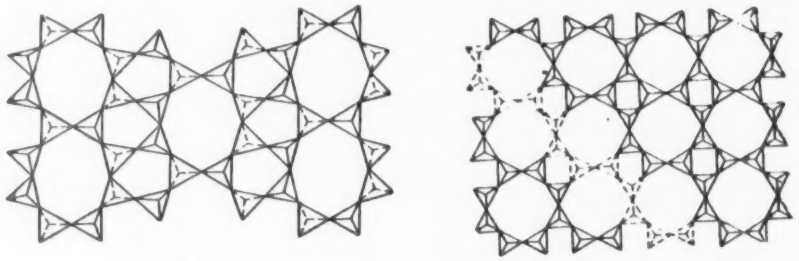

a b

Fig. 6. Single-layer silicon-oxygen networks of the second chapter: a) apophyllite; b) okenite.

The role of Na as an agent for stretching the Si_2O_7 groups appears very clearly in the synthesis of quartz, a mineral that grows very readily in nature, but which proved difficult to grow in the laboratory until solutions of sodium carbonate were used to provide Na cations to extract the Si from the raw material and transfer it to the seed in the best (extended) form.

Any treatment of the processes in silicate masses, ceramics, glasses, and cements must take account of the fact that the main form factor arises from the rods, layers, and plates of Mg(Ti) and Al octahedra in ceramics (mullite), of Ca octahedra in cements, and of Ca and Na octahedra in glasses. These columns and layers are characteristic of most of the structures in the second chapter; to them are fitted the strong but flexible silicon-oxygen radicals. A very notable feature is provided by the thermal-expansion coefficients of glasses, which (see [23]) are entirely determined by the cations and scarcely depend at all on the SiO_2 content.

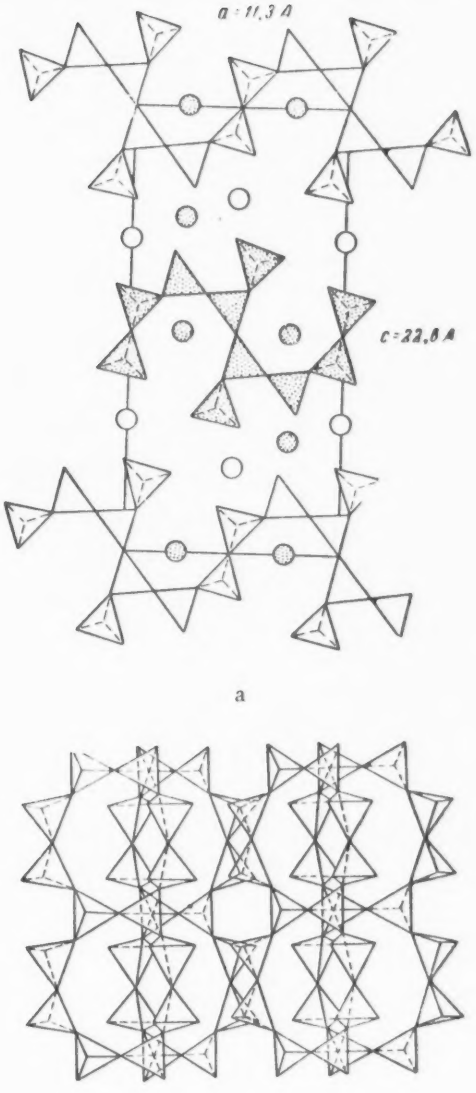

Fig 7. Two-layer tobermorite grid: a) projection taken along xonotlite strips fused into a grid; b) mechanism of folding (mutual superposition of xonotlite rings).

The structure of the minerals listed in the early part of this paper form the main experimental basis of this second chapter in the chemical crystallography of the silicates; the minerals are of two types, namely the Ca hydrosilicates of cement and the alkali silicates containing element such as Zr, Ti, Nb, Ta, Mn, and TR, which have presented us with two principal problems. It appears that all of these structures are govered by the same laws as regards the cation rods and the silicon-oxygen radicals (the latter controlled by the former), in which case the problems become very similar, if not identical. The above elements, especially Zr, and also Ti, Nb, and Ta, give cations that are not so big as by themselves to make the silicates large-cation ones, but they appear in fair amounts in minerals also containing Ca and Na. One outstanding success in the x-ray laboratory at the Institute of Crystallography in 1959 was Simonov's demonstration that the structure of lovenite $(Na, Ca, Mn)_3(Zr, Ti)[Si_2O_7]OF$ (from the Kola peninsula) is one in which the silicon-oxygen and cation patterns of the Ca silicate cuspidine $Ca_4[Si_2O_7]F_2$ are reproduced exactly (the structure of cuspidine was established by Smirnova in the same laboratory in 1954). But, although the patterns are the same in both, the cation columns in the latter are made up of Ca octahedra, whereas the columns in the former (which are precisely analogous) are [13] made up of Zr and Ca octahedra; on the other hand, in other (crystallographically distinct) silicates the Ti(Fe) octahedra are mixed with Ca and Na octahedra (Fig. 8). Previously Simonov had demonstrated that the structure of seidorzerite $Na_4Zr_2TiMn[Si_2O_7]_2O_2F_2$ (also from the Kola peninsula, Fig. 9) contains three crystallographically distinct kinds of columns: in the first kind there are Zr octahedra with Na octahedra; in the second, Ti and Na; and in the third, Mn and Na. In each column octahedra responsible for color (Zr, Ti, Mn) alternate with colorless Na octahedra [12]. The discovery of this feature resolves a number of problems in silicate chemistry, including problems concerned with the varieties of silicon-oxygen radicals and with the forms taken by those radicals, and also problems related to the nature of the titanosilicic and zirconosilicic acids that feature so prominently in the mineralogical literature. It is clear from the examples we have presented that these silicates are not Ca or Na salts of those acids but are complex oxide compounds resembling niobates and tantalates in the form of "polyrutiles": $FeNb_2O_6$, $FeTa_2O_6$.

The results serve as the basic material for the second chapter, and they have revealed the basic laws to be applied, especially that this second class of silicates is primarily one having colorless cations (especially the Ca silicates and hydrosilicates, i.e., cement minerals and artificial compounds). We have elucidated the structures of several such silicates (Mamedov's group has done most of the work on this topic), produced a new scheme for the successive condensations of the new silicon-oxygen chains, and have demonstrated the relations with the cement silicates, especially as regards bonding properties. The feature responsible for those properties (for the tendency of the chains to adapt themselves to different structures) is that the chains are double (we have called these xonotlite chains above); when these chains break up (at high temperatures) into single wollastonite chains, the bonding properties are lost. The strongest cement compound (tobermorite) has the largest number of

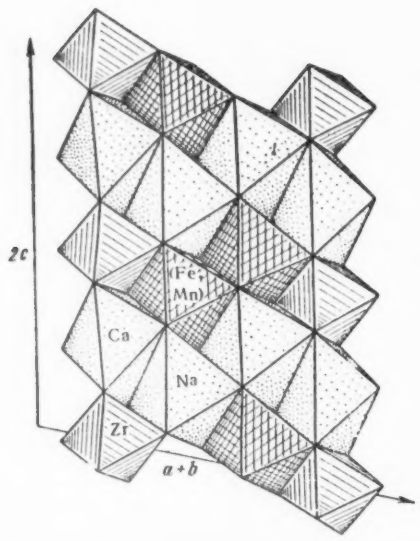

Fig. 8. The basic pattern in the structure of lovenite.

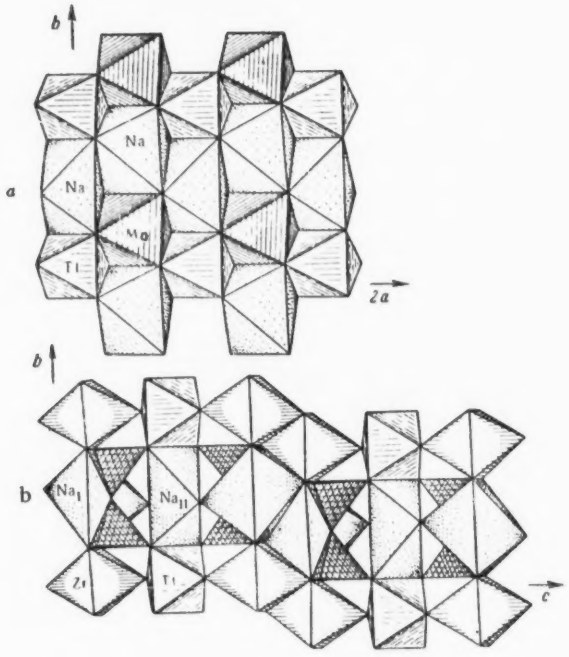

Fig. 9. The basic pattern in the structure of seidozerite: a) xy projection; b) yz projection.

xonotlite configurations (Mamedov). There are many Ca hydrosilicates that form and decompose during all stages of the preparation and use of cement, which gives us an enormous field in which to apply x-ray analysis, whose results may easily be transferred to the chemical crystallography of glass*.

An important feature is that the Li silicates appear in the second chapter, although they appear there in various ways. Mineralogists have long been aware of the analogy between lithium and manganese, but it was unexpected when Simonov [24] demonstrated that the small Li shows a resemblance to the large Ca, in that lithium resembles hydrogen (its analog in the first group of the periodic table) in oscillating in crystal structures, which behavior makes it resemble the large Ca; again, in other cases, Li resembles Si in the sense that Li can form the center of a tetrahedron, in which it is analogous to silicon (Li analogs of the Ca garnets); this in addition to its resemblance to its nearest neighbors, namely Be and B.

* This term is met more and more frequently, and, although it is nonsense if taken literally, the meaning it is meant to convey is clear. The chemistry of silicates for long was a purely empirical subject, in which only oxide formulas were real; in that respect it was blot on the face of modern chemistry, which demands that molecules and radicals must be represented as they actually are (in three dimensions) and that configurations must be represented in terms of linear parameters (bond lengths) and angles (valence angles); whereas the structures of silicates that do not dissolve without decomposition can be derived only by means of x-ray diffraction (occasionally, electron or neutron diffraction) applied to crystals. Modern ideas on the processes occurring in glass are based on the idea that a fixed chemical crystallography is the basis of the elementary silicon-oxygen radicals even for amorphous disordered materials such as glass; this is the reason why the chemistry of glass is sometimes referred to as being part of chemical crystallography.

Nonsense of this kind persisted for a long time in the chemistry of the Ca hydrosilicates (cements). The obstacle to progress here was not that these Ca hydrosilicates are amorphous but that the crystals are extremely small (were too small for analysis). Progress in x-ray methods made it possible to examine these microcrystals, whereupon the chemical crystallography of cements became chemical crystallography in the proper sense of the word; it became little different from the chemical crystallography of silicates having macroscopic crystals.

LITERATURE CITED

1. B.K. Brunovskii, "The structure of catapleiite," Acta phys. chim. USSR 5, 863 (1936).
2. N.V. Belov, V.P. Butuzov, and N.I. Golovastikov, Doklady Akad. Nauk SSSR 37, 156 (1942); 87, 6, 953 (1952).
3. N.V. Belov and L.M. Belyaev, Doklady Akad. Nauk SSSR 69, 6, 805 (1949).
4. N.V. Belov and T.N. Tarkhova, Doklady Akad. Nauk SSSR 69, 3, 365 (1949); Trudy Inst. Kristall. Akad. Nauk SSSR 6, 25 (1949).
5. N.V. Belov and V.I. Mokeeva, Doklady Akad. Nauk SSSR 81, 4, 581 (1951); Trudy Inst. Kristall. Akad. Nauk SSSR 9, 49 (1954).
6. N.V. Belov and I.M. Rumanova, Doklady Akad. Nauk SSSR 89, 5,853 (1953); Trudy Inst. Kristall. Akad. Nauk SSSR 9, 105 (1954).
7. E.G. Fesenko, I.M. Rumanova and N.V. Belov, Doklady Akad. Nauk SSSR 102, 2, 275 (1955); Kristallografiya 1, 2, 171 (1956).
8. R.F. Smirnova, I.M. Rumanova, and N.V. Belov, Zap. Vses. Min. Obshch. 84, 2, 159 (1955).
9. Kh.S. Mamedov and N.V. Belov, Doklady Akad. Nauk SSSR 104, 4, 615 (1955); Zap. Vses. Min. Obshch. 85, 1, 1339 (1956).
10. Kh.S. Mamedov and N.V. Belov, Doklady Akad. Nauk SSSR 107, 3, 463 (1956).*
11. P.V. Pavlov and N.V. Belov, Doklady Akad. Nauk SSSR 114, 4, 884 (1957).*
12. V.I. Simonov and N.V. Belov, Doklady Akad. Nauk SSSR 122, 3, 473 (1958);* Kristallografiya 4, 2, 163 (1959).
13. V.I. Simonov and N.V. Belov, Doklady Akad. Nauk SSSR 131, 1, 133 (1960).*
14. V.V. Ilyukhin and N.V. Belov, Doklady Akad. Nauk SSSR 131, 1, 176 (1960).*
15. E.A. Pobedimskaya and N.V. Belov, Doklady Akad. Nauk SSSR 129, 4, 900 (1959).*
16. Kh.S. Mamedov and N.V. Belov, Doklady Akad. Nauk SSSR 123, 4, 741 (1958).*
17. Kh.S. Mamedov, Doklady Akad. Nauk Azerb. SSR 14, 6, 445 (1958).
18. N.V. Belov, Structures of Ionic Crystals and of Metallic Phases [in Russian] (Izd. AN SSSR, Moscow, 1947).
19. N.V. Belov, "An outline of structural mineralogy, X," Min. Sborn. L'vov. Geol. Obshch. 13, 23 (1959).
20. Kh.S. Mamedov and N.V. Belov, Doklady Akad. Nauk SSSR 121, 4, 720 (1958).*
21. Kh.S. Mamedov and N.V. Belov, Doklady Akad. Nauk SSSR 123, 1, 163 (1958).*
22. N.V. Belov, "Chemical crystallography of the main crystallization process in a magma," in coll.: Geochemistry of the Rarer Elements in the Light of Petrogenesis; An International Symposium, 1957 [in Russian] (Moscow, 1958).
23. St. Naray Szabo, Acta phys. Acad. Scient. Hungaricae IX, 4, 403-422 (1959).
24. V.I. Simonov and N.V. Belov, Doklady Akad. Nauk SSSR 119, 2, 353 (1958);* Kristallografiya 3, 4, 428 (1958).
25. N.V. Belov, "An outline of structural mineralogy," Min. Sborn. L'vov. Geol. Obshch. 14 (1960).

* Original Russian pagination. See C.B. translation.

THE STRUCTURE OF EPIDIDYMITE $NaBeSi_3O_7(OH)$. A NEW TYPE OF $[Si_6O_{15}]$ CHAIN

E.A. Pobedimskaya and N.V. Belov

Lomonosov State University Moscow
Translated from Zhurnal Strukturnoi Khimii, Vol. 1, No. 1, pp. 51-63,
May-June, 1960
Original article submitted December 25, 1959

An x-ray study has been made of epididymite $NaBeSi_3O_7(OH)$. Ordinary and weighted projections have been used to deduce the structure. The coordinates of all Si, Na, O, and Be atoms have been found. The structure is based on columns of Na polyhedra having strips of composition Si_6O_{15} running parallel; these strips are duplicated wollastonite chains. The Si_6O_{15} strips combine with Be tetrahedra to form double layers perpendicular to c.

Epididymite is a rare Na-Be silicate which has been found in the USSR in the Kola peninsula [1]. Recent studies agree with Gossner and Kraus's finding [2] that epididymite (and especially the monoclinic form thereof, eudidymite) resembles the feldspars very considerably (in density and optics), but there is also a considerable resemblance to the micas [3], which appears as perfect cleavage on (001), tabular habit, and pseudohexagonal behavior.

Ito [4] proposed a structure in 1934; the main feature was the $[Si_3O_8]_\infty$ chains (Fig. 1) running parallel to b = 7.34 A*. This was only a tentative proposal, made before Patterson methods were available; the pattern was in agreement with the cell parameters and with the symmetry, but there was no proper x-ray confirmation. The proposed structure had many defects; the Si-Si distances in the silicon-oxygen tetrahedra varied from 1.11 to 2.80 A, and other unacceptable features were Be-Si and Be-O separations of 0.54 and 0.72 A respectively. The Na atom located at a center of symmetry was enclosed (on the common faces of the Na octahedron) by two Si tetrahedra (Fig. 2). Wyckoff [8] pointed out that the structure must be revised.

We had available specimens from Yu.A. Pyatenko's collection and also specimens we collected ourselves during 1958 near Lovozero (Kola peninsula). We used single crystals 0.3-0.5 mm in size, all of which were in the form of plates or tablets. The main results have been derived from eight Weissenberg photographs on b and two (the zeroth and first) on a. Good results were not obtained on c; the spots were irregular in shape, and there were many spots in excess [both effects are caused by the resemblance to mica; the layers are displaced along (001), the perfect cleavage direction].

*Berman [5] proposed a chain of this type for minerals of the wollastonite group (for xonotlite in particular); b is about 7.3 A in nearly every case. Mamedov and Belov rejected Berman's model on the basis of their results for xonotlite [6] and wollastonite itself [7]; they proposed a metasilicate chain $[SiO_3]_\infty = [Si_{2+1}O_9]_\infty$ for wollastonite, this chain differing only in the length of its links from the chain found in diopside. Nevertheless, the geometry of the silicon-oxygen radical in epididymite is closely related to the corresponding feature in wollastonite (see below).

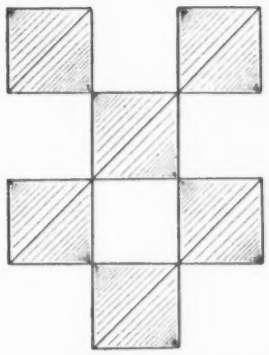

Fig. 1. Berman's $[Si_3O_8]_\infty$ chain.

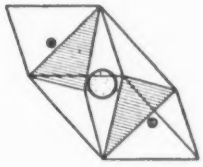

Fig. 2. Combination of a Na octahedron with two Si tetrahedra in Ito's structure for epididymite.

The cell parameters are a = 12.66, b = 7.34, c = 13.48 A which are close to Ito's values [4]; they agree well with the axial ratios given in 1894 by Flink [9] if we double c. The specific gravity (2.55) implies that the cell contains eight formula units $HNaBeSi_3O_8$.

The space group is D_{2h}^{16} = Pnam, as Zachariasen claimed in 1929 [10]. Tests for piezoelectric response (made in the Department of Crystal Physics at Moscow State University) gave negative results, which pointed to the presence of a center of symmetry, as did the intensity statistics [11] and the results obtained by the triplets method applied to the Patterson projections [12].

The resemblance to mica [10] (c is a pseudosixfold axis) appears in the ratio a : b (which is almost $\sqrt{3}$) and in the weakness of the reflections with h + k = 2n + 1 in the xy projection. The latter feature indicates that the lattice is pseudocentered on the C (= ab) plane, as we would expect.

The intensities were estimated visually by reference to 35 calibrated spots. We used different radiations (Mo and Cu) to determine the intensities for the zero layer lines, and then calculated mean values. The strong reflections were corrected by reference to the β spots. The structure amplitudes were calculated in the usual way with allowance for the polarization and kinematic factors. The $|F|^2_{max}$: $|F|^2_{min}$ were in the ratio 1000:1, approximately. Absorption was neglected in calculating the $|F|^2$, because this mineral is effectively semitransparent to x rays and because the specimens were roughly isometric.

The spots numbered about 2000, and the atoms are all similar in a atomic number, so one would expect that Zachariasen's statistical methods would solve the structure. But this laborious work did not give the expected result, because the atoms lie almost entirely in layers (see [13]) and the mineral is pseudohexagonal. Harker-Kasper methods could not be used, because the reference group contained only four reflections having absolute amplitudes ≥0.5. We were forced to use only Patterson functions.

The short axis is b, so we would expect that the P(uw) projection would show the fewest overlapping peaks; but Fig. 3* shows that the pattern is too complex to be interpreted without ambiguity, so we constructed weighted projecting P_1 (uw) and P_2 (uw) (from 303 reflections of h1l type and from 226 of h2l type respectively) in order to ease the task of locating the first-order** Si-Si peaks in P(uw). These projections had only one system of first-order peaks; they gave the x and z of the "heaviest" atom (Si) uniquely. The results were confirmed by taking Harker sections at the levels 0 and ½ along b, for which purpose we used 846 reflections from the first, second, and third layer lines appearing on the rotation photographs taken on b.

We constructed P(vw) (Fig. 4) from 68 0kl reflections and P_1 (vw) from 202 1kl reflections in order to find the third coodinate of this Si. Next we constructed M(uw), the minimal function [15], by superposition. Minimalization of P(uw) gave the coordinates of all the Si, and of six O out of ten. The M(vw) gave only the coordinates of the silicon and those less reliably, because the peaks were less sharp in the vw projection.

The Patterson diagram gave only the coordinates of Si_I unambiguously, so we used these most reliable coordinates to calculate the signs, without reference to the results from the minimalization, in order to construct the electron-density projection along b. Figure 5 shows the projection on the xz plane; we see that Si_I and Si_{III} coincide in σ(xz). The peak for Si_{III} has the same z as the first two, but x is doubled: $x_{I,II} = 10/60$; $x_{III} = 20/60$. This projection, in addition, shows peaks corresponding to the O atoms; almost all peaks in M(uw) have corresponding peaks in σ(xz). There is a rather large peak at the origin in σ(xz), which we at first

*The a' is halved in this projection as a result of the a glide plane normal to b.

**Porai-Koshits's name [14] for the peaks produced by the vectors between atoms in the same regular system.

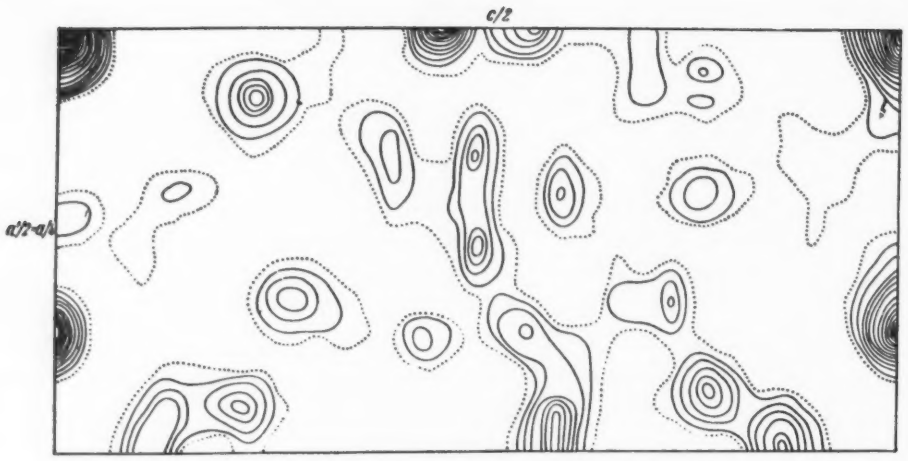

Fig. 3. Epididymite. Patterson projection along b.

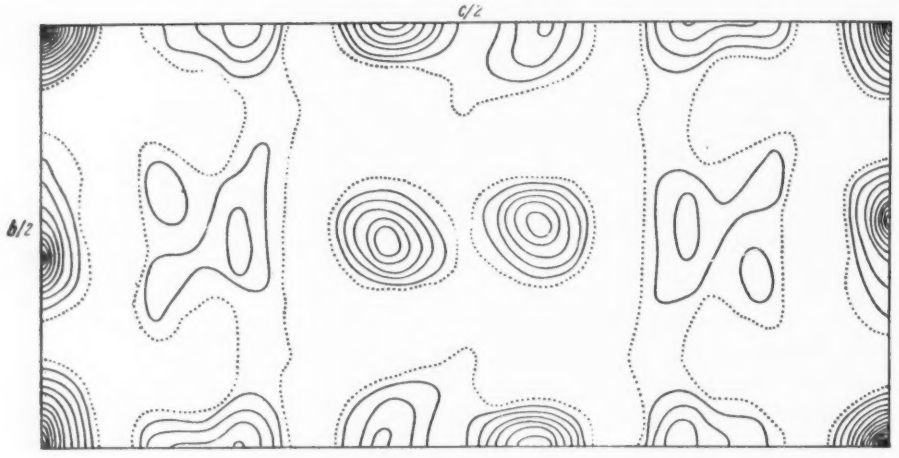

Fig. 4. Patterson projection along a.

took to represent Na; but the volume available for the Na polyhedron is inadequate, so the Na cannot lie at the inversion center. We found later that this peak corresponds to two Be atoms superimposed.

The electron-density projection constructed with allowance for the coordinates of three Si, ten O, and one Be had a further peak, which we naturally took to be Na. The x and z were revised, and then we calculated the structure amplitudes, which are compared with the experimental ones in Fig. 6. The superimposed pairs for Si (I and III) and O appearing in the xz projection facilitated the work on the projection along b, but it hindered the process of refining the coordinates, so R for the h0l reflections remained fairly large: 0.23 ($B = 0.56$ A^2, $\sin\theta/\lambda \leq 1.1$) ; when 17 zero-intensity reflections were allowed for ($\sin\theta/\lambda \leq 0.9$) we found that R was 0.24.

Three Si atoms were located by minimizing P(vw); the approximate y and the reliable z were used to calculate the signs for the 0kl zone. The electron-density projection on a (Fig. 7) gave revised y and confirmed most of the z. An error-series synthesis was used to refine the coordinates of Be and O. Here R for the projection along a was 0.21 ($\sin\theta/\lambda \leq 1$) or 0.225 with allowance for 12 zero-intensity reflections. Figure 8 gives the calculated and experimental 0kl structure amplitudes.

Table 1 gives the coordinates of the 15 basal-plane atoms. Except for the three kinds of O atoms (which lie in mirror planes), all atoms (including Na, of which there is only one kind - see above) lie in general eightfold positions, so the total number of parameters is $(15 \times 3) - (3 \times 1) = 42$.

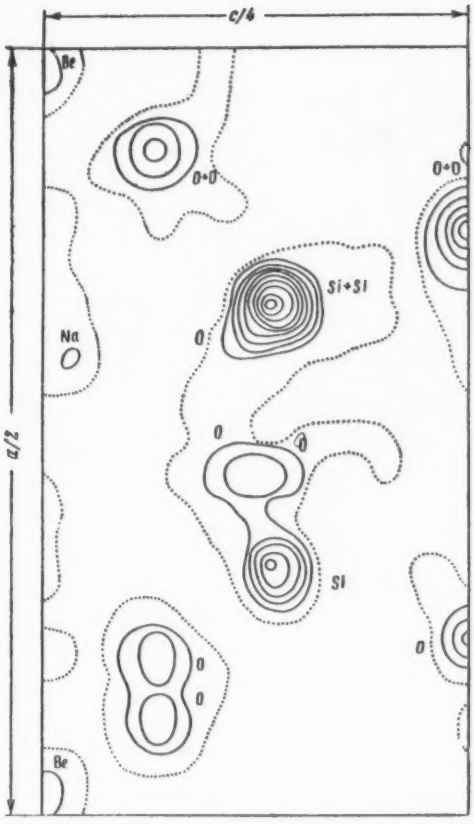

Fig. 5. Electron-density projection along b.

The Si-O distances vary from 1.59 to 1.74 A, and the Na-O from 2.1 to 2.7 A (compare the 2.14 to 2.62 A of [13]). The probable errors are given by Vainshtein's formula [16] as Si ± 0.004 A, Na ± 0.006 A, O ± 0.009 A, Be ± 0.023 A.

The Si-O-Si angles are 130; 134; 135.5; 139; 149 and 160°.

Table 2 gives the distances in each coordination polyhedron. Table 3 gives the same for Ito's coordinates. Table 4 gives the balance of the valencies for each of the ten kinds of O(OH) atoms (see Table 1).

The mineral resembles most other silicates [17] in having columns of oxygen polyhydra arranged around a large cation (here Na). Here the polyhedra have eight corners and take the form of the twisted cubes so characteristic of Ca grossular garnet and of the Na-Li analog cryolithionite ($CuAl_2$ [17] is composed exclusively of such polyhedra). The columns of Na polyhedra extend along the twofold screw axes parallel to b. Two such polyhedra occur in one b repeat distance (Fig. 9a), as in many silicates having columns of Na-Ca polyhydra that have been examined recently*; all of these structures have b very close to 7.3 A.

Here b = 7.3 A, and at three levels along that axis there are three SiO_4 tetrahedra, which form a link of a wollastonite chain $[Si_3O_9] = [Si_{2+1}O_9]$ in which two tetrahedra face one way and one the other.

Two such chains are joined into a band** as in xonotlite $Ca_6[Si_6O_{17}](OH)_2$ [6], although only every third tetrahedron is linked in the latter case, because the symmetry plane is normal to the plane containing the centers of all three tetrahedra in a link; whereas the symmetry plane in epididymite is parallel to the plane containing the centers, so all three tetrahedra in a link are joined. If xonotlite has $2[Si_3O_9] - O = [Si_6O_{17}]$, for the formula of its

TABLE 1

Relative Coordinates of the Basal Atoms in Epididymite†

Atom	x	y	z	Atom	x	y	z
Si_I	0,167	0,500	0,150	IV	0,075	0,017	0,075
Si_{II}	0,334	0,207	0,142	V	0,117	0,900	0,250
Si_{III}	0,152	0,877	0,132	VI	0,075	0,410	0,075
Na	0,194	0,167	0,492	VII	0,278	0,400	0,150
Be	0,025	0,215	0,032	VIII	0,200	0,684	0,095
I	0,400	0,225	0,042	IX	0,267	0,010	0,125
II	0,117	0,483	0,250	OH	0,050	0,780	0,078
III	0,384	0,130	0,250				

† The roman numerals denote the oxygen atoms.

* Cuspidine-tilleyite [19], wollastonite [7], xonotlite [6], foshagite-hillebrandite-tobermorite [20], seidozerite [13], and lovenite [21].

** G.B. Bokii predicted silicon-oxygen patterns of this type in a course of lectures on chemical crystallography he presented at Moscow State University in 1955.

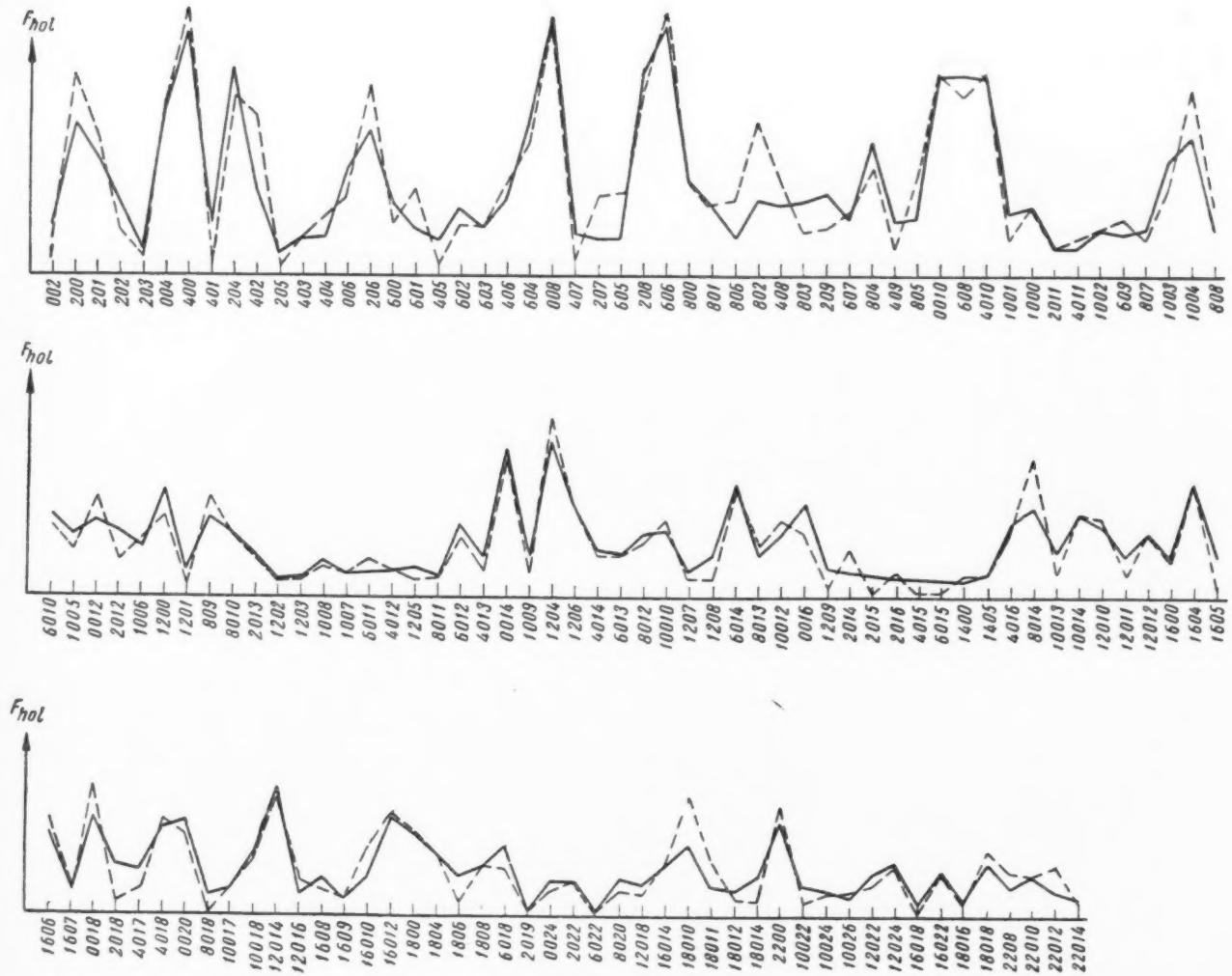

Fig. 6. Calculated and experimental $|F_{hol}|$ (broken and full lines respectively).

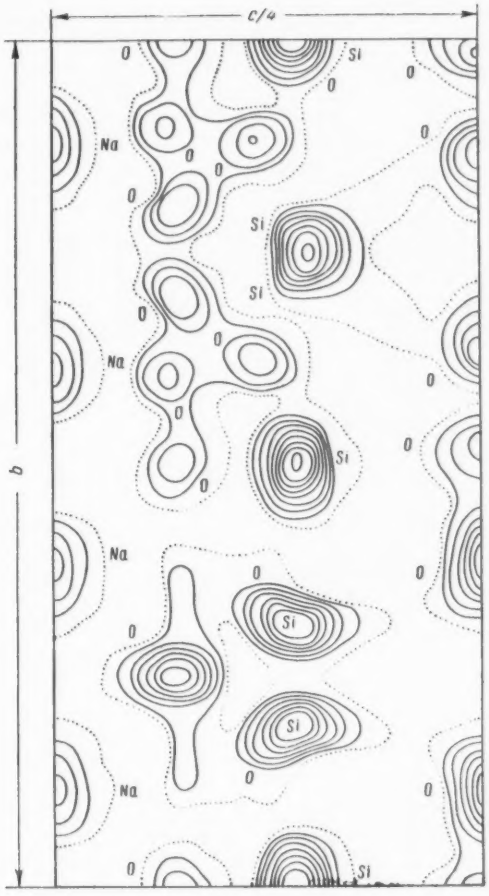

Fig. 7. Electron-density projection along a.

strip, more exactly, $[Si_{4+2}O_{17}]$, epididymite has $2[Si_3O_9] - 3O = [Si_6O_{15}] = [Si_{4+2}O_{15}]$. Figure 10 shows the wollastonite chain and the two kinds of strip produced by combining such chains. Figure 9b shows the $[Si_6O_{15}]_\infty$ strip, while Fig. 9c shows how this $[Si_6O_{15}]_\infty$ strip is combined with the twisted Na cubes. A Si_2O_7 group appearing in one half of the chain is linked to the diagonal square face of a Na polyhedron, while the third (single) Si tetrahedron is (see [17]) linked with the side of a square*. The second chain (half of the strip) is linked with the twisted cubes in another column.

A link of an epididymite chain divided by three is $[Si_2O_5]$, and a double chain having this unit for its links occurs in sillimanite $Al_2SiO_5 = Al^{VI}[AlSi^{IV}O_5]$ [14], although in this case half of the tetrahedra contain Al instead of Si and the centers of gravity of all tetrahedra lie in one plane, so the link is actually $[Si_2O_5]$, or rather $[SiAlO_5]$. Figure 10 illustrates the differences between the two types of chain and the three types of strip (double chain). The combination of chains is controlled (as in the Ca silicates) by the need to match two large polyhedra and three tetrahedra in a distance of 7.3 A when we pass from the columns of Al octahedra in sillimanite [18] to those of Na polyhedra in epididymite, even though Si_2O_5 is still the basic formula. We can see that the Si-O-Si angle in the simple sillimanite Si_2O_5 strip is very much acute; the stress that would otherwise result is avoided by departure from crystallographic identity of all the Si(Al) atoms in a chain (that is, if we displace one third of them from the common plane, as in epididymite - Fig. 9b).

Epididymite shows a clear resemblance to the feldspars. Figure 11 shows the silicon-oxygen structure typical of orthoclase, which is very similar to the structure in epididymite, except that each link has four levels instead of three; $[Si_8O_{20}]_\infty = [Si_{4+4}O_{20}]_\infty$. Such strips may only be dissected from the three-dimensional framework formed by the tetrahedra in the case of the feldspars, whereas the $[Si_6O_{15}]$ links in epididymite are distinct and less tightly couple the single Be tetrahedra into layers; they leave room to fit the large Na atoms in the gaps between the strips (Figs. 12 and 13).

Epididymite resembles beryl and the aluminosilicates in having a framework similar to that found in SiO_2, because its formula corresponds to an (O+OH):(Si+Be) ratio of two. On the other hand, its structure is intermediate between the strip and framework structures found in silicates, because that structure contains dual $[Be_2Si_6O_{14}(OH)_2]$ layers consisting of $[Si_6O_{15}]_\infty$ strips and Be tetrahedra; epididymite must be called a beryllosilicate of layered structure in Bokii's classification of the silicates [23].

The doubled formula of epididymite $Na_2Be_2Si_6O_{14}(OH)_2$ bears to the formula $[Si_6O_{18}]$ a relation such that it is clear that one of the O atoms (out of 15) must be replaced by OH, the true formula being $[Si_6O_{14}OH]$. We cannot say which of the 15 atoms is so replaced, but it can hardly be one of the three (single) O atoms lying in the plane of symmetry, because these three are O atoms joined via two Si tetrahedra. The other 12 such atoms in that plane fall into six crystallographically identical pairs. The atoms O_{VII}, O_{VIII}, O_{IX} belong each to two Si tetrahedra at once, so one OH group is distributed statistically over the six positions of atoms O_I, O_{IV}, O_{VI} (compare the statistical distribution of two OH in afwillite [24] and of six OH

* This shortens one edge of the trigonal prism in which the Si_2O_7 group is inscribed and lengthens another (in favor of the single SiO_4 tetrahedron). Then the central O_{VIII} atom in the Si-O-Si group is displaced very much from the Si-Si axis (the Si-O-Si angle is 160°; see [22]).

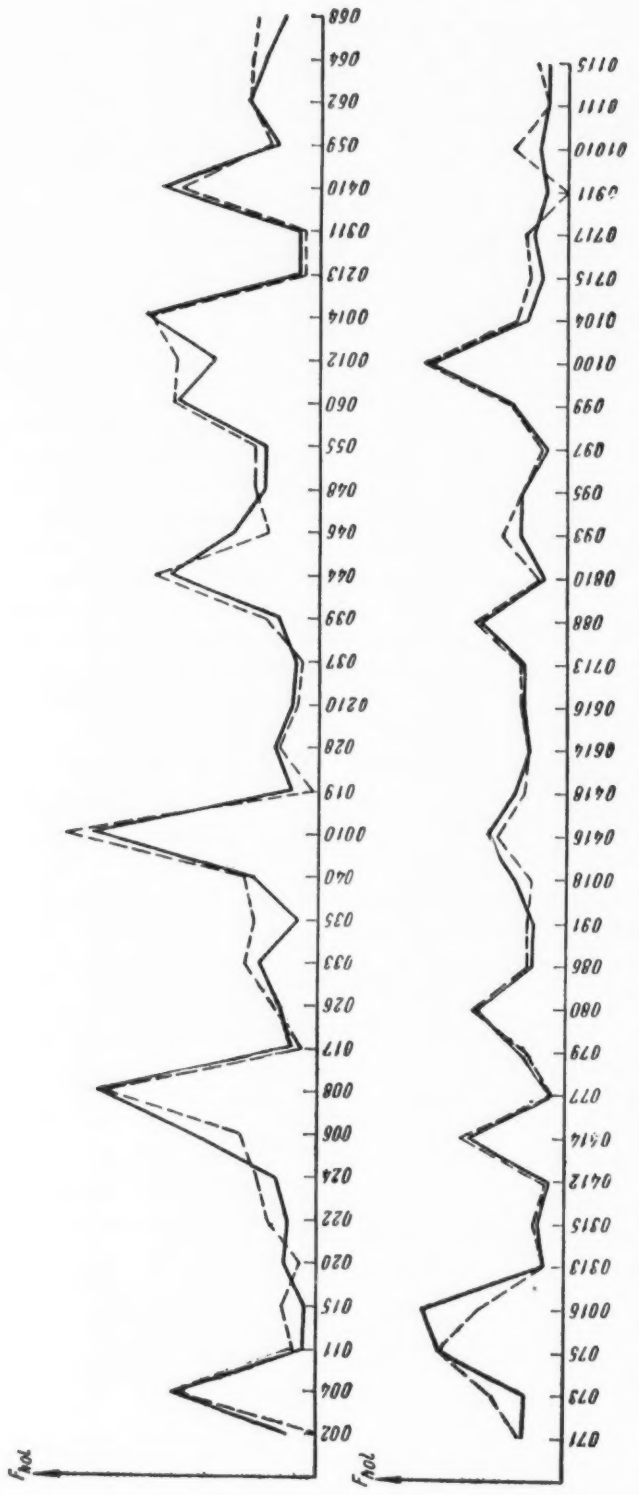

Fig. 8. The calculated and experimental $|F_{0kl}|$ (broken and full lines respectively).

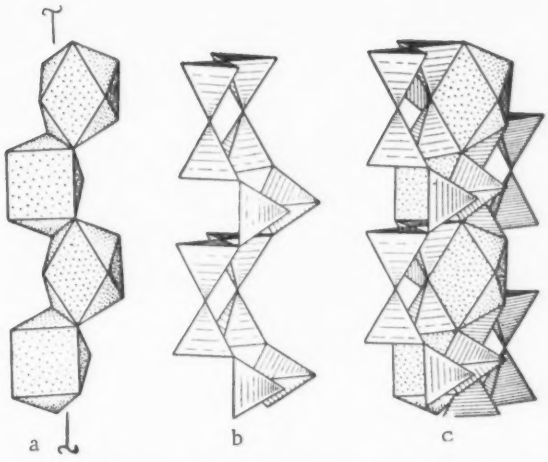

Fig. 9. Two basic patterns in epididymite: a) columns of Na polyhedra; b) double chain of Si tetrahedra; c) combination of the two patterns.

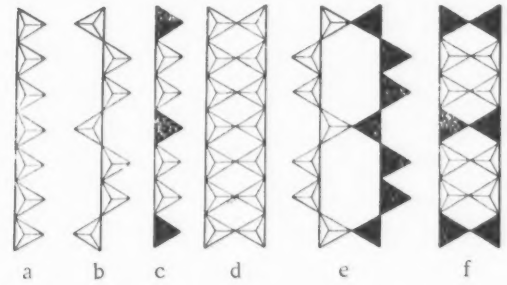

Fig. 10. Silicon-oxygen chains $[SiO_3]_\infty$ having their tetrahedra variously oriented, and some combinations thereof: a) simple $[Si_1O_3]_\infty$ chain; b) wollastonite $[Si_{2+1}O_9]_\infty$ chain (view along a normal to the plane containing the centers of gravity of the tetrahedra); c) the same seen from the side; d) sillimanite strip; e) xonotlite strip; f) epididymite strip.

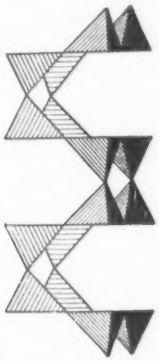

Fig. 11. $[Si_8O_{20}]_\infty$ strips in orthoclase.

TABLE 2

Interatomic Distances (A) in Epididymite

Si_I Tetrahedron		Be Tetrahedron	
Si_I — II	1,60	Be — I	1,65
Si_I — VI	1,65	Be — IV	1,68
Si_I — VII	1,60	Be — VI	1,67
Si_I — VIII	1,60	Be — OH	1,53
II — VIII	2,78	I — IV	2,89
II — VI	2,50	I — VI	2,42
II — VII	2,52	I — OH	2,51
VI — VII	2,66	IV — VI	2,87
VI — VIII	2,56	IV — OH	2,56
VII — VIII	2,43	VI — OH	2,51
Si_{II} Tetrahedron		Na Polyhedron	
Si_{II} — I	1,59	Na — IV	2,11
Si_{II} — III	1,66	Na — VI	2,50
Si_{II} — VII	1,59	Na — VII	2,72
Si_{II} — IX	1,69	Na — IX	2,20
I — III	2,80	Na — VII	2,72
I — VII	2,43	Na — IX	3,10
I — IX	2,52	Na — VIII	2,08
III — VII	2,76	Na — OH	2,63
III — IX	2,42		
VII — IX	2,88		
Si_{III} Tetrahedron			
Si_{III} — IV	1,63		
Si_{III} — V	1,67		
Si_{III} — VIII	1,62		
Si_{III} — IX	1,74		
IV — V	2,59		
IV — VIII	2,90		
IV — IX	2,53		
V — VIII	2,84		
V — IX	2,72		
VIII — IX	2,50		

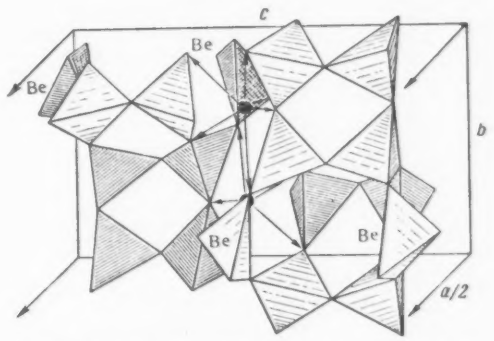

Fig. 12. Axonometric representation of the structure of epididymite.

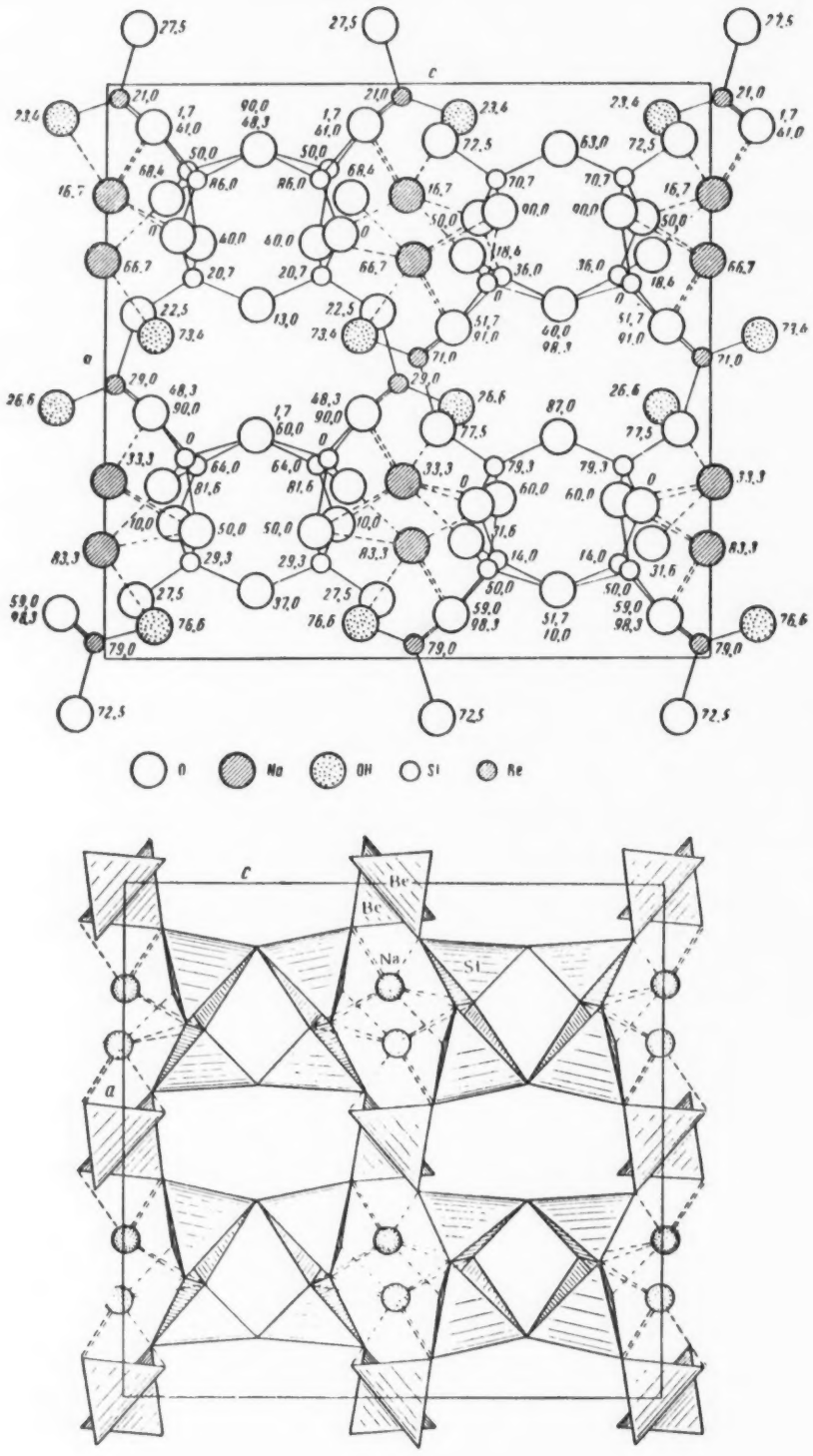

Fig. 13. Structure of epididymite : a) projection along b (the numbers are the heights in hundredths of b); b) xz projection in polyhedra.

TABLE 3

Interatomic Distances (A) in Ito's [4] Structure for Epididymite. a) Tetrahedron; b) octahedron (centrosymmetric)

Si-Tetrahedron		Si-Tetrahedron	
Si — I	1,89	Si — IV	2,86
Si — III	1,43	Si — V	2,56
Si — IV	2,38	Si — VI	2,61
Si — VI	1,79	Si — VII	1,89
I — III	2,84	V — VII	3,01
I — IV	3,03	V — IV	2,36
I — VI	2,64	V — VI	2,91
III — IV	2,91	VI — IV	3,01
III — VI	2,80	IV — VII	2,91
IV — VI	3,01		
Si- Tetrahedron		Na- Octahedron (centrosymmetric)	
Si — II	1,89	Na — III	2,91
Si — III	1,30	Na — IV	2,20
Si — V	2,38	Na — I	2,02
Si — VII	1,79	I — III	2,84
II — III	2,84	I — IV	3,03
II — V	3,03	III — IV	2,91
II — VII	2,64		
III — V	2,91	Na- Octahedron (centrosymmetric)	
III — VII	2,98	Na — III	2,27
V — VII	3,01	Na — II	2,03
		Na — V	2,17
		II — III	2,84
		II — V	3,03
		V — III	2,91

TABLE 4

Balance of Valencies in Epididymite

O (OH)	Na	Be	Si_I	Si_{II}	Si_{III}	Σ
I		2/4		4/4		1½
II			2×4/4			2
III				2×4/4		2
IV	1/8	2/4			4/4	1⅝
V					2×4/4	2
VI	1/8	2/4	4/4			1⅝
VII	2/8		4/4	4/4		2¼
VIII	1/8		4/4		4/4	2⅛
IX	2/8			4/4	4/4	2¼
OH	1/8	2/4				⅝

in lovozerite [25])*; only the corners not coupled to Si atoms in the Be tetrahedra can for certain be assigned to hydroxyl.

The structure explains the physical properties of the mineral, especially the two mutually perpendicular cleavage planes (100) and (001); this feature makes epididymite very similar to orthoclase, the more so since the cause of the cleavage (silicon-oxygen strips extending along b) is the same. Along (001) we have closed double layers of Si tetrahedra with Be tetrahedra, the layers being separated by large Na atoms falling in a strictly hexagonal array; this feature makes the mineral similar to the micas, since tabular (pseudohexagonal) triplets tend to form, and so on** . The cleavage on (100) is not so good, because the silicon-oxygen strips are joined in that plane by Be tetrahedra.

Epididymite is optically positive, in accordance with the chain nature of the radical.

Eudidymite (the monoclinic form of epididymite) contains Si_6O_{15} chains arranged stepwise, but three tetrahedra still form one unit along the axis.

This form of chain explains the perfect cleavage on (110).

LITERATURE CITED

1. L.L. Shilin and E.I. Semenov, Doklady Akad. Nauk SSSR 122, 2, 325 (1957).***
2. B. Gossner and O. Kraus, Zbl. Mineral. A8, 257 (1927).
3. E.S. Dana, Textbook of Mineralogy [Russian translation] (Moscow, 1937).
4. T. Ito, Z. Kristallogr. 88, 142 (1934); X-ray Studies and Polymorphism, (Tokyo, 1950).
5. H. Berman, Amer. Mineralogist 22, 391 (1937).
6. Kh.S. Mamedov and N.V. Belov, Doklady Akad. Nauk SSSR 104, 4, 615 (1955); Zap. Vses. Min. Obshch. 85, 1, 13 (1956).
7. Kh.S. Mamedov and N.V. Belov, Doklady Akad. Nauk SSSR 107, 3, 463 (1956).**
8. R.W.G. Wyckoff, The Structure of Crystals. Suppl. (New York, 1935).

*We cannot put the formula as $Na_2Be_2[Si_6O_{15}]\cdot H_2O$, because water is released only at temperatures above 800°C [1].

**Epitaxis of NaI (or other Na salts) on epididymite is reminiscent of the long-known epitaxis of KI on micas.

***Original Russian pagination. See C.B. translation.

9. G. Flink, Z. Kristallogr. 23, 353 (1894).
10. W.H. Zachariasen, Norsk. geol. tidsskr. 10, 449 (1929).
11. E.R. Howells, D.C. Phillips, and D. Rogers, Acta crystallogr. 3, 216 (1950).
12. Kh. S.Mamedov and N. V.Belov, Doklady Akad. Nauk SSSR 106, 3, 462 (1956).*
13. V.I. Simonov and N.V. Belov, Kristallografiya 4, 163 (1959).
14. M.A. Porai-Koshits, A Practical Course in X-ray Analysis of Structures [in Russian] (Izd. Mosk. Gos. Univ., 1960) Vol. II.
15. M.J. Buerger, Proc. Nat. Acad. Sci. USA 36, 272 (1951); Vector Space (New York, 1959) p. 239.
16. B.K. Vainshtein, Zhur. Éksp. i Teoret. Fiz. 27, 44 (1954).
17. N.V. Belov, "An outline of structural mineralogy. X," Min-Sborn. L'vov. Geol. Obshch. 13, 23 (1959).
18. N.V. Belov, Structures of Ionic Crystals [in Russian] (Moscow, 1947).
19. R.F. Smirnova, et al., Zap. Vses. Min. Obshch. 84, 1, 159 (1958).
20. Kh.S. Mamedov and N.V. Belov, Doklady Akad. Nauk SSSR 121, 5, 901 (1958);* 123, 1, 163 (1958)*; 123, 4, 741 (1958).*
21. V.I. Simonov and N.V. Belov, Doklady Akad. Nauk SSSR 130, 6, 1333 (1960).*
22. N.V. Belov, "A second chapter in the chemical crystallography of silicates", Zhur. Strukt. Khim. 1, 1, 39 (1960).*
23. G.B. Bokii, An Introduction to Chemical Crystallography [in Russian](Izd. Mosk. Gos. Univ., 1960) 2nd edition.
24. H.D. Megaw, Acta crystallogr. 5, 477 (1952).
25. V.V. Ilyukhin and N.V. Belov, Doklady Akad. Nauk SSSR 131, 1, 176 (1960)*

* Original Russian pagination. See C.B. translation.

ON PHASES FORMED IN THE SYSTEM CHROMIUM – BORON, IN THE BORON-RICH REGION

V.A. Epel'baum, N.G. Sevast'yanov, M.A. Gurevich and G.S. Zhdanov

L.Ya. Karpov Physicochemical Scientific Research Institute
Translated from Zhurnal Strukturnoi Khimii, Vol. 1, No. 1, pp. 64-65, May-June, 1960
Original article submitted March 27, 1959

The presence of a new, previously-unknown phase corresponding to the composition CrB_6, in the chromium–boron system has been established. The unit cell dimensions of this phase (tetragonal syngony) were determined: a = 5.458 kX; c = 7.138 kX ; Z = $4CrB_6$.

In our preceding works [1, 2], devoted to the study of the phase composition of synthesis products in the chromium–boron system under certain conditions (temperature and given initial compositions from $CrB_{0.01}$ to CrB_3)*, we reported the formation of a hexagonal modification of chromium (β-phase), due to the solubility of small quantities (up to 0.1%) of boron in the original cubic modification of chromium, and described, among other phases, a new phase corresponding to the composition Cr_5B_3.

The results of investigation of the phase composition in the region richer in boron, i.e., with an initial composition from CrB_5 to CrB_{24}, are given in the present article.

Starting Materials and Method of Synthesis

Samples were prepared under the conditions described by us in [1, 2]–direct synthesis from 99.3-99.6% pure boron obtained by the thermal decomposition of diborane, and 99.9% pure electrolytic chromium. The initial mixtures of finely-divided powders of the given composition were mixed for a long time and then pressed in the cold under a pressure of about 500 kg/cm^2 into moldings 5-8 mm in diameter and 10-15 mm long. The latter were put into silica boats, on the bottom of which was strewn the powder of the sample being investigated. In order to prevent the molding from reacting with the silica and the furnace atmosphere, it was covered with the same powder (a 2-3 mm layer). The synthesis was carried out in vacuo at 1150° for 10 hours and then for 48-60 hours at 1300-1350° in an argon atmosphere. Chemical and x-ray phase analysis was carried out by the methods described by us in [1].

Several series of samples of the following initial compositions were synthesized and investigated:

a) ten samples from CrB_3 to CrB_{12} under the conditions stated above (samples Nos. 185-189 and 209-213);

b) four samples from CrB_6 to CrB_{24}, 1300°, in argon 40 hr (Nos. 257-260);

c) five samples from CrB_3 to CrB_{12}, 2200° in argon 2 hr (Nos. 195-199);

*Gross composition of samples, and not phase composition.

Indices, Interplanar Distances d (kX), and Visually-Estimated* Intensities I of Lines of the CrB_6 Phase (CuK_α Radiation)

No. of line	hkl	d_{calc}	d_{exp}	I_{exp}	No. of line	hkl	d_{calc}	d_{exp}	I_{exp}
1	002	3,569	3,568	s.	16	006	1,190	1,190	v.w.
2	200	2,729	2,729	w.	17	403	1,184	1,181	v.w.
3	201	2,549	2,532	w.	18	305	1,123	1,116	w.
4	210	2,441	2,440	s.	19	500, 206	1,091	1,094	w.
5	300	1,819	1,818	m.	20	510, 216	1,070	1,071	v.w.
6	004	1,785	1,784	w.	21	325	1,039	1,038	w.
7	310	1,726	1,725	s.	22	415	0,971	0,969	w.
8	222, 104	1,696	1,696	w.	23	530, 326	0,936	0,935	s.
9	312	1,554	1,533	m.	24	600	0,910	0,910	m.
10	320	1,514	1,513	w.	25	610, 406	0,897	0,898	w.
11	005, 214	1,434	1,427	w.	26	416	0,885	0,884	v.w.
12	410	1,324	1,326	w.	27	533, 336	0,872	0,873	w.
13	330	1,286	1,286	v.w	28	620	0,863	0,865	v.w.
14	205, 331	1,266	1,266	v.w	29	540, 426	0,852	0,853	s.
15	215	1,232	1,231	w.	30	541, 327	0,846	0,845	v.w.

*s.—strong, m.—medium, w.—weak, v.—very weak.

d) two samples, CrB_6 and CrB_{12}, 2200° in vacuo, 15 min, then in argon, 2100°, 1 hr (Nos. 214 and 215);

e) six samples from CrB_6 to CrB_{24}, 1900°, in vacuo, 1.5 hr (Nos. 266-271).

X-ray and Chemical Analysis

X-ray analysis of samples of the first series of experiments (a) revealed that in the region of compositions from CrB_3 to $CrB_{5.5}$, besides the known hexagonal phase CrB_2, lines of a new phase, not described in the literature, appear. X-ray patterns for a composition close to CrB_6 bear lines only of this new phase, and when the boron content is further increased to the composition CrB_{12} no new lines appear. Lines of pure boron are not observed either; this is possibly explained by the amorphous state of the free boron. Increasing the boron content to CrB_{24} (series b) does not lead to the appearance of free boron lines either; the lines of the main (new) phase are not noticeably shifted.

Increasing the synthesis temperature to 1900-2200° leads to decomposition of the new phase with formation of the compound CrB_2 and the appearance of a crystalline form of free boron.

Chemical analysis of homogeneous samples of the phase found by us gave the following content (in wt. %): B 55.6-55.9; Cr 43.7-43.8; theoretical content for CrB_6 55.52 and 44.48%, respectively; i.e., the discrepancy lies within the limits of analytical error. The density of the new phase, measured pycnometrically, was 3.35 g/cm^3.

Experimental and calculated interplanar distances d and visually-estimated line intensities for the CrB_6 phase are given in the table. It was determined by the analytical method that the compound CrB_6 belongs to the tetragonal system; $a = 5.458 \pm 0.001$ kX; $c = 7.138 \pm 0.001$ kX; $Z = 4CrB_6$; x-ray density $\sigma_x = 3.63$ g/cm^3.

The authors thank Professor B.F. Ormont for critical comments in the discussion of this work.

LITERATURE CITED

1. V.A. Epel'baum, et al., Zhur. Neorg. Khim. 2, 1848 (1957).
2. V.A. Epel'baum, et al., Zhur. Neorg. Khim. 3, 2545 (1958).

CRYSTAL STRUCTURE OF TERNARY PHASES IN THE SYSTEMS Mo (W) – Fe (Co, Ni) – Si

E.I. Gladyshevskii and Yu.B. Kuz'ma

Iv. Franko L'vov State University
Translated from Zhurnal Strukturnoi Khimii, Vol. 1, No. 1, pp. 66-71,
May-June 1960
Original article submitted May 25, 1959

The existence of the ternary phases MoFeSi, MoCoSi, MoNiSi, WFeSi, WCoSi, and WNiSi has been established and their crystal structures determined.

In the systems Mn–Co–Si and Mn–Ni–Si, which we investigated in part, together with Kripyakevich, there were found ternary compounds of the composition $Mn_3Me_3Si_2$ [1] or Mn(Me, Si)$_2$ [2] (where Me=Co or Ni), having a $MgZn_2$-type structure (Laves phases). One of the necessary conditions of formation of ternary Laves phases is that the ratio of atomic radii $r_R/r_{X;Z}$ (where R is the component with the largest atoms and X and Z are the components with the smaller atoms) must lie within the range 1.09-1.50 [3]. In the above-mentioned manganese-containing systems the ratio of atomic radii is less than 1.09, but Laves phases are still formed in them. The radii of molybdenum and tungsten are greater than that of manganese (r_{Mo}=1.39 kX; r_W=1.40 kX; r_{Mn}=1.30 kX). Therefore one may expect the formation of Laves phases in the systems R–Co–Si and R–Ni–Si, where the component R is molybdenum or tungsten. In the binary systems Mo–Co, Mo–Ni, W–Co, and W–Ni binary phases with the $MgZn_2$ structure are not formed [4] but this does not exclude the possibility of the formation of Laves phases by these metals on addition of a third component.

The question of the formation of ternary Laves phases in the systems Mo–Fe–Si and W–Fe–Si is also of interest. Contrary to systems with Co and Ni, the binary systems Mo–Fe and W–Fe contain the binary compounds $MoFe_2$ and WFe_2 with $MgZn_2$-type structure [5].

The ternary Laves phase in the system Mo–Fe–Si (or W–Fe–Si) might be: a) a solid solution of the third component in a binary Laves phase (similar to the solid solution of Mn in $MgZn_2$ [6]); b) a ternary compound with a structure of the same type as the binary (as in the system Ca–Ag–Mg [7]), or c) a ternary compound of different structure (similar to the compounds $MgLi_{0.25}Zn_{1.75}$ and MgLiZn in the system Mg–Li–Zn [8]).

Some of the systems of molybdenum or tungsten with transition metals and silicon of interest to us have already been studied in part. In the system Mo–Ni–Si the ternary compounds Mo_2Ni_3Si and $MoNi_4Si_2$ were found; the latter exists only at temperatures above 850° [9]. The system W–Fe–Si was investigated by the methods of thermal analysis and microstructure [10]. In this system, the compounds WFeSi and W_2FeSi were found. The systems Mo–Fe–Si, Mo–Co–Si, W–Co–Si, and W–Ni–Si have not been investigated until now.

We undertook to make a partial study of the systems Mo–Fe–Si, Mo–Co–Si, Mo–Ni–Si, W–Fe–Si, W–Co–Si and W–Ni–Si in the region up to 33.3 at.% Si in order to find out whether ternary compounds are formed in them, and, if so, to determine their structures.

Experimental Procedure

The alloys were prepared from powdered metals of the following degrees of purity: tungsten 99.95%, molybedum 99.97%, cobalt 99.9%, nickel and iron, reduced by hydrogen from chemically pure oxides, and silicon 99.5%. Weighed samples of the powders were pressed, and then melted in porcelain crucibles under argon in a high-frequency furnace. Ignition losses were negligible, and therefore the alloys were not chemically analyzed.

The alloys, wrapped in tantalum foil, were ignited in silica ampules sealed in vacuo. The ignition continued for 48 hr at 1100°, after which the alloys were cooled to 1000 or 800° and maintained at that temperature for 150 hours more. After this, the alloys were quenched in cold water and pulverized; in order to determine deformation, and for further homogenization, the resulting powders were kept for 8-10 hr more at 1000 or 800° and again quenched. The x-ray investigation was carried out in Debye and Preston cameras.

Systems Mo – Co – Si and Mo – Ni – Si

In the system Mo–Co–Si we investigated 15 alloys located on the section Mo_3Si–Co_3Si and in the central part of the ternary diagram. Alloys containing 33.3-40.0 at. % molybdenum and 22.5-33.3 at. % silicon proved to be homogeneous. The x-ray pattern of the alloy MoCoSi was induced on the basis of a hexagonal lattice with a = 4.73 kX and c/a = 1.61. This indicates the possibility of formation of a ternary compound with a $MgZn_2$-type structure in the system Mo–Co–Si, the given axial ratio being characteristic of this type of structure. In the x-ray pattern the absence of lines with indices $00l$ and hhl where $l \neq 2n$, also indicates the possibility of a $MgZn_2$-type structure (Table 1). In order to test the hypothesis that the ternary compound in the system Mo–Co–Si has a $MgZn_2$-type structure, we calculated the theoretical intensities for the alloy MoCoSi (Table 1).

The following arrangement of atoms in the space group D_{6h}^4 – C6/mmc was assumed:

$$4\text{Mo in } 4(f): \tfrac{1}{3}, \tfrac{2}{3}, z;\ \tfrac{2}{3}, \tfrac{1}{3}, \bar{z};\ \tfrac{2}{3}, \tfrac{1}{3}, \tfrac{1}{2}+z;\ \tfrac{1}{3}, \tfrac{2}{3}, \tfrac{1}{2}-z;\ z=\tfrac{1}{16};$$

$$2\,(\text{Co,Si}) \text{ in } 2(a): 000;\ 00,{}^1/_2;$$

$$6\,(\text{Co, Si}) \text{ in } 6(h): x,\ 2x,\ {}^1/_4;\ 2\bar{x},\ \bar{x},\ {}^1/_4;\ x,\ \bar{x},\ {}^1/_4;\ \bar{x},\ 2\bar{x},\ {}^3/_4;\ 2x,\ x,\ {}^3/_4;$$
$$\bar{x},\ x,\ {}^3/_4;\ x={}^1/_6.$$

The coordination number of the Mo atoms is 16 for the indicated positions, whereas that of the Co and Si atoms is 12 for both positions.

As is evident from Table 1, measured intensities agree well with calculated ones, which indicates that the ternary compound of Mo with Co and Si belongs to the $MgZn_2$ type. The change in the distances between lines for alloys lying in the region of homogeneity, indicates variability of composition of the compound and a change in c/a.

In the system Mo–Ni–Si we investigated the three alloys MoNiSi, Mo_2Ni_3Si, and $MoNi_4Si_2$, which were quenched from the temperatures 1000 and 800°. X-ray patterns of the first two alloys, quenched from 1000°, were identical with those of alloys quenched from 800° and were characteristic of the $MgZn_2$-type structure (Table 1). The x-ray pattern of the alloy $MoNi_4Si_2$ had not only lines of the $MgZn_2$ structural type, but also secondary lines apparently belonging to nickel silicides.

In the system W–Co–Si the alloys WCoSi, $W_{33.3}Co_{42.7}Si_{25}$, $W_{35}Co_{35}Si_{30}$ and $W_{37.5}Co_{37.5}Si_{25}$ were investigated. In the x-ray pattern of the alloy WCoSi lines of the $MgZn_2$ structural type, as well as two very weak secondary lines, appeared (Table 2). Every one of the other alloys proved to be homogeneous and consisted only of a ternary, $MgZn_2$-type compound. The assignment of the compound to this type is confirmed by the agreement of measured intensities with those calculated for the $MgZn_2$-type (composition of WCoSi, Table 2).

Systems W – Co – Si and W – Ni – Si

In the system W–Ni–Si the alloys WNiSi, $W_{33.3}Ni_{42.7}Si_{25}$, $W_{35}Ni_{35}Si_{30}$ and $W_{37.5}Ni_{37.5}Si_{25}$ were investigated. They all proved to be heterogeneous: the main lines of the x-ray patterns belonged to the $MgZn_2$ structural type, but other weak lines belonging to tungsten were observed (Table 2).

TABLE 1*

X-ray Powder Patterns of the Alloys MoCoSi, MoNiSi, and MoFeSi (Fe-K radiation, camera diameter 57.3 mm)

hkl	MoCoSi				MoNiSi			MoFeSi		
	$\sin^2\vartheta$		I		$\sin^2\vartheta$		I	$\sin^2\vartheta$		I meas.
	meas.	calc	meas.	calc.	meas.	calc	meas.	meas.	calc.	
100	—	0,056	0	4	—	0,056	0	0,050	0,055	5
002	—	0,066	0	2	—	0,065	0	—	0,064	0
101	0,080	0,072	5	4	—	0,072	0	0,070	0,071	5
102	0,120	0,121	10	9	0,122	0,123	10	0,119	0,119	10
110	0,167	0,167	50	50	0,165	0,167	50	0,165	0,166	50
103	0,204	0,203	80	80	0,203	0,202	80	0,198	0,199	80
200	0,223	0,222	10	14	0,225	0,222	10	0,221	0,221	10
112	0,232	0,232	90	96	0,233	0,232	80	0,229	0,230	90
201	0,240	0,238	60	57	0,240	0,238	50	0,237	0,237	50
004	0,263	0,262	10	8	0,261	0,261	5	0,255	0,255	10
202	0,288	0,287	5	2	0,286	0,287	5	0,285	0,289	5
104	0,319	0,317	10	6	0,318	0,317	5	0,310	0,311	10
203	—	0,369	0	2	—	0,369	0	—	0,365	0
210	—	0,389	0	1	—	0,389	0	—	0,387	0
211	—	0,405	0	1	—	0,405	0	—	0,403	0
114	—	0,428	0	0	—	0,428	0	—	0,421	0
212	0,451	0,454	10	4	0,453	0,454	5	—	0,451	0
105	0,466	0,465	20	12	0,463	0,464	20	0,454	0,454	20
204	—	0,484	0	1	—	0,483	0	—	0,477	0
300	0,501	0,500	20	16	0,495	0,500	20	—	0,498	0
301	—	0,516	0	0	—	0,516	0	—	0,514	0
213	0,538	0,536	60	60	0,535	0,536	60	0,533	0,531	60
302	0,566	0,565	50	41	0,565	0,565	50	0,561	0,562	50
006	0,590	0,589	10	7	0,587	0,588	10	0,575	0,574	10
205	0,633	0,631	60	57	0,632	0,630	60	0,622	0,620	60
106	0,649	0,645	20	7	0,649	0,643	10	0,630	0,630	10
303		0,647		0		0,646			0,642	
214		0,650		7		0,650			0,643	
220	0,666	0,666	60	56	0,669	0,666	60	0,664	0,664	60
310	0,717 **	0,721	20	9	0,717 **	0,722	20	—	0,720	0
222	—	0,731	0	2	—	00731	0	—	0,728	0
311	—	0,738	0	1	—	00738	0	—	0,735	0
116	—	0,756	0	2	—	0,754	0	—	0,740	0
304	—	0,761	0	0	—	0,761	0	—	0,753	0
312	—	0,787	0	4	—	0,787	0	—	0,783	0
215	0,800	0,798	40	29	0,796	0,797	40	0,786	0,786	40
206	0,814	0,811	40	35	0,816	0,810	40	0,797	0,796	40
107	0,860	0,857	10	14	0,858	0,855	10	0,840	0,837	10
313	0,872	0,869	100	100	0,872	0,869	100	0,864	0,863	100
400	0,887	0,888	10	10	0,889	0,888	10	0,885	0,886	10
401	0,907	0,904	60	49	0,907	0,904	60	0,901	0,902	60
305	—	0,909	0	0	—	0,908	0	—	0,897	0
224	0,931	0,928	60	59	0,931	0,927	60	0,921	0,920	60
402	0,958	0,953	10	4	0,958	0,953	10	0,954	0,949	10
216	0,978	0,978	60	66	0,977	0,976	50	0,963	0,962	50
314		0,979		26	0,983	0,983	20	0,974	0,975	20

* Only α-lines are given in the table.

For MoCoSi $\sin^2\vartheta = 0{,}04162 \left[\frac{4}{3}(h^2 + k^2 + hk) + 0{,}3932\, l^2\right]$,

" MoNiSi $\sin^2\vartheta = 0{,}04163 \left[\frac{4}{3}(h^2 + k^2 + hk) + 0{,}3921\, l^2\right]$,

" MoFeSi $\sin^2\vartheta = 0{,}04151 \left[\frac{4}{3}(h^2 + k^2 + hk) + 0{,}3844\, l^2\right]$.

** The 310 line coincides with the 313 β-line.

TABLE 2 *

X-ray Powder Patterns of the Alloys WCoSi, WNiSi, and WFeSi (Fe-K radiation, camera diameter 57.3 mm)

hkl	WCoSi				WNiSi			WFeSi		
	$\sin^2\vartheta$		I		$\sin^2\vartheta$		I_{meas}	$\sin^2\vartheta$		I meas.
	meas.	calc.	meas.	calc.	meas.	calc.		calc.	calc.	
100	0,054	0,056	10	14	0,055	0,056	10	0,056	0,056	10
002	0,062	0,063	5	9	0,064	0,066	5	0,064	0,064	5
101	0,071	0,072	10	12	0,071	0,072	10	0,067	0,072	10
102	0,117	0,119	10	13	0,120	0,121	10	0,120	0,121	10
110	0,165	0,167	50	55	0,165	0,167	50	0,168	0,169	60
103	0,195	0,197	70	72	0,202	0,202	70	0,197	0,202	70
200	0,220	0,223	10	13	0,223	0,223	20	0,223	0,225	10
112	0,229	0,230	80	70	0,232	0,232	70	0,231	0,233	70
201	0,236	0,239	40	31	0,239	0,239	40	0,240	0,241	40
004	0,253	0,251	5	3	—	0,261	0	0,255	0,258	5
202	—	0,286	0	1	—	0,288	0	—	0,290	0
104	0,306	0,307	5	2	—	0,317	0	0,311	0,314	5
203	0,361	0,364	20	12	0,368	0,370	20	0,366	0,370	20
210	0,387	0,390	10	5	—	0,390	0	0,390	0,394	10
211	0,405	0,406	10	5	—	0,406	0	0,406	0,410	10
114	—	0,419	0	0	—	0,428	0	—	0,427	0
212	0,448	0,453	30	7	0,453	0,455	10	0,457	0,458	40
105		0,449		19	0,463	0,463	30		0,459	
204	—	0,474	0	0	—	0,484	0	—	0,483	0
300	0,499	0,502	30	19	0,500	0,502	30	0,503	0,506	30
301	—	0,518	0	0	—	0,518	0	—	0,523	0
213	0,530	0,532	70	60	0,535	0,537	60	0,535	0,539	70
302	0,563	0,565	50	32	0,565	0,567	50	0,568	0,571	50
006		0,566		5	0,585	0,587	10	0,576	0,580	10
205	0,614	0,616	60	44	0,629	0,630	60	0,625	0,628	60
106		0,622		6	0,640	0,643	10	0,633	0,637	10
303	—	0,643	0	0	—	0,648	0	—	0,651	0
214	0,638	0,642	20	22	0,656	0,651	5	0,649	0,652	10
220	0,668	0,669	60	40	0,669	0,669	60	0,672	0,675	60
310	0,721	0,725	10	16	0,721	0,724	10	0,731	0,731	10
222	—	0,732	0	9	0,733	0,734	10	0,743	0,740	10
311	—	0,741	0	4	—	0,741	0	—	0,748	0
116	0,730**	0,733	20	9	0,752	0,754	5	—	0,749	0
304	—	0,753	0	0	—	0,762	0	—	0,764	0
312	—	0,788	0	8	0,785	0,790	5	—	0,796	0
215	0,783	0,783	60	47	0,797	0,798	60	0,791	0,797	60
206	0,786	0,789	10	20	0,811	0,810	20	0,799	0,805	20
107	0,827	0,826	10	14	0,855	0,855	10	0,850	0,846	10
313	0,867	0,866	100	100	0,871	0,861	100	0,872	0,877	100
400	—	0,892	0	1	0,891	0,892	5	—	0,900	0
401	0,908	0,908	40	29	0,911	0,908	40	0,911	0,916	50
305	—	0,895	0	0	—	0,909	0	—	0,909	0
224	0,921	0,921	40	20	0,933	0,930	30	0,926	0,933	50
402	—	0,955	0	1	—	0,957	0	—	0,965	0
216	$0,957\alpha_1$	0,960	40	42	0,976	0,977	40	0,978	0,974	40
314	0,968	0,976	10	10	0,985	0,985	10	0,990	0,989	20

* Only α-lines are given in the table.

For WCoSi $\sin^2\vartheta = 0{,}03914 \left[\frac{4}{3}(h^2+k^2+hk) + 0{,}4025l^2\right]$,

" WNiSi $\sin^2\vartheta = 0{,}04179 \left[\frac{4}{3}(h^2+k^2+hk) + 0{,}3903l^2\right]$,

" WFeSi $\sin^2\vartheta = 0{,}04220 \left[\frac{4}{3}(h^2+k^2+hk) + 0{,}3820l^2\right]$.

Secondary lines in the x-ray patterns: WCoSi $\sin^2\vartheta = 0.890$; 0.936; WNiSi $\sin^2\vartheta = 0.964$; WFeSi $\sin^2\vartheta = 0.839$; 0.893; 0.965.

** The 116 and 222 lines.

TABLE 3

Lattice Constants of the Crystal Structures of Ternary Phases

Phase composition	a in kX *	c in kX *	c/a	Phase composition	a in kX *	c in kX *	c/a
MoFeSi	4,741	7,647	1,613	WFeSi	4,728	7,651	1,618
MoCoSi	4,735	7,555	1,596	WCoSi	4,724	7,706	1,630
MoNiSi	4,735	7,563	1,597	WNiSi	4,725	7,563	1,601

* Values of a and c were determined with accuracies of ± 0.003 and ± 0.004 kX, respectively.

TABLE 4

Interatomic Distances in the Structures of the Ternary Phases RXSi (in kX)

Distance	MoFeSi	MoCoSi	MoNiSi	WFeSi	WCoSi	WNiSi
R — 1R	2,87	2,83	2,84	2,87	2,89	2,84
R — 3R	2,90	2,89	2,89	2,89	2,89	2,89
R — 6X (*h*)	2,75	2,73	2,73	2,75	2,77	2,73
R — 3X (*h*)	2,77	2,76	2,76	2,77	2,77	2,76
R — 3X (*a*)	2,77	2,77	2,77	2,77	2,76	2,76
X (*h*) — 2X (*a*)	2,35	2,33	2,33	2,35	2,36	2,33
X (*h*) — 4X (*h*)	2,37	2,37	2,37	2,36	2,36	2,36
X (*h*) — 2R	2,77	2,76	2,76	2,77	2,77	2,76
X (*h*) — 4R	2,75	2,73	2,73	2,75	2,77	2,73
X (*a*) — 6X (*h*)	2,35	2,33	2,33	2,35	2,36	2,33
X (*a*) — 6R	2,77	2,77	2,77	2,77	2,76	2,76

Systems Mo − Fe − Si and W − Fe − Si

In connection with the presence of binary compounds with the $MgZn_2$ structure ($MoFe_2$ and WFe_2) in the systems Mo−Fe and W−Fe and the existence of the compound WFeSi [10], we investigated the sections $MoFe_2$−MoFeSi and WFe_2−WFeSi. We prepared seven alloys corresponding to each section, with a constant Mo(W) content equal to 33.3 at.% and a silicon content from 0 to 33.3 at.%. In the system W−Fe−Si the alloy W_2FeSi also was investigated. It was found that in the systems Mo−Fe−Si and W−Fe−Si, for constant concentrations of 33.3 at.% Mo(W) and compositions ABC, phases with $MgZn_2$-type structures are formed (calculations for the x-ray patterns of MoFeSi and WFeSi are given in Tables 1 and 2). The question as to whether they are ternary phases or solid solutions based on the binary compounds $MoFe_2$ and WFe_2 remains obscure, since we were unable to prepare the binary compounds in pure form.

We did not confirm the existence of the compound W_2FeSi: the x-ray pattern of the alloy of composition W_2FeSi contained not only lines belonging to the $MgZn_2$ structural type, but also intense tungsten lines.

DISCUSSION OF RESULTS

By x-ray structural investigation of the systems Mo−Fe−Si, Mo−Co−Si, Mo−Ni−Si, W−Fe−Si, W−Co−Si, and W−Ni−Si we established that a ternary phase with a $MgZn_2$-type structure is formed in each of them. In systems containing nickel or cobalt these phases are ternary compounds; in systems containing iron they are ternary compounds or solid solutions based on the binary compounds $MoFe_2$ and WFe_2. Two of the indicated phases−MoNiSi (Mo_2Ni_3Si) and WFeSi−were known earlier [9, 10], but their structure has not been studied until now; the rest of the phases have not yet been described in the literature.

The unit-cell constants of the ternary $MgZn_2$-type phases (for the composition RXSi, where R = Mo, W; X = Fe, Co, Ni) are given in Table 3. The constant a is less for tungsten compounds than for those of molybdenum, despite the fact that the radius of the first is somewhat greater than that of the second. A similar relation is observed in other series of isostructural compounds of elements in Periods V and VI: Mo_2C-W_2C ([11], p. 332) and $NbFe_2-TaFe_2$ ([11], p. 301). The value of c/a for most of the phases investigated is less than the ideal (1.63) and approaches it only in the case of WCoSi (Table 3).

Interatomic distances in the RXSi structures are given in Table 4.

From the viewpoint of crystal chemistry the investigated phases are most similar to compounds in the systems Mn–Co–Si and Mn–Ni–Si [1, 2]. They are not only isostructural with the latter, but also characterized by low values of c/a. The unit-cell constants for phases containing molybdenum and tungsten are greater than for manganese compounds; this is due to replacement of manganese atoms by the larger molybdenum and tungsten atoms.

The authors thank P.I. Kripyakevich for a discussion of the questions dealt with in this article.

SUMMARY

Forty-three alloys of the ternary systems Mo(W)–Fe(Co, Ni)–Si were investigated by the method of x-ray structural analysis. The existence of the following ternary phases with $MgZn_2$-type structures was established:

MoFeSi ($a = 4{,}741$ kX, $c = 7{,}647$ kX) WFeSi ($a = 4{,}728$ kX, $c = 7{,}651$ kX)
MoCoSi ($a = 4{,}735$ kX, $c = 7{,}555$ kX) WCoSi ($a = 4{,}724$ kX, $c = 7{,}706$ kX)
MoNiSi ($a = 4{,}735$ kX, $c = 7{,}563$ kX) WNiSi ($a = 4{,}725$ kX, $c = 7{,}563$ kX).

LITERATURE CITED

1. E.I. Gladyshevskii, P.I. Kripyakevich, and Yu.B. Kuz'ma, Dopovidi Akad. Nauk UkrRSR 1, 67 (1956).
2. E.E. Cherkashin, E.I. Gladyshevskii, P.I. Kripyakevich, and Yu.B. Kuz'ma, Zhur. Neorg. Khim. 3, 3, 650 (1958).
3. P.I. Kripyakevich and E.E. Cherkashin, Uspekhi Khim. 19, 361 (1950).
4. W. Loskiewicz and M. Orman, Uktady równowagi pódwójnych stopów metali (Warsaw, 1956).
5. R.P. Zaletaeva, N.F. Lashko, M.D. Nesterova, and S.A. Yuganova, Doklady Akad. Nauk SSSR 81, 3, 415 (1951).
6. E.I. Gladyshevskii and E.E. Cherkashin, Zhur. Neorg. Khim. 1, 6, 1394 (1956).
7. H. Nowotny, Struct. Reports 10, 31 (1953).
8. P.I. Kripyakevich, Khimichnii Zbirnik L'vivs'k. Derzh. Univ. 46, 5, 107 (1958).
9. H. Pfautsch, Z. Metallkunde 17, 48 (1925).
10. R. Vogel and H. Topker, Arch. Eisenhüttenwesen 13, 183 (1939/40).
11. G.B. Bokii, Introduction to Crystal Chemistry [in Russian] (Izd. MGU, 1954).

COMPLEX COMPOUNDS WITH MULTIPLE BONDS IN THE INNER SPHERE

G.B. Bokii

Institute of Inorganic Chemistry SO, Academy of Sciences of the USSR
Translated from Zhurnal Strukturnoi Khimii, Vol. 1, No. 1, pp. 72-79,
May-June, 1960
Original article submitted November 29, 1959

A hypothesis is advanced on the existence of a special group of complex compounds differing from ordinary ones in that they have one or several multiple bonds in the inner sphere, between the central atom and the ligands. The properties of these compounds are discussed. A crystallochemical criterion for relating a compound to this group is pointed out.

In the most typical complex compounds ligands, as a rule, are univalent anions or neutral groups for instance, Cl^-, Br^-, I^-, NO_2^-, OH^-, CN^-, SCN^-, NH_3, and other amines, H_2O et al.,

If the complex compound contains a polyatomic bivalent ligand, it often forms two bonds and occupies two coordination positions (e.g., the oxalate ion, ethylenediamine, α-dioximes, etc.). These substances, particularly dimethylglyoxime, can saturate the main valences of the central metal atom and also can form bonds with the central atom through a nitrogen atom, remaining neutral in this case. In both cases the character of the metal–ligand chemical bond is the same as with the univalent and neutral ligands mentioned above. Of the compounds metioned in A.A. Grinberg's book, "Introduction to the Chemistry of Complex Compounds [in Russian], compounds of these types constitute, probably, over 95%. Below we shall call them "ordinary complex compounds."

Metal–ligand bonds of very similar types are characteristic of all this enormous number of complex compounds; they are most simply expressed by a two-electron covalent bond. The difference in bond type among different ligands lies in the extent of their deviation from purely covalent toward ionic.

In compounds of this type, according to modern coordination theory, there is no difference between primary and secondary valences. For this reason the characteristic structural criterion of these compounds is the fact that the coordination number of the central atom is always greater than its valence*

The question arises: what peculiarities will the compounds have if their ligands are bound to the central atom by bonds of a sharply (qualitatively) different type?

Qualitatively different types of chemical bond appear in the case where a different number of electrons participate therein. Of course, two types of bond may differ qualitatively from one another even in the case where an equal number of electrons take part, but the converse statement is unconditionally valid: if a different number of electrons participate in the bonds, the bond types must be different. Such are bond types with which we shall deal in the present article.

---

* The concept "valence" is used here by us in that sense in which it is usually employed in analytical chemistry. It is similar to the concepts "state of oxidation" and "degree of oxidation," used in the works of G. Seaberg and other authors. Thus, for instance, in K_2PtCl_6 the valence of Pt in this sense is four. We denote this degree of oxidation of platinum by Pt^{4+}, without of course, implying that the symbol represents a quadruply-charged ion.

In this connection the clearest demarcation of compounds is made in organic chemistry, since the latter is systematized essentially according to bond types. Thus, in organic chemistry, the division of aromatic compounds, characterized by sesquiple (benzene) bonds, is always distinguished. Among the acyclic compounds the division of saturated compounds and their derivatives, always characterized by only single (two-electron) bonds, is always distinguished. In turn unsaturated compounds of the ethylene and acetylene series are distinguished from them.

The C−C bonds in paraffins, benzene, ethylene, and acetylene are essentially different and cannot be continuously and gradually interchanged. A different number of electrons, equal to two, three, four, and six, respectively, take part in each of these bond types.

Each type of bond between identical atoms has a corresponding interatomic distance, which varies within certain but, as a rule, narrow limits depending on the presence of other atoms in the molecule. Changes in the interatomic distances in this case are quantitative in character and remain within the limits of one qualitative type of chemical bond. The physical, particularly the energetic, characteristics of the chemical bond−primarily its stability, which may be determined, for instance, from heats of dissociation−are related to the interatomic distance. As we stated earlier [1], in exceptional special cases different bond types may be characterized by equal interatomic distances. It was of extreme interest to us to make a comprehensive study of such pairs of bonds and to compare them. However, this hypothesis was not supported by organic chemists, and hence remained insufficiently developed.

In any case different types of chemical bond, in general, correspond to different average interatomic distances. For the series C−C, C=C, C=C, and C≡C the interatomic C−C distances will be 1.54, 1.40, 1.35-1.30, and 1.20 A, respectively. From these numbers we may conclude that a change in distance of 0.1 A leads, as a rule, to a qualitative change in the character of the chemical bond. Here we have discussed chemical facts well known to all chemists− multiple bonds of nonmetallic atoms. Chemists have paid very little attention to multiple bonds of metallic atoms.

Multiple bonds of metal atoms apparently were first mentioned by Pauling [2]. This idea was developed by Syrkin and Dyatkina [3]. Zachariasen (see below) first compared U−O distances for single and double bonds. In recent years similar comparisons were made by Hanic [4] for compounds of chromium and certain other elements. In the present article we shall consider multiple bonds between the central metal atom and the ligands in complex compounds.

In the present article, speaking of complex compounds and being guided by their analogy with organic compounds, we propose to distinguish among them the group of compounds containing multiple bonds between the central atom and the ligand. The idea of a detailed consideration of the properties of such compounds occurred to the author in connection with the very interesting and rather unexpected results obtained in the Crystal Chemistry Laboratory of IONKh Academy of Sciences, USSR, by Parpiev, Khodasheva, and Atovmyan [5] in a structural investigation of complex ruthenium and osmium compounds.

This group of compounds containing multiple bonds differs from ordinary complex compounds in the same way that unsaturated hydrocarbons and their derivatives differ from saturated ones. Clearly, the characteristic ligands for this group of complex compounds will be different from those for the group of "ordinary complex compounds" mentioned at the beginning of the article. In particular, if these ligands are single atoms, their valence must be at least two. In polyatomic ligands the valence of the atom, by which the ligand is bound to the central atom, must be at least three. The simplest compounds of this type will be those containing an oxygen or nitrogen atom as ligand. However, if these atoms are components of a polyatomic ligand, the complex compounds may be of the ordinary type, e.g., compounds containing the groups OH_2, OH^-, NO_2^-, NH_3 and other amines, and the like as ligands.

Complex compounds, in which there are multiple bonds between the central atom and certain ligands, must have other properties distinguishing them from ordinary complex compounds. Thus, for instance, the bonds in such complexes are highly nonequivalent. For this reason, the basic rule for "ordinary complex compounds", to the effect that all bonds in the complex belong to the same type and that there is no difference between primary and secondary valences, does not apply. The characteristic peculiarity that distinguishes them from ordinary complex compounds consists namely in this fact.

Complex osmium compounds are of great interest. The coordination polyhedron for complex compounds of this metal is an octahedron, e.g., in $K_2[OSO_2Cl_4]$. Hence, the rule stated above, that the coordination number in ordinary complex compounds is always greater than the valence of the central atom, does not hold here in most cases. In the given case, both these quantities are equal to six, which is one more characteristic peculiarity of complex compounds with multiple bonds in the inner sphere. The coordination number may even be less than the valence of the central atom, as is the case, for instance, in the tetrahedral complex $[OsO_3N]$, found in the compound $KOsO_3N$. The valence of osmium is eight, whereas the coordination number is four.

In $KOsO_3N$ we encounter a very unusual ligand—a single nitrogen atom. Os—N bonds of the same character are encountered in the compounds K_2OsNCl_5 and $KOsNBr_4 \cdot 2H_2O$ [5], whose remarkable isomorphism was discovered by Atovmyan. In the first structure the fact that one of the five Os—Cl distances is greatly shortened is especially noteworthy; on the basis of this fact it may be assumed that the linear group $N \equiv Os - Cl$ analogous to osmyl or uranyl [5], is present in this compound. The degree of shortening of the Os—Cl distance is even greater than that observed on passing from a single to a double bond. Similar shortening of the $Os-OH_2$ distances in the second salt was not found.

The number of complex compounds with multiple bonds in the complexes is apparently not so small; they simply have not received the proper attention until now. Even now it may be said that the ability to form multiple bonds is apparently characteristic of multivalent metals which are located in the fifth, sixth, seventh, and eighth A-subgroups of the Periodic System, and also in the actinide group, and have the greatest electronegativity. Their most characteristic valence is six. For instance, let us mention chromium, molybdenum, and tungsten compounds of the types Me^+CrO_4, $Me^{++}WO_4$, and $Me_2^{++}[OsO_2Cl_4]$. Septivalent manganese and rhenium form compounds of the type Me^+ReO_4. Complex compounds with multiple bonds in the complexes are formed also by sexivalent uranium and certain other transuranic elements.

The character of the bond between a given ligand and the central atom may be varied; in particular, the bond may be single or multiple. This fact greatly complicates the isolation of the class of complex compounds with multiple bonds in the inner sphere from ordinary complex compounds. As an example, let us consider the nitroso compounds of ruthenium. It is generally known that their chemical behavior is so diverse that their existence can be explained only by assuming that the nitroso groups in them have very different electronic structures [6].

This question has been considered theoretically by Syrkin and Belova [7]. They established two extreme types of electronic structure for the nitroso group in such compounds:

(the case of $Me^- = N^+ = O$ with the bond angle 180° is difficult to distinguish from the second, although it is essentially intermediate between the two extremes mentioned above).

The works of the author together with Parpiev and Khodasheva [5, 8, 9] confirm these theoretical conclusions. As Table 1 shows, experimental Me—N—O bond angles have intermediate values between 105 and 180° and indicate that the bonds in these compounds are intermediate in character. But this in turn gives rise to certain difficulties of classification, since it predetermines a gradual transition in some cases from ordinary complex compounds to complex compounds with multiple bonds.

Our problem involves the finding of such macroscopic properties as might make it possible to determine the character of the nitroso group immediately. In a conversation with the author on this subject, D. Hodgkin advanced the hypothesis that, if the nitroso group is bound to the central atom at an angle, the compounds will be colorless, whereas if this group is attached "in a straight line," they will be colored. Unfortunately, this hypothesis was incorrect, but the very idea of determining the type of the nitroso-group bond on the basis of some easily-measured property seems very sound to us, and it should be developed in every possible way. It is inexpedient to calculate the crystal structure each time in order to learn the structure of the nitroso group, since x-ray structural investigations are too laborious for this.

TABLE 1

Me — N, A	N — O, A	< Me — N — O	Compound	Lit. cited
		~135°	$Co[S_2CN(CH_3)_2NO]$	10
2,07	1,14	~150°	$[RuNO(OH)(NH_3)_4]Cl_2$	8
2,04	1,13	153°	$(NH_4)_2[RuNO(OH)Cl_4]$	9
1,70	1,25	177°	$K_2[RuNOCl_5]$	5
1,57and1,67	1,20	~180°	$CsFe_4S_3(NO)_7H_2O$	11

We shall obtain typical complex compounds with multiple bonds in the inner sphere if, for instance, individual oxygen or nitrogen atoms act as ligands in them. Attachment of one or two oxygen atoms to the metal atoms to form very stable groups is well known to chemists. It is sufficient to mention here the bivalent vanadyl and uranyl ions, VO^{++} and UO_2^{++}. These groups are so stable that some synthetic chemists suggest that they be regarded wholly as "central pseudoatoms" surrounded by the first coordination sphere. This idea is essentially incorrect but would quite naturally occur to chemists far removed from structural chemistry, since reactions leading to substitution of ligands alone in the complex go much more readily than the replacement of such oxygen atoms. The latter replacement requires very severe conditions leading to complete disintegration of the complex. If the uranyl ion has six ligands, it is quite incorrect to assume that they have an octahedral arrangement, or to draw any chemical conclusions from this, especially on the types of isomers that may exist. Structure determination for similar compounds shows that all ligands, including the two oxygen atoms of the uranyl group, are located at the corners of a more or less distorted cube whose "uranyl diagonal" is only 10% shorter than the rest (all other conditions being equal). Thus, it must be assumed that the central atom, uranium in this case, has a coordination number of eight, and the coordination polyhedron is a deformed cube or, in the limit, a hexagonal bipyramid. In this complex the bonds between the central atom and the ligands are wholly nonequivalent: two of them are multiple.

When multiple bonds are present in the complex, the rest of the bonds become much more ionic. Because of this the number of such ligands will not always be strictly constant for a given type of central atom. Thus, for instance, the uranyl group is often surrounded by four, five, or six peripheral ligands [12]. This constitutes one more peculiarity of complex compounds with multiple bonds. It is easy to understand why the above-mentioned uranium compounds are unstable and readily dissociate in aqueous solutions, the uranyl ion remaining unchanged. For this reason, as Khodasheva observed, the formation of UO_2 complexes with thiocarbamide and other ligands tending to give covalent bonds is less probable. Complex compounds of uranium may be compared with those of platinum. In the latter the coordination number is practically always six for quadrivalent platinum and four for bivalent.

An octahedral arrangement of ligands is characteristic of complex osmium compounds even in those cases in which the complexes contain the osmyl group. This is due to the fact that osmium is a stronger complex-former than uranium. Hence, even when the osmyl group is present in the complex, the bonds between the other four ligands and the central atom are more covalent than in the analogous uranium compounds.

In two structures of nitroso compounds of ruthenium, determined by the author together with Parpiev, the hydroxyl group was found in the trans-position relative to the nitroso group. By the way, the type of isomer in these compounds was not established by chemists; its determination was the result of direct deciphering of the crystal structure. If there is a stable bond between the central atom and one of its ligands, the density of the electron cloud on the opposite side of the atom will inevitably be less than the average value, and the bond formed by the central atom in this coordination position of the complex must be the most ionic. Hence, an anionic ligand, and not a neutral molecule, will more probably be attached in this position; of different competing anions, the one having the greatest electronegativity will most likely be attached. Hence the finding of the hydroxyl group in the trans-position relative to the nitroso group evidently is not fortuitous.

The study of the Ru—NO bond was continued with the compound $K_2[RuNOOH(NO_2)_4]$ which was previously treated as $K_2Ru(NO_2)_5$, where either the ruthenium must be assigned the coordination number five, or one of the ligands occupies two coordination positions. New chemical, magnetic, and spectral data have

TABLE 2

Me — X	A	Compound	Lit. cited
Me — OH_2	~2,10	$KOsNBr_4 \cdot 2H_2O$	5
Me — OH	2,03	$(NH_4)_2[RuNO(OH)Cl_4]$	9
	1,98		8
Me — O	1,85	$K_2[OsO_2Cl_4]$	15
Me — NH_3	2,23	$[RuNO(OH)(NH_3)_4]Cl_2$	8
	2,07	$[RuNO(OH)(NH_3)_4]Cl_2$	8
Me — NO	2,04	$(NH_4)_2[RuNO(OH)Cl_4]$	9
	1,70	$K_2[RuNOCl_5]$	5
Me — N	~1,60	$KOsNBr_4 \cdot 2H_2O$	5

led to the formula written above, which contains NO and OH groups as ligands [13]. The structure of this compound was studied at IONKh, Academy of Sciences, USSR, by research student Wang Ang-p'u. This work confirmed that the ruthenium is surrounded by six ligands in an octahedron. It is remarkable that, when a hydroxyl group is present in the structure, the bond between the ruthenium and the nitroso group tends to become ordinary (see the Ru—N—O bond angles and interatomic distances in Table 1). Apparently these peculiarities are connected with the character of the Ru—OH bond. When a hydroxyl group is present in the complex, an ordinary Ru—N bond is formed instead of a triple Ru≡N bond. We must consider ruthenium quadrivalent in this case, but sexivalent in the compound $K_2[RuNOCl_5]$. The Ru≡No triple bond apparently occurs only in compounds in which there is no bond between the central atom and oxygen. If this reasoning is correct, one may expect the Pt^{IV}—NO bond angle in complex compounds of platinum with the nitroso group to be less than 150° and the Pt—N distance to be greater than 2 A, since a change in the valence of the central atom from four to six is improbable in these compounds.

A comparison of the Me—N and Me—O interatomic distances, where Me = Ru or Os, with respect to the group containing the nitrogen or oxygen atom, is given in Table 2. In such compariosns the atomic radius of the metal is usually equated to the covalent radius, which is quite correct for ordinary complex compounds. The atomic radii of Ru and Os are equal to 1.34 and 1.35 A, respectively, and the covalent radius of nitrogen in an ordinary bond is 0.70 A. The sum of the radii agrees well with the experimental distance (Table 2). With ammonia the bond apparently has the character of ion-dipole interaction.

The atomic radius of nitrogen decreases with respect to the bond type as follows: ordinary bond 0.70, sesquiple 0.66, double 0.63, and triple, 0.55 A. If the minimum value for nitrogen is taken and added to the atomic radii of osmium and ruthenium, the sums obtained for the last three compounds are much greater than the experimental values. Only one conclusion can be drawn. The discrepancy is due to the fact that we have used an incorrect value for the size of the metal atom.

In the literature there are no data on changes in the size of metal atoms with multiple bonds. For nonmetallic atoms, there is a well-known rule to the effect that, as the bond multiplicity increases from single to double, the atomic radii decrease by an amount slightly less than 0.1 A. As regards metals, this subject is scarcely mentioned anywhere. Works by Zachariasen [14], in which the covalent radii of actinide-metal atoms in different valence states are given for the ordinary bond, are the only exception. By this, the author obviously implies that the values will be different in the case of the nonordinary bond; however, he does not give them. He further discusses the character of the U—O bond in the uranyl group and comes to the conclusion that double bonds are present therein.

The answer to the question of changes in the size of metal atoms with multiple bonds is given by the experimental data of Table 2. It follows from the latter that the "radius" of $\equiv Ru^{6+}$ is about 1.15 A, whereas the "radius" of $\equiv Os^{6+}$ is about 1.05 A. These values are obtained as the differences 1.70 - 0.55 and 1.60 - 0.55 A, respectively, whence it follows that the "radius" of Ru or Os in the sexivalent state with a triple covalent bond is about 0.2-0.3 A less than its usual value for an ordinary bond.

The "radius" of $=Os^{6+}$ with a double bond may be obtained for the structure of $K_2OsO_2Cl_4$ [15]. The Os=O distance in the latter is about 1.85 A, whereas the radius of an oxygen atom with a double bond is 0.59 A, whence the radius of $=Os^{6+}$, of interest to us, is about 1.26 A. In the case of the ordinary bond the covalent radii of uranium, according to Zachariasen, will be: for $-U^{4+}$ 1.62, $-U^{5+}$ 1.50, and $-U^{6+}$ 1.42 A. To this series of numbers may be added $R(=U^{6+}) = 1.32$ A, obtained as the difference between the U–O distance in the uranyl group, 1.91 A, and the covalent radius of oxygen with a double bond, 0.59 A.

Hence it follows that the decrease in the covalent radius of a metal on increase of the bond multiplicity by one approximately coincides with its decrease on increase of the valence by one. These quantities may be determined more precisely when the parameters of the atoms in the structures of the corresponding compounds are more accurately known. It is interesting to note that the changes in the size of metal atoms with covalent multiple bonds are even greater than in the case of nonmetals. Insofar as they are determined, these quantities evidently will play a certain part in the study of the chemistry of ruthenium, osmium, molybdenum, tungsten, uranium, and other metals which can form multiple bonds. It would be extremely interesting to study organometallic compounds with the Me = C< bond.

The above leads to a crystallochemical criterion for judging the types of complex compounds in doubtful cases. On the basis of interatomic distances we can judge whether a compound is an "ordinary" complex one or a complex compound with multiple bonds in the inner sphere. It must be considered that a qualitative change of the bond occurs when the interatomic distances are changed by an amount of the order of 0.2 A (0.1 A on account of the decrease in radius of the metal and 0.1 A for that of the nonmetal). The stated values characterize transition from a single to a double bond.

Let us turn to the question of bond types. It was noted above, that on formation of a multiple Me– ligand bond the bonds of all the other ligands, particularly the ligand situated in the trans-position relative to the first, become more ionic. This sharp increase in the asymmetry of the external electron shell of the atom, which obviously is accompanied by a change in the character of hybridization of the wave functions taking part in the bond, causes asymmetry in the electric field and hence splitting of levels in the inner shells of the atom. This means that the electron cloud formed by the inner electrons is affected tosome extent when multiple bonds appear. This is equivalent to the hypothesis that all electrons of the atom take part in the chemical bond, but under "ordinary conditions," i.e., with weak bonds, we do not notice the effect of the inner electron shells. The change in the symmetry of the electron cloud in the atom should probably have some effect on the atomic nucleus and be manifested in the first place, for instance, in a change in the magnetic properties of the nucleus and certain other characteristics of the latter. The very weak interactions among the particles of a substance can now be studied experimentally by radio-spectroscopic methods.

Atoms joined by such a stable bond as the Os≡N form a group whose exceptional stability and structural isolation in complex compounds we showed above. It may be thought, therefore, that under certain severe conditions, where ordinary chemical bonds are ruptured, these formations of the types $Os^{8+}=O$ and $Os^{8+}\equiv N$ may exist independently in the form of molecular ions; in this case metal–oxygen and metal–nitrogen bonds should, naturally, be even further strengthened. Such particles may appear, for instance, in the first stages of element formation as a result of nuclear transformations, and in all measurements involving the mass of atoms or ions they should be very difficult to distinguish from polonium and bismuth ions, respectively. Analogous molecular ions probably can be formed also from ions of other multivalent metals with other light atoms –primarily carbon and boron.

If a complex compound with multiple bonds is heated, such groups of atoms probably dissociate last and hence may be called "fragmentary radicals." If we proceed from the opposite direction, i.e., from higher temperatures, such particles will be formed first on cooling of the corresponding systems. The practical value of our structural investigations may consist in this: data obtained at ordinary temperatures can be used in high-temperature chemistry.

Compounds of the considered type e.g., nitroso compounds of ruthenium, are of practical importance even now. It is well known, for instance, that in the treatment of nuclear fuel with nitric acid in order to remove radioruthenium in the form of K_2RuO_4, the greater part of the ruthenium is converted to nitroso compounds and therefore cannot be completely removed in this way. The high stability of these compounds gives rise to great difficulties in purifying industrial solutions [16, 17].

In conclusion, we should like to note that the purpose of the present article is to provoke discussion of the questions dealt with, for the purpose of sounder, more efficient planning of scientific research work in this field, which, in the author's opinion, receives less attention than it deserves, despite its obvious importance.

LITERATURE CITED

1. G.B. Bokii, Collection: State of Chemical Structure Theory in Organic Chemistry [in Russian] (Izd. AN SSSR, Moscow, 1952) p. 383.
2. L. Pauling, Nature of the Chemical Bond [Russian translation] (Goskhimizdat, Moscow, 1947).
3. Ya.K. Syrkin and M.E. Dyatkina, The Chemical Bond and Molecular Structure [in Russian] (Goskhimizdat, Moscow, 1946).
4. F. Hanič, Chem. zvesti 10, 268 (1956).
5. G.B. Bokii, L.O. Atovmyan, and T.S. Khodasheva, Doklady Akad. Nauk SSSR 128, 1, 78 (1959).*
6. E.E. Addison and J. Lewis, Uspekhi Khim. 25, 9, 1120 (1959).
7. Ya.K. Syrkin and V.I. Belova, Izvest. Akad. Nauk SSSR, Otdel. Khim. Nauk 12, 1492 (1958).*
8. G.B. Bokii and N.A. Parpiev, Kristallografiya 2, 5, 691 (1957).
9. N.A. Parpiev and G.B. Bokii, Zhur. Neorg. Khim. 2, 8, 1927 (1957).
10. P. Alderman and P.Q. Owston, Nature, 178, 1071 (1956).
11. G. Jahansson and W. Lipscomb, J. Chem. Phys. 27, 6, 1417 (1957).
12. W. Zachariasen, Fedorov Session on Crystallography (Abstracts of Proceedings) [in Russian] (Izd. AN SSSR, 1959) p. 22.
13. J.M. Fletcher, I.L. Jenkins, F.M. Lever, F.S. Martin, A.R. Powell, and R. Todd, J. Inorg. and. Nucl. Chem. 1, 378 (1955).
14. W. Zachariasen, Actinides [Russian translation] (IL, Moscow, 1955) p. 623.
15. J.L. Hoard and I.D. Grenko, Z. Krist. (A) 87, 100 (1934).
16. O.E. Zvyagintsev, Proceedings of the International Conference on Peaceful Uses of Atomic Energy [in Russian] (Geneva, 1955) p. 216.
17. A.V. Nikolaev and N.M. Sinitsyn, Doklady Akad. Nauk SSSR 127, 1, 117 (1959).*

* Original Russian pagination. See C.B. translation.

QUANTITATIVE EVALUATIONS OF MAXIMA IN THE THREE-DIMENSIONAL PATTERSON FUNCTION

V.V. Ilyukhin and S.V. Borisov

Crystallography Institute, Academy of Sciences of the USSR;
Institute of Inorganic Chemistry SO, Academy of Sciences of the USSR
Translated from Zhurnal Strukturnoi Khimii, Vol. 1, No. 1, pp. 80-85,
May-June, 1960
Original article submitted December 23, 1959

In the case of the three-dimensional Patterson function for the recently-deciphered structure of the Zr silicate lovozerite, experimental values of the maxima of this function are compared with values calculated by the proposed formulas. The effect of the temperature factor is analyzed.

The role of the Patterson function in direct methods of structural analysis, which has grown enormously in recent years, has made this function the object of many-sided study (works of Buerger [1], Simonov [2], et al.,). For even more extensive use of it in direct methods it is desirable to have reliable methods for the theoretical calculation of "forms" of the Patterson function, which would give numbers coinciding satisfactorily with that given by a harmonic analysis based on experimental values – some form of measured intensities of the diffraction pattern. In the first place formulas are required, which estimate the value (height) of the Patterson peaks and their form for the different atom pairs generating each individual peak. The necessary evaluations are obtained quite rapidly and easily by using the methods of calculating integral characteristics, well developed in [3, 4], and atomic factor tables [5].

For this the Patterson function

$$P(r) = \frac{1}{V} \sum\sum\sum F_H \times F_H^* \cos 2\pi (\vec{H}\vec{r}) \tag{1}$$

will be considered to represent the electron density as a function of a certain centrosymmetric structure with all positive amplitudes

$$F'_H = F_H \cdot F_H^* = \sum_{n=1}^{N} f_n e^{2\pi i(\vec{H}\vec{r}_n)} \times \sum_{j=1}^{N} f_j e^{-2\pi i(\vec{H}\vec{r}_j)} =$$

$$= \sum_{n=1}^{N} f_n^2 + \sum_{n \neq j} f_n f_j e^{2\pi i[\vec{H}(\vec{r}_n - \vec{r}_j)]}. \tag{2}$$

Such a "structure" has an "atom" at the beginning of the unit cell, with the scattering power $\sum_{n=1}^{N} f_n^2$ and N(N-1) more atoms with the scattering power $f_n \times f_j$ in the positions $(\vec{r}_n - \vec{r}_j)$. Obviously values of Patterson-function maxima and their form can be calculated by the formulas derived in [3] for the electron density function, by replacing f_j by $f_n \times f_j$ everywhere.

In order to calculate the height of a maximum produced by a certain pair of atoms, the following approximate formulas from [3, 4] may be used:

$$P'_{ij}(0) = kZ_{av}^{\alpha} p \text{ el}^2/\text{A}^2. \tag{3}$$

Here $P_{ij}(0) = P(\vec{r}_{ij})$, the average "atomic" number $Z_{av} = \sqrt{Z_i Z_j}$, and k, α, and p are taken from the tables for G_1 in [3]. However, far more accurate values are obtained by approximately calculating the integral itself:

$$P_{ij}(0) = \frac{1}{2\pi^2}\int_0^{\infty} f_i(s) f_j(s) s^2 ds \simeq \frac{1}{2\pi^2} \sum_{k=0}^{k\,\max}{}' f_i(s_k) f_j(s_k) s_k^2 \Delta s_k. \tag{4}$$

Here, as usual, $s = 4\pi \sin \theta/\lambda$ s_k is the value of s in the kth interval of some "width" Δs_k (the entire region s, used in the experiment, is divided into these intervals): f_i and f_j include (here and everywhere below) the temperature factor, determined, for instance, by the Wilson method [6] or from comparison of F_{exp} with F_{calc}: i.e., $f_i = f_{i,\,table} \exp(-B \sin^2\theta/\lambda^2)$, and similarly f_j. Calculation by Formula (4) is laborious and requires preliminary construction of graphs of the function

$$D(s) = \frac{1}{2\pi^2} f_i(s) f_j(s) s^2 \tag{5}$$

(a simpler approximate calculation by means of (3) gave a deviation up to 20% in our case). Graphs of D(s), shown in Figs. 1 and 2, were constructed for several values of the temperature factor B. As the latter increased, the maximum value of D(s) is appreciably decreased and the half-width of the maximum, which, to a certain extent and in any case most simply, characterized the sharpness of the peak, is somewhat decreased.

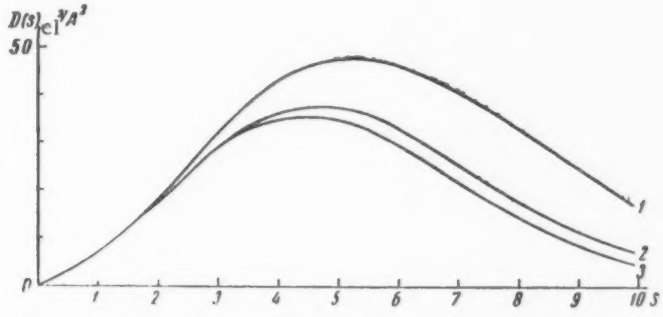

Fig. 1. Radial function D(s) for the Si–Si peak. In Curves 1, 2, and 3, B = 1.0, 1.75, and 2.0 A^2, respectively.

Values of $P_{ij}(0)$, calculated by Formula (4) for four peaks from atoms with different values of Z and for different values of the temperature factor, are given in Table 1. To calculate the form of maxima of the three-dimensional Patterson function, assuming that, as usual, they have spherical symmetry in the first approximation, it is necessary to evaluate the expression

$$P_{ij}(r) = \frac{1}{2\pi^2}\int_0^{\infty} f_i(s) f_j(s) s^2 \frac{\sin(sr)}{sr} ds, \tag{6}$$

or approximately:

$$P_{ij}(r) \approx \frac{1}{2\pi^2} \sum_{k=0}^{k\,\max}{}' f_i(s_k) f_j(s_k) s_k^2 \frac{\sin(s_k r)}{s_k r} \Delta s_k. \tag{7}$$

TABLE 1

Peaks	$Z_i Z_j$	$P_{ij}(0)$		
		$B = 1,0$	$B = 1,75$	$B = 2,0$
Zr — Si	560	1002	725	657
Zr — Na	440	725	537	490
Zr — O	320	420	318	290
Si — Si	196	302	213	201

Using tables of the function sin (sr)/sr [7], we calculate the radial distribution of the function P_{ij} (r) near the maximum. Comparison of the form of the peak for different values of the temperature factor B shows that thermal motion strongly affects not only the maximum value of the peak, but also its form (Fig. 3). The half-width of the maximum δ increases with B:

$B(A^2)$	1,0	1,75	2,0
δ (A)	0,32	0,37	0,38

For comparison of calculated value of the Patterson maxima and their form with experimental ones, the three-dimensional Patterson synthesis of the recently-deciphered silicate $Na_2ZrSi_6O_{15} \cdot 3H_2O \cdot 0,5NaOH$ [12] was used. The P-function was drawn to the absolute scale in which all calculations were performed. To increase the accuracy, the drawing was carried out according to a somewhat modified formula [3, 4]:

$$kP(000)_{exp} = \sum_{i=1}^{N} P_{ii}(0) - \frac{F_{000}^2}{V}; \qquad (8)$$

here $P(000)_{exp}$ is the value of the unnormalized function at the beginning of the Patterson unit cell $F_{000}^2 = \left(\sum_{i=1}^{N} Z_i\right)^2$, V is the unit-cell volume, and the $P_{ii}(0)$ are calculated by Formula (4). Thus the absolute value of the function P at any point will be:

$$P(xyz)_{abs} = kP(xyz)_{exp} + \frac{F_{000}^2}{V}. \qquad (9)$$

The appearance of the additional term F_{000}^2/V is due to the fact that in finding $P(xyz)_{exp}$ one cannot take into account the zeroth term, since it cannot be given in relative units.

It is more difficult to establish the exact value of the constant temperature factor B. The best solution probably would be to determine it from the form of the initial peak of the Patterson function, with regard to which we usually know beforehand, of which $P_{ii}(0)$ maxima it is composed. But for this we must have a normalized value of P(000), and normalization is impossible without knowing the temperature factor. In the Patterson function of lovozerite, chosen for illustration, the temperature factor was established after several successive approximations through a certain variation of it relative to the approximately-known value determined by the Wilson method [6]; the result obtained was B = 1.75 A^2. The rather close coincidence of form of the zeroth peak $P(xyz)_{abs}$ and the theoretical peak $\sum_{i=1}^{N} P_{ii}(r)$ obviously may serve to confirm the correctness of the assumed (average for all atoms) isotropic temperature factor.

A comparison of the form of experimental and theoretical peaks (taking their multiplicity into account) is given in Figs. 5 and 6. As was to be expected, curves of "heavier" maxima give the best correspondence: two peaks (Zr−Si) with coordinates x=0.29, y=0, z=0.73 and x=0.49, y=0.225, z=0.71 (which made it possible to find the approximate coordinates of the Si atoms), and also two summary peaks (Zr−Na)+(Si−Si) with the coordinates x=0, y=0, z=0.50 and x=0.25, y=0.25, z=0.25. For "lighter" peaks of the three-dimensional synthesis of Zr−O, Si−Si, and Na−Na the errors in F^2_{exp} have a substantial effect, which (together with deviation from a centrosymmetric arrangement of atoms [12]) leads to distortion of their form. However, the height of the maximum remains close to the theoretical value (within the limits of error).

A series of calculations, carried out with respect to P(xyz) for lovozerite, showed that uncontrolled approximations often lead to relatively large errors. As an example we give those values of P(xyz), which result from calculations based on the well-known Booth approximations for the electron density function [8, 9]

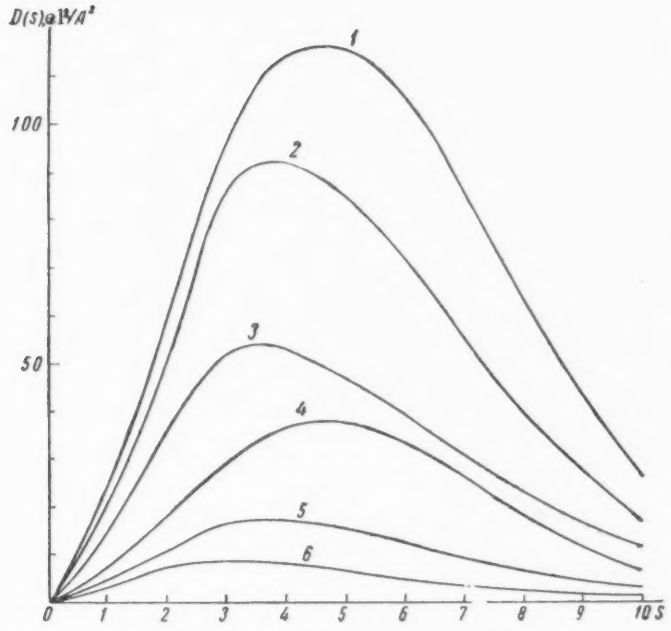

Fig. 2. Radial function D(s) for B = 1.75 A^2 and various $Z_i \times Z_j$ values: Zr–Si(1), Zr–Na(2), Zr–O(3), Si–Si(4), Si–O(5), O–O(6).

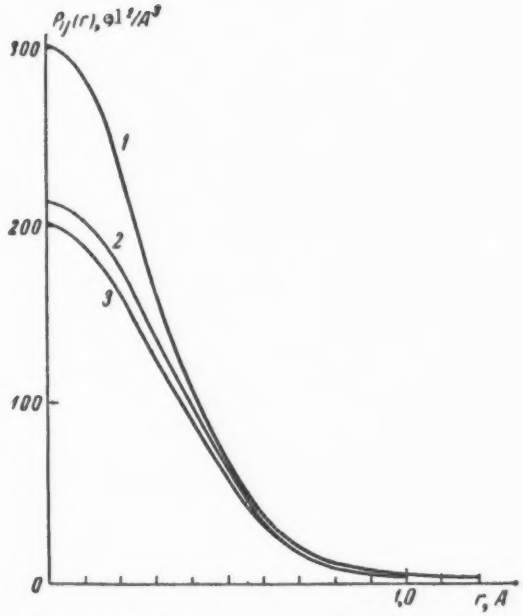

Fig. 3. Effect of thermal motion on the form of the peak of the Patterson function P_{Si-Si} (r). In Curves 1, 2, and 3, B = 1.0, 1.75, and 2.0 A^2, respectively.

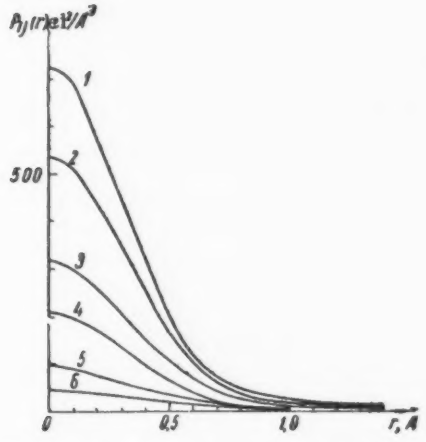

Fig. 4. Function P_{ij} (r), calculated in the vicinity of the maximum for peaks Zr–Si (1), Zr–Na(2), Zr–O(3), Si–Si(4), Si–O (5), O–O(6), B = 1.75 A^2.

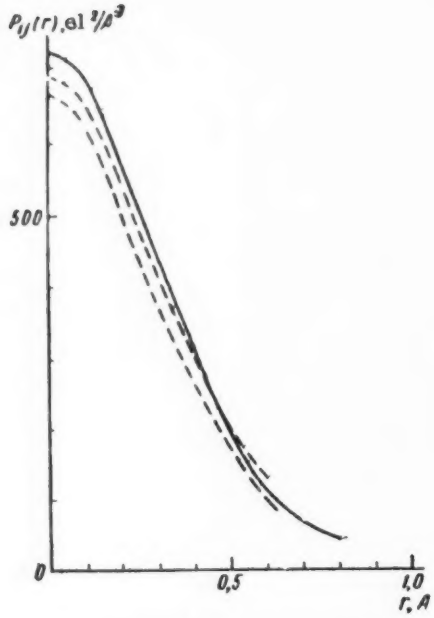

Fig. 5. Function $P_{Zr-Si}(r)$. Solid lines – theoretical curve; dashed lines – experimental curves.

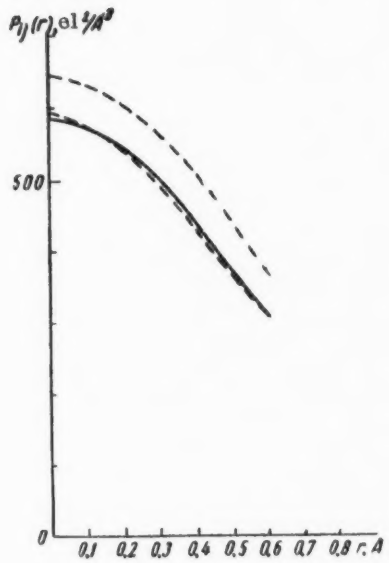

Fig. 6. Function $P_{Zr-Na}(r) + P_{Si-Si}(r)$. Solid line – theoretical curve; dashed lines – experimental curves. The theoretical curves of the (Si–Si) and (Zr–Na) peaks are superposed with a displacement corresponding to the vector $\underline{r}$ (see [12]).

$$\rho''(r) = A \exp(-mr^2) \tag{10}$$

and those of Kitaigorodskii [10, 11]

$$\rho'''(r) = \frac{\beta t}{(r^2 + \beta^2)^2 \pi^2}. \tag{11}$$

The arbitrary parameters in these functions may be determined by using the normalization

$$Z = \int_0^\infty \rho(r)\, 4\pi r^2\, dr \tag{12}$$

and the value of $\rho(0)$, taken from [3]. The functions then acquire the form:

$$\rho_i''(r) = kpZ_i^\alpha \exp[-\pi(kpZ_i^{\alpha-1})\, r^2] \tag{13}$$

$$\rho_i'''(r) = kpZ_i^{\alpha+4/3}\{r^2\pi^{4/3}(kpZ_i^\alpha)^{4/3} + Z_i^{4/3}\}^{-2}. \tag{14}$$

Calculating the value of P_{ij} at the center of the maximum

$$P_{ij}(0) = \int_0^\infty \rho_1(r)\, \rho_2(r)\, 4\pi r^2\, dr, \tag{15}$$

we obtain for the Booth approximation

$$P''_{ij}(0) = kp\,(Z_i Z_j)^{\alpha+1}\,[(Z_i^{\alpha} Z_j)^{1/3} + (Z_i Z_j^{\alpha})^{1/3}]^{-3/2} \tag{16}$$

and

$$P''_{ii}(0) = \frac{kpZ_i^{\alpha+1}}{2\sqrt{2}} \tag{16a}$$

and for the Kitaigorodskii approximation

$$P'''_{ij}(0) = kp\,(Z_i Z_j)^{\alpha+1}\,[(Z_i Z_j^{\alpha})^{1/3} + (Z^{\alpha} Z_j)^{1/3}]^{-3} \tag{17}$$

and

$$P'''_{ii}(0) = \frac{kpZ_i^{\alpha+1}}{8}. \tag{18}$$

Numerical values of $P''_{ij}(0)$ and $P'''_{ij}(0)$ are given in Table 2.

TABLE 2

Peaks	$Z_i Z_j$	$P_{ij}(0)$	$P''_{ij}(0)$	$P'''_{ij}(0)$	Peaks	$Z_i Z_j$	$P_{ij}(0)$	$P''_{ij}(0)$	$P'''_{ij}(0)$
Zr — Zr	1600	2377	2970	1050	Si — Si	196	213	274	97
Zr — Si	560	725	890	320	Si — O	112	97	145	51
Zr — Na	440	537	675	240	O — O	64	44,5	78	27,5
Zr — O	320	318	470	165	Na — Na	121	124	159	56

Testing on the comparatively complex structure of lovozerite showed that the method of quantitative evaluations can be used to great advantage in the deciphering of three-dimensional Patterson syntheses of unknown structures.

LITERATURE CITED

1. M. Buerger, Acta crystallogr. 4, 531 (1951).
2. V.I. Simonov, Kristallografiya 4, 3, 302 (1959).
3. B.K. Vainshtein, Zhur. Eksp. i Teoret. Fiz. 27, 44 (1954).
4. B.K. Vainshtein, Structural Electronography [in Russian] (Izd. AN SSSR, Moscow, 1956).
5. Internationale Tabellen zur Bestimmung von Kristallstrukturen (Berlin, 1935) No. 1, II, pp. 571-573.
6. A.J.C. Wilson, Nature 150, 152 (1942).
7. J. Sherman, Z. Kristallogr. 85, 404 (1933).
8. A.D. Booth, Proc. Roy. Soc. A 188, 77, 1012 (1946).
9. D.W.J. Cruickshank, Acta crystallogr. 2, 65 (1949).
10. A.I. Kitaigorodskii, X-ray Structural Analysis [in Russian] GITTL, Moscow, 1950).
11. A.I. Kitaigorodskii, Theory of Structural Analysis [in Russian] (Izd. AN SSSR, Moscow, 1957).
12. V.V. Ilyukhin and N.V. Belov, Doklady Akad. Nauk SSSR 131, 1, 176 (1960).*

* Original Russian pagination. See C.B. translation.

APPLICATION OF INFRARED SPECTROSCOPY TO THE DETERMINATION OF SILICATE STRUCTURES

I. REFLECTION SPECTRA OF SODIUM SILICATE CRYSTALS IN THE 7.5-15 μ REGION

V.A. Florinskaya and R.S. Pechenkina

S.I. Vavilova Leningrad State Optical Institute
Translated from Zhurnal Strukturnoi Khimii, Vol. 1, No. 1, pp. 86-98, May-June, 1960
Original article submitted June 19, 1959

We have studied the reflection spectra of crystallized two-component glasses containing from 12 to 55 mole % Na_2O. We have also shown that the phase diagram of the $Na_2O - SiO_2$ system does not reflect the entire set of crystalline silicates capable of existing in this system.

INTRODUCTION

The infrared spectra of silica [1-17] and silicates [18-27] in the 8-30 μ region contain a series of bands corresponding to the fundamental frequencies of silicon and oxygen atoms in the crystal lattics of these compounds. The number of bands, their position in the spectrum, their structure, intensities, and polarization depend on the crystal structure. Hence, not only different compounds, but also different crystalline forms of any one compound will give distinct spectra [11, 13, 14]. This fact makes it possible to use infrared spectroscopy for the physicochemical analysis of silicates.

We have studied the crystallization of glasses in the Na_2O-SiO_2 system and the resulting products. Our results will be presented in several papers, the first of which deals with the study of the reflection spectra of the glass crystallization products; subsequent papers will describe the study of the crystallization process itself and some solid state reactions.

EXPERIMENTAL

The Glass. In our study we have used primarily glasses containing from 12 to 50 mole % Na_2O. All of them were fused under ordinary industrial conditions, either in one hundred-liter, or twenty-two-liter, or five-liter quartz pots. In addition to this, a large amount of similar glasses (as well as glasses containing 55.60 and 66.6 mole % Na_2O) were also fused under laboratory conditions in platinum crucibles, in a platinum resistance furnace, by using a high-speed platinum stirrer (of these glasses the last three crystallized out while the melt was cooling). In this case the mixture was prepared from ultrapure materials. We obtained our SiO_2 by grinding high-quality quartz crystals between millstones made of the same quality quartz. Sodium carbonate was purified by the Voano method. In certain melts we also used the Kalbaum brand of soda. Both the industrial and the laboratory quality glasses, particularly those containing 14.20, 25.5, 30, 33.3, and 50 mole % Na_2O, were fused several times; in this way results obtained from various melts could be compared. Glass samples fused in the glass-maker were checked for waviness under the same conditions as are used for testing optical glass. Experimental samples were made up of flawless glass. Not all of our glasses were annealed. The glasses were crystallized in a continuous constant temperature annealing oven. The temperature was regulated and maintained constant to within several degrees by means of an automatic model SP-3 – P-1 potentiometer. The temperature

itself was measured on a portable model PP-1 potentiometer. The absolute temperature could be determined with a precision of several degrees. The samples were inserted into the oven on platinum foil. The thermal processing was varied from 1 to 1000-3500 hr at a constant temperature.

When the Na_2O content was 33.3 mole % or higher the glass would crystallize completely after only one or several hours. However, our experiments have shown that in many cases upon being left at a constant temperature many newly formed crystals changed their form. And therefore in an attempt to determine the nature of these changes in several cases we extended considerably the duration of the heat treatment.

Samples. The experimental samples were made in the form of flat discs 20-30 mm in diameter and 5-10 mm thick. All the glasses were polished under anhydrous kerosene. The reflections were measured immediately after the samples were polished. All the discs were kept in a desiccator before and after the heat treatment. To prevent the possibility of surface film interference with the crystallization process, every sample of once polished glass was repolished right before being inserted into the oven. Since it frequently happens that when a sample crystallizes the outer layers contain one kind of silicate while the interior another, we studied portions of both the crust and the underlying layers. When reflections from the crust were studied the discs were not repolished after the heat treatment. Due to diffused reflections from such surfaces some of the light was lost during the measurements, and consequently the corresponding selective reflection curves frequently had slightly lower intensities; otherwise the curves retained the correct shapes. After the reflection spectrum of the outer layers was recorded these were removed from the samples by grinding. Usually a layer 1-2 mm thick was ground away. After that the discs were repolished and the reflection spectra of the inner portions were studied. In certain cases the results were checked by examining 5-10 layers at different depths.

Apparatus. The glass reflections were studied in the 7-15μ region, where some of the fundamental silicate absorption bands are located. We used in our work a model IKS-11 spectrometer having a NaCl prism with a 60° refracting angle. A Kozyrev vacuum thermocouple served as energy receiver. The reflections were measured in unpolarized light at an almost 25° angle. The reflections from our samples were compared with reflections from an aluminum reflector. All of our measurements were recorded visually and checked several times.

EXPERIMENTAL RESULTS

Phase diagrams of the Na_2O-SiO_2 system reveal the existence of the following compounds: $Na_2O \cdot 2SiO_2$, $Na_2O \cdot SiO_2$, $3Na_2O \cdot SiO_2$, and $2Na_2O \cdot SiO_2$ [28-31]; also some workers [29-30] mention only one, others [30], at least two modifications of sodium disilicate. This last paper also mentions the existence of mixed crystals in the examined system. These crystals are spread on both sides of the sodium disilicate composition though not very far. A study of the transmission and reflection spectra [26, 27] of crystallized glasses containing from 12 to 66.6 mole % Na_2O showed that crystalline sodium silicates are actually much more numerous and diverse than has been previously assumed on the basis of other experimental methods. The lack of fuller knowledge of these silicates and of their transformations is to a large extent responsible for the many problems that one faces in the study of sodium silicate glasses.

Figures 1 and 2 show the reflection spectra of glasses containing from 12 to 55 mole % Na_2O, which crystallized completely at 620°. The abscissa gives the wave length λ in microns, while the ordinate gives the relative reflection coefficient R in percent. All the spectra are from the inner portions of crystallized samples, layers at least 1-2 mm from the surface. The length of heat treatment τ (in hours) is given beside each curve. The differences in the length of heat treatment are unimportant, since we were primarily interested in showing what general kinds of silicates can exist in the system.

Curves 4, 5, and 6 (Fig. 1) show some typical spectra of crystallized glasses of the sodium disilicate composition. Crystallized glasses from various melts either exhibited spectra which could be related to one of these three types or had spectra which gradually changed into one of the three given types.

An optical crystal analysis (carried out by E.Ya. Mukhin) revealed that crystals yielding spectrum 4 and 5 have the same outside appearance and refractive index and have optical properties identical with $Na_2O \cdot 2SiO_2$. On the other hand crystals yielding spectrum 6 differ from the preceding two types in their outside appearance—they grow in the form of fibers instead of plates like the others. The corresponding refractive index data is rather contradictory. Earlier determinations indicate that it is identical with the refractive index of sodium disilicate, while more recent results indicate it is higher. This problem will be resolved later on.

A comparison of Curves 4, 5, and 6 shows that they differ in the structure of their strongest bands and in the position of their maxima (9.60-9.65 μ, 9.80 μ, and 10.20 μ); consequently we must be dealing with different crystal structures.

We would like to point out that none of these spectra, or the spectrum of $Na_2O \cdot SiO_2$ for that matter, agree with the infrared spectra calculated by Stepanov and Prima [32] and used as a basis for the interpretation of sodium silicate glass structures.

Curves 10 and 11 (Fig. 1) show the spectra of various crystallized glasses of the sodium metasilicate composition. The first of these two curves was recorded on a glass sample prepared from high-purity materials; normal grade materials were used for the glass represented by the second curve. According to Mukhin's data the crystals which form under these conditions represent the normal sodium metasilicate. The most intense reflection maximum of $Na_2O \cdot SiO_2$ lies at 10.20-20.25 μ Besides it, the spectrum contains another intense maximum at 11.4 μ. The latter most likely does not belong to the metasilicate but to sodium carbonate, which is always present in crystallized glasses containing 50 mole % Na_2O. This conclusion is confirmed by the fact that the sodium carbonate spectrum contains three strong bands, at 7 μ, 11.4 μ, and 14 μ respectively. All these bands can be found in the spectra of crystallized glasses containing 50 mole% or more of Na_2O, and their intensities increase with the Na_2O content. In addition to this, just as in the case of sodium carbonate, the intensities of the 7μ and the 14 μ bands increase sharply when the water content of the examined sample is raised.

The spectra of products obtained from the crystallization of all the other glasses could not be represented as a simple super-position of the spectra of SiO_2, $Na_2O \cdot 2SiO_2$, $Na_2O \cdot SiO_2$, and $2Na_2O \cdot SiO_2$, all of which are known from the phase diagrams.

Besides these, the system may contain either compounds with a high silica content or a high Na_2O content.

Thus, for example, curve 12, which represents the spectrum of a crystallized glass containing 55 mole% Na_2O reveals that besides the metasilicate (the 10.25 μ peak) the crystallization product also contains some other silicate richer in Na_2O (the 10.75 μ band); this last one differs also from $2Na_2O \cdot SiO_2$, the spectrum of which has the strongest maximum at 10.3 μ.

The high Na_2O content of this silicate can be deduced from the following observations:

1) With increasing content of the metal oxide component the strongest absorption band of a silicate usually shifts towards longer wave lengths.

2) The observed chemical reactions (taking place in the solid phase) between silicates with bands at $\lambda \geq$ $\geq 10.4\mu$ and silica indicate that the formation of silicates with a maximum at 10.2-10.3 μ reduces the amount of both of the initial components.

The spectrum of the glass containing 45 mole % Na_2O also shows that besides sodium disilicate (the 9.65 μ maximum) the crystallized glass contains some other kind of silicate rich in Na_2O having a reflection maximum at 10.55 μ. It is still impossible to tell if these large silicates constitute distinct chemical compounds or if they are just solid solutions. At this stage it was simply important to establish the fact that these silicates actually exist.

The spectra of crystallized glasses containing less than 33.3 mole % Na_2O cannot be reproduced either by superimposing the spectrum of silica on that of sodium disilicate, as one would have expected from the phase diagram. For example, the spectrum of a glass containing 25.5 mole % Na_2O (the composition at the eutectic between the silica and the sodium disilicate phases) can not be reproduced by superimposing curves 4,5, and 6 of Fig. 1 over curves 1, 2, and 5 of Fig. 3, which represent some very stable compound with a silica content higher than that of sodium disilicate. Budnikov and Matveev have proposed [33] that the compound may be $Na_2O \cdot 3SiO_2$, but it is also possible that the compound is $Na_2O \cdot 4SiO_2$, since such a silicate is indeed found in crystallized glasses containing 22 and 20 mole % Na_2O. The actual composition range of this compound will be discussed in a later communication.

When the Na_2O content of glasses is reduced to 12-14 mole % we get some other unknown crystalline silicates with selective reflection bands at 9.42-9.45μ and 9.68-9.70 μ. The first one of these apparently is a compound with a silica content exceeding that of the compound discussed in the preceding paragraph. As evidence that we are dealing with an actual compound we can cite the fact that a silicate with the same maximum

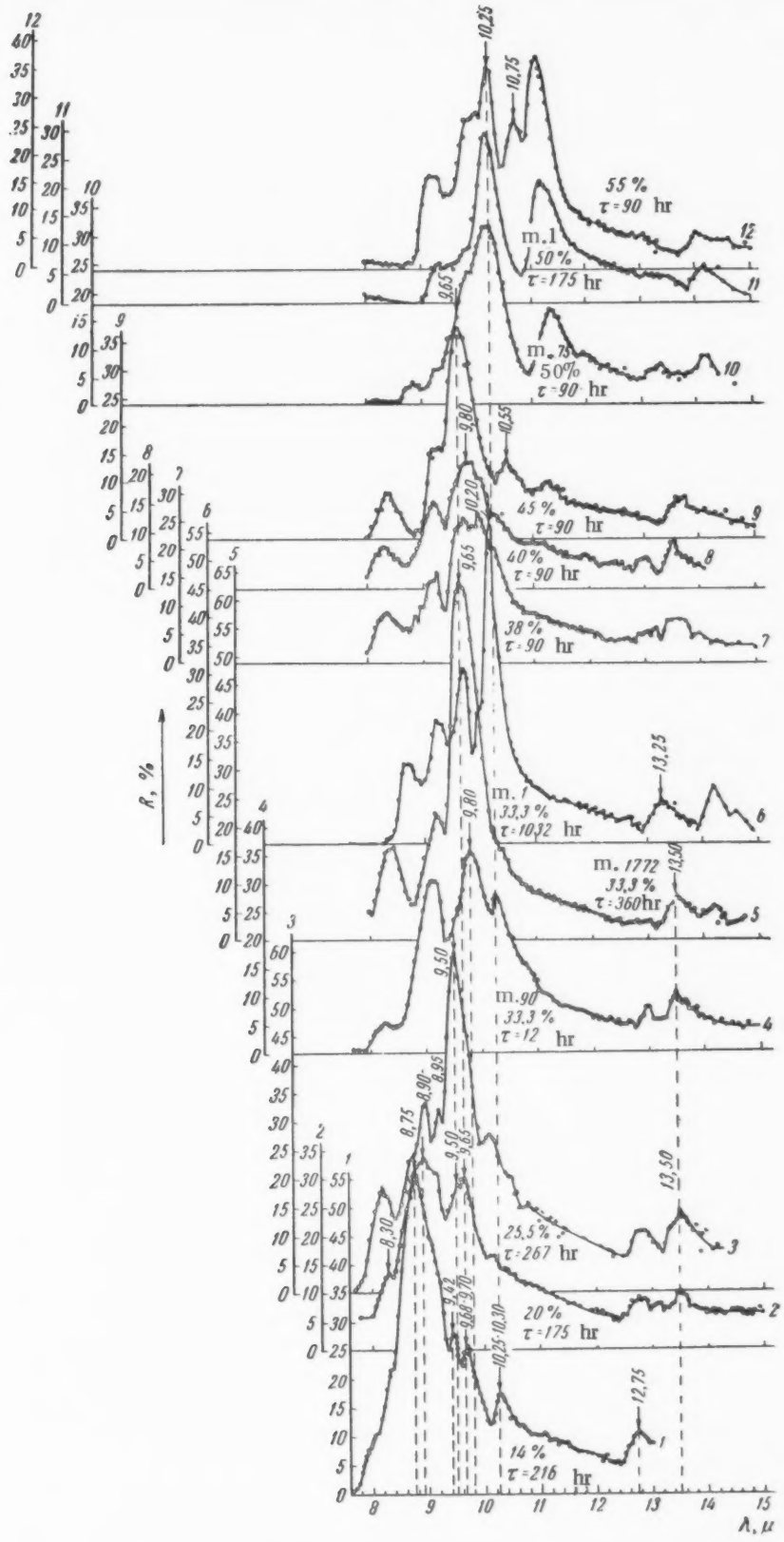

Fig. 1. The reflection spectra of crystallized glasses containing from 14 to 55 mole% Na_2O. Inner portions, t = 620° (m. = melt).

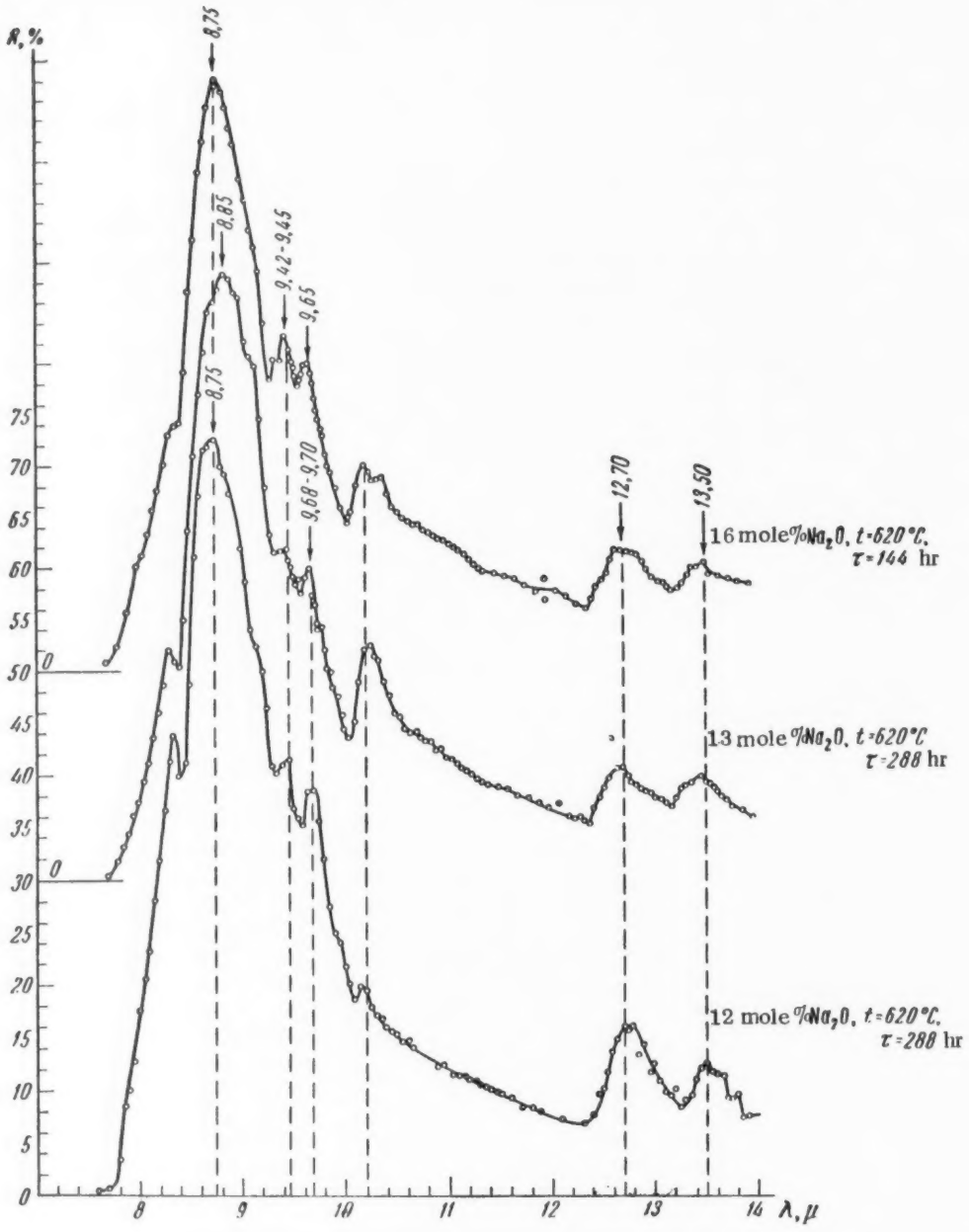

Fig. 2. The relection spectra of crystallized glasses containing 12, 13, and 16 mole % of Na_2O. Inner portions, t = 620°.

frequently appears in quite a number of crystallized glasses of very high silica content. The fact that the maximum occurs always at the same wave length indicates that the shift from 9.50 μ (curve 3) to 9.42-9.45 μ could not possibly be attributed to any kind of lattice defects in the newly formed crystals, since in various samples these defects would be different and consequently produce different spectra. The spectrum of the silica constituting the bulk of crystallized high-silica-content glasses (the 8.75 μ and the 12.7 μ bands on curve 1 in Fig. 1) is very different from the spectra of α-quartz [14], α-tridymite [17], and α-cristobalite [14], as can be seen in Fig. 3 where the spectra are presented alongside each other. A similar type of silica is encountered in many glasses of various compositions which had been crystallized under diverse conditions. At the same time the fact that the most intense reflection bands constantly appear in the same place indicates that we must be dealing

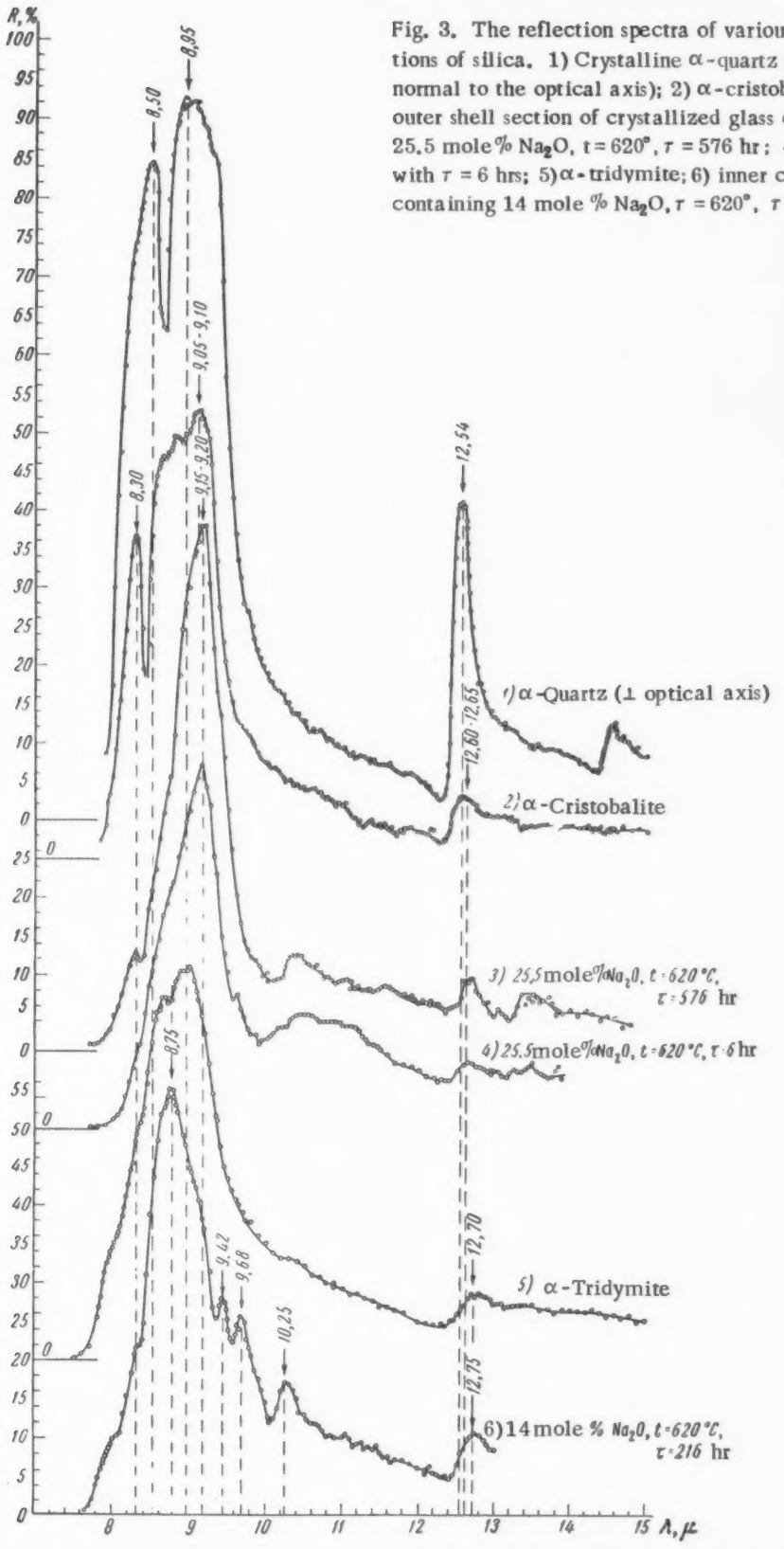

Fig. 3. The reflection spectra of various modifications of silica. 1) Crystalline α-quartz (a slice cut normal to the optical axis); 2) α-cristobalite; 3) outer shell section of crystallized glass containing 25.5 mole % Na_2O, t = 620°, τ = 576 hr; 4) same but with τ = 6 hrs; 5) α-tridymite; 6) inner core of glasses containing 14 mole % Na_2O, τ = 620°, τ = 216 hrs.

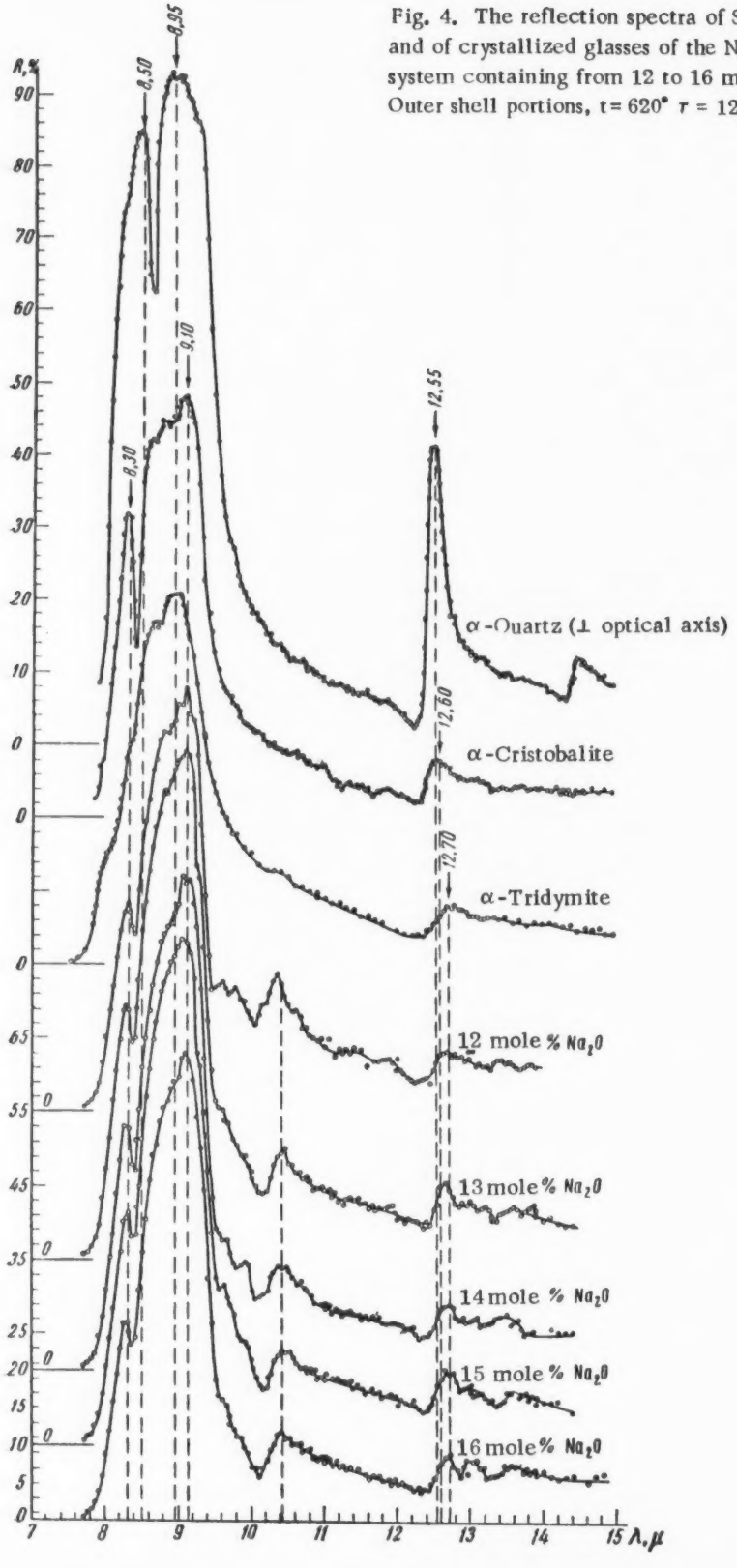

Fig. 4. The reflection spectra of SiO_2 crystals and of crystallized glasses of the Na_2O-SiO_2 system containing from 12 to 16 mole % Na_2O. Outer shell portions, $t = 620°$ $\tau = 12$ hr .

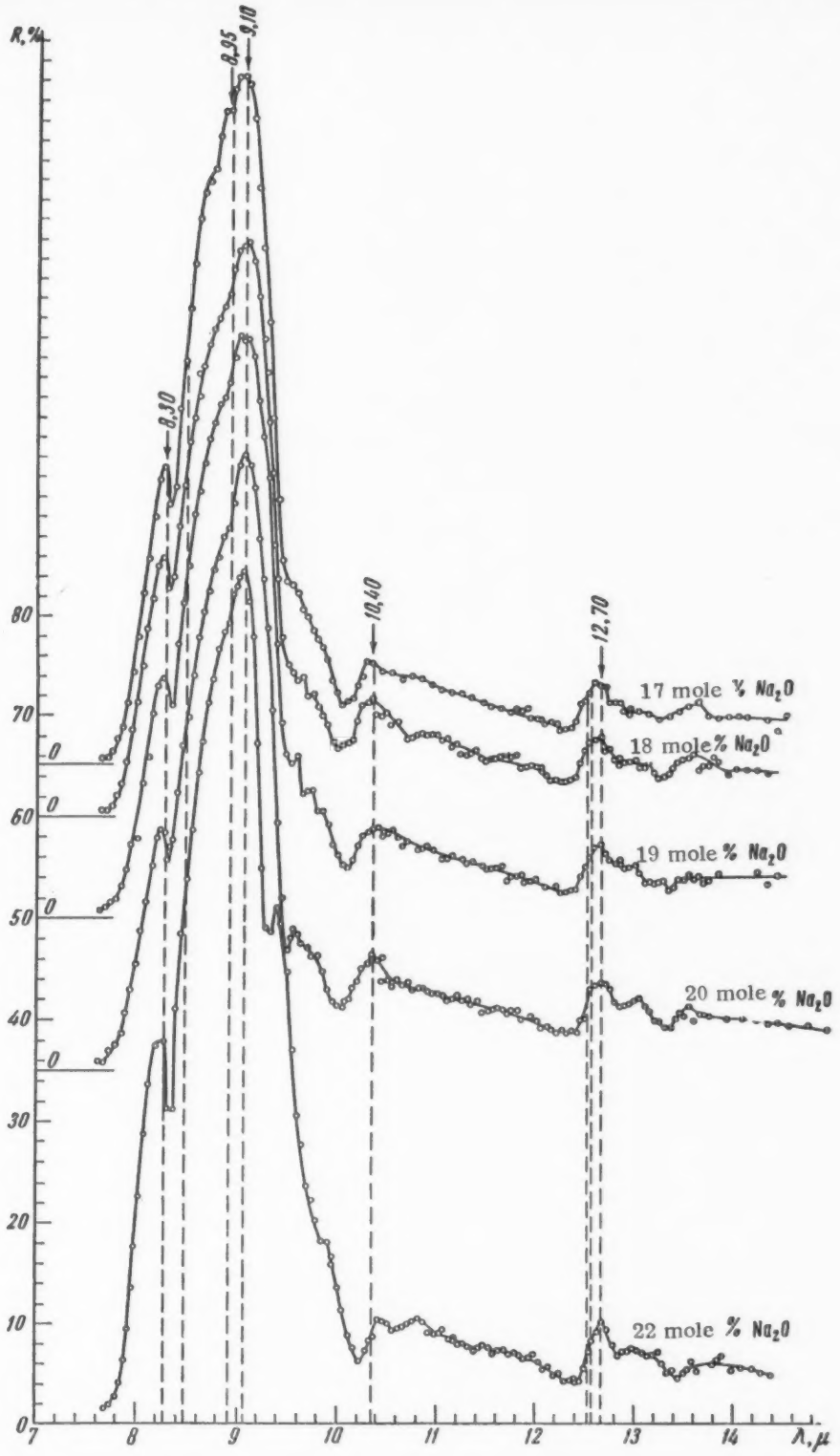

Fig. 5. The reflection spectra of crystallized glasses containing from 17 to 22 mole % Na_2O. Outside shell portions, t = 620°, τ = 12 and 288 hr for glasses containing 17-20 and 22 mole % Na_2O respectively.

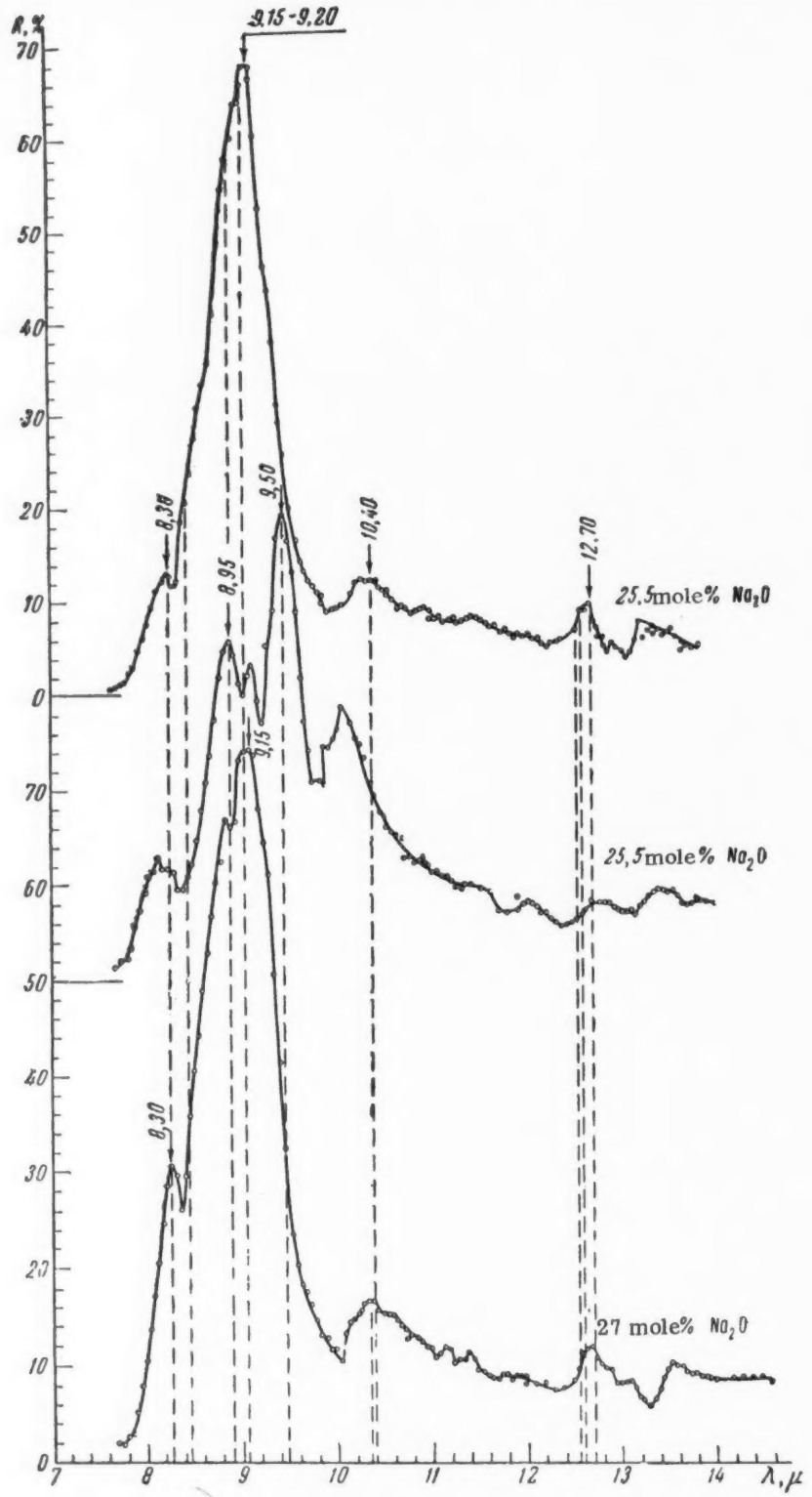

Fig. 6. The reflection spectra of crystallized glasses (outside shell portions). The uppermost curve is for 25.5 mole % Na_2O, t = 620°, and τ = 576 hr; the middle one is for 25.5 mole % Na_2O, t = 570°, τ = 288 hrs; the lowest one is for 27 mole % Na_2O, t = 620°, τ = 24 hr.

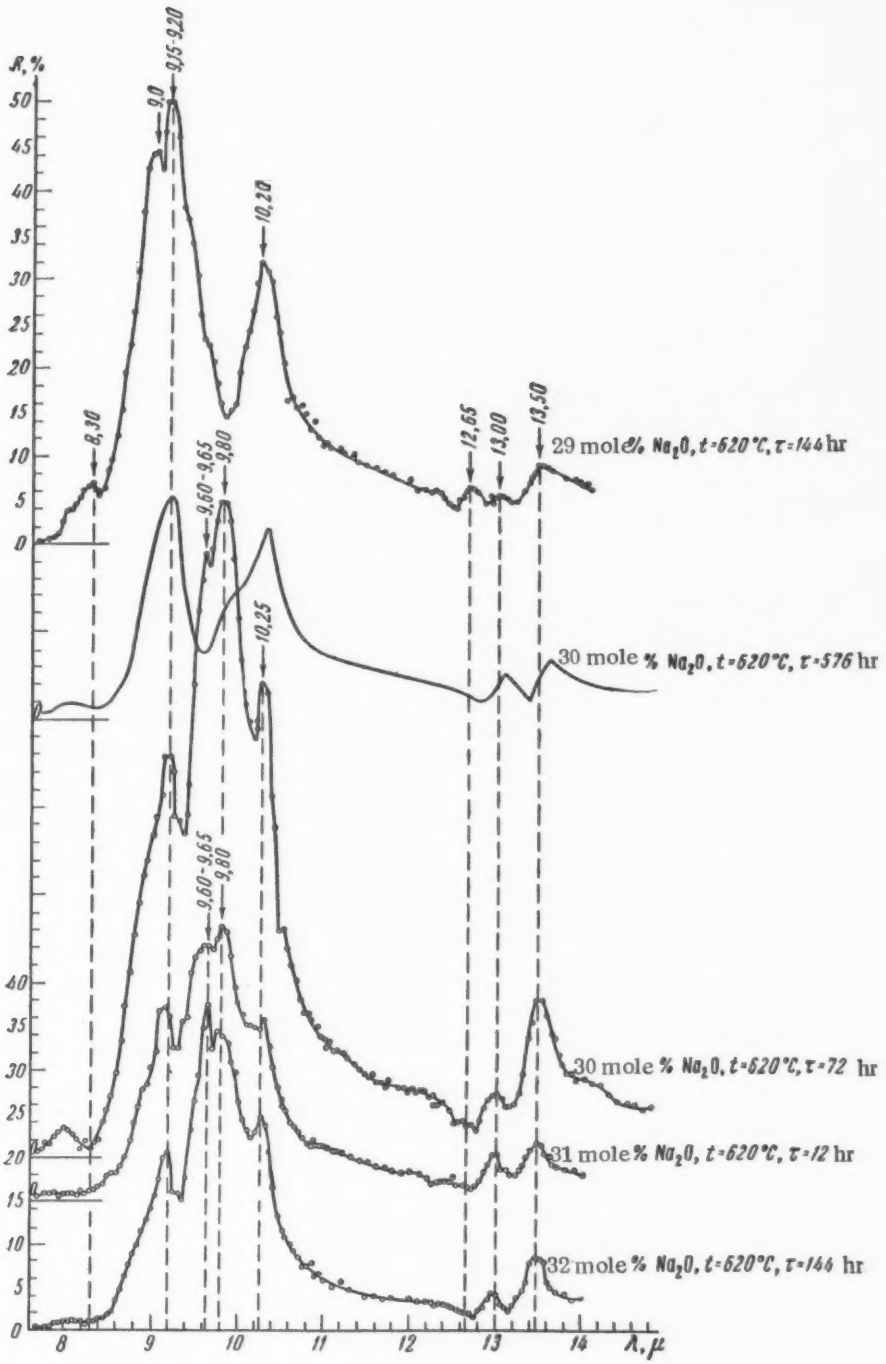

Fig. 7. The reflection spectra of crystallized glasses containing from 29 to 32 mole % Na_2O. Outside shell portions, t = 620°.

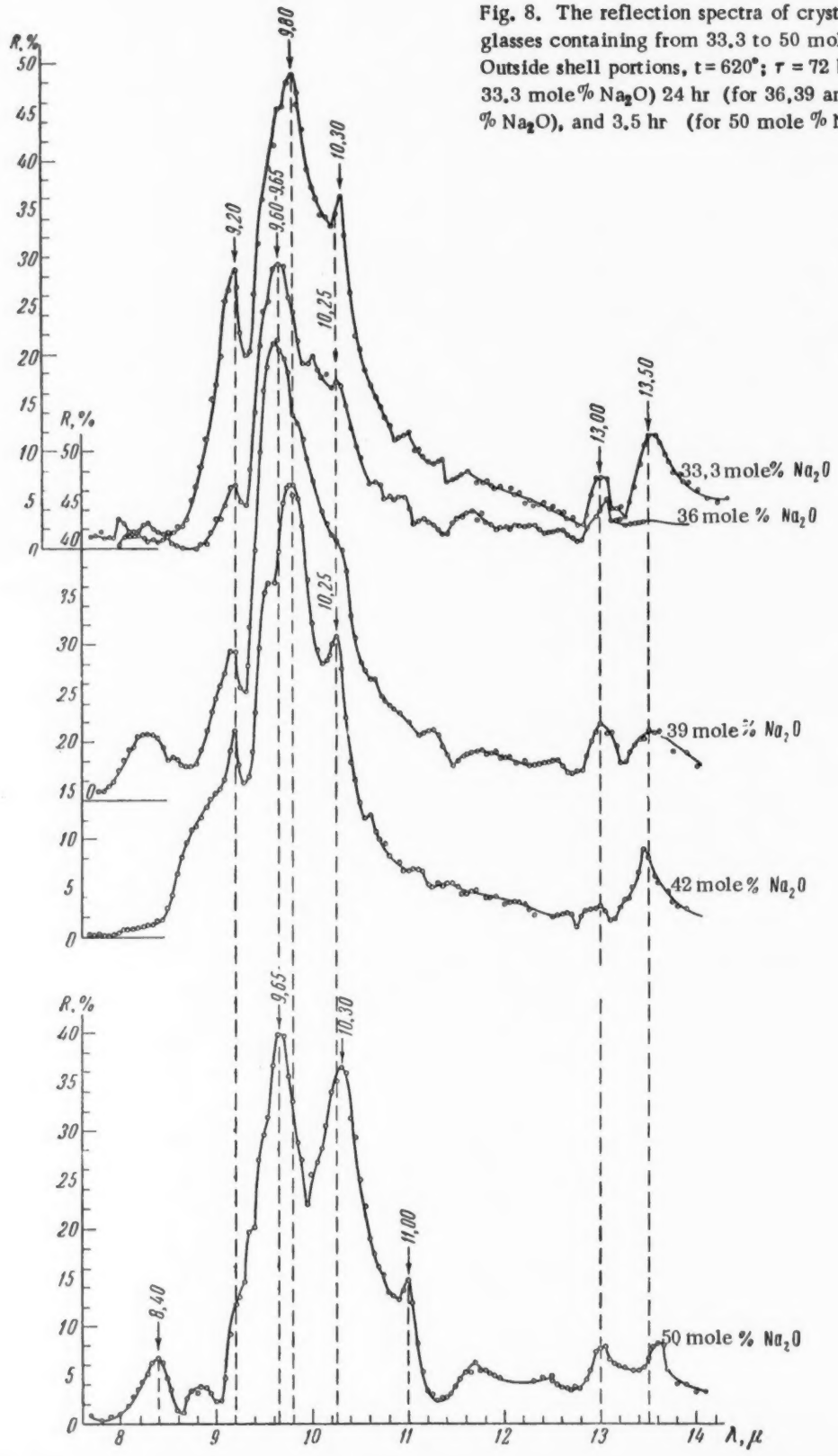

Fig. 8. The reflection spectra of crystallized glasses containing from 33.3 to 50 mole % Na_2O. Outside shell portions, t = 620°; τ = 72 hr (for 33.3 mole% Na_2O) 24 hr (for 36,39 and 42 mole % Na_2O), and 3.5 hr (for 50 mole % Na_2O).

with another form of SiO_2. In Figs. 4-8 we have reproduced the reflection spectra of silica [14, 17] and of the outside shell of glasses of the Na_2O-SiO_2 system crystallized at 620°. The heat treatment of most of these samples extended from 3.5-12 to 24 hr, i.e., most of the spectra shown in Figs. 4-8 represent glasses in the early stages of crystallization.

For the glasses containing 25.5 mole % Na_2O we have reproduced the spectra of samples crystallized at 620 and 570°, since the crystals formed at these two temperatures are entirely different. For precisely the same reason two spectra are given for the glass containing 30 mole % Na_2O. Silica, which is responsible for the bands at 8.30 μ, 9.10-9.20 μ, and 12.6-12.7 μ, constitutes the major portion of products formed when glasses containing from 12 to 29 mole % Na_2O are crystallized; in addition to silica these glasses yield also silicates with a high content of Na_2O, as is indicated by the presence of bands at 10.4-10.6 μ and 13-14 μ. The most intense band in the spectra of crystallized glasses containing less than 22 mole % Na_2O is a doublet with peaks at 9.05-9.10 μ and 8.30 μ – the characteristic wave-lengths of α-cristobalite. Therefore the silica crystallizing out under these conditions can be identified only with this form of SiO_2. In glasses containing 25.5 mole % or more Na_2O the strongest maximum shifts towards longer wave-lengths, to 9.15-9.20 μ, and becomes much sharper in the process than the corresponding peak of α-cristobalite (Fig. 3); at the same time the intensity of the side-band at 8.30 μ declines. We are apparently dealing in this case with a more "primitive"* form of cristobalite. It in its turn is preceded by an even more "primitive" silica. This last one can be found at the earliest stages of glass crystallization, as soon as the first fogging appears on the glass surface. In Fig. 3 (curve 4) we have reproduced a spectrum of such a fogged surface. When glasses containing 29 mole % or more of Na_2O crystallize the outside shell portions of the samples consist of a mixture of silica, sodium disilicate, sodium metasilicate, and other silicates with a higher Na_2O content. This can be readily seen by comparing the corresponding curves.

The described investigation of crystallized sodium silicate glasses clearly demonstrates how inadequate are phase diagrams for the detection of all the silicates that can exist in the given system.

It is still uncertain which of the discovered crystals represent actual compounds. But since glasses themselves constitute nonequilibrium systems, in studying the structure and properties of glasses one has to consider all of the crystalline silicates which may exist under one or another set of conditions in a given system. The x-ray crystallographic data on these same crystallized glasses are in good agreement with the results of our spectroscopic investigation.

The authors are grateful to A.G. Alekseev and G.O. Bagdyk'yants for their x-ray diffraction study of our samples. We also wish to express our gratitude to Academician A.A. Lebedev for suggesting this project and for all the assistance rendered towards the completion of this work, and to A.G. Vlasov for his valuable advice and aid.

LITERATURE CITED

1. H. Rubens, Ann. Physik, 45, 23 (1872).
2. W.W. Coblentz, Investigations of I.R. Spectra Carnegie Inst. (Washington Publ.,1906) Vol. 65, Part 3, p. 21.
3. E.F. Nichols, Phys. Rev. 4, 297 (1897).
4. O. Reinkober, Ann. Physik, 34, 343 (1911).
5. T. Liebisch and H. Rubens, Berl. Ber., 199 (1919).
6. C. Schaefer and M. Schubert, Z. Phys. 7, 313 (1921).
7. M. Czerny, Z. Phys. 53, 317 (1929).
8. J.D. Hardy and S. Silvermann, Phys. Rev. 37, 176 (1931).
9. S. Silvermann, Phys. Rev. 45, 158 (1934).
10. R.L. Henry, J. Opt. Soc. Am. 38, 9 (1948).
11. V.A. Florinskaya and R.S. Pechenkina, Doklady Akad. Nauk SSSR 85, 6 (1952).
12. J. Simon and McMahon, J. Chem. Phys. 21, 23 (1953).
13. M. Haceuria, Bull. Soc. chim. Belg. 62, 428 (1953).
14. N.A. Sevchenko and V.A. Florinskaya, Doklady Akad. Nauk SSSR 109, 6 (1956).
15. N.A. Sevchenko and V.A. Florinskaya, Optika i Spektroskopiya 4, 189 (1958).

* One with a simpler crystal lattice than low-temperature cristobalite (relative to silica).

16. N.A. Sevchenko and V.A. Florinskaya, Optika i Spektroskopiya 4, 261 (1958).
17. N.A. Sevchenko, Inzh. -Fiz. Zhur. 1, 8 (1958).
18. C. Schaefer, F. Matossi and R. Wirtz, Z. Phys. 89, 210 (1934).
19. F. Matossi and H. Krüger, Z. Phys. 99, 1 (1936).
20. F. Matossi and O. Bronder, Z. Phys. 111, 1 (1938-1939).
21. F. Matossi, Z. techn. Phys. 12, 585 (1937).
22. F. Matossi and H. Bluschke, Z. Phys. 108, 295 (1938).
23. F. Matossi, J. Chem. Phys. 17, 679 (1949).
24. R. Launer, Am. Mineralogist 37, 764 (1952).
25. V.A. Florinskaya and R.S. Pechenkina, Glass Structure, Trans. of the Confer. on Glass Structure [in Russian] Leningrad, November 23-27, 1953 (Izd. AN SSSR, 1955).
26. V.A. Florinskaya and R.S. Pechenkina, Optika i Spektroskopiya 1, 690 (1956).
27. V.A. Florinskaya, Optika i Spektroskopiya 2, 724 (1957).
28. G.W. Morey and N.W. Bowen, J. Phys. Chem. 28, 1167 (1924).
29. I.V. Grebenshchikov and K.A. Krakau, Trans. State Optical Institute [in Russian](1929) Vol. 5, p. 45.
30. F.E. Kracek, J. Phys. Chem. 34, 1588 (1930).
31. J. Löffler, Dissertation, Univ. Berlin (1930).
32. B.I. Stepanov and A.M. Prima, Optika i Spektroskopiya 4, 734 (1958); 5, 15 (1958).
33. P.P. Budnikov and M.A. Matveev, Doklady Akad. Nauk SSSR 107, 4 (1956).*

*Original Russian pagination. See C.B. translation.

THE APPLICATION OF ELECTRON PARAMAGNETIC RESONANCE TO THE STUDY OF MOLECULAR STRUCTURE OF CARBONS

N.N. Tikhomirova, I.V. Nikolaeva, and V.V. Voevodskii

Institute of Chemical Physics, Academy of Sciences of the USSR
Translated from Zhurnal Strukturnoi Khimii, Vol. 1, No. 1, pp. 99-102,
May-June, 1960
Original article submitted December 11, 1959

The electron paramagnetic resonance (EPR) line structure method of analysis, developed earlier, has been used to investigate the change in structure of the conjugated aromatic system of coconut charcoal, which results from different effects.

It has been shown that repeated treatment of charcoal with a mixture of 5% KOH + alcohol–pyridine at 100° decreases ω_e, the frequency of electron exchange between separate aromatic networks.

During reversible adsorption of oxygen, ω_e increases, indicating facilitation of exchange in the presence of oxygen. Adsorption of one oxygen molecule leads to a decrease in the effective number of unpaired electrons by approximately 60. Conclusions have been made as to the possible nature of the formation of unpaired electrons in charcoals.

A method of determining the frequency of exchange interaction ω_e for the paramagnetic resonance singlet line was given in [1] for those cases where ω_e approximates to the width of the line in order of magnitude. For the determination, the interactions between an unpaired spin and the surrounding medium are given by the essential parameters: the exhange frequency ω_e and the value of ω_g, which is characteristic of the spin distribution of the system in the absence of any exchange interaction. According to van Vleck's theory [2], the relation $\omega_g^2/\omega_e \cdot \omega_L \approx 1$ must hold, where ω_L is the parameter which characterizes the central portion of the line, which obeys the Lorentz relation in the presence of exchange interactions. For a sufficiently strong exchange interaction, i.e., for $\omega_e > \Delta\omega_{1/2}$, the majority of the lines are described by this law and ω_L is found on the half-widths of the lines determined experimentally. From these considerations the parameter ω_L clearly does not have an independent value, since it is linked with ω_e and ω_g in a well-defined manner.

It was shown in the paper quoted that in PVC (polyvinylchloride) chars, obtained at 600°, the values of ω_g and ω_e were $0.67 \cdot 10^7$ and $1.2 \cdot 10^7$ sec^{-1}. The value of ω_g can be evaluated independently for a system of spins uniformly distributed in space, for a given spin concentration. This evaluation leads to a somewhat smaller value because it does not take into account the possibility of the line being widened through forbidden hyperfine structure, which would obey the Gauss law. On the basis of analysis of the EPR line for PVC chars, obtained at different temperatures, the following conclusions were drawn: 1) with increasing carbonization temperature, the aromatic networks were enlarged, i.e., the regions of delocalized electrons increased, resulting in a decrease in ω_g, and 2) the relative amount of the irregular surrounding structure, through which exchange takes place, was decreased, i.e., ω_g decreased.

These conclusions are confirmed by known carbon chemistry and by x-ray structure analysis of charcoals [3]. Analogous changes in ω_g and ω_e are observed for sugar chars, obtained in the temperature range 400–650°. There is good reproducability of ω_g and ω_e values for chars from different series of preparations (for example, for samples from different series ω_g equals $0.73 \cdot 10^7$ and $0.67 \cdot 10^7$ sec^{-1} and ω_e equals $1.05 \cdot 10^7$ and $1.05 \cdot 10^7$ sec^{-1}).

TABLE 1

The Variation of Exchange Frequency ω_e on Removing the Irregular Surrounding Structure of Charcoals

Sample	Exchange frequency ω_e, sec^{-1}	
	"old"	"young"
Initial sample	$5.2 \cdot 10^7$	$4.5 \cdot 10^7$
First treatment	$3.2 \cdot 10^7$	–
Second "	$3.8 \cdot 10^7$	$3.2 \cdot 10^7$
Third "	–	$3.0 \cdot 10^7$
Fourth "	$3.2 \cdot 10^7$	$3.0 \cdot 10^7$

TABLE 2

p_{O_2}, mm Hg	N, g^{-1}	ΔN, g^{-1}	$(nO_2)_{ads}$, g^{-1}	$\Delta N/(nO_2)_{ads}$
0	$458 \cdot 10^{18}$	—	—	—
10	$200 \cdot 10^{18}$	$258 \cdot 10^{18}$	$3,8 \cdot 10^{18}$	~68
20	$152 \cdot 10^{18}$	$306 \cdot 10^{18}$	$4,1 \cdot 10^{18}$	~74
30	$116 \cdot 10^{18}$	$342 \cdot 10^{18}$	$5,2 \cdot 10^{18}$	~66
40	$76 \cdot 10^{18}$	$382 \cdot 10^{18}$	$5,7 \cdot 10^{18}$	~67

We consider that here we are dealing essentially with exchange between separate spin systems, and the frequency will be considerably less than the exchange frequency in individual molecules with conjugated bonds, where it is 10^{14} – 10^{15} sec^{-1}. Values for the exchange frequency, found by us, are of the same order of magnitude as the rate constants for elementary reactions of chemically activated particles (e.g., radicals), which suggests that exchange of the type under consideration could play an essential part in the course of complex chemical processes.

We were interested in explaining how the ω_e value changed in two cases: 1) on removal of the surrounding structure, which facilitates exchange, by chemical reaction, and 2) on formation of other opportunities for exchange by inserting into the structure bridges between the separate networks of aromatic systems. In the first case, natural carbons were studied, which gave intensive narrow peaks in air with a g-factor practically coinciding with that of DPPH (Diphenylpicrylhydrazyl). Repeated treatment of such carbons with a mixture of 5% KOH + alcohol-pyridine at 100° led to a gradual elimination of the surrounding structure.* Analysis of the structure of the narrow peak showed that in fact ω_e decreased as the surrounding structure was removed. Table 1 contains values for ω_e obtained from analysis of the experimental curves for two sorts of chars ("old and "young").

This data indicates that the exchange interactions between separate networks of aromatic systems occur through the irregular surrounding structure.

The construction of synthetic bridges between the networks is a more interesting and complex point, and it was found expedient to study the effect of oxygen on EPR spectra of chars. There have been many references to an increase in the line width at half-height, i.e., an increase of ω_L due to the action of oxygen, which is generally accepted as an indication of a decrease in exchange and in the amplitude of the peak [4]. For most of the chars, those effects were completely reversible, and the initial form and amplitude of the peak could be regained after evacuation at room temperature. Most of the investigators assumed that there was no change in the concentration of unpaired electrons during oxygen adsorption [5]; others assumed that the number of unpaired electrons decreased [6]. Our method of analysis of the linear structure has, in our opinion, settled this question. From what has been said, it can be seen that it is possible on the basis of this analysis to determine on the one hand ω_g or ω_e, and on the other to evaluate much more exactly the total concentration of paramagnetic particles, since it is possible to evaluate absorption at the extremes of the Gauss section of the curve.

* These carbon samples were supplied by a colleague at I.G.I. Akademii Nauk SSSR, to whom the authors are very grateful.

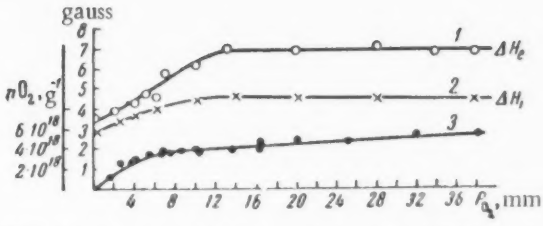

The change in ω_e (1) and ω_g (2) of the EPR line of sugar char in relation to the oxygen pressure; 3) adsorption of oxygen at room temperature.

Such a detailed analysis was carried out on sugar charcoal, and during oxygen adsorption both a widening of the peak and a decrease in the concentration of paramagnetic particles were observed.

First we studied the effect of oxygen on the parameters ω_g and ω_e. Experimental data for sugar charcoal showing the change of these parameters with the oxygen pressure is given in the diagram.* The increase in ω_g is probably determined by the local magnetic field of the adsorbed oxygen molecules. The increase in ω_e indicates an increase in the exchange interaction in the presence of oxygen (not a decrease of it, as could be assumed from a consideration of just one value of ω_g).

These results are comparable with those put forward by Frumkin in 1935 [7], who proposed the existence of a type of oxygen adsorption on charcoal in which the oxygen molecules penetrated between neighboring sections of aromatic networks. Taking into account the fact that an oxygen molecule has initially two unpaired electrons, a model of this type would fit in well with the assumptions given above, i.e., those concerning the possible easing of electron exchange between neighboring sections during oxygen adsorption.

It should also be noted that ω_e and ω_g vary with the amount of adsorbed oxygen (Fig. 1, curve 3). This confirms that changes in ω_e and ω_g depend on the adsorbed oxygen molecules. Table 2 gives the values of N, ΔN, and the number of oxygen molecules $(nO_2)_{ads}$ adsorbed by 1 g charcoal for a sample of sugar charcoal at different oxygen pressures p_{O_2}.

Thus, adsorption of one oxygen molecule changes the number of effective spins by approximately 60. Oxygen also has a very effective influence on the values of ω_e and ω_g. In fact, the results show that adsorption of $\sim 10^{19}$ oxygen molecules results in a change in the exchange frequency and the ω_g parameter by a total of $5 \cdot 10^{20}$ spins for the sample.

The above results make it possible to come to certain conclusions about the nature of the free valencies in charcoals and other carbonization products of organic substances. It has been established in the literature that paramagnetism of carbons is due to the distorted chemical bonding in the irregular structure [8]. From data on delocalized unpaired electrons, the authors of [9] came to conclusions about the π-character of the electron cloud. However, for some time past, data has been published on EPR in systems having conjugated double bonds and aromatic rings, which give, in our opinion, some idea of the nature of EPR peaks for carbonized compounds.

For dinaphthosemiquinone for example, a clear EPR absorption peak with g ~2.0 was observed [10]. Determination of the concentration of unpaired spins showed that there is one unpaired electron for 400 dinaphthosemiquinone molecules. An analagous result was obtained in a study of a series of quinoline dyestuffs [11]. In these compounds, paramagnetic resonance absorption peaks were discovered, which corresponded on the average to one unpaired electron for 5000 dyestuff molecules. EPR studies of polymers consisting of macromolecular chains with conjugated bonds [12] showed that at a certain degree of polymerization a narrow EPR peak (~5 gauss) appeared, due to the unpaired electrons being delocalized throughout the polymeric chains.

In all the cases examined, like the case of carbons, the EPR peak increases with decreasing temperature, which completely excludes the hypothesis of a thermal excitation to the triplet state. The appearance of EPR peaks in these systems are considered to be due to the emergence of "anomalous" paramagnetism, dependent not on distorted chemical bonds, but on some new magnetic interaction of electrons (as yet unknown), which results in a complex bond system. There is no theory of this phenomenon, and it is only possible to characterize a degree of paramagnetism which represents the number of unpaired electrons (measured experimentally) in relation to the number of conjugated systems.

It therefore follows that adsorbed oxygen molecules not only act as "little bridges" in facilitating exchange, but by virtue of their paramagnetism, distort the interactions of the electronic system of conjugated bonds.

*ΔH and ω are proportional to each other ($\Delta H \cong 3 \cdot 10^{-7} \omega$).

Data in Table 2 confirm the conclusion that oxygen adsorption results in a decrease of the effective number of paramagnetic particles. The ready desorption of oxygen, and complete reduction of the peak on evacuation, clearly suggests that stable chemical bonds are not formed during adsorption; the decrease in intensity of the peak during adsorption is linked with a decrease in the average degree of paramagnetism through the action of the magnetic moment of oxygen. It is possible that a decrease of N_{eff} at oxygen pressures greater than 10 mm Hg, once adsorption equilibrium has been attained, is also linked with the change in paramagnetism due to an increasing number of collisions between paramagnetic oxygen molecules and the lattice surface. This point needs further investigation.

LITERATURE CITED

1. N.N. Tikhomirova and V.V. Voevodskii, Optika i Spektroskopiya 7, 829 (1959).
2. J.H. van Vleck, Nuovo cimento, Suppl. 6, Ser. X, 993 (1956).
3. N.N. Tikhomirova, B.V. Lukin, L.L. Razumova, and V.V. Voevodskii, Doklady Akad. Nauk SSSR 122, 264 (1958).*
4. D.E.G. Austen, D.J.E. Ingram, and J.G. Tapley, Trans. Faraday Soc. 54, 400 (1958).
5. L.S. Singer and W.J. Spry, Bull. Am. Phys. Soc. 1, 214 (1956).
6. R.C. Pastor, J.A. Weil, T.H. Brown, and J. Turkevich, Phys. Rev. 102, 918 (1956).
7. S. Lweina, A. Frumkin, and A. Lunew, Acta physicochim. USSR 3, 397 (1935).
8. D.J.E. Ingram, J.G. Tapley, R. Jackson, R.L. Bond, and A.R. Murnaghan, Nature 174, 797 (1954).
9. F.H. Winslow, W.O. Baker, and W.A. Jager, J. Am. Chem. Soc. 77, 4751 (1955).
10. J. Matsunaga, Canad. J. Chem. 37, 1003 (1959).
11. Yu.Sh. Moshkovskii, Doklady Akad. Nauk SSSR 130, 6, 1277 (1960).*
12. A.A. Berlin, L.A. Blyumenfel'd, M.I. Cherkashin, A.É. Kalmanson, and O.S. Sel'skaya, Vysokomolek. Soed. 1, 9, 1361 (1959).

*Original Russian pagination. See C.B. translation.

NEW MAGNETIC PROPERTIES OF MACROMOLECULAR COMPOUNDS CONTAINING CONJUGATED DOUBLE BONDS

L.A. Blyumenfel'd, A.A. Berlin, A.A. Slinkin, and A.E. Kalmanson

Institute of Chemical Physics of the Academy of Sciences of the USSR
Translated from Zhurnal Strukturnoi Khimii, Vol. 1, No. 1, pp. 103-108, May-June, 1960
Original article submitted December 17, 1959

Polymers with conjugated double bonds give narrow electronic paramagnetic resonance signals with the free spin g-factor. The intensity of the signals increases with increase in the conjugation. The effect is an intramolecular one, independent of dissolution, and characterizes the fundamental state of the π-electron cloud of the molecule. In the solid state, polymers with conjugated double bonds, especially those containing nitrogen atoms and polar groups in the macromolecular chain, are characterized not only by the narrow lines mentioned above, but also by the broad asymmetrical electronic paramagnetic resonance lines of very great integral intensity. These structures possess positive static magnetic susceptibility, though with increase in the magnetic field intensity, the susceptibility diminishes; the magnetizability, however, remains constant, which makes it permissible to speak of the ferromagnetic properties of the systems under discussion. The effect referred to appears to be purely structural.

In the current work, we have attempted to generalize some results obtained earlier, together with certain new results, on the investigation of the electronic paramagnetic resonance (EPR) spectra of macromolecular compounds, and also data on the measurement of the static magnetic susceptibility of these compounds. The compounds discussed include both hydrocarbon polymers, and polymers containing heteroatoms, each with a system of conjugated double bonds in the polymer chain. As the development will show, these structures exhibit anomalous magnetic properties which are not provided for within the framework of existing concepts. Although there is up to the present no theoretical explanation of the effects which we have observed, it seems to us none the less timely to attempt a systematization of the facts which have been obtained, and to formulate some general suggestions which emerge from them.

The experimental technique involved in the investigation, and the characteristics of the compounds studied, have been described in previous publications (see the literature).

More than ten years have passed since Kozyrev [1] discovered that straight chain hydrocarbons, with a continuous chain of conjugated bonds of the polyene type, give EPR spectra whose intensity increases with increase in the length of the conjugated chain. He suggested that these signals arose from thermal excitation of the molecules in the triplet (biradical) state. He did not, however, measure the temperature dependence of the signal intensity, and, apparently, his explanation is erroneous.

Moshkovskii, while investigating the EPR spectra of cyanine dyes [2], observed the appearance of narrow EPR signals in the fundamental state of the molecules, which was plainly indicated by the nature of the temperature dependance of the intensity of these signals. In the work of Berlin, Blyumenfel'd, Cherkashin, Kalmanson and Sel'ska [3], the EPR spectra of a series of polyphenylactylenes were obtained. All these compounds proved to give narrow EPR signals, with a breadth ΔH between the points of maximum slope of ~ 4-8 oe.

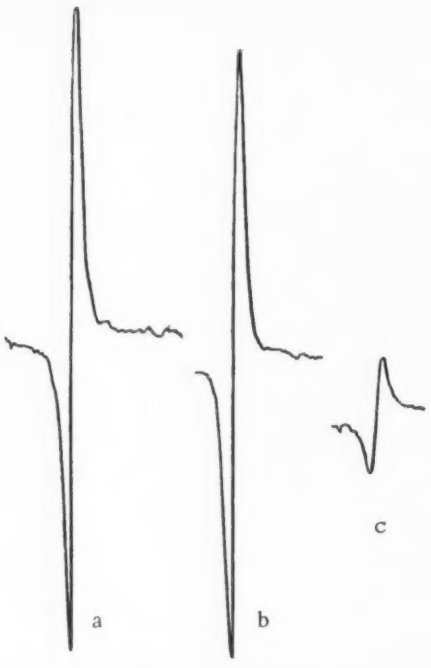

Electronic paramagnetic resonance spectra of polyphenylacetylene.

The following basic results of this investigation may be set out:

1) The position of the EPR spectral lines corresponds practically exactly with the pure spin value of the g-factor.

2) The narrowness of the EPR signal and the absence of superfine structure shows that there must be considerable delocalization of the nonpaired electrons.

3) The intensity of the EPR lines depends sharply on the length of the chain of conjugated bonds and, therefore, on the molecular weight. Increasing the molecular weight from 1100 for compound $(-CPh=CH-)_{11}$ to ~ 2000 for the higher polymer $(-CPh=CH-)_{20}$ (where $Ph=C_6H_5$) leads to an increase in the effective number of unpaired electrons from $\sim 5 \times 10^{17}$ to $\sim 3 \times 10^{19}$ particles/g. Further increase in the degree of conjugation by means of copolymerization, and the formation of two or three dimensional networks, does nor result in increase in the signal.

4) The highest attained signal intensities correspond approximately to a content of 1 unpaired electron per 10 molecules.

5) The intensity of the EPR signals is increased with reduction of temperature in accordance with the Curie law. This makes impossible any explanation of the observed effect as due to thermal excitation in the triplet state. The possibility that the triplet level is the fundamental one, or that it is separated from them by an energy $\Delta E \ll kT$ is excluded by the low magnitude of the effect. For polymers of low molecular weight there are no more than 1 unpaired electron for each 1000 molecules, and in the case of the cyanine dyes [2], no more than 1 for each 10,000 molecules.

6) The intensity and shape of the EPR signals are maintained in solution, and unaffected by the dilution of the solution.

This last fact is very important, and, as we shall see later, is apparently contradictory to the results of measuring the static magnetic susceptibility. For this reason we undertook an additional investigation of the EPR spectra of polyphenylacetylene preparations which give a comparatively intense EPR signal in various solvents (benzene and acetone). The experiments showed that the intensity, shape, and breadth of the EPR lines was not changed by dissolution, and, when recalculated in terms of unit weight of the dissolved material, did not depend on the dilution either. Comparison of the intensities was conducted by reference with the lines produced by an internal standard. The glass ampoule in which the specimen was contained served this purpose, since, as is well known, it gives a clear line with $g \cong 4$ because of metallic impurities in the glass. The figure gives as an example the EPR spectrum of one of the polyphenylacetylene specimens in the solid state (a), in the same amount in saturated solution in benzene (b), and after five-fold dilution of the benzene solution (c).

It may thus be concluded that the appearance of unpaired electrons giving the narrow lines of the EPR spectrum in systems of conjugated double bonds, is a property of separate, individual molecules. Taking into account the fact that signals with corresponding properties are given by an isodisperse system possessing sufficient conjugation, and also that in the interaction of n-diethynylbenzene with these compounds, the polymers are almost quantitatively converted into nonfusible, insoluble block copolymers [4], it can be concluded that the EPR data demonstrate, apparently, that not one molecule in 10 nor one in 100, in the given sample, contains an unpaired electron, but that each molecule "contains" 0.1 or 0.01 unpaired spin. We may, in this sense, speak of "the degree of unpairedness" of the π-electron cloud in a system of conjugated bonds. The theory of this phenomenon still remains to be formed. It may be thought that the narrow EPR lines in coals* of different origin, characterized by the developed chain of conjugated double bonds, are not due, as numerous investigations have presupposed, to ruptured carbon-carbon bonds, but must be connected with the same general phenomenon (see also the article by Tikhomirova, et al., [5] in this issue p. 89).

*It is uncertain whether the authors really mean "coals" here, or simply "natural" carbons from various sources. The latter is more probable, but in either case the introduction of the EPR spectrum of these materials is somewhat abrupt and unexplained. – Translator's note.

Number of specimen	Type of polymer	Molecular weight	$\chi \cdot 10^6$					H, oersteds	$\sigma_{20^\circ} = \chi \cdot H$
			20°	42°	80°	105°	160°		
1	Polyphenylacetylene	1100	−0,07	—	—	—	—	3500	—
			−0,07	—	—	—	—	4000	—
			−0,07	—	—	—	—	4500	—
2	The same	1500	+0,24	+0,25	+0,24	—	—	3500	$0,84 \cdot 10^{-3}$
			+0,20	+0,20	+0,20	—	—	4000	$0,80 \cdot 10^{-3}$
			+0,17	+0,17	+0,17	—	—	4500	$0,77 \cdot 10^{-3}$
3	"	1800	+1,05	+1,05	+1,04	—	—	3500	$3,7 \cdot 10^{-3}$
			+0,93	+0,92	+0,92	—	—	4000	$3,7 \cdot 10^{-3}$
			+0,80	+0,81	+0,80	—	—	4500	$3,7 \cdot 10^{-3}$
4	"	2000	+3,1	+3,1	+2,9	+2,9	—	3500	$1,32 \cdot 10^{-2}$
			+2,6	+2,6	$+2,4_4$	$+2,4_4$	—	4000	$1,30 \cdot 10^{-2}$
			+2,3	+2,3	+2,92	+2,2	—	4500	$1,33 \cdot 10^{-2}$
5	Polyaminoquinone	—	+1,68	—	—	—	—	3500	$5,9 \cdot 10^{-3}$
			+1,56	—	—	—	—	4000	$6,2 \cdot 10^{-3}$
			+1,40	—	—	—	—	4500	$6,3 \cdot 10^{-3}$
6	Polyaminoquinone, structurized by Cu^{2+} ions	—	+4,1	—	+3,7	—	+2,6	3500	$1,43 \cdot 10^{-2}$
			+3,9	—	+3,5	—	+2,4	4000	$1,55 \cdot 10^{-2}$
			+3,8	—	+3,4	—	$+2,2_5$	4500	$1,70 \cdot 10^{-2}$

In the work of Topchiev and co-authors [6], attempts have been made to correlate the EPR spectra of polymers containing conjugated double bonds with their electrical conductivity (for solid specimens). It is clear on the basis of everything which has been said above that this correlation does not emerge from the experimental results, since the two effects have quite different dependences on the temperature. In all probability the electrons (or holes) responsible for the electrical conductivity of solid specimens are not the same as the unpaired electrons which give the EPR lines.

The table gives the results of measurements on the static magnetic susceptibility of some polymers containing conjugated bonds. It must be added that the quantity of unpaired electrons which is determined from the narrow EPR spectral lines cannot lead to the paramagnetism of these compounds. The corresponding paramagnetic susceptibilities are either less than the diamagnetic components, or lie outside the limits of sensitivity of the method of magnetic weights. But, as can be seen from the table, the polyphenylacetyleneswhich have been studied are characterized by comparatively large values of χ, which correspond, if we assume pure spin paramagnetism, to about 10^{21} unpaired electrons per gram of specimen. It is interesting to note that although dissolution of the polymers in benzene or acetone leads to no change in the shape or intensity of the EPR spectrum (as we have seen above), the magnetic susceptibility measured in solution in benzene is approximately -0.6×10^{-6}: that is, the entire magnetism which characterizes solid polymers disappears completely in solution. This fact, to a practical certainty, yet again testifies to the phenomenon of unpaired spins, which give rise to the narrow EPR lines, being a molecular effect and independent of the structure of the sample, while the value of χ, on the other hand, reflects the structural peculiarities of the lattice of the solid material. As we have shown in one of our previous publications [7], certain polymers possessing a conjugated bond system, and containing nitrogen atoms and polar groups in the conjugated chains, give wide, asymmetric EPR lines with a very great integral intensity. An example of this type of polymer is found in the polyaminoquinones. If the assumption of pure paramagnetism is made, then the signal intensity corresponds to 10^{21} or more unpaired electrons per gram. But it would seem that such calculations have no meaning, since the shape, breadth and temperature characteristics of the EPR signals (the sudden extinction of the signal at a definite, sufficiently low, temperature) are reminiscent of the corresponding properties found in antiferromagnetic materials, and not those in paramagnetic substances. The sizes of the effects determined from EPR spectrum and from the static measurement

of χ for these polymers are practically identical. It would seem that the appearance of the wide EPR lines and of static paramagnetism in solid polymers are both explained by the structural effect, and are due to the same structural peculiarity. But these broad EPR lines are not found with all polymers possessing static paramagnetism. A possible explanation for this is given below.

It is seen from the table that the static paramagnetism of these systems exhibits very unexpected peculiarities: 1) the relationship between χ and the field strength; 2) saturation at relatively low field strength (that is the magnetization σ is paractically constant). Such properties are known to be characteristic of ferromagnetism, the materials exhibiting which show cooperative spin interaction, and, consequently, there ought to exist in the polymers studied sufficiently well-ordered parts for this cooperative interaction to be possible in them. It seems that these parts may be present in the samples as "bundles" [8]. It should be observed that the values of χ for polymers 2, 3 and 4 shown in the table are practically independent of temperature, which may point to the antiferromagnetic character of the spin interaction, since the Neél point for similar substances may either be only weakly emphasized, or lie in the high temperature region. Since the ordered regions ("bundles") in the polymers may be supposed to consist of strongly defective microcrystals, it would be difficult to imagine the existence in them of compensated antiferromagnetism, and one might expect the possible development of uncompensated antiferromagnetism: this is in fact suggested by the relationship between χ and H*.

Within the framework of what has been suggested above, it is easy to understand why some molecules which possess positive values of χ do not reveal broad EPR lines. This is apparently either due to the fact that the EPR is measured below the Neél point, or that the absorption line is very broad. If the magnetic properties of polymers with a high degree of conjugation, which have been determined, depend on their macrostructure and the manner in which they are packed into the lattice of the solid material, then every change in the structure must have a direct effect on their properties. The change in structure may take place both through the formation of a network in the polymers and through arrangement into "bundles." Both effects would lead to change in the magnetic properties, the former because of increase in the degree of coordination in the system, and the latter because of the enhancing of the cooperative interaction of the spins. Thus, polymer 6, which consists of polymer 5 which has been structurized by means of cupric ions, at once possesses increased susceptibility, and this increase of χ cannot be fully ascribed to the introduction of copper into the polymer, since similar effects may be produced by merely thermal structurizing of the compound without the use of metal. There is a sharper change in magnetic properties in polymers of the type:

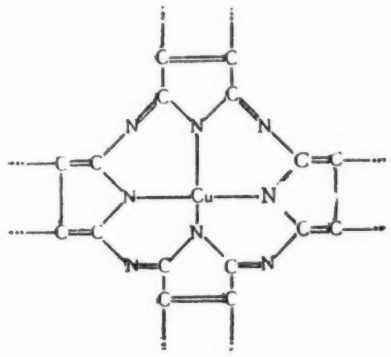

When this compound is heated for six hours at 500°, its susceptibility is increased from $\sim 10 \times 10^{-6}$ to $\sim 50 \times 10^{-6}$, the copper content in the initial and heated polymers being approximately the same. It should also be pointed out that narrow EPR lines are found in the spectrum of the polyaminoquinones, due to the presence in the system of conjugate double bonds. Their appearance under different conditions is completely analogous to the appearance of EPR signals in the polyphenylacetylenes.

*Strictly speaking, it is not correct to apply the term "antiferromagnetism" to the systems under consideration, since saturation in a magnetic field is observed at all temperatures, even those lying higher than the specific point of "antiferromagnetic" transition.

The broad EPR lines, and the anomalous static paramagnetic susceptibility in the synthetic macromolecular compounds which have been studied, is completely analogous to the corresponding properties in the nucleic acids and nucleoproteins [9, 10]. In both cases the properties appear to be purely structural effects, and are completely determined by the high degree of organization (in the macrospecimen) of the multiple molecular structure with local systems of conjugated double bonds.

The presence of nitrogen atoms in the conjugated chain, and of regularly located polar groups and metal atoms, apparently, leads to an increase in the effect.

SUMMARY

It has been shown that macromolecular compounds possessing conjugated double bonds reveal new magnetic properties. In the first place, the presence of a sufficiently developed system of conjugate double bonds produces the phenomenon of "unpairedness" in the basic state of the system, which is manifested in pure spin paramagnetism. It may be suggested that this effect occurs for all molecules possessing conjugated double bonds, but may only be observed experimentally with the experimental techniques at present available for sufficiently large molecules. In the second place, the macromolecular systems which have been studied are characterized by properties closely similar to the antiferromagnetic properties revealed by substances with incompletely compensated antiferromagnetic interaction. This effect depends essentially on a regularized structure within the organization of all the specimens. The authors believe that further investigation involving the synthesis of polymers of this class may lead to the creation of polymeric materials with magnetic properties which, not only qualitatively but also quantitatively, will approximate to the magnetic properties of the ferrites.

LITERATURE CITED

1. B.M. Kozyrev, Doctorate Dissertation, Kazan' Branch of AN SSSR [in Russian] (Kazan', 1956).
2. Yu.Sh. Moshkovskii, Doklady Akad. Nauk SSSR, 130, 6, 1277 (1960).*
3. A.A. Berlin, L.A. Blyumenfel'd, M.I. Cherkashin, A.E. Kalmanson, and O.G. Sel'skaya, Vysokonolek. Soed. 1, 1362 (1959).
4. A.A. Berlin, M.I. Cherkashin, O.G. Sel'skaya, and V.E. Limanov, Vysokomolek. Soed. 1, 12 (1959).
5. N.N. Tikhomirova, I.V. Nikolaeva and V.V. Voevodskii, Zhur. Strukt. Khim. 1, 1, 99 (1960) [this issue].
6. A.V. Topchiev, et al., Doklady Akad. Nauk SSSR 128, 312 (1959).*
7. L.A. Blyumenfel'd, A.A. Berlin, N.G. Matveeva, and A.E. Kalmanson, Vysokomolek. Soed. 1, 11, 1647 (1959).
8. V.A. Kargin, A.I. Kitaigorodskii and G.L. Slonimskii, Kolloidn. Zhur. 19, 131 (1959).*
9. L.A. Blyumenfel'd, A.E. Kalmanson, and Sheny Pei-Keng Doklady Akad. Nauk SSSR 124, 1144 (1959).*
10. L.A. Blyumenfel'd, Biofizika 5, 515 (1959).

* Original Russian pagination. See C.B. translation.

THE MOLECULAR ORBITAL SELF-CONSISTENT-FIELD DETERMINATION OF THE GROUND STATE OF FERROCENE

E.M. Shustorovish and M.E. Dyatkina

M.V. Lomonosov Moscow Institute of Fine Chemical Technology
and the N.S. Kurnakov Institute of General and Inorganic Chemistry
Translated from the Zhurnal Strukturnoi Khimii, Vol. 1, No. 1, pp. 109-121,
May-June, 1960
Original article submitted December 17, 1959

The ground state of ferrocene, $Fe(C_5H_5)_2$, was determined using the molecular orbital (MO) self-consistent field treatment (Roothaan's modification). The molecular orbitals of the complex consisted of ten MO's representing the ring π-electrons, which were constructed from the $2p_z$ atomic orbitals (AO) of carbon, and of nine $3d^5 4s4p^3$ AO's of iron. The atomic orbitals were represented in the form of Slater wave functions. The formulas used for calculating the necessary matrix elements are discussed and their numerical values tabulated. The form and the energies of the MO's in the complex are given. The calculated ionizational potential (6.39 ev) is in a satisfactory agreement with the experimental value (7.05 ev). A detailed discussion of our results will be postponed till after the calculations for similar molecules $(C_6H_6)_2Cr$, $(C_5H_5)_2Co^+$, and $(C_5H_5)_2Cr$ are completed.

As a result of the work done by a number of workers [1], it became apparent that a satisfactory description of the electronic structure of ferrocene and of other metal complexes of aromatic compounds can only be achieved by the molecular orbital treatment. The symmetry of the atomic orbitals of the central atom and of the π-orbitals of the aromatic ring electrons indicated the possibility of having many-center molecular orbitals throughout the molecule. Three types of bonding are possible in bis-cyclopentadienyl compounds: 1) ordinary covalent bonds involving unpaired electrons on the central atom and in the ring, 2) coordination donor-acceptor bonds involving pairs electrons on the ring and vacant orbitals on the central atom, and 3) dative bonds involving paired electrons on the central atom and free antibonding orbitals in the ring.

However, despite the fact that the problem of the bond formation itself has essentially been solved, the data concerned with the molecular orbitals of the metal complexes of aromatic compounds remain qualitative in nature and leave completely unsolved such important problems as the relative energy levels of these molecular orbitals, the relative importance of single and multiple bonds in molecules with various central atoms and aromatic rings, and the electron density distribution in such molecules. In an attempt to solve at least some of these problems we undertook a quantitative determination of the molecular orbitals of metal complexes of aromatic compounds using the MO self-consistent field treatment (Roothaan's modification [2]). In this paper we are reporting the calculations involved in evaluating the ground state energy of ferrocene, $(C_5H_5)_2Fe$, and in subsequent papers we intend to present the calculations on the cobalticenium ion, $(C_5H_5)_2Co^+$, dibenzene chromium $(C_6H_6)_2Cr$, chromocene $(C_5H_5)_2Cr$, and other aromatic complexes.

One previous attempt to apply Roothaan's method to ferrocene is reported in the literature (Yamazaki [3]). Though the results of these calculations were published in 1956 in the form of a brief communication to the editor, no detailed presentation of the calculations involved have appeared until now.

Essentially, Roothaan's method involves the assumption that all the electrons in a molecule are located in one-electron MO's, which can be expressed as LCAO's of the type

$$\varphi_i = \sum_p c_{ip}\chi_p, \tag{1}$$

where the index i denotes a molecular orbital; index p, an atomic orbital, and c_{ip}, a certain arbitrary coefficient.

The condition that MO's be orthogonal is expressed by the equation

$$\int \bar{\varphi}_i \varphi_j d\tau = \sum_{p,\ q} \bar{c}_{ip} S_{pq} c_{jq} = \delta_{ij},$$

where the overlap integrals S_{pq} between AO's are defined by the equation

$$S_{pq} = \bar{S}_{qp} = \int \bar{\chi}_p \chi_q d\tau. \tag{2}$$

The complete normalized 2N electron wave function Φ_{2N} for the singlet ground state of the molecule comes out in the form of an antisymmetrized product of such LCAO−MO functions:

$$\Phi_{2N} = \frac{1}{[(2N)!]^{1/2}} \begin{vmatrix} (\varphi_1\alpha)^1 & (\varphi_1\beta)^1 & \cdots & (\varphi_N\alpha)^1 & (\varphi_N\beta)^1 \\ (\varphi_1\alpha)^2 & (\varphi_1\beta)^2 & \cdots & (\varphi_N\alpha)^2 & (\varphi_N\beta)^2 \\ \vdots & \vdots & & \vdots & \vdots \\ (\varphi_1\alpha)^{2N} & (\varphi_1\beta)^{2N} & \cdots & (\varphi_N\alpha)^{2N} & (\varphi_N\beta)^{2N} \end{vmatrix}$$

where α and β are the two possible electron spin functions, and $(\varphi_i\alpha)^j$ denotes a wave function of the jth electron with a spin $+\frac{1}{2}(h/2\pi)$ located in the MO φ_i. The electronic energy of 2N electrons in the ground state of the molecule is

$$E = \int \bar{\Phi}\, \mathcal{H}\, \Phi\, d\tau,$$

where

$$\mathcal{H} = \sum_\mu H^\mu + \frac{1}{2} \sum_{\substack{\mu,\ \nu \\ \mu \neq \nu}} \frac{e^2}{r^{\mu\nu}}.$$

In this case H^μ is the Hamiltonian for the μth electron located in the field of the nuclei only and unperturbed by other electrons, so that the first part of the summation includes all the one-electron components of the complete energy operator; the second portion of the summation includes all the two-electron operators (where e is the charge of the electron and $r^{\mu\nu}$ – the distance between the μth and νth electrons), and as a result it takes into account the contributions from electron−electron interactions. Due to the requirement that the ground state have a minimum energy, we get the following matrix equation for the determination of coefficients giving the best LCAO-MO's:

$$(\mathbf{H} + \mathbf{G})c_i = \varepsilon_i S c_i, \tag{3}$$

where the c_i vectors form a single-column matrix and represent the AO coefficients in the ith LCAO-MO, S is a Hermitian matrix the elements of which are defined by Eq. (2), and **H** is the energy matrix in the field of only the nuclei; this last term includes both the kinetic and the potential energy of an electron exposed to the field (attraction) of all the nuclei. The respective matrix elements can be calculated from the equation:

$$H_{pq} = \overline{H}_{qp} = \int \bar{\chi}_p H \chi_q d\tau,$$

where

$$H = -\frac{h^2}{2m}\Delta_i - \sum_i \frac{Z_i e^2}{r_i}$$

or in atomic units

$$H = -\frac{1}{2}\Delta_i - \sum_i \frac{Z_i}{r_i}.$$

For the electronic interaction matrix **G**, composed of elements G_{pq}, we get

$$G_{pq} = \overline{G}_{qp} = \sum_i \left(2\int \frac{\bar{\varphi}_i^{\mu}\bar{\chi}_p^{\nu}\varphi_i^{\mu}\chi_q^{\nu}}{r^{\mu\nu}}\, d\tau^{\mu\nu} - \int \frac{\bar{\varphi}_i^{\mu}\bar{\chi}_p^{\nu}\varphi_i^{\nu}\chi_q^{\mu}}{r^{\mu\nu}}\, d\tau^{\mu\nu}\right),$$

with the summation carried out only over all the filled MO's φ_i.

If we define L = H + G then Eq. (3) can be simplified to

$$\mathbf{L}\, c_i = \varepsilon_i \mathbf{S}\, c_i. \tag{4}$$

This short matrix formula represents a system of n homogeneous equations of the type:

$$\begin{aligned}
&c_{i1}(L_{11} - S_{11}\varepsilon_i) + c_{i2}(L_{12} - S_{12}\varepsilon_i) + \ldots + c_{in}(L_{1n} - S_{1n}\varepsilon_i) = 0\\
&c_{i1}(L_{21} - S_{21}\varepsilon_i) + c_{i2}(L_{22} - S_{22}\varepsilon_i) + \ldots + c_{in}(L_{2n} - S_{2n}\varepsilon_i) = 0\\
&\qquad\vdots \qquad\qquad\qquad\vdots \qquad\qquad\qquad\vdots\\
&c_{i1}(L_{n1} - S_{n1}\varepsilon_i) + c_{i2}(L_{n2} - S_{n2}\varepsilon_i) + \ldots + c_{in}(L_{nn} - S_{nn}\varepsilon_i) = 0
\end{aligned} \tag{5}$$

(where n is the number of AO's and consequently MO's). Thus the best LCAO-MO's can be expressed as the eigenfunctions of the Hermitian operator L. To determine the eigenvalues of the energy ϵ_i (energy of the LCAO-MO) we have to solve the secular equation:

$$|L_{pq} - S_{pq}\varepsilon| = 0,$$

i.e., a determinant of the nth order:

$$\begin{vmatrix}
L_{11} - S_{11}\varepsilon & L_{12} - S_{12}\varepsilon & \ldots & L_{1n} - S_{1n}\varepsilon\\
L_{21} - S_{21}\varepsilon & L_{22} - S_{22}\varepsilon & \ldots & L_{2n} - S_{2n}\varepsilon\\
\vdots & \vdots & & \vdots\\
L_{n1} - S_{n1}\varepsilon & L_{n2} - S_{n2}\varepsilon & \ldots & L_{nn} - S_{nn}\varepsilon
\end{vmatrix} = 0. \tag{6}$$

This in turn requires that we compute the matrix elements $L_{pq} = H_{pq} + G_{pq}$ and S_{pq}.

The principal difficulties are encountered in the determination of the G_{pq} elements, which depend on the arbitrary coefficients c_{ip}. The self-consistent field method involves essentially the following procedure: an arbitrary set of coefficients c_{ip} substituted into the secular Eq. (6) yield a corresponding set of eigenfunctions ϵ_i, which are then substituted into Eq. (5) to yield a new set of coefficients c_{ip} (the condition that the MO's be orthonormal must be kept in mind); these in turn are used to get new values of ϵ_i and the process is reiterated until a self-consistent set of coefficients c_{ip} is found.

The solution of Determinant (6) yields n real roots for ϵ_i (i=1,2,....,n) which represent the energies of the LCAO-MO's. If the molecule contains 2N electrons then N lowest MO's will be filled in the ground state while the remaining n-N MO's will remain free.

An electronic transition from a filled ground-state MO φ_i into a free MO φ_j may give rise to singlet and triplet excited states in the molecule. The transition energies would then be

$$^1E = \varepsilon_j - \varepsilon_i - J_{ij} + 2K_{ij}, \tag{7}$$

$$^3E = \varepsilon_j - \varepsilon_i - J_{ij}, \tag{8}$$

where ϵ_i and ϵ_j are the roots of Determinant (6) corresponding to the MO's φ_i and φ_j,

$$J_{ij} = \int \frac{\bar{\varphi}_i^{\mu}\bar{\varphi}_j^{\nu}\varphi_i^{\mu}\varphi_j^{\nu}}{r^{\mu\nu}} d\tau^{\mu}d\tau^{\nu}, \quad K_{ij} = \int \frac{\bar{\varphi}_i^{\mu}\bar{\varphi}_i^{\nu}\varphi_i^{\nu}\varphi_j^{\mu}}{r^{\mu\nu}} d\tau^{\mu}d\tau^{\nu}.$$

Since $K_{ij} > 0$ the triplet state always lies $2K_{ij}$ units below the singlet.

Equations (7) and (8) can be written in the form:

$$^{1,3}E = (\varepsilon_j - \varepsilon_i) - (J_{ij} - K_{ij}) \pm K_{ij}, \tag{9}$$

or by representing the average energy of the singlet and triplet states by $\epsilon_j^{(i)} = \epsilon_j - (J_{ij} - K_{ij})$, in the form:

$$^{1,3}E = (\varepsilon_j^{(i)} - \varepsilon_i) \pm K_{ij}, \tag{9'}$$

where the plus sign is used for the singlet state and the minus for the triplet.

Equation (9') shows that in Roothaan's method the roots of Determinant (6) can only have a physical significance for filled MO's in the ground state of the molecule, while to represent the energy of free MO's it is more appropriate to use functions of the type $\epsilon_j^{(i)}$.

From Eq. (7)–(9') it follows that the first ionization potential of the molecule is equal to the absolute energy of the upper filled MO φ_i, i.e., that

$$I_1 = -\varepsilon_{i'}.$$

To evaluate the matrix G we have to know which MO's are filled with electrons, since only filled molecular orbitals contribute to the matrix elements G_{pq}. In most cases the set of filled MO's is known beforehand. However, one may encounter some more complex cases where the correct choice of lower filled MO's can only be deduced after completing the self-consistent field treatment.

If the molecule is symmetrical the solution of Eqs. (5) and (6) may be considerably simplified. This is done by constructing MO's not by the usual linear combination of AO's [Eq. (1)] but by the linear combination of the so-called "symmetrical orbitals." The latter ones are obtained from the original AO's in the form of linear combinations belonging to certain irreducible representations of the molecular symmetry groups. As a result, an nth order determinant can be broken up into several determinants of orders equal to the respective numbers of symmetrical orbitals belonging to each irreducible representation. In the case of degenerate irreducible representations, the corresponding determinants can be further broken up to the extent permitted by the order of degeneracy. The aromatic complexes of metals possess fairly high degrees of symmetry (bis-cyclopentadienyl compounds are D_{5d}, while dibenzene chromium and related compounds are D_{6h}). Therefore from now on (in this paper as well as in examining other aromatic complexes) we will always use symmetrical orbitals. Moreover, χ_{pp} in Eq. (1), and in subsequent equations, denotes a symmetrical orbital.

We used the following approximations and assumptions in order to simplify the ferrocene calculations:

TABLE 1

Atomic function	Effective charge	
	C	Fe
$2p$	1,6	—
$4s$, $4p$	—	1,0
$3d$	—	2,0

1) The MO's of the molecule were limited to the π-MO's of the ring, which are constructed from the atomic $2p_z$ carbon orbitals, and nine $3d^5 4s 4p^3$ AO's of the central atom.

2) The electrons of the complex were regarded as located in a field arising from a positive central atom shell (Fe^{8+}) and from the shells of the rings in which each carbon represented a unit positive charge.

3) For the AO's Slater wave functions with the effective charges listed in Table 1 were used.

4) In the S matrix all the off-diagonal terms S_{pq} ($p \neq q$) were assumed to be zero.

5) In computing the matrix elements H_{pq} (the operator which includes only one-electron terms) all the resonance integrals between nonadjacent carbon atoms were taken as zero, while for neighboring atoms the value $\beta_{CC} = -2.39$ ev was used; matrix elements H_{pq} between AO's of the central atom and ring MO's of like symmetry were assumed to be proportional to the overlap integrals. In computing the diagonal matrix elements H_{pp}, which represent the $2p\pi$ atomic orbitals of carbon, we took into account the valence (oxidation state) energy ($W_{2p} = -11.28$ ev); this is usually done in calculations involving π-electron systems of conjugated hydrocarbons.

6) In the electron–electron interaction matrix only integrals of the type shown below were considered:

$$\int \frac{\bar{\sigma}_p^{\mu} \bar{\sigma}_q^{\nu} \sigma_p^{\mu} \sigma_q^{\nu}}{r^{\mu\nu}} d\tau^{\mu\nu}.$$

7) We assumed that the interaction between the $3d_{z^2}$ AO's and the ring MO's of like symmetry can be disregarded (the calculated overlap integrals presented later in the paper confirm the validity of this assumption).

8) Only one-center and two-center integrals were evaluated.

The formulas used in evaluating some of the integrals have been previously derived [4, 5] and are presented in this paper without explanatory comments. We used 2.03 A for the Fe–C distance and 1.43 A for the C–C distance [6].

The Form of Initial MO's

Self-consistent field treatment was applied to the 19 MO's of the complex which were built from the 10 ring MO's and the 8 AO's of the central atom. By using symmetrical orbitals (for a D_{5d} molecular symmetry) we broke up the 19th order secular equation into: three 4th order equations (e_{1g}, e_{1u}, e_{2g}), one 3rd order equation (a_{1g}), and two 2nd order equations (a_{1u} and e_{2u}).

If we use only the real symmetrical ring orbitals (Table 2) then each 4th order equation splits into two identical 2nd order equations (the 2nd order equation representing orbitals with a e_{2u} symmetry also splits into two identical first order equations).

In Table 3 we have listed the symmetrical orbitals of the complex and in Table 4 all the MO's of the complex.

The Evaluation of Matrix Elements S_{pq} and L_{pq}

In evaluating the matrix elements S_{pq} and $L_{pq} = H_{pq} + G_{pq}$ used in Eq. (5) and (6) it is important to remember that the fivefold molecular axis of symmetry (along which the AO's are quantized) does not coincide with the Fe–C bonds. Hence, we have to carry out a transformation into a new coordinate system where the z' axis is taken along the line of a Fe–C bond. Thus, the AO's are transformed in the following way [7]:

$$\text{(Carbon AO's)} \quad \psi_{p_z} = \psi_{p_{z'}} \cos\omega + \psi_{p_{x'}} \sin\omega$$

(Iron AO's)

$$\begin{cases} \psi_s = \psi_{s'} \\ \psi_{p_z} = \psi_{p_{z'}} \cos\omega - \psi_{p_{x'}} \sin\omega \\ \psi_{p_x} = \psi_{p_{z'}} \sin\omega + \psi_{p_{x'}} \cos\omega \\ \psi_{d_{z^2}} = \psi_{d_{z'^2}} (\cos^2\omega - {}^1/_2 \sin^2\omega) - \dfrac{\sqrt{3}}{2} \psi_{d_{x'z'}} \sin 2\omega + \dfrac{\sqrt{3}}{2} \psi_{d_{x'^2-y'^2}} \sin^2\omega \\ \psi_{d_{xz}} = \dfrac{\sqrt{3}}{2} \psi_{d_{z'^2}} \sin 2\omega + \psi_{d_{x'z'}} \cos 2\omega - \dfrac{1}{2} \psi_{d_{x'^2-y'^2}} \sin 2\omega \\ \psi_{d_{x^2-y^2}} = \dfrac{\sqrt{3}}{2} \psi_{d_{z'^2}} \sin^2\omega + \dfrac{1}{2} \psi_{d_{x'z'}} \sin 2\omega + \dfrac{1}{2} \psi_{d_{x'^2-y'^2}} (1 + \cos^2\omega). \end{cases}$$

TABLE 2

C_5H_5 Ring MO's*

Symmetry	Type of wave function: complex	Type of wave function: real
a	$\psi_0 = \frac{1}{\sqrt{5}} (\theta_1 + \theta_2 + \theta_3 + \theta_4 + \theta_5)$	$\psi_0 = \frac{1}{\sqrt{5}} (\theta_1 + \theta_2 + \theta_3 + \theta_4 + \theta_5)$
		$F_1 = \frac{1}{\sqrt{2}} (\psi_{+1} + \psi_{-1}) =$
	$\psi_{+1} = \frac{1}{\sqrt{5}} (\theta_1 + \theta_2\omega + \theta_3\omega^2 + \theta_4\omega^3 + \theta_5\omega^4)$	$= \sqrt{\frac{2}{5}} [\theta_1 + (\theta_2 + \theta_5) \cos 72° - (\theta_3 + \theta_4) \cos 36°]$
e_1	$\psi_{-1} = \frac{1}{\sqrt{5}} (\theta_1 + \theta_2\omega^{-1} + \theta_3\omega^{-2} + \theta_4\omega^{-3} + \theta_5\omega^{-4})$	$\Phi_1 = \frac{-i}{\sqrt{2}} (\psi_{+1} - \psi_{-1}) =$
		$= \sqrt{\frac{2}{5}} [(\theta_2 - \theta_5) \sin 72° + (\theta_3 - \theta_4) \sin 36°]$
		$F_2 = \frac{1}{\sqrt{2}} (\psi_{+2} + \psi_{-2}) =$
e_2	$\psi_{+2} = \frac{1}{\sqrt{5}} (\theta_1 + \theta_2\omega^2 + \theta_3\omega^4 + \theta_4\omega^6 + \theta_5\omega^8)$	$= \sqrt{\frac{2}{5}} [\theta_1 - (\theta_2 + \theta_5) \cos 36° + (\theta_3 + \theta_4) \cos 72°]$
		$\Phi_2 = \frac{-i}{\sqrt{2}} (\psi_{+2} - \psi_{-2}) =$
	$\psi_{-2} = \frac{1}{\sqrt{5}} (\theta_1 + \theta_2\omega^{-2} + \theta_3\omega^{-4} + \theta_4\omega^{-6} + \theta_5\omega^{-8})$	$= \sqrt{\frac{2}{5}} [(\theta_2 - \theta_5) \sin 36° - (\theta_3 - \theta_4) \sin 72°]$

* θ_j stands for a $2p_z$ AO of the jth carbon atom, $\omega = e^{2\pi i/5}$ are the normalization constants if the $2p_z$ carbon orbitals are left nonorthogonal.

To simplify the calculations, all the off-diagonal matrix elements S_{pq} ($p \neq q$) were assumed to be zero (for diagonal terms $S_{pp} \equiv 1$). From now on, nonzero matrix elements S_{pq} between the symmetrical orbitals of any nonreducible representation were evaluated solely for the purpose of finding matrix elements H_{pq} in accordance with the assumptions made above.

Within the framework of the above-made assumptions the operator H in the matrix elements $H_{pq} = H_{qp} = \int \chi_p H \chi_q \, d\tau^*$ has the form:

$$H = -\frac{1}{2}\Delta_i - \sum_i \frac{Z_i}{r_i} =$$

$$= -\frac{1}{2}\Delta_i - \frac{1}{r_{C_1'}} - \frac{1}{r_{C_2'}} - \frac{1}{r_{C_3'}} - \frac{1}{r_{C_4'}} - \frac{1}{r_{C_5'}} - \frac{1}{r_{C_1''}} - \frac{1}{r_{C_2''}} - \frac{1}{r_{C_3''}} -$$

$$- \frac{1}{r_{C_4''}} - \frac{1}{r_{C_5''}} - \frac{8}{r_{Fe}},$$

where Z_i/r_i represents the attraction between an electron and a corresponding atomic shell.

TABLE 3

Symmetrical Orbitals of $(C_5H_5)_2Fe$*

Symmetry	Type of wave function	Symmetry	Type of wave function
a_{1g}	$\chi_1 = \frac{1}{\sqrt{2}}(\psi_0' + \psi_0'')$	e_{1u}	$\chi_{12} = \frac{1}{\sqrt{2}}(\Phi_1' - \Phi_1'')$
	$\chi_2 = 4s$		$\chi_{13} = 4p_y$
	$\chi_3 = 3d_{z^2}$	e_{2g}	$\chi_{14} = \frac{1}{\sqrt{2}}(F_2' + F_2'')$
a_{1u}	$\chi_4 = \frac{1}{\sqrt{2}}(\psi_0' - \psi_0'')$		$\chi_{15} = 3d_{x^2-y^2}$
	$\chi_5 = 4p_z$		$\chi_{16} = \frac{1}{\sqrt{2}}(\Phi_2' + \Phi_2'')$
e_{1g}	$\chi_6 = \frac{1}{\sqrt{2}}(F_1' + F_1'')$		$\chi_{17} = 3d_{xy}$
	$\chi_7 = 3d_{xz}$	e_{2u}	$\chi_{18} = \frac{1}{\sqrt{2}}(F_2' - F_2'')$
	$\chi_8 = \frac{1}{\sqrt{2}}(\Phi_1' + \Phi_1'')$		$\chi_{19} = \frac{1}{\sqrt{2}}(\Phi_2' - \Phi_2'')$
	$\chi_9 = 3d_{yz}$		
e_{1u}	$\chi_{10} = \frac{1}{\sqrt{2}}(F_1' - F_1'')$		
	$\chi_{11} = 4p_x$		

* The prime and double prime denote LCAO's in the first and second C_5H_5 rings respectively.

All the off-diagonal terms H_{pq} ($p \neq q$) are presumed to be proportional to the corresponding S_{pq} elements. The resonance integral between the $2p_Z$ functions of adjacent carbon atoms was assumed to be equal to that in benzene($\beta = -2.39$ ev), since only the one-center and two-center integrals are considered while the three center integrals $\int 2p_{z_i} \frac{8}{r_{Fe}} 2p_{z_j} d\tau$ are neglected. Hence, we can use the β value for a molecule unperturbed by the metal atom. The formulas used for evaluating the elements S_{pq} were taken directly out of [7]** and [8].

* Since all the symmetrical orbitals are real the respective complex conjugates of these functions are identical, and therefore we will henceforth drop the asterisk.

** A printing error was found in the cited paper: we should have $\sqrt{3}/2$ instead of $\sqrt{\frac{3}{2}}$ in the equation for $S(a_{1g}, 3d_{z^2})$.

TABLE 4

The MO's of a $(C_5H_5)_2M$ Complex

Symmetry	Type	Symmetry	Type
$1a_{1g}^{*}$	$c_{11}\chi_1 + c_{12}\chi_2 + c_{13}\chi_3$ **	$1e_{1u}^{*}$	$c_{1010}\chi_{10} + c_{1011}\chi_{11}$
$2a_{1g}^{*}$	$c_{21}\chi_1 + c_{22}\chi_2 + c_{23}\chi_3$	$2e_{1u}$	$c_{1110}\chi_{10} + c_{1111}\chi_{11}$
$3a_{1g}$	$c_{31}\chi_1 + c_{32}\chi_2 + c_{33}\chi_3$		
$1a_{1u}^{*}$	$c_{14}\chi_4 + c_{45}\chi_5$	$1e_{1u}^{''*}$	$c_{1212}\chi_{12} + c_{1213}\chi_{13}$
$2a_{1u}$	$c_{54}\chi_4 + c_{55}\chi_5$	$2e_{1u}^{'}$	$c_{1312}\chi_{12} + c_{1313}\chi_{13}$
$1e_{1g}^{*}$	$c_{66}\chi_6 + c_{67}\chi_7$	$1e_{2g}^{*}$	$c_{1414}\chi_{14} + c_{1415}\chi_{15}$
$2e_{1g}$	$c_{76}\chi_6 + c_{77}\chi_7$	$2e_{2g}$	$c_{1514}\chi_{14} + c_{1515}\chi_{15}$
$1e_{1g}^{''*}$	$c_{88}\chi_8 + c_{89}\chi_9$	$1e_{2g}^{''*}$	$c_{1616}\chi_{16} + c_{1617}\chi_{17}$
$2e_{1g}^{'}$	$c_{98}\chi_8 + c_{99}\chi_9$	$2e_{2g}^{'}$	$c_{1716}\chi_{16} + c_{1717}\chi_{17}$
		$2e_{2u}$	χ_{18}
		$2e_{2u}$	χ_{19}

* The asterisk * denotes bonding MO's.

** As will subsequently become apparent we can safely assume that $c_{21} = c_{22} = c_{13} = c_{33} = 0$ and consequently that $c_{23} = 1$.

The method used for evaluating the matrix elements H^{ii} depends on whether the χ_p function represents an AO of the central atom or a ring MO (see Table 3). For the first case we used Roothaan's method [9]. At the same time, though we used the kinetic energy integrals listed in Roothaan's work, we calculated the nuclear attraction integrals using the equations we had previously [4, 5] derived for closed-shell distributions involving 4s, 4p, and 3d electrons, which were similar to Roothaan's equations for closed-shell distributions involving 1s, 2s, and 2p electrons. In the second case we simply applied the previously mentioned approximations:

$$H_{pp} = \int \chi_p H \chi_p d\tau \equiv \int \chi_p \left(-\Delta/2 - \sum_i \frac{1}{r_{C_i}} - \frac{8}{r_{Fe}} \right) \chi_p d\tau \approx$$

$$\approx C + n\beta + \int (2p_{z_i}) \left(\frac{-8}{r_{Fe}} \right) (2p_{z_i})\, d\tau,$$

where

$$C \equiv \int (2p_{z_i}) \left(-\Delta/2 - \sum \frac{1}{r_{C_i}} \right) (2p_{z_i})\, d\tau \text{ and } \beta \equiv \int (2p_{z_i})\, H\, (2p_{z_j})\, d\tau = -2{,}39 \text{ ev}$$

(i and j denote adjacent carbon atoms).

These are the respective coulomb and resonance integrals of the normal LCAO-MO treatment with the n determined by the symmetry of the MO (Tables 2 and 3). The integral C was evaluated using the method described by Goppert-Mayer and Sklar [10] and with the valence energy of the carbon atom taken into account ($W_{2p} = -11.28$ ev). The integral $\int (2p_{z_i}) \left(\frac{-8}{r_{Fe}} \right) (2p_{z_i})\, d\tau$ was treated as an ordinary one-electron two-center integral equal to:

$$\int (2p_z)_a \left(-\frac{Z}{r_b}\right)(2p_z)_a d\tau = -Z\,[K(\sigma\sigma)\cos^2\omega + K(\pi\pi)\sin^2\omega],$$

where

$$K(\sigma\sigma) = \int (2p\sigma)_a \frac{1}{r_b}(2p\sigma)_a d\tau,$$

$$K(\pi\pi) = \int (2p\pi)_a \frac{1}{r_b}(2p\pi)_a d\tau.$$

In evaluating the matrix elements G_{pq} we only used coulomb integrals of the type $\int \frac{\sigma_p^\mu \sigma_q^\nu \sigma_p^\mu \sigma_q^\nu}{r^{\mu\nu}} d\tau^\mu d\tau^\nu$, which for the sake of simplicity will henceforth be denoted by

$$[\sigma_p\sigma_p \mid \sigma_q\sigma_q]^*.$$

The evaluation of these integrals can be handled in three distinct ways depending on the form of σ_p and σ_q 1) σ_p and σ_q are the $2p_z$ atomic orbitals of carbons; 2) σ_p and σ_q are the AO's of the central atom; 3) σ_p is the $2p_z$ AO of carbon while σ_q is the AO of the central atom.

Let us now examine these three cases in more detail.

1) Linear combinations of integrals of the first type are encountered in computing the coulomb $[\chi_p\chi_p|\chi_q\chi_q]$ and exchange $[\chi_p\chi_q|\chi_p\chi_q]$ integrals, where χ_p and χ_q are the ring MO's, i.e., linear combinations of σ_p and σ_q – the $2p_z$ AO's of carbon.

We determined the contributions of various one-center (i = j) and two-center ($i \neq j$) integrals to the integral $[\chi_1\chi_1|\chi_1\chi_1]$ (see Table 3). Numerical integration was done with the help of Kitani's Tables [11]. We found that coulomb integrals of the type $[p_{z_i}p_{z_i}|p_{z_j}p_{z_j}]$ contribute 68%, ionic integrals of the type $[p_{z_i}p_{z_i}|p_{z_i}p_{z_j}]$ 29%, and exchange integrals $[p_{z_i}p_{z_j}|p_{z_i}p_{z_j}]$ only 3%** to the entire integral. Hence in computing integrals such as $[\chi_p\chi_p|\chi_q\chi_q]$ and $[\chi_p\chi_q|\chi_p\chi_q]$ we only considered coulomb terms of the type $[p_{z_i}p_{z_i}|p_{z_j}p_{z_j}]$ ($i = j$, $i \neq j$) which are equal to:

$$[p_{z_i}p_{z_i}|p_{z_j}p_{z_j}] = \cos^4\omega\,[p\sigma p\sigma|p\sigma p\sigma] + \sin^4\omega\,[p\pi p\pi|p\pi p\pi] + \\ + \tfrac{1}{2}\sin^2 2\omega\,[p\pi p\pi|p\sigma p\sigma] - \sin^2 2\omega\,[p\sigma p\pi|p\sigma p\pi],$$

where ω is the angle between the direction of a p_z AO of carbon and the $C_i - C_j$ bond. For any two carbon atoms on the same ring $\omega = 90°$ and, thus $[p_{z_i}p_{z_i}|p_{z_j}p_{z_j}] = [p\pi p\pi|p\pi p\pi]$. The evalutation of integrals $[\chi_p\chi_p|\chi_q\chi_q]$ and $[\chi_p\chi_q|\chi_p\chi_q]$ is then reduced to the evaluation of the linear combination of coulomb integrals of the following six types:

$$[p_{z_1}p_{z_1}|p_{z_1}p_{z_1}],\ [p_{z_1}p_{z_1}|p_{z_2}p_{z_2}],\ [p_{z_1}p_{z_1}|p_{z_3}p_{z_3}],\ [p_{z_1}p_{z_1}|p_{z_1'}p_{z_1'}],\ [p_{z_1}p_{z_1}|p_{z_2'}p_{z_2'}] \text{ and } [p_{z_1}p_{z_1}|p_{z_3'}p_{z_3'}].$$

2) We have previously [5] derived exact equations for the evaluation of coulomb integrals of the 2nd type.

3) Third type integrals were computed by means of the formulas shown below. In the integral $[\alpha\alpha/\beta\beta]$ α denotes a 2p AO of carbon and β and 4s, 4p, or 3d AO of Fe. We will now get:

$$[p_zp_z|ss] = [p\sigma p\sigma|ss]\cos^2\omega + [p\pi p\pi|ss]\sin^2\omega,$$

$$[p_zp_z|p_zp_z] = [p\sigma p\sigma|p\sigma p\sigma]\cos^4\omega + [p\pi p\pi|p\pi p\pi]\sin^4\omega + \\ + \{[p\sigma p\sigma|p\pi p\pi] + [p\pi p\pi|p\sigma p\sigma]\}\sin^2\omega\cos^2\omega,$$

$$[p_zp_z|p_xp_x] = \{[p\sigma p\sigma|p\sigma p\sigma] + [p\pi p\pi|p\pi p\pi]\}\sin^2\omega\cos^2\omega + \\ + [p\sigma p\sigma|p\pi p\pi]\cos^4\omega + [p\pi p\pi|p\sigma p\sigma]\sin^4\omega.$$

---

* These were, however, computed for both the coulomb $[\varphi_i\varphi_i|\chi_p\chi_q]$ as well as the exchange $[\varphi_i\chi_p|\varphi_i\chi_q]$ components of the matrix element G_{pq}.

** In other integrals involving ring MO's the relative contribution of the coulomb term is even greater.

$$[p_z p_z | d_m d_m] = C_1 [p\sigma p\sigma | d\sigma d\sigma] + C_2 [p\sigma p\sigma | d\pi d\pi] + C_3 [p\sigma p\sigma | d\delta d\delta] +$$
$$+ C_4 [p\pi p\pi | d\sigma d\sigma] + C_5 [p\pi p\pi | d\pi d\pi] + C_6 [p\pi p\pi | d\delta d\delta].$$

The coefficients C_i of this last expression are listed in Table 5.

TABLE 5

	m		
C_i	z^2	xz	$x^2 - y^2$
C_1	$\cos^2\omega(\cos^2\omega - 1/2\sin^2\omega)^2$	$\frac{3}{4}\cos^2\omega\sin^2 2\omega$	$\frac{3}{4}\cos^2\omega\sin^4\omega$
C_2	$\frac{3}{4}\cos^2\omega\sin^2 2\omega$	$\cos^2\omega\cos^2 2\omega$	$\frac{1}{4}\cos^2\omega\sin^2 2\omega$
C_3	$\frac{3}{4}\cos^2\omega\sin^4\omega$	$\frac{1}{4}\cos^2\omega\sin^2 2\omega$	$\frac{1}{4}\cos^2\omega(1+\cos^2\omega)^2$
C_4	$\sin^2\omega(\cos^2\omega - 1/2\sin^2\omega)^2$	$\frac{3}{4}\sin^2\omega\sin^2 2\omega$	$\frac{3}{4}\sin^2\omega\sin^4\omega$
C_5	$\frac{3}{4}\sin^2\omega\sin^2 2\omega$	$\sin^2\omega\cos^2 2\omega$	$\frac{1}{4}\sin^2\omega\sin^2 2\omega$
C_6	$\frac{3}{4}\sin^2\omega\sin^4\omega$	$\frac{1}{4}\sin^2\omega\sin^2 2\omega$	$\frac{1}{4}\sin^2\omega(1+\cos^2\omega)^2$

The interaction integrals found on the right hand side of these equations were evaluated with the help of previously derived [5] approximate formulas.

Numerical Values of Matrix Elements

Matrix Elements S_{pq}

$$S(a_{1g}, 4s) = S_{12} = 0{,}359,$$

$$S(a_{1g}, 3d_{z^2}) = S_{13} = 0{,}023,$$

$$S(a_{1u}, 4p_z) = S_{45} = 0{,}063,$$

$$S(e_{1g}, 3d_{xz}) = S_{67} = S_{89} = 0{,}339,$$

$$S(e_{1u}, 4p_x) = S_{10,11} = S_{12,13} = 0{,}380,$$

$$S(e_{2g}, 3d_{x^2-y^2}) = S_{14,15} = S_{16,17} = 0{,}192$$

Matrix Elements H_{pq}*

$H_{11} = -4{,}5341$
$H_{12} = -0{,}1302$
$H_{22} = -4{,}5546$
$H_{33} = -6{,}0052$
$H_{44} = -4{,}5341$
$H_{45} = -0{,}0229$
$H_{55} = -4{,}7093$
$H_{66} = H_{88} = -4{,}4128$
$H_{67} = H_{89} = -0{,}1230$
$H_{77} = H_{99} = -6{,}0706$
$H_{10,10} = H_{12,12} = -4{,}4128$
$H_{10,11} = H_{12,13} = -0{,}1379$
$H_{11,11} = H_{13,13} = -4{,}4741$
$H_{14,14} = H_{16,16} = -4{,}2164$
$H_{14,15} = H_{16,17} = -0{,}0697$
$H_{15,15} = H_{17,17} = -5{,}8619$
$H_{18,18} = H_{19,19} = -4{,}2164$

*In atomic units: 1 a.u. = 27.21 ev.

TABLE 6

Matrix Elements G_{pq}*

1	2	3	4	5	6	7	8	9	10	11	12	13	14	15	16	17	18	19	
0,24638	0,23	0,27	0,24638 0,09584	0,26	0,24638 0,04262	0,28	0,24638 0,04262	0,28	0,24638 0,05289	0,23	0,24638 0,05289	0,23	0,24638 0,02366	0,26	0,24638 0,02366	0,26	0,24638 0,02285	0,24638 0,02285	1
	0,22952	0,28282	0,23	0,22952	0,23	0,28282	0,23	0,28282	0,23	0,22952	0,23	0,22952	0,23	0,28282	0,23	0,28282	0,23	0,23	2
		0,56308	0,27	0,29333	0,27	0,51104	0,27	0,51104	0,27	0,27754	0,27	0,27754	0,27	0,49814	0,27	0,49814	0,27	0,27	3
			0,24638	0,26	0,24638 0,05289	0,28	0,24638 0,05289	0,28	0,24638 0,04262	0,23	0,24638 0,04262	0,23	0,24638 0,02285	0,26	0,24638 0,02285	0,26	0,24638 0,02366	0,24638 0,02366	4
				0,24942	0,26	0,28808	0,26	0,28808	0,26	0,21957	0,26	0,21957	0,26	0,27232	0,26	0,27232	0,26	0,26	5
					0,25821	0,28	0,23455 0,01183	0,28	0,25821 0,10727	0,23	0,23455 0,01143	0,23	0,24638 0,03314	0,26	0,24638 0,03314	0,26	0,24638 0,03787	0,24638 0,03787	6
						0,56308	0,28	0,50244	0,28	0,28808	0,28	0,27232	0,28	0,50244	0,28	0,50244	0,28	0,28	7
							0,25821	0,28	0,23455 0,01143	0,23	0,25821 0,10727	0,23	0,24638 0,03314	0,26	0,24638 0,03314	0,26	0,24638 0,03787	0,24638 0,03787	8
								0,56308	0,28	0,27232	0,28	0,28808	0,28	0,50244	0,28	0,50244	0,28	0,28	9
									0,25821	0,23	0,23455 0,01183	0,23	0,24638 0,03787	0,26	0,24638 0,03787	0,26	0,24638 0,03314	0,24638 0,03314	10
										0,24942	0,23	0,21957	0,23	0,28808	0,23	0,28808	0,23	0,23	11
											0,25821	0,23	0,24638 0,03787	0,26	0,24638 0,03787	0,26	0,24638 0,03314	0,24638 0,03314	12
												0,24942	0,23	0,28808	0,23	0,28808	0,23	0,23	13
													0,26769	0,26	0,22507 0,02131	0,26	0,26769 0,12229	0,22507 0,02644	14
														0,56308	0,26	0,51534	0,26	0,26	15
															0,26769	0,26	0,22507 0,02644	0,26769 0,12229	16
																0,56308	0,26	0,26	17

* The numbers in the pq squares give the values of the coulomb integrals $[\chi_p\chi_p|\chi_q\chi_q]$. In cases where our approximation does not yield a zero exchange integral $[\chi_p\chi_q|\chi_p\chi_q]$, the value of the latter is then given below that of the coulomb integral. All the values are in atomic units.

TABLE 7

The Matrix Elements, and the MO Coefficients and Energies* in the Last Cycle of SCF Calculations

L_{pq}	C_{ij} and ε_i	Assigned	Obtained
$L_{11} = -0,4620$	c_{11}	0,871	0,872
$L_{22} = -0,1828$	c_{12}	0,491	0,489
$L_{12} = -0,2286$	ε_1	−0,589	−0,590
	ε_2	−0,053	−0,055
$L_{33} = -0,3105$	ε_3	−0,305	−0,310
$L_{44} = -0,5008$	c_{44}	0,997	0,996
$L_{55} = +0,0165$	c_{45}	0,090	0,088
$L_{45} = -0,0463$	ε_4	−0,504	−0,505
	ε_5	+0,024	+0,020
$L_{66} = -0,3161$	$c_{66} = c_{88}$	0,927	0,927
$L_{77} = +0,1392$	$c_{67} = c_{80}$	0,374	0,374
$L_{67} = -0,2202$	$\varepsilon_6 = \varepsilon_8$	−0,404	−0,405
	$\varepsilon_7 = \varepsilon_9$	+0,232	+0,228
$L_{10,10} = -0,2858$	$c_{10,10} = c_{12,12}$	0,811	0,810
$L_{11,11} = -0,1225$	$c_{10,11} = c_{12,13}$	0,585	0,586
$L_{10,11} = -0,2469$	$\varepsilon_{10} = \varepsilon_{12}$	−0,463	−0,464
	$\varepsilon_{11} = \varepsilon_{13}$	+0,057	+0,056
$L_{11,14} = +0,0663$	$c_{14,14} = c_{16,16}$	0,526	0,525
$L_{15,15} = -0,1199$	$c_{14,15} = c_{16,17}$	0,850	0,851
$L_{14,15} = -0,1850$	$\varepsilon_{14} = \varepsilon_{16}$	−0,231	−0,235
	$\varepsilon_{15} = \varepsilon_{17}$	+0,183	+0,181
	$\varepsilon_{18} = \varepsilon_{19}$	+0,105	+0,103

* In atomic units

SCF Calculations

Using the matrix elements listed above we improved the molecular orbitals by means of the self-consistent field treatment worked out by Roothaan for molecules with a singlet ground state. In Table 7 we have listed the values of the matrix elements L_{pq} after the last cycle of the SCF calculations, while alongside we have compiled the assumed and the calculated (after the last cycle) energies and coefficients c_{ij} of the molecular orbitals; a comparison between the calculated and the assigned values indicates the degree of self-consistency.

The Final Form of the SCF MO's of Ferrocene and the Orbital Energies

We are now going to present the final form of the self-consistent bonding molecular orbitals of ferrocene in the form $C_1\theta_1 + C_2\theta_2$; the corresponding antibonding orbitals of the same symmetry are expressed in the form $C_2\theta_1 - C_1\theta_2$. The energies of the orbitals are given in parentheses (in electron volts), where the first number refers to bonding and the second to antibonding orbitals:

a_{1g}	$0,87a_{1g} + 0,49s$	$(-16.05;\ -1,50)$
a'_{1g}	d_{z^2}	$(-8,44)$
a_{1u}	$0,99a_{1u} + 0,10p_z$	$(-13,74;\ +0,54)$
e_{1u}	$0,81e_{1u} + 0,59p_x$	$(-12.62;\ +1,52)$
e_{1g}	$0,93e_{1g} + 0\ 37d_{xz}$	$(-11,02;\ +6,20)$
e_{2g}	$0,52e_{2g} + 0,85d_{xy}$	$(-6,39;\ +4,92)$
e_{2u}		$(+2,80).$

The energy of the highest filled orbital (with the sign reversed, + 6.39 ev) gives the first ionization potential of $Fe(C_5H_5)_2$ which agrees well with the experimental value (7.05 ev).

We computed the excitation energies of ferrocene for the following one-electron transitions:

$$a'_{1g} \rightarrow a'_{1u}\ (^1A_{1g} \rightarrow {}^{1,3}A_{1u}) \text{ and } a'_{1g} \rightarrow e'_{1u}\ (^1A_{1g} \rightarrow {}^{1,3}E_{1u}).$$

[Equation (9') was used to determine the average excitation energies to singlet and triplet states with the configuration interaction neglected]. These energies turned out to be 1.0 and 2.5 ev respectively*. The last transition seems to correspond to the absorption band observed in the spectrum of ferrocene at 4300 A (in solution) or 4400 A (in the solid state), which represents an energy of 2.85 ev.

* Our calculated values came out fairly close to the transition energies calculated by Yamazaki (0.9 and 2.5 ev) despite the fact that the energies of our MO's and symmetries of upper filled levels were different. This agreement is apparently due to the fact that in Roothaan's method the energies of free orbitals [given by the roots of the Determinant (6)] have no physical meaning.

The MO energies calculated by us differ from those reported by Yamazaki in the following respect. Whereas we get positive energies for our antibonding orbitals (except for the a''_{1g} orbital, which has a small negative energy) Yamazaki gets large negative energies for all of his (from -7.07 to - 3.64ev). The energy range of our bonding orbitals is in close agreement with that found by Yamazaki; the positions of the lowest orbital a_{1g} (-16.80 ev in Yamazaki's case) and the second bonding orbital of symmetry a'_{1g} (-8.57 ev in Yamazaki's case) are also in close agreement. At the same time, in Yamazaki's case the last orbital mentioned above is a hydrid, whereas in our case it is a pure dz^2 orbital. The positions and sequence assigned by us to the other orbitals differ somewhat from Yamazaki's assignments. We are unable to account for these differences because Yamazaki still has not published a detailed paper with his calculations.

We intend to postpone any broader discussion of our results and conclusions based on these data until similar calculations on $(C_6H_6)_2Cr$, $(C_5H_5)_2Co^+$, and $(C_5H_5)_2Cr$ have been completed.

LITERATURE CITED

1. H.H. Jaffe, J. Chem. Phys. 21, 156 (1953); W. Moffitt, J. Am. Chem. Soc. 76, 3386 (1954); E. Ruch and E.O. Fisher, Z. Naturforsch 7b, 676 (1952); M.E. Dyatkina, Izvest. Akad. Nauk SSSR, Otdel Khim. Nauk, 1025 (1959).*
2. C.C.J. Roothaan, Revs. Mod. Phys. 23, 69 (1951).
3. M. Yamazaki, J. Chem. Phys. 24, 1260 (1956).
4. E.M. Shustorovich and M.E. Dyatkina, Zhur. Fiz. Khim. 34, 644 (1960).
5. E.M. Shustorovich and M.E. Dyatkina, Zhur. Fiz. Khim. 34, 8 (1960).
6. E.A. Seibold and L.E. Sutton, J. Chem. Phys. 23, 1967 (1955).
7. J.D. Dunitz and L.E. Orgel, J. Chem. Phys. 23, 954 (1955).
8. D. Brown, J. Chem. Phys. 29, 1086 (1958).
9. C.C.J. Roothaan, J. Chem. Phys. 19, 1445 (1951).
10. M. Göppert-Mayer and A.S. Sklar, J. Chem. Phys. 6, 645 (1938).
11. M. Kotani, et al., Tables of Molecular Integrals (Tokyo, 1955).

*Original Russian pagination. See C.B. translation.

BRIEF COMMUNICATIONS

PROTON RELAXATION IN AQUEOUS SOLUTIONS OF DIAMAGNETIC SALTS

II. ALKALI METAL CATIONS AND HALIDE ANIONS

V.M. Vdovenko and V.A. Shcherbakov

V.G. Khlopin Leningrad Radium Institute, Academy of Sciences of the USSR
Translated from Zhurnal Strukturnoi Khimii, Vol. 1, No. 1, pp. 122-124,
May-June, 1960
Original article submitted January 7, 1960

In an earlier paper [1] we have shown how nuclear magnetic resonance (NMR) measurements can be used to determine the τ_i/τ ratio for hydrated ions. According to the theory developed by Samoilov [2], this number gives the ratio between the time spent by a water molecule in the equilibrium position nearest to the ion in the solution structure (τ_i) and the average time a water molecule spends in an equilibrium position in the water structure (τ). By studying the proton relaxation of diamagnetic solutions we can get the value of τ_c^i/τ_c^0, the ratio between the correlation time of the dipole interaction for protons in an aqueous solution of diamagnetic compounds (τ_c^i) and the same function in pure water (τ_c^0). The value of τ_c^i/τ_c^0 is probably close to that of τ_i/τ We had previously determined the τ_c^i/τ_c^0 ratios for the nitrates of group II elements [1]. However, the literature contains very little data on the τ_i/τ ratios for these ions, and consequently we could not tell definitely how similar these two ratios actually are.

The most thorough study of local hydration has been done for the alkali metal and halide ions [2]. Below we are going to present some of our preliminary results obtained from the proton relaxation measurements in aqueous solutions of these ions.

The experimental technique, the preparation of samples, and the calculations did not differ in any important details from those reported in Communication I. Since these ions produce very weak relaxation effects, conditions were slightly altered so as to make the experiment more sensitive, which is reflected in the precision of our measurements. The data are given in arbitrary units as before.

In the table we have listed the molar relaxation shifts Δ_M and the τ_c^i/τ_c^0 ratios for alkali metal ions and ammonium nitrates, sodium halides, sodium perchlorate, and sodium sulfate; we have also listed the τ_i/τ ratios calculated from ionic mobility and water self-diffusion data [2].

Our ratios for the alkali metal ions exceeded the literature values by about one unit, and in the case of halide anions our ratios were about double the literature values. This is not entirely unexpected, since our data included the effects of both the cations and the anions. At the same time we would like to point out how consistent the potassium and sodium data are. It turns out that not only is the difference between the τ_i/τ_c^0 and the τ_i/τ ratio of each metal about the same (1.04 and 0.93), but that both of the sodium ratios differ by almost the same magnitude from the corresponding potassium ratios (0.92 and 0.81).

In the case of lithium, these relationships are not as clear-cut. A qualitative explanation for this irregularity is possible by attributing it to the different type of electron cloud around the lithium ion (a helium as opposed to a neon configuration), which might be expected to produce different bonding between the ion and the water molecule. Since the relaxation shift also depends on the ionic radius one might have predicted this difference (see the figure).

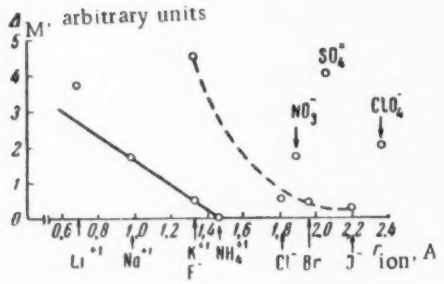

Molar relaxation shift as a function of the ionic radius.

Compound	Δ_M (± 0,5), arbitrary units	The τ_c^i/τ_c^0 ratio		Lit. values of the τ_i/τ ratios for the ions [2]
		for the salts	for the ions	
$LiNO_3$	3,7	3,9	3,0	3,48
$NaNO_3$	1,7	2,5	1,5	1,46
KNO_3	0,5	1,5	0,5	0,65
NH_4NO_3	0	1,0	0,1	—
NaF	4,5	5,0	5,9 ($n_- = 3,3$)*	—
NaCl	0,5	1,4	0,9	0,65
NaBr	0,4**	1,2	0,8	0,61
NaJ	0,2**	1,1	0,7	0,58
$NaNO_3$	1,7	1,9	1,7 ($n_- = 4,5$)*	—
$NaClO_4$	2,0	2,0	1,7 ($n_- = 5,5$)*	—
Na_2SO_4	4,0	2,3	2,6 ($n_- = 5,0$)*	

*Extrapolated from the curve of n_ vs. ionic radius.

**Conditions were chosen to make the measurements even more sensitive.

Using the available data, one can attempt to separate the effects of anions and cations. The first problem connected with this involves the determination of a correction for the effects produced by the nitrate ion, and after the correction is introduced one can attack the sodium and potassium data. The figure shows that the Δ_M values of sodium nitrate, perchlorate, and sulfate do not fall on a curve resembling the one obtained for the halides. This unusual behavior can probably be attributed to the specific charactor of these ions: the oxygen atoms promote hydrogen bonding and consequently, despite a greater ionic radius, the hydration is more positive than in the case of the halide ions. The Raman and ultraviolet spectra of aqueous solutions of these ions lead to a similar conclusion [3].

This would indicate that the τ_c^i/τ_c^0 ratio (and probably τ_i/τ too) for the nitrate ion should be slightly greater than unity. We would now like to propose a solution for the problem, and our approach may be vindicated by the above-mentioned agreement between the literature and our data. Equation (5) of Communication I assumes the following form for 1-1 electrolytes:

$$N_0 K = K_+ + K_-, \tag{1}$$

where

$$K_\pm = \left(\frac{\tau_c^i}{\tau_c^0} - 1\right) n_\pm \tag{2}$$

($n_\pm$ is the hydration number of the respective anion or cation). Our choice of standard state was based on the τ_c^i/τ_c^0 ratio of sodium nitrate and we selected the following value:

$$(\tau_c^i/\tau_c^0)_{Na^+} = 1{,}50. \tag{3}$$

This gives a $(\tau_c^i/\tau_c^0)_{NO_3^-} = 1.70$. In one of the columns in our Table we have listed the τ_c^i/τ_c^0 ratios of individual ions calculated by the above-described method.

It is quite apparent that the agreement with literature data depends entirely on the accuracy of our measurements. It is also interesting to note that by correcting the sodium halide data for the cation effect we not only get reasonable τ_c^i/τ_c^0 values for the halide ions but also find that both ratios show a consistent change as one proceeds from the chloride to the iodide.

The most important result of our work is the discovery of a regular decrease in the τ_c^i/τ_c^0 ratio as one proceeds from lithium to potassium, with the latter having a ratio of less than one. This fact is in full accord with the negative nature of the K^+ hydration pointed out by Samoilov [2]. Even only a qualitative agreement would warrant the use of this simple NMR technique for the determination of the τ_c^i/τ_c^0 ratios. At the same time the good quantitative agreement between the τ_c^i/τ_c^0 and the τ_i/τ ratios indicate that the results obtained by this method are sufficiently reliable.

The authors express their sincere gratitude to Yu.V. Gurikov for his valuable advice.

LITERATURE CITED

1. V.M. Vdovenko and V.A. Shcherbakov, Zhur. Strukt. Khim. 1, 1, 28 (1960) [present issue].
2. O.Ya. Samoilov, The Structure of Aqueous Solutions of Electrolytes and the Hydration of Ions [in Russian] (Izd. AN SSSR, Moscow, 1957).
3. J.Bochris, Collection: Some Problems in Contemporary Electrochemistry, [Russian translation] (IL, Moscow, 1958).

THE NUCLEAR QUADRUPOLE RESONANCE SPECTRUM OF 1,2,3- TRICHLOROBENZENE

É.I. Fedin

Institute of Heteroorganic Compounds, Academy of Sciences of the USSR
Translated from Zhurnal Strukturnoi Khimii, Vol. 1, No. 1, p. 124,
May-June, 1960
Original article submitted September 11, 1959

The nuclear quadrupole resonance spectrum of 1,2,3-trichlorobenzene has previously been investigated by Bray and co-workers[1,2]. The first paper lists five bands for the spectrum of this compound, whereas the second paper gives six. The discrepancy between the results was not discussed. To be more explicit, we might mention that the conflict is caused by the fact that in his second paper Bray reports a band at 36,238 Mcs, located between two previously reported at 36,214 and 36,268 Mcs belonging to the original quintuplet.

An x-ray diffraction study of 1,2,3-trichlobenzene (undertaken in the x-ray analysis laboratory of the INEOSa of the Academy of Sciences of the USSR by Yu. T. Struchkov and I.N. Strel'tsova) shows that a unit cell contains two crystallographically distinct molecules located in general positions. Therefore, there are three different Cl atoms in each 1,2,3-trichlorobenzene molecule, while in the crystalline state we have six different chlorines [3]. It was therefore interesting to find some unequivocal evidence for the presence of six peaks in the nuclear quadrupole resonance spectrum of this compound.

The reason for the discrepancy observed by Bray is quite obvious. He used the super-regenerative method [4] in which every resonance band is surrounded by side-bands. In the case of 1,2,3-trichlorobenzene the side-bands are about the same distance apart as are the primary components of the spectrum, which renders any interpretation of the spectrum very difficult.

We examined the quadrupole resonance spectrum of 1,2,3-trichlorobenzene by using a regenerative spectrometer free of this defect [5, 6]. The spectrum was recorded under a cosine regime [6] at 77°K. Our spectrum showed six bands the spacing of which agreed quite well with the frequency separations given in [2].

Thus, it is important to consult the available crystallographic data in interpreting the number of bands shown in the nuclear quadrupole resonance spectrum of a compound, especially if one deals with splittings on the order of several tens of kilocycles per second.

We will postpone the discussion of the specific arrangement of the bands in the spectrum of 1,2,3-trichlorobenzene until after the x-ray study is completed.

The author wishes to express his deep gratitude to A.I. Kitaigorodskii and Yu.T. Struchkov for their interest in this work.

LITERATURE CITED

1. P.I. Bray, R.G. Barnes and R. Bersohn, J. Chem. Phys. 25, 813 (1956).
2. P.I. Bray and R.G. Barnes, J. Chem. Phys. 27, 551 (1958).
3. A.I. Kitaigorodskii, Organic Crystal Chemistry [in Russian] (Izd. AN SSSR, Moscow, 1955).
4. T.P. Das and E.L. Hahn, Nuclear Quadrupole Resonance Spectroscopy (New York, 1958).

5. É.I. Fedin and G.K. Semin, Radiotechnology and Electronics [in Russian] (1959) Vol. 1, p. 127.
6. É.I. Fedin and Yu.S. Konstantinov, Pribor. i Tekh. Éksp. 2, 27 (1959).

THE COORDINATION OF NICKEL IN $Ni(CN)_2NH_3 \cdot nH_2O$ Crystals

M.A. Porai-Koshits

N.S. Kurnakov Institute of General and Inorganic Chemistry,
Academy of Sciences of the USSR
Translated from Zhurnal Struckturnoi Khimii, Vol. 1, No. 1, pp. 125-126,
May-June, 1960
Original article submitted October 22, 1959

Rayner and Powell [1] have shown that solid $Ni(CN)_2NH_3 \cdot nH_2O$ consists of a two-dimensional network of $Ni(CN)_2NH_3$ molecules (with square loops) in which octahedral 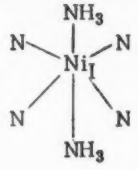 units alternate with square planar units. Successive planes are superimposed in such a way that the octahedral units of one lie over the center of the loop of another (see figure), which leads to the closest packing of layers. The planes are slightly crimped—the units are displaced by about 0.4 A from the average lattice plane. Water molecules are located between the planes and lie on the normals passing through the Ni_{II} atoms.

The position of water has not been fixed unequivocally. The x-ray diffraction data used in [1] did not permit a clear cut choice between the two possible values for the z coordinate of H_2O (0.809 and 0.691). The knowledge of the correct position of these molecules is of primary importance. The first value would yield a $Ni_{II}-H_2O$ distance of 3.10 A, which corresponds to the sum of the Van der Waals radii, while the second one would yield 2.07 A, which is equal to the sum of the covalent radii. In the first choice the Ni_{II} atoms would have a dsp^2 configuration, whereas in the second case they would have a square-pyramid dsp^3 configuration and a coordination number of 5.

It is our opinion, however, that the over-all atomic distribution in the solid favors the first possibility. In fact, if the structure were to be based on the covalent $Ni_{II}-H_2O$ bond then due to the fact that the Ni_I-NH_3 and the $Ni_{II}-H_2O$ covalent radii are very similar (2.10 and 2.07 A respectively) one could achieve the closest packing without having to distort the lattice planes (the NH_3-H, NH_3-C, H_2O-N, and H_2O-C contacts are responsible for the distortion). The crimping of the layers would then increase the H_2O-N and the H_2O-C distances to 3.9 and 4.1 A respectively, greatly in excess of the known intermolecular distances. The consequent bending of the $-C\equiv N$ angle, which in itself requires some energy, would lead to a loss of about half the contacts between the layers and the loss could only be partially compensated by the new possibility of C—C interaction between the layers (the C—N = 3.82 A and the N—N = 3.97 A distances would still exceed the intermolecular distance). It is then quite obvious that the second of the two possibilities is energetically unfavorable.

Distance between bound atoms, A	Distance between unbound atoms, A	
	NH — A	H_2O — A
Ni_I — N = 2,11 (4)	NH_3 — C = $3,5_2$ (2)	H_2O — Ni_{II} = $3,1_0$ (1)
Ni_I — NH_3 = 2,10 (2)	NH_3 — C = $3,5_3$ (2)	H_2O — C = $3,3_7$ (4)
Ni_{II} — C = 1,86 (4)	NH_3 — N = $3,5_4$ (2)	H_2O — N = $3,1_8$ (4)
C — N = 1,15 (1)	NH_3 — N = $3,5_6$ (2)	H_2O — H_2O = $3,7_6$ (2)
	NH_3 — NH_3 = $3,6_2$ (2)	H_2O — NH_3 = $3,2_2$ (1)
	NH_3 — H_2O = $3,2_3$ (1)	C — C = $3,7_2$ (1)

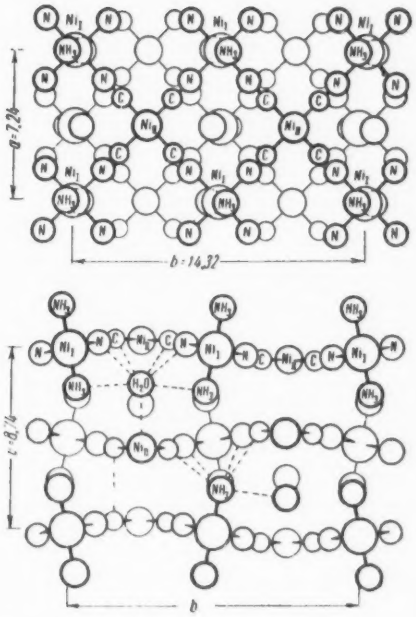

On the other hand, if the first possibility is chosen; the lattice crimping can be readily explained by attributing it to the inclusion of water molecules between the layers: the displacement of individual network loops leads to normal Van der Waals distances between the H_2O molecules and the nearest neighbors (Ni_{II} on one side 3.10 A away, C and N on the other at a distance of 3.18 A and 3.37 A respectively), and at the same time it allows for contact between the carbons of adjacent lattices.

The fact that water molecules fail to fill all the available positions in the crystal but utilize only about 50% of them (n = 0.25) provides an additional argument in favor of the first structural possibility. If the Ni_{II} atoms had shown any tendency to assume a pentavalent state the fifth bond would have probably been formed before complete crystallization had taken place. In actual fact the H_2O molecules act as a "binder" holding the layers together, and the crystal takes up only an amount of water sufficient to promote a satisfactory Van der Waals interaction between layers.

Magnetic susceptibility data support the square planar configuration of Ni_{II} (i.e., a coordination number of four). As is well known, nickel assumes the same configuration in the $Ni(CN)_2NH_3 \cdot C_6H_6$ complex, though the layers are stacked somewhat differently [2]. Belova, Syrkin, and Avdeeva [3] have found that the values and the temperature dependence of the magnetic susceptibilities of the two compounds are very similar, which indicates a similarity in the configuration of Ni. Hence there is no doubt that the lattice of the compound examined in this paper consists of square planar NiC_4 and octahedral $NiN_4(NH_3)_2$ units, while the water acts as a zeolite.

It seems that the dsp^3 configuration (a coordination number of five) is not favored by divalent nickel (unlike divalent copper in the crystals of $Cu(NH_3)_4SO_4 \cdot H_2O$ [4], and copper dimethylglyoxime [5]). So far, no one has reported a crystalline Ni_{II} compound with pentacoordinated nickel; the example examined in this paper shows that such coordination fails to arise even under the most favorable conditions, where we have an additional atom or molecule capable of donating electron pairs to the metal.

We have also compiled a complete table of interatomic distances in the crystal of $Ni(CN)_2NH_3 \cdot nH_2O$ (only some of the distances were tabulated in [1]). The figures in parenthesis give the number of identical atoms at the given distance from the atom listed on the left.

LITERATURE CITED

1. J.H. Rayner and H.M. Powell, J. Chem. Soc., 3412 (1958).
2. J.H. Rayner and H.M. Powell, J. Chem. Soc., 319 (1952).
3. V.I. Belova, Ya.K. Syrkin, and A.I. Avdeeva, Zhur. Neorg. Khim. 2, 1488 (1957).
4. M. Simerskaya, Czech. Phys. J. 4, 277 (1954).
5. E. Frasson, R. Zannetti, R. Bardi, and S. Bezzi, J. Inorg. and Nucl. Chem. 8, 452 (1958).

CHRONICLE

PROBLEMS OF STRUCTURAL INORGANIC CHEMISTRY AT THE THIRD ALL-STATE CONFERENCE ON INORGANIC CHEMISTRY IN BRATISLAVA

T.S. Khodashova

N.S. Kurnakov Institute of General and Inorganic Chemistry,
Academy of Sciences of the USSR
Translated from Zhurnal Strukturnoi Khimii, Vol. 1, No. 1, pp. 127-128,
May-June, 1960
Original article submitted November 20, 1959

The Third All-State Conference on Inorganic Chemistry, organized by the Division of Inorganic Chemistry of the Chemical Institute of the Slovak Academy of Sciences, was held in Bratislava (Czechoslovakia) from June 29 to July 4, 1959. Scientists from Czechoslovakia, USSR, German Democratic Republic, Poland and Hungary took part in the work of the conference. More than 70 papers were presented and discussed. Academician I.I. Chernyaev and Corresponding Member of the Academy of Sciences USSR G.B. Bokii presented papers from the Soviet Union.

Papers by Corresponding Member of the Slovak Academy of Sciences, M.Gregor and by Academician I.I. Chernyaev were presented at the first plenary session. M. Gregor began his paper: "Tasks of Czechoslovak inorganic chemistry in the light of the decisions of the Eleventh Congress of the Czechoslovak Communist Party" with a review of the period since the Second All-State Conference on Inorganic Chemistry. After a survey of the achievements of the Czechoslovak inorganic chemistry during this period, he turned to its tasks imposed by the plan for the development of the national economy, confirmed at the Eleventh Congress of the Czechoslovak Communist Party, and in conjunction with the results of the Twenty-first Congress of the Communist Party of the Soviet Union. The second part of the paper dealt with the fulfillment of the Government decision for construction of a new building for the Institute of Inorganic Chemistry of the Czechoslovak and Slovak Academies of Sciences, and the consequent considerable expansion of their work. A special section of M. Gregor's paper was devoted to the results of the Eighth Mendeleev Congress on General and Applied Chemistry. In conclusion, he reviewed the prospects for development of inorganic chemistry in Czechoslovakia and for training of chemists, and problems of coordination of scientific research work both within the country and with scientific institutions in the USSR, the Peoples' Democracies, and capitalist states.

In his paper "Platinum pentammines," Academician I.I. Chernyaev presented the results of recent research in the field of chemistry of quadrivalent platinum, with special reference to a new method for synthesis of pentammines by the action of ammonia on platinum iodohydroxotetrammines, which was extended to cyclic and bicyclic pentammines. It was shown in the paper that iodine has a strong trans-influence and that this accounts for difficulties in synthesis of iodopentammine salts. The properties of iodopentammine salts are similar to those of bromo- and chloropentammine salts, but differ from the properties of nitropentammines (the latter are much more stable). Absence of any appreciable trans-influence of the nitro group in quadrivalent platinum compounds was confirmed once again by chemical methods.

The conference covered a wide range of problems in inorganic chemistry. In this report attention is devoted mainly to papers dealing with structural inorganic chemistry. Corresponding Member of the Academy of Sciences USSR G.B. Bokii presented a paper entitled: "Significance of crystal-chemical investigations in the

chemistry of complex compounds." He defined complex compounds and pointed out that introduction of the coordination number concept into chemistry marked the appearance of a new branch of the subject—the chemistry of complex compounds. However, it is not always possible to determine the coordination numbers of atoms in actual compounds by purely chemical methods, while in principle the coordination number can always be determined by crystal-chemical methods. Owing to crystal chemistry the concept of coordination number was extended to the simplest chemical compounds. The role of crystal chemistry in studies of isomerism was demonstrated in the paper. Apart from direct determination of the types of known isomers, crystal chemistry makes it possible to predict completely new instances of isomerism and to solve other problems in structural chemistry. The coordination numbers of ions in the outer sphere can be determined by the methods of crystal chemistry. In the concluding section of his paper G.B. Bokii emphasized that as the result of direct determinations of interatomic distances crystal chemistry introduced a quantitative content into all qualitative aspects of stereo-chemistry.

The work of F. Hanic and his associates (Chemical Institute of the Slovak Academy of Sciences) was presented in three papers. They determined the structure of copper salicylate. It was shown that the structure consists of $Cu[C_6H_4(OH)CO_2]_2 \cdot 2H_2O$, molecules joined by hydrogen bonds; pairs of water molecules fill the channels in the structure. Copper is in square coordination. The authors consider that this compound should be classified with the chelate type. The second paper dealt with determination of the structure of zeunerite, a uranyl compound. The structure was found to contain layers of $[UO_2(AsO_4)]$, with water molecules and copper ions between them. The postulated structure satisfactorily explains the physical and chemical properties of the mineral. The UO_2 group is asymmetric (U—O = 1.94 and 1.85 A); this is attributed to asymmetric arrangement of water molecules around the group. G.B. Bokii stated in the discussion that this result contradicts all known structural data, according to which the UO_2 group is symmetric, and that the difference in the distances in the case of zeunerite should probably be attributed to insufficient accuracy in determination of the coordinates of the oxygen atoms. In the newly determined structure of CrO_3, built up of chains of tetrahedrons, two types of Cr—O distances have been found: 1.78 A in the chain, and 1.53 A outside it. The authors suggest that the latter distance corresponds to multiple bonding.

V. Kupcic and S. Durovic (Kamensky University, Bratislava) presented a paper entitled: "The crystal structure of $CuPy_2Br_2$." They showed that this compound is not isomorphous with the corresponding chloro derivative, although its structure is very similar.

K.H. Fost reported on the results of determinations of the structures of sodium Kurrol salt $(NaPO_3)_X$, which contains spiral chains of PO_4 tetrahedrons joined by sodium ions. O. Yarkhov reported on the structure of periodic acid. Both speakers are members of the Institute of Structural Research, Academy of Sciences of the German Democratic Republic (Berlin).

In a paper entitled: "Structure and properties of inorganic substances" N. Zikmund (Chemical Institute of the Slovak Academy of Sciences, Bratislava) considered the influence of the theory of chemical structure on the development of inorganic chemistry. In his opinion, significant progress in inorganic chemistry began only after chemistry had adopted new concepts of ths structure of electron shells in atoms and of the quantum-mechanical theory of the chemical bond, and also as the result of the use of new physical investigation methods. The speaker presented certain data to demonstrate the dependence of the reactivity of substances on their structure. Special attention was devoted in the paper to the solid state. Connections between the physico-chemical properties and lattice defects and between the structure and physical properties of substances were noted.

In addition to papers concerned with the structure of inorganic compounds, papers dealing with other branches of chemistry were presented at the conference: synthesis and properties of complex compounds, investigations of the reactions of halogens, work on technology and analytical chemistry, and research associated with the silicate industry. Much attention was devoted to work on polarography, a field in which Czechoslovak scientists hold the world priority. Several papers were concerned with problems of physicochemical analysis. M. Malinovsky (Slovak Polytechnic Institute) presented a long paper on the significance of physicochemical analysis in studies of inorganic systems. He analyzed the main trends of this branch of science and reviewed its present status in Czechoslovakia and other countries.

Most of the papers provoked lively discussions. The conference demonstrated the very high level of development of chemical science in Czechoslovakia.

SIGNIFICANCE OF ABBREVIATIONS MOST FREQUENTLY ENCOUNTERED IN SOVIET PERIODICALS

FIAN	Phys. Inst. Acad. Sci. USSR.
GDI	Water Power Inst.
GITI	State Sci.-Tech. Press
GITTL	State Tech. and Theor. Lit. Press
GONTI	State United Sci.-Tech. Press
Gosenergoizdat	State Power Press
Goskhimizdat	State Chem. Press
GOST	All-Union State Standard
GTTI	State Tech. and Theor. Lit. Press
IL	Foreign Lit. Press
ISN (Izd. Sov. Nauk)	Soviet Science Press
Izd. AN SSSR	Acad. Sci. USSR Press
Izd. MGU	Moscow State Univ. Press
LEIIZhT	Leningrad Power Inst. of Railroad Engineering
LET	Leningrad Elec. Engr. School
LETI	Leningrad Electrotechnical Inst.
LETIIZhT	Leningrad Electrical Engineering Research Inst. of Railroad Engr.
Mashgiz	State Sci.-Tech. Press for Machine Construction Lit.
MEP	Ministry of Electrical Industry
MES	Ministry of Electrical Power Plants
MESEP	Ministry of Electrical Power Plants and the Electrical Industry
MGU	Moscow State Univ.
MKhTI	Moscow Inst. Chem. Tech.
MOPI	Moscow Regional Pedagogical Inst.
MSP	Ministry of Industrial Construction
NII ZVUKSZAPIOI	Scientific Research Inst. of Sound Recording
NIKFI	Sci. Inst. of Modern Motion Picture Photography
ONTI	United Sci.-Tech. Press
OTI	Division of Technical Information
OTN	Div. Tech. Sci.
Stroiizdat	Construction Press
TOE	Association of Power Engineers
TsKTI	Central Research Inst. for Boilers and Turbines
TsNIEL	Central Scientific Research Elec. Engr. Lab.
TsNIEL-MES	Central Scientific Research Elec. Engr. Lab.–Ministry of Electric Power Plants
TsVTI	Central Office of Economic Information
UF	Ural Branch
VIESKh	All-Union Inst. of Rural Elec. Power Stations
VNIIM	All-Union Scientific Research Inst. of Metrology
VNIIZhDT	All-Union Scientific Research Inst. of Railroad Engineering
VTI	All-Union Thermotech. Inst.
VZEI	All-Union Power Correspondence Inst.

Note: Abbreviations not on this list and not explained in the translation have been transliterated, no further information about their significance being available to us. – Publisher.

RESEARCH BY SOVIET EXPERTS

Translated by Western Scientists

BORATE GLASSES

by L. Ya. Mazelev

Boron as an element has been known for a long time, but the role of its oxide in glass has been studied little. This book is based mainly on the results of investigating silicate and borosilicate glasses. The purpose of the author's work was a systematic study of the technology of glass melting, the processes and reactions of glass formation, the crystallisation of glasses and the composition of the crystallisation products, the physicochemical properties and their relation to the composition and structure of glass and methods of calculating these properties. This book is important for all those interested in the problems of the structure of glass.

Cloth **176 pages** **$10.00**

SILICON AND ITS BINARY SYSTEMS

by A. S. Berezhnoi

Data accumulated on the physical chemistry of silicon and its binary systems are critically reviewed. The properties and descriptions of the crystal structures of silicon and all its binary compounds known at present are given in detail and the most important ways of using these substances in practical applications are indicated. Silicon carbide is treated in detail, as are silicon compounds of the transition metals. All sections have been provided with a historical outline and the basic literature is cited with each problem considered.

Cloth **265 pages** **$8.50**

CRYSTAL CHEMISTRY OF SIMPLE COMPOUNDS OF URANIUM, THORIUM, PLUTONIUM AND NEPTUNIUM

by E. S. Makarov

This book represents the first attempt to correlate crystal structure data on the simplest compounds of the most thoroughly studied actinide elements. No books dealing specifically with crystal chemistry of the actinides have been published hitherto either abroad or in the Soviet Union, although separate surveys by Zachariasen have appeared in various collective volumes.

The abundant factual data on crystal structures of actinide compounds are summarised in compact form. This work will enable research workers and engineers to make wider use of crystal structure data which, until now, have been scattered throughout numerous literature sources.

The author considers certain questions of general crystal chemistry, gives full details of the crystalline structures of the polymorphic modifications of the actinides and their simplest compounds, adopts Seaborg's cautious position regarding the parent of the "5f" family of elements, and advances an interesting theory concerning the dual chemical nature of the actinides.

Cloth **146 pages** **Illus.** **$5.25**

Payment may be made in sterling to Barclay's Bank in London, England.

Tables of contents upon request

CONSULTANTS BUREAU

227 W. 17th ST., NEW YORK 11, N. Y.

RESEARCH BY SOVIET EXPERTS

Translated by Western Scientists

INSTABILITY CONSTANTS OF COMPLEX COMPOUNDS

by K. B. Yatsimirskii and V. P. Vasil'ev

Instability constants quantitatively characterize the equilibrium in solutions of complex compounds and, in this connection, are very widely used by chemists in different fields (analytical chemistry, electrochemistry, technology of nonferrous and rare metals, etc.) for appropriate calculations.

The instability constants of 1381 complex compounds are given. The authors have prefaced the summary of instability constants with an introductory section which examines methods of calculating instability constants from experimental data, the effect of external conditions (temperature and ionic strength) on the stability of complexes and the main factors determining the stability of complex compounds in aqueous solutions.

Cloth 200 pages $6.75

SOVIET RESEARCH ON COMPLEXES AND CO-ORDINATION CHEMISTRY

This collection consists of 372 articles by Russian scientists in the general area of the chemistry of complexes. These reports have been complied from the Consultants Bureau translations of the following Soviet journals:

Journal of General Chemistry
Journal of Analytical Chemistry
Bulletin of the Academy of Sciences
Division of Chemical Sciences
Proceedings of the Academy of Sciences
Journal of Applied Chemistry
Soviet Journal of Atomic Energy

The articles have been grouped into five volumes, each of which may be purchased separately.

I. Inorganic Complexes—103 articles $65.00
II. Metal-Organic Complexes—86 articles $45.00
III. Thermodynamic and Kinetic Studies—57 articles .. $37.50
IV. Complexes in Analytical Chemistry—57 articles .. $37.50
V. Condensed Inorganic Systems; —38 articles ..
Miscellaneous —31 articles .. $45.00

Complete collection .. $200.000

Tables of contents on request

Payment in sterling may be made to Barclays Bank in London, England

CONSULTANTS BUREAU

227 West 17th Street · New York 11, N. Y.